Virginia Tech
NSF/REU Site
Interdisciplinary Water Sciences and Engineering

Proceedings of Research: Summer 2012
Site Duration: June 3 – August 10, 2012
Host Department: Department of Engineering Education
Project Director: Dr. Vinod K. Lohani[@&] (vlohani@vt.edu)
Project Assistant: Stephanie Welch[&]
Faculty Mentors: Fred Benfield[*], Andrea Dietrich[&], Mark Edwards[&], Erich Hester[&], John Little[&], Vinod K. Lohani[@&], Amy Pruden[&], and Mark Widdowson[&], and Kang Xia[#]
*Biological Sciences, &Civil and Environmental Engineering, #Crop and Soil Environmental Sciences, @ Engineering Education

Host Lab: www.lewas.centers.vt.edu

LEWAS LAB
LabVIEW Enabled Watershed Assessment System

Table of Contents

Acknowledgements

We would like to express our sincere thanks to REU/NSF Site Research Mentors for their kind cooperation and excellent mentoring during summer 2012. Our thanks are also to our graduate student mentors, REU Fellows for their dedication and excellent performance, laboratory staff, seminar speakers, professionals who assisted in field trips and all other individuals who directly/indirectly contributed to the success of our 10-week research program at VT. The program is supported by the National Science Foundation (NSF-REU Grant No. 1062860).

Editorial Staff

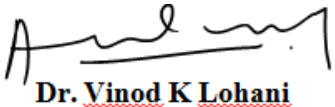

Dr. Vinod K Lohani

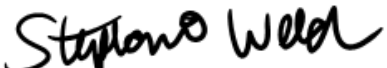

Ms. Stephanie Welch

Disclaimer`

The opinions, findings, and conclusions or recommendations expressed in this proceedings are those of the authors and do not necessarily reflect the views of the National Science Foundation or Virginia Tech.

Summary

This Research Proceedings includes papers of undergraduate research that was conducted on Virginia Tech campus during summer 2012 as part of an NSF/REU Site on Interdisciplinary Water Sciences and Engineering. This was the 2nd year of our 2011-14 NSF/REU Site. Our current Site follows a very successful NSF/REU Site that was implemented at VT during 2007-09. Research Proceedings of 2007, 2008, 2009, and 2011 Sites are available at: www.lewas.centers.vt.edu.

Investigation of interdisciplinary research issues in water sciences and engineering is the key goal of this REU Site. Faculty members from three departments (Engineering Education, Civil and Environmental Engineering, and Crop and Soil Environmental Sciences) mentored 9 excellent undergraduates who were recruited out of a nation-wide competition. Ten graduate students from these departments assisted the faculty mentors and got a valuable experience in mentoring undergraduate research students. Figure 1 shows a word cloud of the keywords that describe the research activities undertaken during the 10-week research at VT.

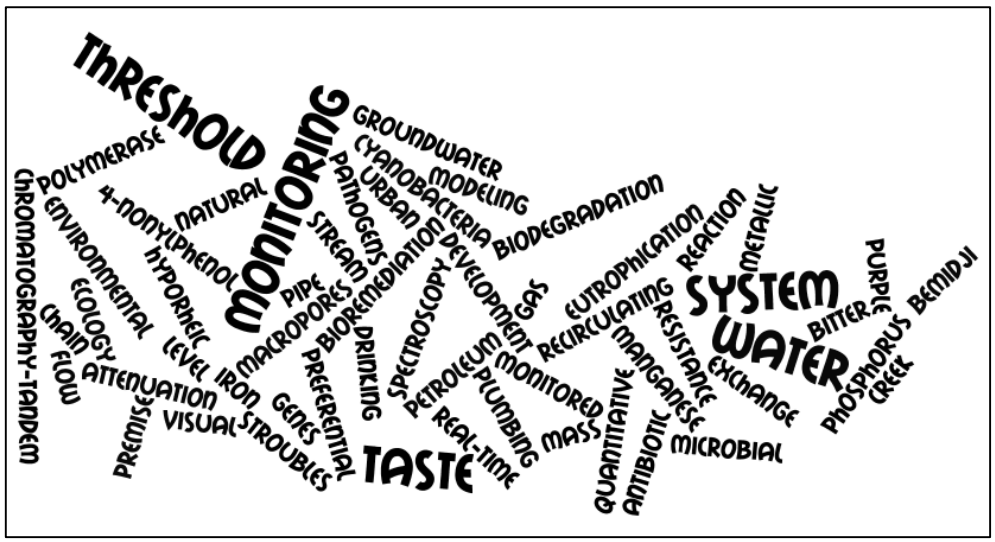

Figure 1: Word Cloud of Keywords – 2012 Research Work

Kate (an REU Fellow from University of Delaware) and her co-authors documented their research work in a paper titled "Macropores As Preferential Flow Paths And Their Effects On Surface Water-Groundwater Exchange Within Hyporheic Zones." Their results suggest that macropores are common geomorphic features (0.812 macropores per meter within the three streams of study) whose dimensions vary within different reaches. By acting as preferential flow paths, macropores increase bank storage and may increase the effects of hyporheic exchange and benefit water quality or stream ecology. Zach (an REU Fellow from University of Maryland-Baltimore County) and his co-authors contributed a paper titled "Applications of Molecular Tools For Exploration of Microbial Community Structure and Function at the Bemidji, Minnesota Oil Spill Site" to study the fate and impacts of petroleum hydrocarbons in groundwater. The goal of their research was to gain a better understanding of the microbial community structure and function involved in oil biodegradation and used data/samples from

the Bemidji Minnesota terrestrial oil spill research site. This research compliments geochemical work done by the USGS and will inform remediation efforts at current and future oil spill sites. In a paper titled "Hot Water Recirculating System Design: Effects on Water Quality Parameters Affecting Premise Plumbing Pathogen Growth" Josh (an REU Fellow from University of Georgia) and his co-authors investigated opportunistic premise plumbing pathogens (OPPPs), which pose special challenges because they grow (amplify) in building plumbing systems beyond the jurisdictional reach of water treatment authorities. In a model hot water heater system, the researchers investigated the effects of pipe orientation and hot water heater temperature settings on temperature stratification, disinfectant residual concentrations, and mixing rates. Ashley (an REU Fellow from Auburn University) and her co-authors contributed a paper titled "Taste and Visual Thresholds of Manganese in Drinking Water" documenting results of their research that had a goal to determine the human taste threshold for aqueous reduced Mn (II) to know if consumers could protect themselves by detecting an off-taste. Thirty-one volunteers (15 female) participated in the study and results indicate that 108 mg/L is the population taste threshold, which is much higher than typical Mn concentrations in water. In a paper titled "Antibiotic Resistance Genes in Recycled Water" Maureen (an REU Fellow from Colorado School of Mines) and her co-authors examined occurrence of antibiotic resistant bacteria (ARB), an example of potentially persistent pathogens, in recycled water samples from irrigation systems in Flagstaff, AZ and Santa Barbara, CA. Antibiotic resistant genes (ARGs), which are the markers of ARB presence, were detected in all but two of the twenty-three samples. Manuel (an REU fellow from Virginia Tech) and his co-authors contributed a paper titled "Study and Application of a Real-Time Environmental Monitoring System" in which they discussed the calibration procedures for water and weather hardware of a real-time monitoring system called LabVIEW Enabled Watershed Assessment System (LEWAS). Using the real-time data, the authors discussed a case study to describe the environmental impacts of a water main break in the town of Blacksburg in summer 2012. In a paper titled "Investigating the Occurrence and Fate of 4-Nonylphenol in a Watershed Impacted by Urban Development" Jennifer (an REU Fellow from Worcester Polytechnic Institute) and her co-authors investigated the occurrence of 4-nonylphenol within the Stroubles Creek Watershed in Blacksburg, Virginia to understand the environmental impacts of urban development. Water and sediment samples were collected at six different locations and the levels of 4-nonylphenol in the water samples were detected at 100's ng/L, while in the sediment samples they were detected at 1000's µg/kg. William (an REU fellow from University of Notre Dame) and his co-authors documented their research in a paper titled "Effect of Bioavailable Fe^{3+} on the Sustainability of Monitored Natural Attenuation of Petroleum Hydrocarbons" which included results of numerical modeling of the fate and transport of gasoline—including an ethanol-enriched fuel known as gasohol—in hypothetical groundwater systems using SEAM3D (Sequential Electron Acceptor Modeling in 3-Dimensions). Meghan (an REU Fellow from Texas Tech University) and her co-authors reported their research findings in a paper titled "Influence of The Phosphorus Circulation on the Eutrophication and Algal Blooms at Falling Creek Reservoir." The goal was to understand the conditions in which cyanobacteria bloom in the reservoir and data such as the amount of phosphorus going into the lake, as well as that in the lake at different depths, temperature, dissolved oxygen, and turbidity were recorded and analyzed.

REU Fellows created two YouTube videos to document their experiences of 10-week work at VT:

http://www.youtube.com/watch?v=85OErf7d6T0

http://www.youtube.com/watch?v=Cw_R4fj84Ms

Research Papers

Macropores As Preferential Flow Paths And Their Effects On Surface Water-Groundwater Exchange Within Hyporheic Zones

Kate E. Aulenbach*, Garrett T. Menichino**, Erich T. Hester**

** NSF-REU fellow, Virginia Polytechnic Institute and State University*
(Home Institution: Environmental Engineering, University of Delaware)
***Department of Civil and Environmental Engineering, Virginia Polytechnic Institute and State University*

ABSTRACT

Hyporheic exchange, the mixing of surface water and groundwater, is beneficial to water quality and stream ecology as it can buffer in-stream temperatures, increase the occurrence and rates of important biogeochemical reactions, attenuate pollutants, and create habitat for organisms. Bank storage is a subset of hyporheic exchange in which stream stage fluctuations cause surface water to temporarily infiltrate the banks and interact with the groundwater within their riparian and parafluvial zones. Macropores are physical void spaces within the bed and banks of streams that may act as preferential flow paths and increase hyporheic exchange. However, previous studies have not quantified their abundance or impact. The objectives of this study are to (1) survey and quantify reach scale macropore abundance and dimensions (i.e., diameter, depth, height above water level at baseflow), (2) determine reach scale temporal variation of macropore activity (i.e., when macropores are saturated), and (3) quantify macropore impact on bank storage rates and hyporheic zone size at the patch scale. Objective (2) was addressed by analyzing differences in the percentages of macropores which were activated (i.e., saturated) by water level increases due to storm events. Objective (3) will be met by monitoring and comparing water levels in piezometers at two stream bank faces: one with, and one without, macropores. Though this study is part of an ongoing research project, preliminary results suggest that macropores are common geomorphic features (0.812 macropores per meter within the three streams of study) whose dimensions vary within different reaches. Macropore engagement (i.e., saturation) varies temporally and may be most important during storm flows. By acting as preferential flow paths, macropores increase bank storage and may increase the effects of hyporheic exchange and benefit water quality or stream ecology.

Keywords: Stream, Groundwater, Macropores, Hyporheic Exchange, Preferential Flow, Water Level

Introduction

One-third of streams in the United States are listed as impaired or polluted, resulting in degraded water quality and the loss of aquatic ecosystems (Bernhardt et al., 2005). Pollutants such as thermal pollution, dissolved inorganic nitrogen, organic chemicals, and heavy metals commonly enter streams and groundwater (Brunke and Gosner 1997). Establishing and preserving beneficial environmental and ecological conditions is important to maintaining the functionality of streams. One such mechanism necessary for the life cycles of streams is hyporheic exchange (Sawyer et al., 2009). Hyporheic exchange, the mixing of stream surface water with groundwater both beneath and adjacent to stream beds, can mitigate thermal pollution, enhance the occurrence of beneficial nutrient exchange, and provide bank storage within streams (Brunke and Gosner 1997 and Hester and Gooseff 2010). Groundwater maintains constant temperatures which are impacted solely by cyclic seasonal temperature gradients while surface water temperature tends to fluctuate daily due to the effects of solar radiation. Hyporheic exchange can therefore cool, buffer, and lag surface water temperature (Arrigoni et al., 2008). This phenomenon ensures the survival of organisms that cannot function in environments with significant temperature variations. Surface water generally contains higher concentrations of dissolved oxygen and organic carbon than groundwater which tends to be high in inorganic solutes, promoting the biogeochemical reactions necessary to sustain stream ecology (Brunke and Gosner 1997). Bank storage is one type of

hyporheic exchange that occurs when water level increases caused by storm events or other stage fluctuations force surface water to infiltrate stream banks and interact with groundwater (Boulton et al., 1998). Bank storage is advantageous because it provides a source of flood mitigation and the transient storage of solutes (Brunke and Gosner 1997 and Boulton et al., 1998), however, the extent of these benefits are typically conceived as dependent upon the permeability of the bank sediment. As the permeability of sediment increases, flow rates increase along with the potential benefits of hyporheic exchange (Sawyer et al., 2009).

Preferential flow paths are located within streams and rivers, characterized as regions of high permeability, and facilitate the mixing of surface water and groundwater (Franklin et al., 2007). Macropores are one type of preferential flow path in which a physical void space exists. These macropores can span various depths, extend from bank faces into the floodplain, and can be filled with either air or water depending upon stage (see Figure 1). Macropores are formed by a variety of mechanisms such as bank erosion, root decay, and bioturbation (Luo et al., 2010). Though recognized as preferential flow paths, the abundance, dimensions, and extent of the effects of macropores on hyporheic exchange have not been previously studied or quantified. The objectives of this research, therefore, are to (1) quantify reach scale macropore abundance, dimensions (i.e., diameter, depth, height above water level at baseflow), and location (i.e., geomorphic feature, sediment type), (2) determine reach scale temporal variation of macropore activity (i.e., when macropores are saturated), and (3) quantify macropore impact on bank storage rates and hyporheic zone size at the patch scale.

Figure 1. Left frame shows a cluster of macropores in the bank of a stream. Right frame is an inset of the left and suggests crayfish were their mechanism of formation.

Research Methods

Site Description

Five streams in the southwest region of Virginia varying in size, sediment type, and land use were surveyed within this study (Table 1, Figure 2). Slate Branch Creek is a second order stream which flows through the urban town of Christiansburg. Stroubles Creek is a second order urban stream located downstream of Virginia Tech's campus in downtown Blacksburg. Craig Creek, a third order stream, flows through a forested area near Blacksburg. Poverty Creek, the outfall of Pandapas Pond and a second order stream, is also located in a forested area near Blacksburg. Also being surveyed is a first order tributary of Tom's Creek located in a region near Blacksburg classified as both urban and agricultural.

Table 1. Site Descriptions and Information

Stream Name	Stream I.D.	Stream Order	Land Use	Typical Bank Sediment Type	Bankfull Width (m)
Slate Branch Creek	1	2	Urban	Clay	5.2
Stroubles Creek	2	2	Urban and Agriculture	Sand and Clay Loam	5.7
Craig Creek	3	3	Forest	Bedrock, Cobble, and Clay Loam	8.2
Poverty Creek	4	2	Forest	Silty Clay	5.3
Tom's Creek Tributary	5	1	Forest and Agriculture	Clay	1.8

Figure 2. Site locations. Sites 1-5 are Slate Branch Creek, Stroubles Creek, Craig Creek, Poverty Creek, and Tom's Creek Tributary.

Macropore Survey

Macropore surveys were conducted along a selected primary reach of each stream whose length was set as twenty times the bankfull width of each respective stream. Macropore aperture, linear depth, height above water level at baseflow, and distance along the survey stretch were surveyed. Qualitative observations associated with each macropore were also documented. These included bank and bed sediment type, geomorphic feature (i.e., pool, riffle), orientation (i.e., open upstream, open downstream, perpendicular to stream), and creation mechanism for individual macropores. The presence of macropores in regions beyond the primary study reaches were confirmed by quantifying their longitudinal distributions both upstream and downstream of the site. Upstream and downstream surveying extended an additional primary reach length in each direction. Simple statistical analyses, primarily the

determination of central tendency, were performed on the recorded macropore abundance, dimensions, and locations.

Macropore Activation

At the midpoints of the primary survey reaches, stream gauges were installed into the banks of each site to measure and record water level fluctuations with the aid of pressure transducers. Stream gauges were constructed by joining two 1-1/4" PVC pipes with a ninety degree 1-1/4" PVC elbow and installed in each stream bank so that one pipe would lay parallel to the bed beneath the water's surface at baseflow and the other would be capped and positioned perpendicular to the top of the bank (Figure 3). Holes were drilled in the top of each PVC cap in order to provide ventilation in the gauge so that surface water that entered the gauge through the inlet was collected in the vertical pipe. The height of the water in the stream gauge represented the water level within the stream. Pressure transducers located at the bottom of each vertical PVC pipe measured and collected absolute pressure data every fifteen minutes for twelve days. In order to analyze the pressure due solely to the water within each vertical PVC pipe, the barometric pressure recorded at Stroubles Creek was subtracted from the absolute pressure. The equation for static fluid pressure, $P = \rho g h$, was used to calculate the height (h) of water above each pressure transducer, where g is the acceleration due to gravity and ρ is the density of water. Temporal macropore activation was determined by comparing stage fluctuations reported by each stream gauge and the heights of individual macropores as collected during the macropore survey.

Figure 3. Stream gauge at Slate Branch site.

Bank Storage Experiment

In order to quantify the effect of macropores on hyporheic exchange within the riparian zones of streams, two perpendicular transects of four piezometers each were installed extending from the bank face into the floodplain of Slate Branch Creek (Figure 4). One piezometer transect was installed perpendicular to a section of the bank that contained a cluster of six macropores ranging in depth, diameter, and height above the stream bed. Approximately 9.19 meters downstream, the second transect of piezometers was constructed perpendicular to a bank face similar to the previous in sediment type and height, but lacked macropores. In both transects, the first piezometer was installed 0.5 meters back from the bank; the second, 1 meter from the bank; the third, 2 meters from the bank; and the forth, 4 meters from the bank. An additional piezometer was placed eight meters from the bank and directly in between the macropore and non-macropore transects to provide a floodplain groundwater level reference.

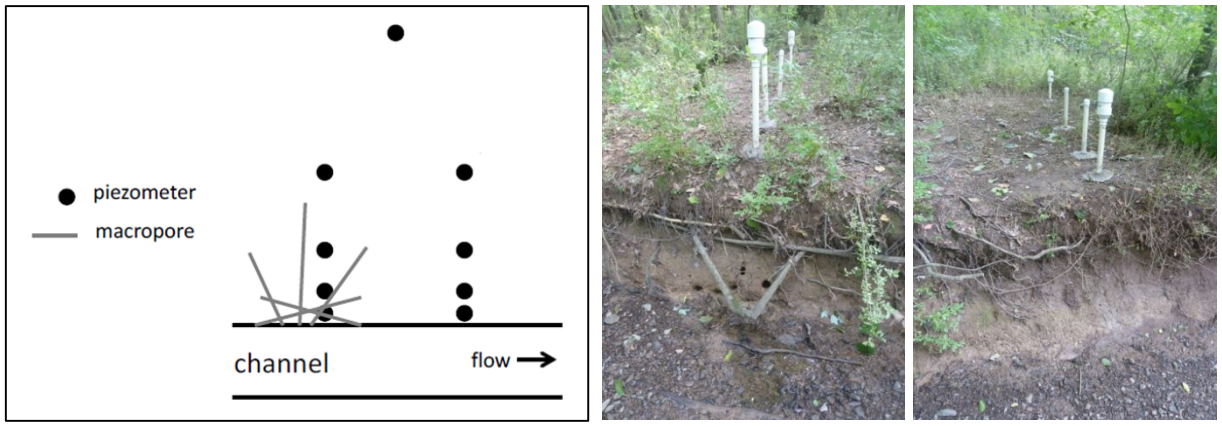

Figure 4. Bank storage experimental setup and construction – plan view schematic (left) and photographs (right).

Each piezometer was constructed from 1.525 meter PVC pipes with diameters of 1-1/4" which was sealed on both ends with 1-1/4" PVC caps. Water permeable screens were attached to the bottom of each PVC pipe by drilling 3/16" inch holes 1-1/2 centimeters apart and covered with filter fabric secured by electrical tape. Screens began approximately nine centimeters from the bottom of each PVC pipe and averaged 64.5 centimeters in length. A 5/16" hole was drilled into the cap of each PVC pipe in order to allow atmospheric ventilation.

Boreholes to house the piezometers were dug using a hand auger. The distances from the ground surface to the bottom of each channel varied as it was dependent upon the depth of the water table at each location. Once the piezometers were installed in the boreholes, the remaining void space was filled with filter sand. Bentonite was used to seal the boreholes at the ground surface and prevent rain water or surface runoff infiltration alongside the each piezometer.

Following installation, each pipe was equipped with a pressure transducer which logged absolute pressure data every fifteen minutes for twelve days. The pressure due solely to the groundwater levels within each piezometer was determined using the same technique applied to the stream gauge data. Given the adjusted pressure values reported by the probes, the water level within each piezometer was determined using the same calculations presented in the description of the stream gauges. The effect of macropores on bank storage rates can be quantified by comparing the temporal variation in water levels across the macropore piezometer transect to that of the non-macropore piezometer transect.

Results and Discussion

This paper focuses on the preliminary results gathered from the macropore surveys performed at Slate Branch Creek, Stroubles Creek, and Craig Creek as well as the macropore activation and bank storage experiments conducted at Slate Branch Creek.

Macropore Survey

Macropore survey results including average aperture, linear depth, and height above water level of the macropores surveyed within each primary stream reach of Slate Branch Creek, Stroubles Creek, and Craig Creek are shown in Table 2. The macropore density, or number of macropores per meter, in each stream was also evaluated. These values were derived by dividing the total number of macropores within each extended survey reach by the length of the respective reach.

Table 2. Macropore survey results.

Stream Name	Survey Reach Length (m)	Number of Macropores Surveyed Within Primary Reach	Number of Macropores Surveyed Within Extended Reach	Reach-Averaged Aperture (cm)		Depth (cm)	Distance to Water Level at Baseflow (cm)	Macropore Density (# of Macropores per Meter)
				Width	Height			
Slate Branch Creek	104	112	293	5.3	4.0	18.2	8.3	0.939
Stroubles Creek	114	111	354	5.0	4.0	21.6	13.9	1.04
Craig Creek	164	106	225	3.9	3.0	15.2	50.3*	0.457
Averages across All Reaches				4.7	3.7	18.3	24.2	0.812
*Measurements taken from bottom of bank rather than baseflow water level due to lack of water flow on day of survey.								

The average number of macropores per meter within both Slate Branch and Stroubles Creek is approximately one. The smaller value determined for macropore density at Craig Creek was due primarily to the sediment type comprising its banks. Stretches of the survey reach at Craig Creek were constrained by bedrock, cobble, and gravel banks and the existence of surface-connected macropores in these areas was rare. Qualitative observations recorded for each macropore surveyed within this study helped to provide additional insight into the sediment types in which macropores are likely to be found. While bank sediment types within each of the streams ranged from loose silt to cobble and bedrock, 99.1 percent of the macropores surveyed within the primary reaches of Slate Branch, Stroubles, and Craig Creek were located in either clay or silty clay loam. Similarly, notes taken during the macropore survey regarding the morphology of the stream at the site of each macropore also indicate the environments in which they often exist. Figure 5 illustrates the longitudinal distribution of macropores across the primary survey reach of each stream. The red line which appears above each graph denotes the geomorphic features present along each reach. Apparent in the analysis of the graphs, macropores are concentrated within riffles and have less of a tendency to appear in pools. Approximately 91 percent of the macropores studied within the primary reaches of each stream were located along riffles while the remainder of those surveyed were found near pools.

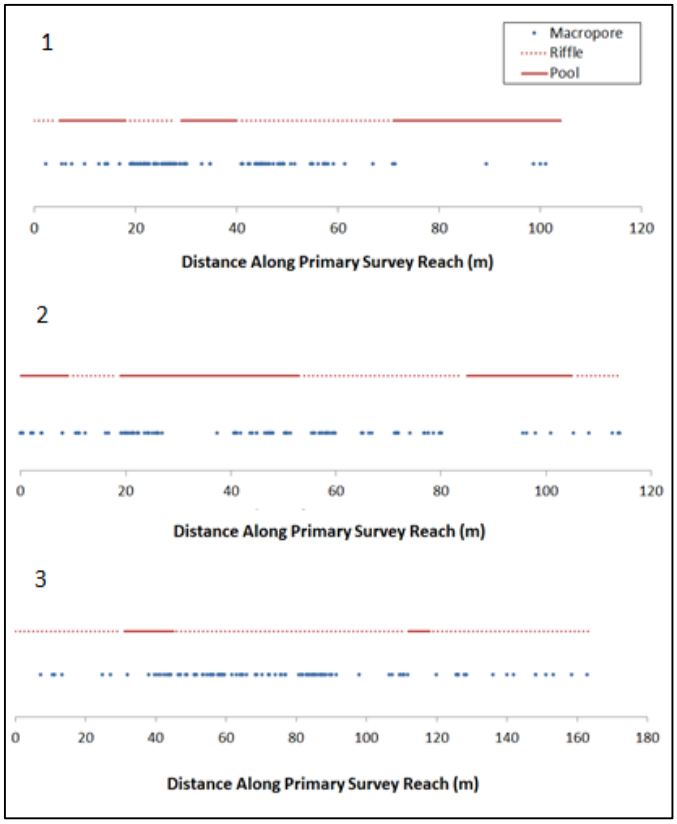

Figure 5. Longitudinal distribution of macropores for sites 1-3 (i.e., Slate Branch Creek, Stroubles Creek, and Craig Creek, respectively).

Macropore Activation

In order to determine the temporal engagement (i.e., saturation) of macropores, macropore survey data collected at Slate Branch Creek was compared to the water level data recorded by the stream gauge installed at the site. Figure 6 below presents the longitudinal distribution of macropores at Slate Branch Creek and the distance of each macropore to the water level at baseflow. On the graph, baseflow water level is denoted by the y-value of zero. The value for baseflow water level at the site of the stream gauge fluctuated about an average of 3.8 centimeters. Under these conditions, only 33.9 percent, 38 of the 112 macropores within the primary survey reach were submerged.

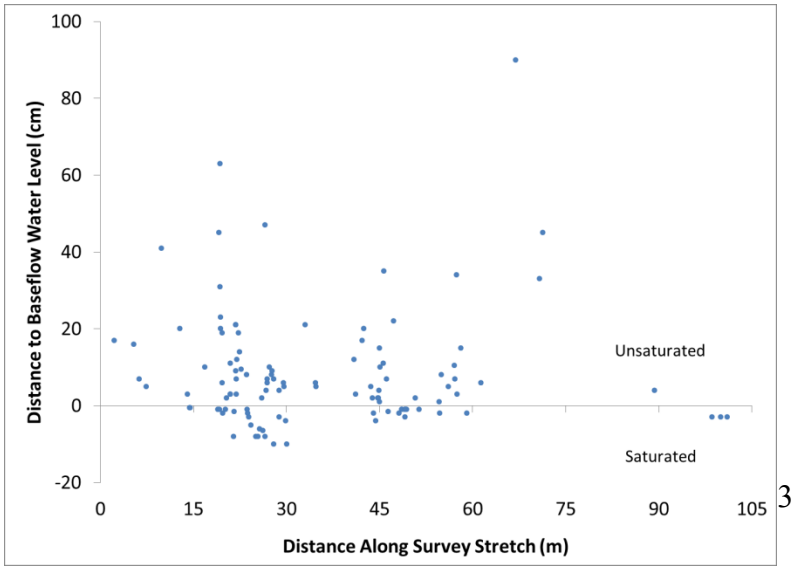

Figure 6. Plot of macropore engagement at baseflow longitudinally along the survey reach.

During the course of the twelve day data logging period, two storm events were observed, indicated by increases in the water level data reported by the stream gauge installed at Slate Branch Creek. A small storm on July 10, 2012 caused the water level to reach a maximum of approximately 5.02 centimeters above baseflow water level at the site of the stream gauge. If this peak water level change is assumed to have occurred throughout the entire survey reach, this storm triggered the saturation of 23 macropores in addition to those saturated at baseflow and increased the percentage of active macropores to 54.5 percent. Similarly, on July 14, a larger storm caused the water level to rise 12.14 centimeters above baseflow and caused the activation of 76.8 percent of the surveyed macropores. These fluctuations in stage and their effect on the number of activated macropores are illustrated in Figure 7. Though only representing two weeks of stream gauge data, these preliminary results demonstrate the drastic variation of macropore saturation as influenced by water level fluctuation during storm events.

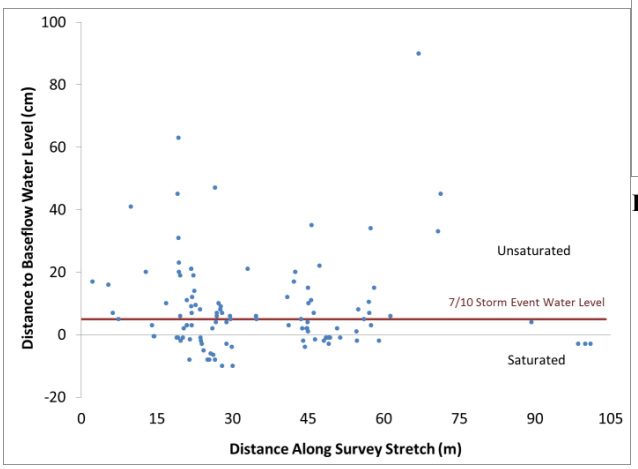

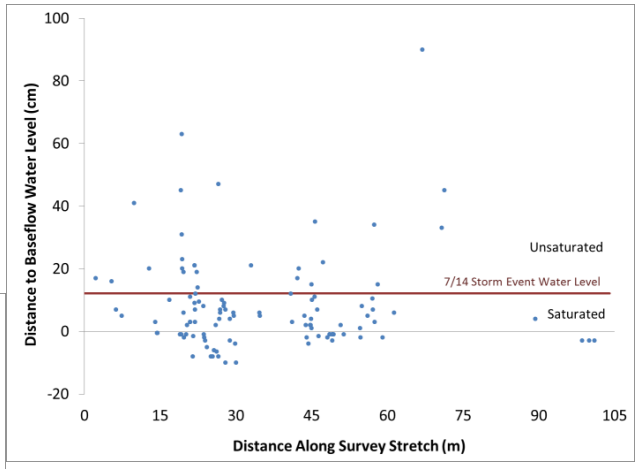

Figure 7. Macropore engagement for two storm events.

Bank Storage Experiment

In order to determine the effects of macropores on bank storage and hyporheic exchange, the water levels within both the non-macropore transect piezometers and the macropore transect piezometers installed at Slate Branch Creek were examined and compared. These results, collected during the two week study period are presented within Figures 8, 9, and 10. Two curves are constant and common to each of these graphs. The purple colored curve present in each graph denotes the water level of the stream as recorded by the stream gauge. Representative of the groundwater level within the floodplain reference piezometer is the blue curve. Because the water level within the floodplain reference piezometer is less than that reported by the stream gauge, the stream can be characterized as a hydrologically losing stream.

Figure 8 illustrates the water levels within the non-macropore transect piezometers over the two week data collection period. The four orange curves depicting these values decrease in color intensity as the piezometers move further into the floodplain. Consistent with a losing stream, water levels decrease with increasing distance from the bank. Slight elevations in water level corresponding to the spikes in the

stage of the stream during the July 10th and 14th storm events can be detected within the piezometers located closest to the bank face labeled NM-A and NM-B.

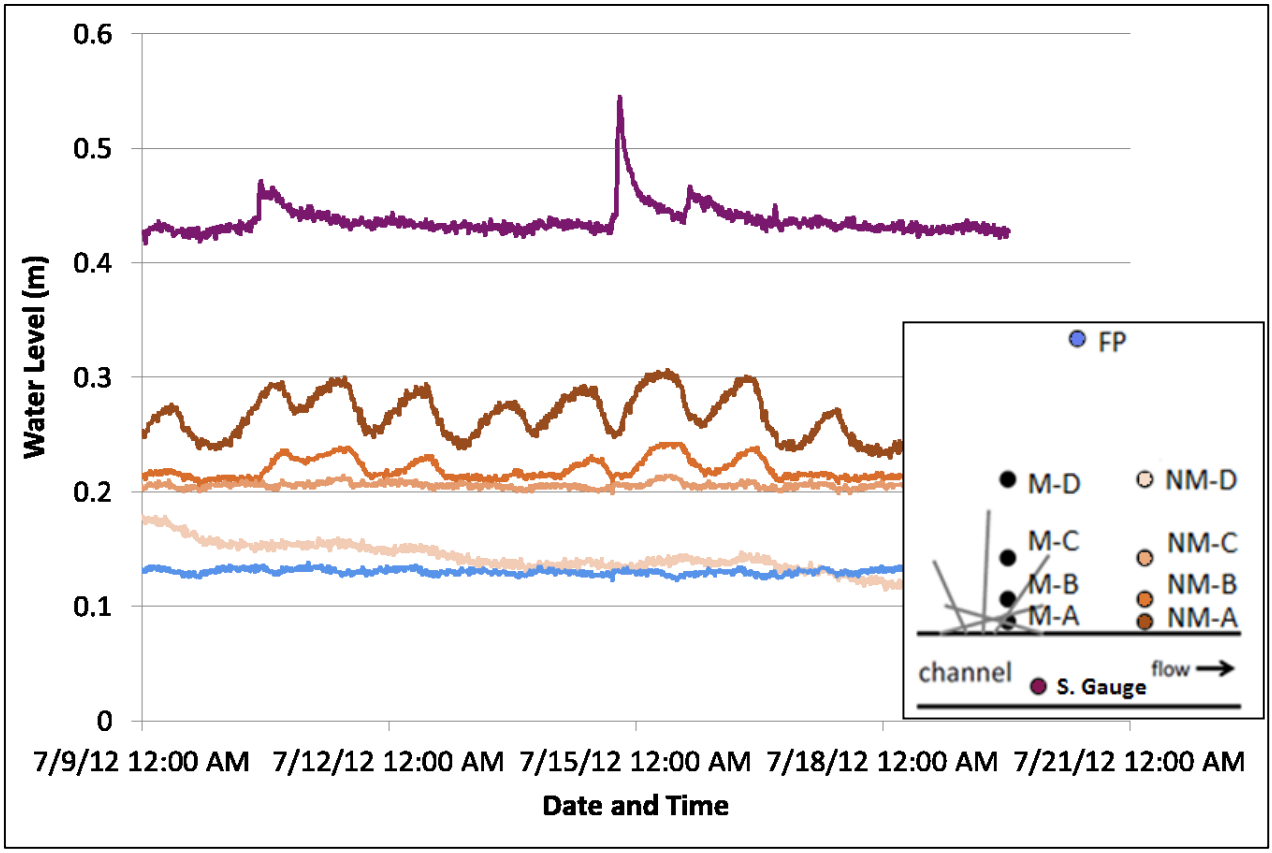

Figure 8. Water levels within non-macropore transect piezometers at Slate Branch Creek.

Figure 9 shows the water levels within the macropore transect piezometers collected throughout the two week duration of study. Like in Figure 8, the four curves representing the water level within each piezometer decrease in color intensity as they move further into the floodplain. Unlike Figure 8, however, the water levels within the two piezometers located closest to the bank do not merely reflect the stream gauge water level during storm events. Instead, the water levels within piezometers M-A and M-B very closely and continuously mimic the water level within the stream.

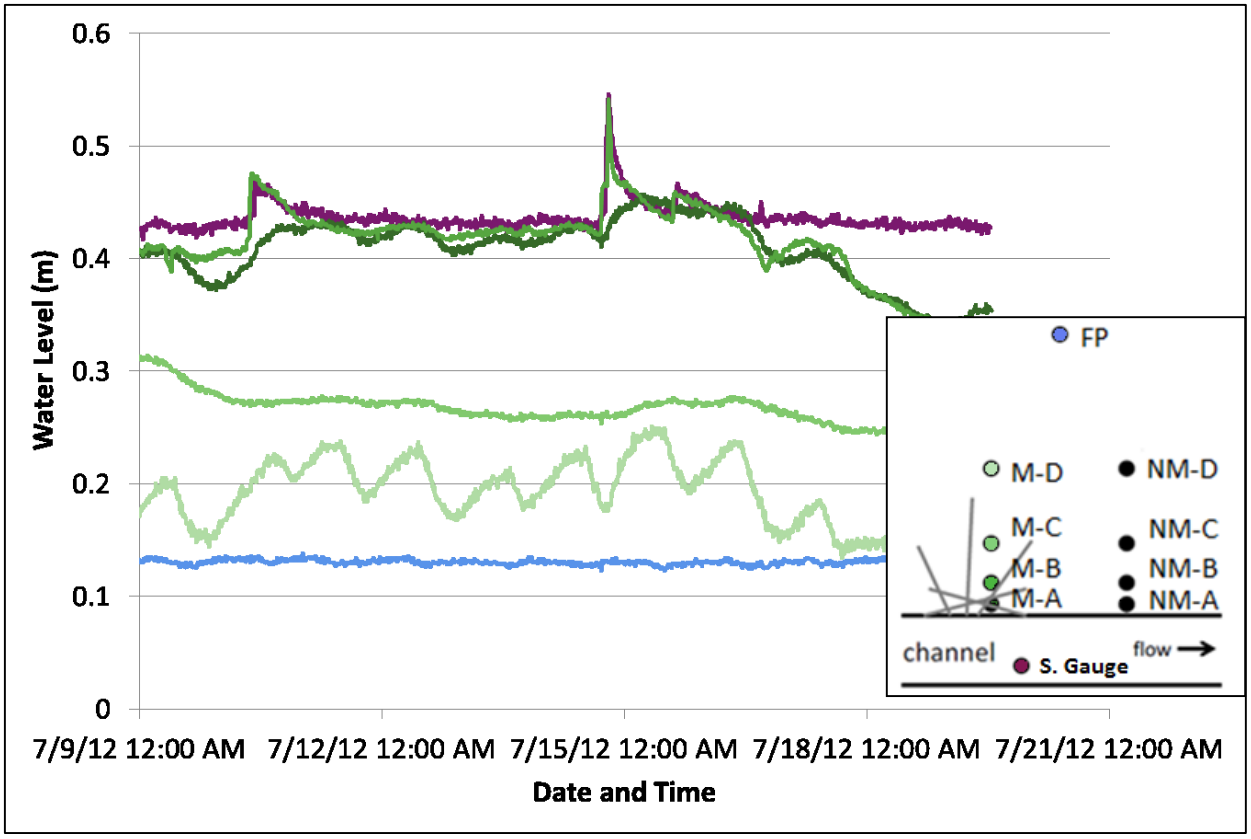

Figure 9. Water levels within macropore transect piezometers at Slate Branch Creek.

Figure 10 overlays the data presented within Figures 8 and 9. Each of the piezometers along the macropore transect contain higher levels of water than the piezometers within the non-macropore transect to which they correspond. For example, the curve representing the water level within the piezometer labeled M-A is consistently higher than that within the piezometer labeled NM-A. Also notable is the tendency of the piezometer located 0.5 meters from the bank face at the non-macropore site (NM-A) to behave, with respect to water level, similarly to the piezometer located 2 meters from the bank face at the macropore site (M-C). These observations indicate the increased rate of bank storage and hyporheic exchange which exist within the macropore transect of piezometers.

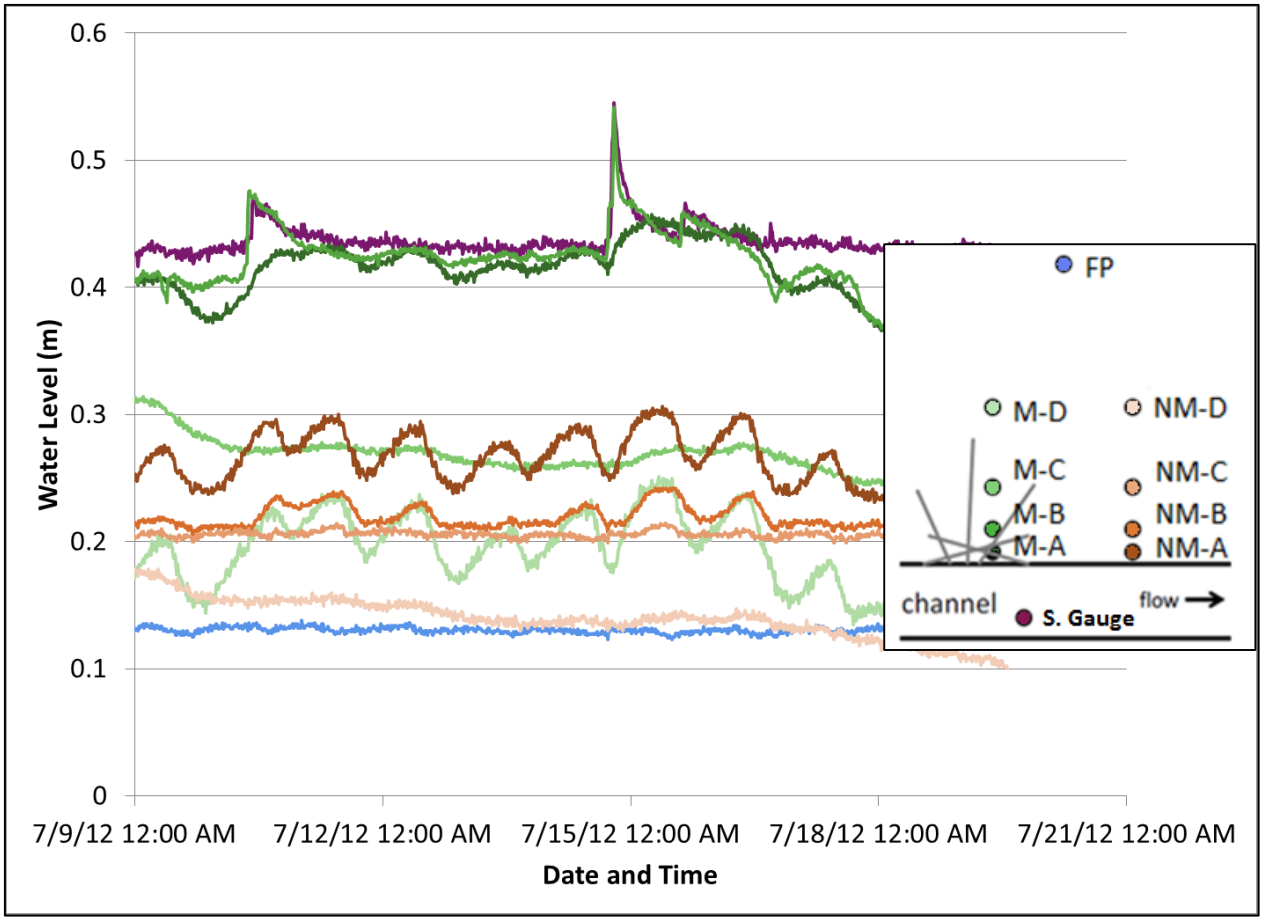

Figure 10. Combined water level data within piezometers at Slate Branch Creek.

Conclusions

The preliminary results presented within this paper suggest that macropores are common geomorphic features within streams that act as preferential flow paths to influence hyporheic exchange by increasing bank storage during storm events and natural stage fluctuation.

The frequency of macropores within streams is indicated by the average macropore density in Slate Branch Creek, Stroubles Creek, and Craig Creek. This value, determined to be 0.812 macropores per meter, suggests that macropore abundance within streams is significant and should be considered when analyzing hyporheic exchange and stream ecology. Macropores were common in riffles as well as regions of streams with banks of clay or silty clay loam. A clear direction for the future study of macropores would be to determine the pathways of individual macropores as well as their connectivity (i.e., if and how macropores are connected).

While the two weeks of stream gauge data analyzed within this study exemplified the impact of stage fluctuation on temporal macropore saturation, the continuation of water level data collection will provide additional insight into the activation of macropores over time. Of particular interest are differences among seasons, particularly summer and winter. Furthermore, a more accurate means of measuring and predicting macropore activation will be implemented by combining macropore survey data, spatial survey data, and discharge measurements to model each of the five study sites within hydraulic modeling software.

Bank storage experiment results suggest that macropores increase rates of bank storage and therefore hyporheic exchange. However, more data collection and analysis is necessary to confirm these effects and quantify their magnitude and any temporal variation.

Acknowledgements

I would like to extend the utmost of thanks to Garrett Menichino for allowing me to participate in his doctoral research and for his mentorship regarding the execution of research and the presentation of its results through the duration of the REU program. Similarly, I'd like to recognize and express my gratitude for Dr. Erich Hester's advisement throughout the process of preparing both a presentation of my project to my peers as well as a research paper for submission to the National Science Foundation. I would also like to express my appreciation for Dr. Lohani and Virginia Tech for hosting and giving me the opportunity to partake in the 2012 NSF/REU Interdisciplinary Water Sciences and Engineering Program. We acknowledge the support of the National Science Foundation through NSF/REU Site Grant EEC-1062860. Any opinions, findings, and conclusions or recommendations expressed in this paper are those of the author(s) and do not necessarily reflect the views of the National Science Foundation.

References

Arrigoni, A.S., G.C. Poole, L. A. K. Mertes, S. J. O'Daniel, W. W. Woessner, and S. A. Thomas, 2008. Buffered, lagged, or cooled? Disentangling hyporheic influences on temperature cycles in stream channels. Water Resources Research, 44: 1-13.

Benhardt, E.S., et al., 2005. Synthesizing U.S. River Restoration Efforts. Science, 308: 636-637.

Boulton, A.J., S. Findlay, P. Marmonier, E.H. Stanley, and H.M. Vallett, 1998. The Functional Significance of the Hyporheic Zone in Streams and Rivers. Annual Review of Ecology and Systematics, 29: 59-81.

Brunke, M. and T. Gosner, 1997. The ecological significance of exchange processes between rivers and groundwater. Freshwater Biology, 37(1): 1-33.

Franklin, D. H., L. T. West, D. E. Radcliffe, and P.F. Hendrix, 2007. Characteristics and Genesis of Preferential Flow Paths in a Piedmont Ultisol. Soil Science Society of America Journal,71(3): 752-758.

Hester, E.T., M.N. Gooseff, 2010. Moving Beyond the Banks: Hyporheic Restoration Is Fundamental to Restoring Ecological Services and Functions of Streams. Environmental Science and Technology, 44(5): 1521-1525.

Luo, L., H. Lin, and J. Schmidt, 2012. Quantitative Relationships between Soil Macropore Characteristics and Preferential Flow and Transport. Soil Science Society of America Journal, 74(6): 1929-1937.

Sawyer, A. H., M.B. Cardenas, A. Bomar, and M. Mackey, 2009. Impact of dam operations on hyporheic exchange in the riparian zone of a regulated river. Hydrological Processes, 23: 2129-2137.

Applications of Molecular Tools For Exploration of Microbial Community Structure and Function at the Bemidji, Minnesota Oil Spill Site

Zach Bailey*, Dr. Nicole Fahrenfeld**, Dr. Amy Pruden**

** NSF-REU fellow, Virginia Polytechnic Institute and State University*
(Home Institution: Civil Engineering, University of Maryland- Baltimore County*)*
***Department of Civil and Environmental Engineering, Virginia Polytechnic Institute and State University*

ABSTRACT

The Bemidji Minnesota terrestrial oil spill research site has provided the unique opportunity to study the fate and impacts of petroleum hydrocarbons in groundwater. While research to date has primarily focused on geochemical understanding of the spill, the goal of this project was to gain a better understanding of the microbial community structure and function involved in oil biodegradation. Several molecular tools were applied including Polymerase Chain Reaction (PCR), Denaturing Gradient Gel Electrophoresis (DGGE), and Real-Time Polymerase Chain Reaction (qPCR). Samples were examined from *in-situ* microcosms, with different electron accepting conditions, to characterize population and functional changes with time. Aquifer sediment cores from different regions of the plume and sampled at various depths were also investigated to explore microbial heterogeneity at the site with respect to depth and dominant electron accepting conditions. Cluster analysis of DGGE fingerprints of aquifer sediment cores illustrated significant changes in the microbial community structure imposed by different electron accepting regions of the oil plume, but not with depth. DGGE of *in-situ* microcosms comparing methane and nitrate as electron acceptors for hydrocarbon degradation revealed significant changes in microbial population only in the microcosms treated with nitrate. Community function was investigated by screening for several functional genes involved in the anaerobic degradation pathway of aromatic compounds found in crude oil. This work compliments geochemical work done by the USGS and will inform remediation efforts at current and future oil spill sites.

Keywords: Oil, BTEX, Microbial Ecology, Bemidji, PCR, DGGE, Biodegradation

Introduction

Background

In August of 1979, near Bemidji Minnesota, a high-pressure crude-oil pipeline burst releasing 10,700 barrels of oil (Essaid et al., 2012). The oil percolated through the unsaturated zone to the water table where it formed three subsurface oil bodies (Figure 1). Remediation efforts began with pumping the oil from the subsurface pools and excavating the soil (Essaid et al., 2012). Approximately 8,100 barrels were removed within the next year. However, due to financial constraints and lack of efficiency, clean up efforts were stopped leaving 2,500 barrels of oil on the water table (Essaid et al., 2012). The remaining oil is now subject to extensive scientific research and observation. Scientists have investigated hydrology (Bennet

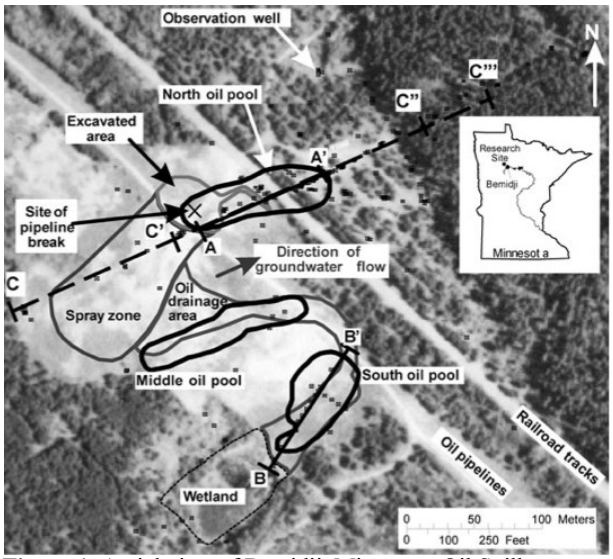

Figure 1. Aerial view of Bemidji, Minnesota Oil Spill**. (USGS, 2001)**

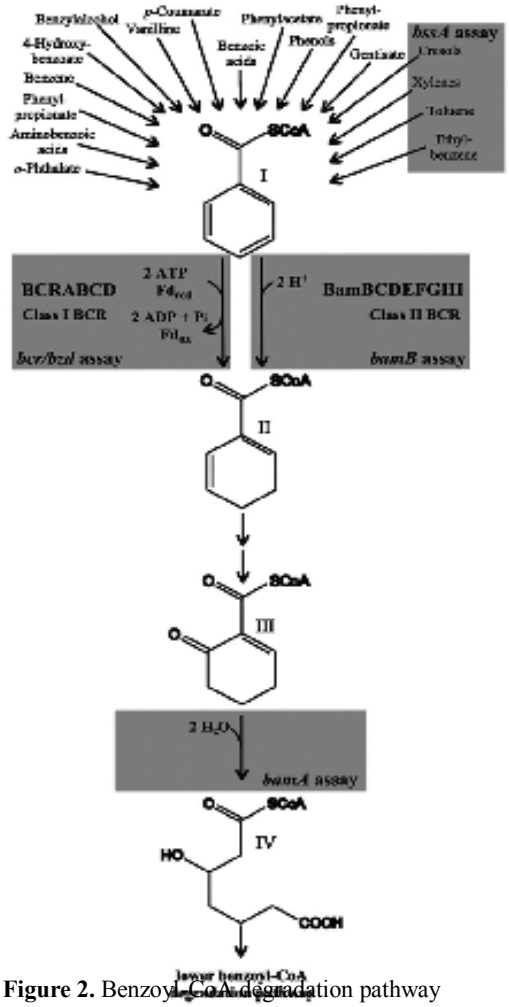

Figure 2. Benzoyl-CoA degradation pathway (Kuntze et al., 2011)

et al., 1993) geochemical interactions (Cozzarelli et al., 1994b), microbial population (Bekins et al., 2001) and biodegradation (Cozzarelli et al., 1994a)

In the summer of 2010, collaborators at the USGS performed *in-situ* microcosms to study natural attenuation processes. These microcosms minimized disturbance of microbial population, maintained geochemical integrity and targeted one redox zone. The study found that benzene and ethylbenzene begin degrading only after toluene was depleted in the iron-reducing sediment, but degraded before toluene and much quicker under methanogenic conditions. Thus leading to the conclusion that the methanogenic wetlands were better adapted to degrade benzene and toluene (Cozzarelli, personal communication).

Petroleum fuels contain toxic hydrocarbons including, benzene, toluene, xylene, and ethylbenzene (BTEX). Once released in terrestrial environments, these compounds pose challenges to remediation through sorption processes and low solubility (Cozzarelli, personal communication). Natural attenuation often becomes the most effective remediation process. This process occurs when microorganisms facilitate the degradation of crude oil and its toxic components. The biodegradation process of BTEX is not yet completely understood, but significant insight has been obtained from the Bemidji site. BTEX is particularly challenging to degrade under anaerobic conditions.

Figure 2 shows a common anaerobic biodegradation pathway of BTEX hydrocarbons, the benzoyl coenzyme A (CoA) degradation pathway (Kuntze et al. 2011). The reductive dearomatization can be catalyzed by class I or class II benzoyl-CoA reductases (BCR). Class I BCRs are dependent on ATP and encoded by *bcr*C and *bzd*N while class II BCRs are ATP-independent and encoded by *bam*B. The final ring cleavage is controlled by the expression of the *bam*A gene that codes for the ring-cleaving hydrolase (Kuntze et al., 2011) Quantification of *bcr*C, *bzd*N, *bam*A, and *bam*B will be performed. Key functional genes related to methanogenesis (*mcr*A) will also be quantified to help define electron accepting conditions within the plume (Pereyra, 2010). These assays will provide insight into microbial community function throughout the plume and across time for *in-situ* microcosm experiments. .

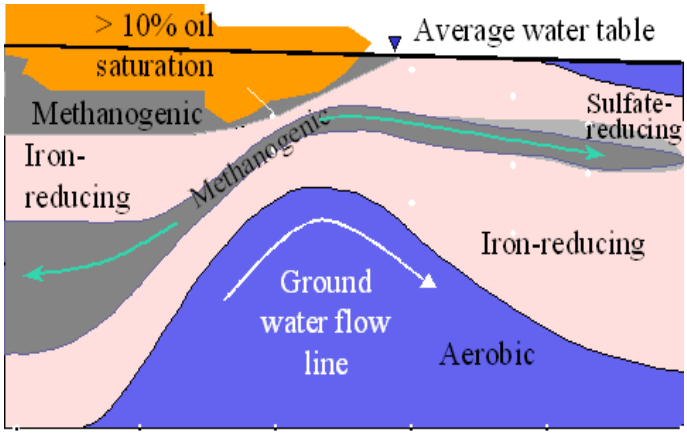

Figure 3. Geochemical zones of the Bemidji oil plume (USGS, 2001)

Five distinct geochemical zones of the plume below the water table have been identified (Baedecker et al. 1989, 1993; Bennett et al. 1993). These zones differ by availability of electron acceptors, which has been shown to affect degradation rates (Cozzarelli, personal communication). Methanogenic and iron-reducing regions have been defined for the Bemidji plume. The methanogenic region is anoxic and the contaminating hydrocarbons serve as the electron acceptor. The iron reducing regions have ferric iron available as a

terminal electron acceptor. Biodegradation of petroleum hydrocarbons in oxic environments is generally quicker than in anoxic environments, due to role of monooxygenases in BTEX ring cleavage (REF). However, research has shown that biodegradation in anoxic conditions can remove substantial amounts of hydrocarbons from the groundwater (Baedecker et al. 1993; Eganhouse et al. 1993; Cozzarelli et al., 1994).

Despite previous work, little is known about microbial structure and function throughout an oil plume and how it pertains to BTEX biodegradation rates. Samples were taken from *in-situ* microcosms and aquifer sediment cores. The *in-situ* microcosms will provide information of the degradation of BTEX with time while the cores will illustrate population and function variation with depth.

The goal of this project is to gain an understanding of the microbial community structure and function and the changes within different regions and depths of the plume. Molecular tools will be applied to investigate changes with time in sediments taken from the *in-situ* microcosms. This research, and collaborative efforts from the USGS, are relevant to current and future oil spill remediation efforts.

Research Methods

Sample Collection

The *in-situ* microcosm samples were provided by the USGS. *In-situ* microcosms were performed in the wetland (methanogenic) region of Bemidji, which was potentially subject to spray during the oil spill but currently has no contamination. Wetland sediment was collected by coring, homogenized, and packed in Teflon sleeves to allow for sediment collection after microcosm sacrifice. The microcosm consisted of a stainless steel cylindrical body that was open at the end to allow it to fill with aquifer sediment. The body of the microcosm isolated a volume of soil for the push-pull test and held the Teflon soil sleeves in contact with aquifer sediments. The top of the microcosm had a sampling port that extended down into the test chamber. The microcosms were installed and allowed to equilibrate for 6 days. BTEX solution was prepared using Bemidji groundwater with either no electron acceptor addition (M samples) or with nitrate as the electron acceptor (N samples). BTEX solution was injected into the microcosm test chamber and periodically sampled. Samples were also taken of sediment before experiment (To). Microcosms were periodically sacrificed and Teflon bagged sediment was retrieved and frozen until analysis, these samples served as controls. BTEX and geochemical analyses were performed by USGS.

The aquifer sediment cores were collected using direct push technology (i.e. Geoprobe) in sterile acetate liners. Cores were cut into 3ft sections in field, capped with rubber caps, taped to preserve anaerobic conditions, and frozen until sampling. Cores were taken near well 423 known methanogenic, and near well 1101 iron-reducing regions. Two iron-reducing cores were taken, one was contaminated with oil, the other was in the same region but not contaminated. A fourth core was taken from the wetland area (Figure 1) using a hand corer. This core served as a control because the wetland provides a naturally anaerobic environment.

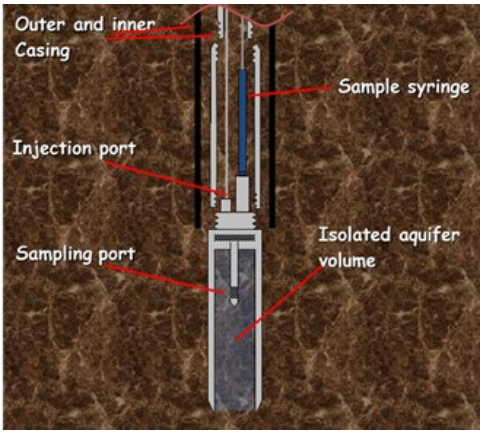

Figure 4. Diagram of in-situ microcosm (Cozzarelli, personal communication)

Upon receipt in the laboratory, cores were sampled in duplicate at various depths, targeting regions with varying particle sizes.

DNA was extracted using a FastDNA SPIN Kit for Soil (MP Biomedicals, Solon, OH) according to the manufacturer's instructions.

After comparing PCR efficiencies of several dilutions of select samples, a 1:100 dilution of DNA extract was found to minimize PCR inhibition for *in-situ* microcosm samples. A 1:110 dilution of DNA extract was chosen for aquifer sediment core samples. Both were respectively implemented in all downstream analyses.

Community Structure Analysis

A nested PCR was performed using this PCR product as template to obtain PCR product suitable for DGGE. Total bacterial population was amplified by16S rRNA PCR using forward primer 8f and reverse primer 1492r ((Weisburg et al. 1991)). PCR was performed using an GenScript Taq kit in a 25 µL reaction volume. The PCR conditions following were used: 3 min at 95°C and 35 cycles of 30 s at 95°C; 30 s at 50°C; 90 s at 72°C and 10 min at 72°C. The following PCR conditions were used with a 25 µL reaction mixture and 341GC/533r primers: 2 min at 94°C and 2 cycles of 15 s at 94°C; 15 s at 52°C; 20 s at 72°C and 2 cycles of 15 s at 94°C; 15 s at 51°C; 20 s at 72°C and 2 cycles of 15 s at 94°C; 15 s at 50°C; 20 s at 72°C and 2 cycles of 15 s at 94°C; 15 s at 49°C; 20 s at 72°C and 2 cycles of 15 s at 48°C; 15 s at 52°C; 20 s at 72°C and 40 cycles of 15 s at 94°C; 15 s at 47°C; 20 s at 72°C and 7 min at 72°C. Product from each PCR reaction was validated on 1.2% agarose gel at 110V for 20 minutes and documented using a Gel Doc XR system (BioRad).

The bacterial community was characterized by DGGE. DGGE was performed using D Code system (Bio-Rad, Hercules, CA). The gels were prepared using 8 % acrylamide with a denaturing gradient form 35 to 55 % for ISMs and 35-65% for cores and electrophoresed at 50 V for 18 h. The gels were stained with 1X SYBR Gold (Molecular Probes) and documented as described above. Bands of interest were excised, placed in 36 µL ddH2O, amplified with PCR using 341GC/533r, and sequenced by the Virginia Bioinformatics Institute (VBI) (Blacksburg, VA).

DGGE fingerprints were digitized using Quantity One software (Bio-Rad). A cluster analysis was performed with PRIMER6 software (Prime E, United Kingdom).

Community Function Analysis

PCR was performed to detect *bam*A, *bam*B, *bcr*C, and *bzd*N. Primers and thermocycler conditions were obtained from Kuntze et al. (2011). A 25 µL reaction mixture of Evagreen (## Concentration), primers (final Concentration ##), and 1µL sample provided product. A temperature gradient was run to find ideal annealing temperature for each primer pair.

PCR product was cloned using the TOPO TA Cloning Kit for Sequencing (Invitrogen, Carlsbad, CA). Clones (20 per reaction) were randomly selected for analysis . A restriction digest was performed using restriction enzyme *MspI*. Unique samples were purified with ExoSAP-IT (Affymetrix, Santa Clara, CA) to eliminate excess primers and dNTPs. Sequencing was performed as described above to ensure specific priming. Sequencing results were analyzed with FinchTV software and Basic Local Alignment Search Tool (BLAST).

Upon confirmation of correct product, qPCR was performed on *in-situ* microcosm and aquifer sediment core samples for each primer with the addition the *mcr*A gene. PCR inhibition was minimized at a 1:50 dilution for *in-situ* microcosm samples, and at 1:10 for aquifer sediment core samples. All qPCR standard curves were constructed from serial dilutions of cloned genes ranging from 10^8 to 10^2 gene copies per µL. qPCR cycle conditions were as described by Singh et al (2011). Samples were analyzed in triplicate.

Results

In-situ Microcosms-Community Structure Analysis

DGGE analysis of *in-situ* microcosm samples showed a complex array of bands, which is indicative of a diverse community. Cluster analysis of band intensity obtained from the DGGE fingerprint of the *in-situ* microcosm, illustrated differences in microbial structure between treatments but little changes over time (Figure 5.).

Figure 5 illustrates no differences between control and no treatment microcosms. This is important because it demonstrates that the added treatments to the microcosms do not affect the microbial community.

The cluster analysis results show microbial community structural differences between methanogenic and nitrate treatments, each of which are significantly different from the control treatment, but not the groundwater treatment. Differences in the microbial community between treatments are expected given the difference in electron accepting conditions. These results can potentially account for the differences observed in biodegradation rates of benzene and toluene in the methanogenic and nitrate treatment by Cozzarelli et al. (2011)

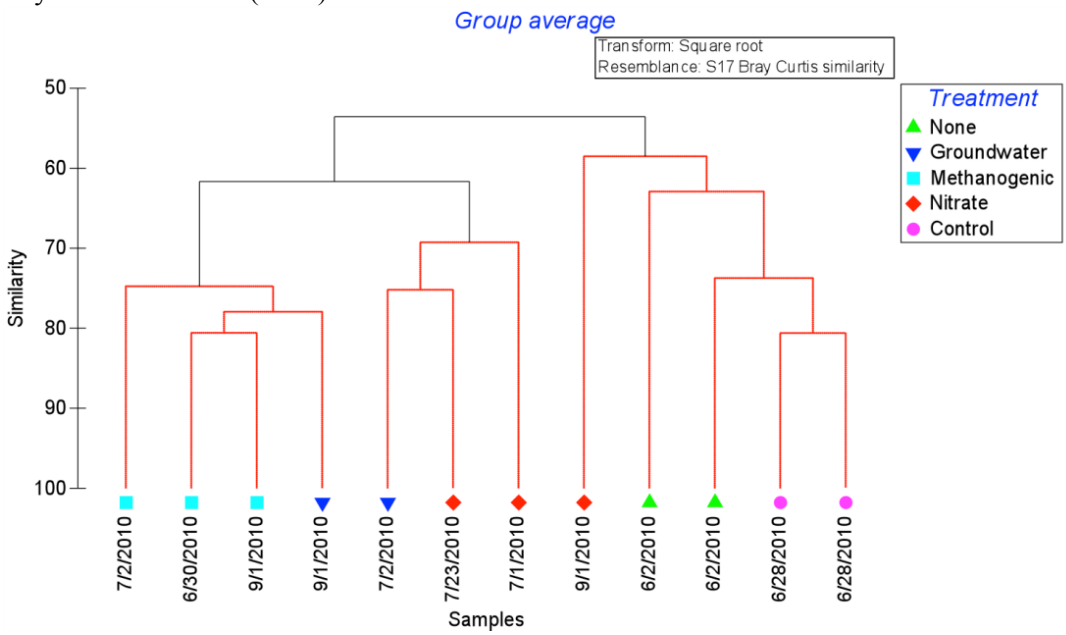

Figure 4. Cluster Analysis of DGGE of *in-situ* microcosm samples

No significant changes were detected in community structure with time during the sampling time period, except in nitrate conditions. The groundwater (blue triangles) replicate microcosms clustered separate from one another and from initial conditions, indicating either a change with time or that structural differences observed across treatments were similar to spatial variation. The final nitrate sample was most similar to the initial conditions suggesting the microcosm underwent a change from nitrate stimulated to the initial conditions. This could be a result of the nitrate being consumed by natural attenuation resulting in a return to the structure prior to contamination.

In-situ Microcosms- mcrA Analysis

qPCR assays were prepared to quantify the presence of known methanogenic genes. *mcr*A genes were detected in all of the *in-situ* microcosm samples. To compare between samples, *mcr*A gene copies were normalized to 16S gene copies. Figure 6 shows the normalized gene copies as it changes with time and sample treatment. Data has been arranged to emphasize changes with time within a given region of the plume.

Day 1 represents the installment of the *in-situ* microcosms (Figure 6). Injections of BTEX and BTEX with Nitrate into respective microcosms were made on day 27. The control samples of day 26 were taken while the microcosm was still open, equilibration with the surroundings. The latter control samples were taken after the microcosms were closed on the 27th day.

The control microcosm samples show a significant decrease in *mcr*A gene numbers over the course of the two-month experiment. Samples treated with BTEX and no electron acceptor show increased methanogensis gene copies from days 28 to 91. The methanogenic samples increased at a rate of 0.1894 normalized *mcr*A gene copies per day, while the nitrate treatment samples showed a negligible decrease of 0.0224 normalized gene copies per day. With a negligible decrease detected, the microcosms with nitrate available as an electron acceptor were assumed to show constant levels of gene copies over the course of the experiment. This is expected, as nitrate is energetically favorable terminal electron acceptor to BTEX compounds.

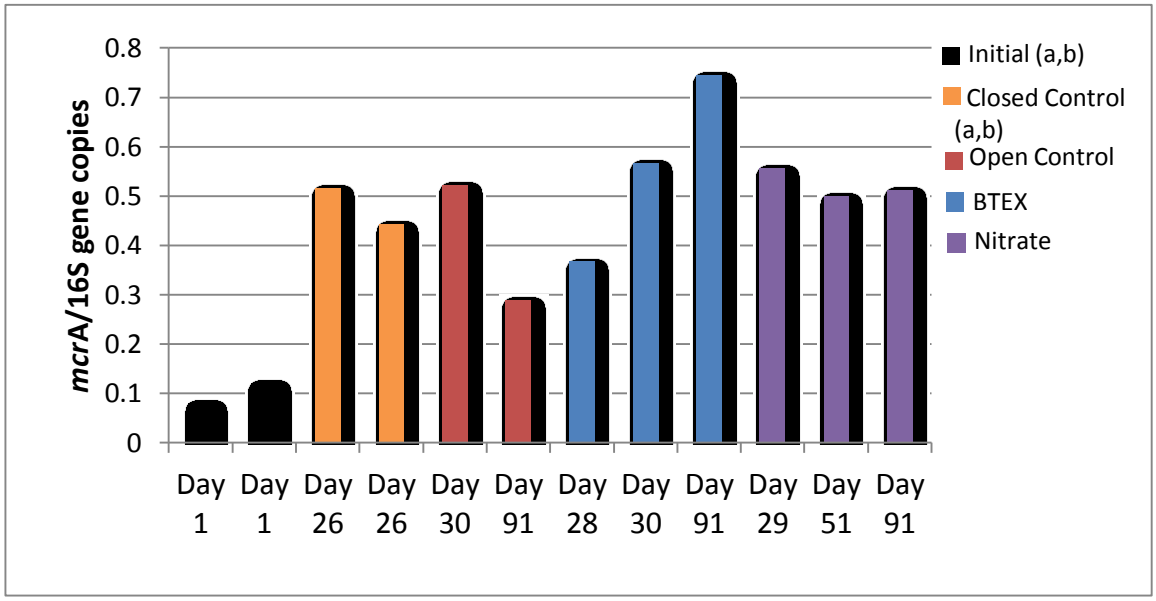

Figure 5. Normalized *mcr*A gene copies to 16s gene copies detected *in-situ* microcosm samples. (a and b denote replicates of the same sample).

Aquifer Sediment Cores- Community Structure Analysis

DGGE analysis of iron-reducing samples (Figure 7) shows a diverse microbial community. No significant differences were observed with depth or with various degrees of contamination However, DGGE is biased towards dominant community members and it is possible that deep sequencing could provide adequate sensitivity to discern structural differences with depth and particle size.

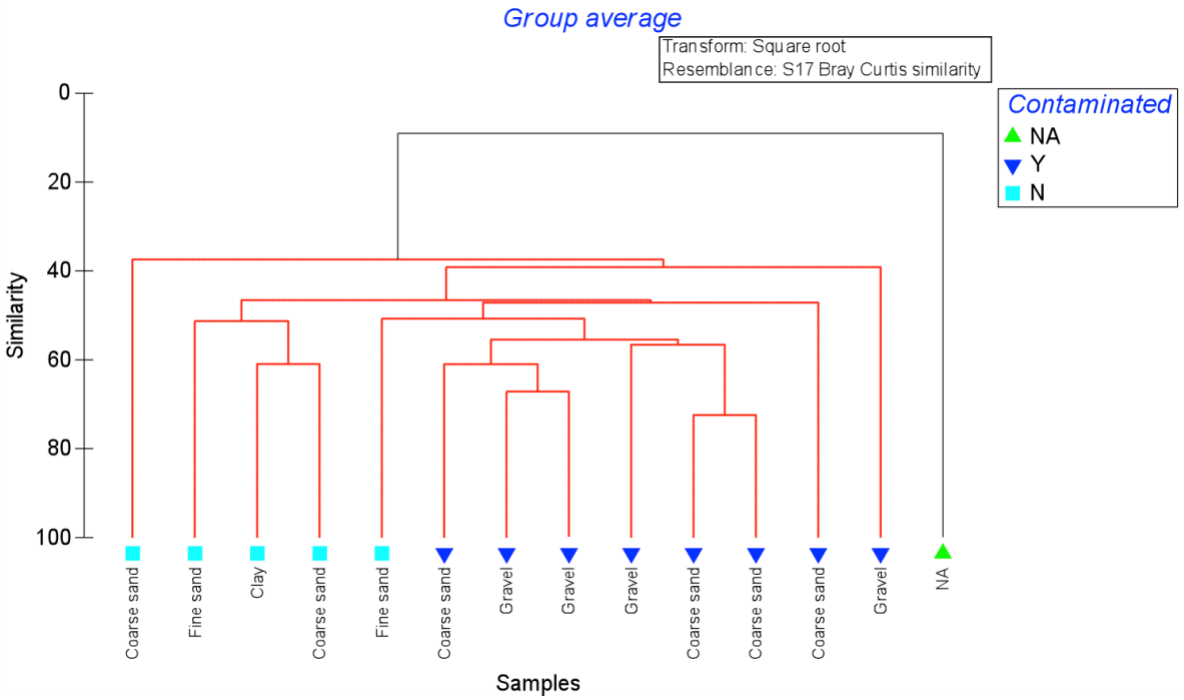

Figure 7. Iron Reducing Cluster Analysis of Aquifer Sediment Core

Cluster analysis (Figure 8) of aquifer sediment cores in the wetlands and methanogenic regions revealed three significantly different clusters. Wetland samples formed two clusters that were significantly different from one another and from the methanogenic core. Thus, despite the fact that both the wetland and methanogenic cores are under methanogenic conditions, the bacterial community structures are significantly different. This indicates that availability of natural organic carbon (greater in the wetland) may be the driver.

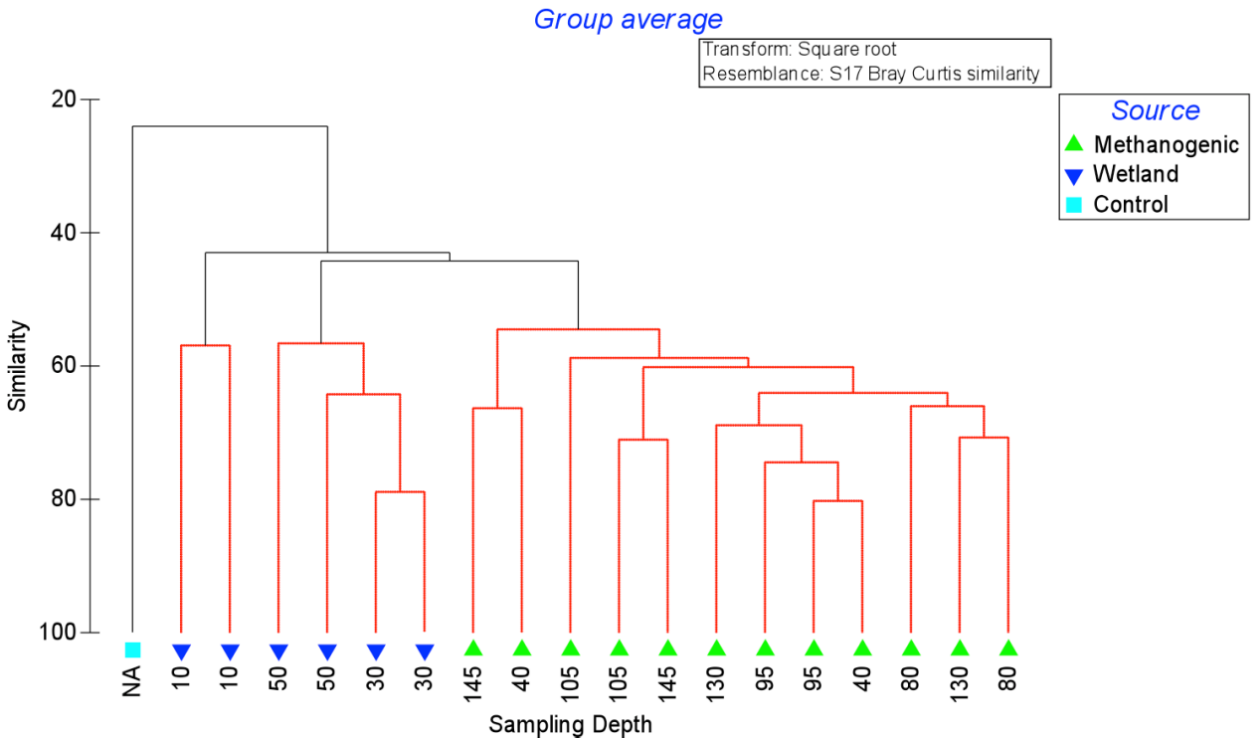

Figure 8. Cluster Analysis of Aquifer Sediment Core taken in the methanogenic and wetland regions of the oil plume at various depth (cm)

Figure 8 also illustrates differences within the wetland core as a function of depth. From 10 cm to 30 cm below beginning of the core (core began 4 feet and 2 inches below the surface), the community changes significantly. However, from 30-50 cm the community is similar. This trend is unique to the wetland environment, as no trends with depth were observed in the methanogenic or iron reducing regions. This may be a result of the natural stratification of the sediment causing differences in conditions at different depths in the wetland region. We may not see these differences in the methanogenic and iron reducing regions, as the oil contamination could be very influential on the microbial population. Also, the areas of the wetlands closer to the surface may be exposed to O_2 stratification that would allow create a more favorable electron accepting environment.

Aquifer Sediment Cores- mcrA Analysis

Normalized detection of *mcr*A gene copies in the aquifer sediment core samples are shown below in Figure 9. No obvious trend is immediately apparent. An obvious peak appears in the methanogenic region but significant copies of the *mcr*A gene are seen in the iron reducing region as well. Sample 2, a wetland sample, should be excluded from analysis due to experimental error.

This data will be analyzed further for trends with depth within each region and significant differences between each region.

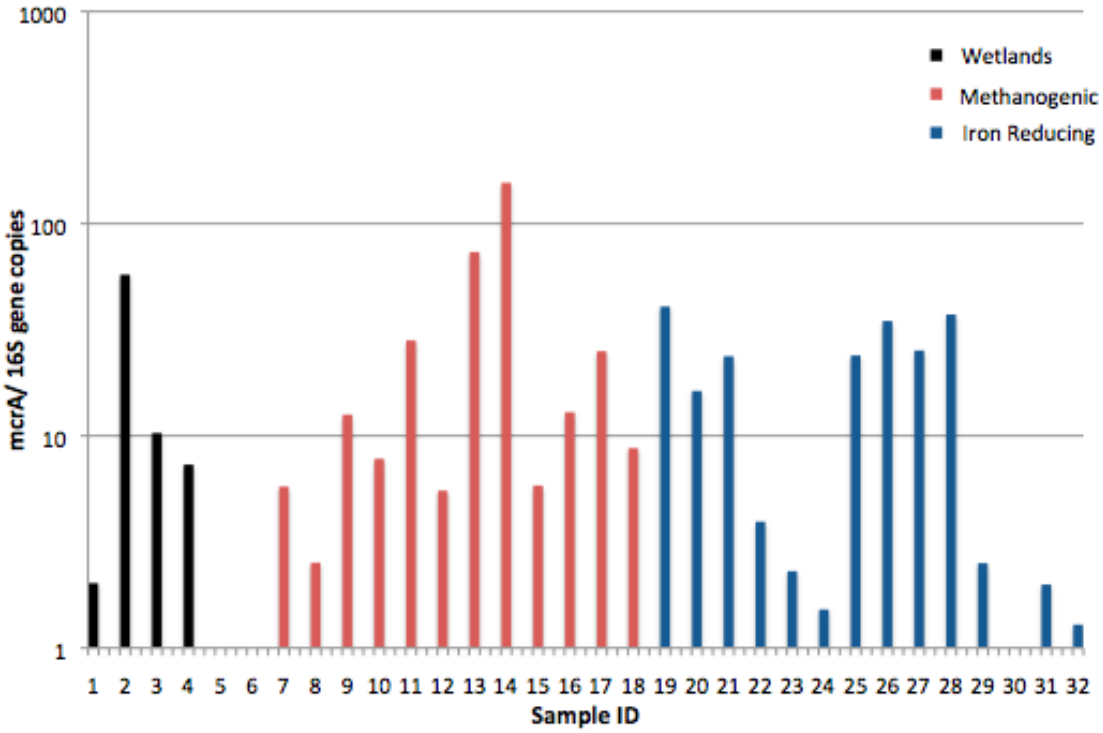

Figure 9. Normalized *mcr*A gene detection in core samples

BTEX Functional Analysis

Progress has been made in analyzing microbial function in the benzoyl-CoA degradation pathway but sequencing results have been obtained for only *bcr*C thus far.

Table 1. Blast Analysis of *bcr*C product

Sample ID	Accession	Bacteria	Gene	Coverage
C4	CP000283.1	*Rhodopseudomonas palustris* BisB5, complete genome	Benzoyl-CoA reductase gamma subunit	96%
I3	CP001281.2	*Thauera* sp. MZ1T, complete genome	Benzoyl-CoA reductase subunit C	94%
I4	CP002418.1	*Rhodopseudomonas palustris* DX-1, complete genome	Benzoyl-CoA reductase subunit C	85%
I5	CP000463.1	*Rhodopseudomonas palustris* BisA53, complete genome	Benzoyl-CoA reductase gamma subunit	98%

Table 1 lists sequencing results from cloning PCR product and demonstrates that specificity of the primers to benzoyl-CoA reductase gene. Results showed high sequence similarity to *bcr*C genes in 3 strains of *Rhodopseudomonas palustris* and one *Thauera* sp. bacteria. This is the gene that we had hoped to isolate and therefore we are able to conclude specific priming and correct function of the primers. This validation was made by comparison of phylogeny observed by Kuntze et al (2011). Analysis of clones from *bzd*N, *bam*A, and *bam*B are in progress.

Conclusions

This work provides new insight into the microbial community structure and function within different regions, depths, and times at the Bemidji, Minnesota terrestrial oil spill site. Cluster analysis of a DGGE of *in-situ* microcosm samples shows the microbial population is significantly different between different electron accepting conditions of the oil plume. No significant changes with time were detected within the sediment treated with BTEX without addition of electron acceptor. However, *in-situ* microcosms biostimulated with nitrate demonstrate community shifts with time to ones more similar to the microbial community before contamination. This observation is most likely a result of the depletion of the amended nitrate electron acceptor. Quantification of methanogenesis, measured by *mcr*A gene copies, demonstrated differences under certain conditions with respect to time. While the closed control showed a decrease in methanogens over the sampling period, we observed an increase under methanogenic conditions and no change in the presence of nitrate as an electron acceptor. This is as expected given that nitrate is energetically favorable electron acceptor, and it may also have been toxic to methanogens.

Cluster analysis of a DGGE of the aquifer sediment core samples shows microbial community differences between oil plume regions, which are consistent with *in-situ* microcosm sample analyses. Specifically, we are able to conclude that microbial community at the Bemidji oil spill site differs significantly between the wetlands, methanogenic and iron-reducing regions. The analysis shows detectable differences with depth in the wetland. However, we see no detectable differences with depth in the methanogenic or iron-reducing regions of the oil plume.

While this work provides some information about the microbiology of the oil plume, further research is required. DGGE band sequences of *in-situ* microcosm and aquifer sediment core samples should be identified using the BLAST tool. Products of the functional primers involved in the BTEX degradation process should be sequenced and analyzed. Once specific priming is verified, all samples can be screened for the presence of *bam*A, *bam*B, *bzd*N and *bcr*C. Further analysis of *mcr*A presence in aquifer sediment cores should be made. Further information about the microbial community structure and function will provide a greater understanding of the anaerobic biodegradation of BTEX and can be potentially relevant to aide in current and future bioremediation efforts.

Acknowledgements

We acknowledge the support of the National Science Foundation through NSF/REU Site Grant EEC-1062860. Any opinions, findings, and conclusions or recommendations expressed in this paper are those of the author(s) and do not necessarily reflect the views of the National Science Foundation.

I acknowledge Dr. Nicole Fahrenfeld for her continuous guidance and support throughout this project. I am very thankful for the laboratory experience and valuable insight into graduate research.

I acknowledge Dr. Amy Pruden for the guidance and her instrumental role in making this opportunity possible. I am very appreciative of the advice on graduate school and career options she has provided.

I acknowledge all of Dr. Amy Prudens lab members for their help around the lab and constructive feedback on my project and presentation.

I acknowledge Dr. Lohani for all his hard work into organizing and overseeing the 2012 Interdisciplinary Water Sciences and Engineering NSF/REU.

I acknowledge all the 2012 Interdisciplinary Water Sciences and Engineering REU fellows for the support and experiences.

References

Baedecker, M.J., Cozzarelli, I.M., Eganhouse, R.P., Siegel, D.I., and Bennett, P.C., 1993, Crude oil in a shallow sand and gravel aquifer 3: Biogeochemical reactions and mass balance modeling in anoxic groundwater, Applied Geochemistry, v. 8, p. 569-586.

Bekins, Barbara A., Isabelle M. Cozzarelli, Michael E. Godsy, Ean Warren, and Hedeff I. Essaid. "Progression of natural attenuation processes at a crude oil spill site: II. Controls on spatial distribution of microbial populations." *Journal of Contaminant Hydrology* 53 (2001): 387-406. Web. 26 July 2012.

Bennett, P.C., Siegel, D.I., Baedecker, M.J., and Hult, M.F., 1993, Crude oil in a shallow sand and gravel aquifer: I. Hydrogeology and inorganic geochemistry, Applied Geochemistry, v. 8, p. 529-549.

Cozzarelli, I.M., Baedecker, M.J., Fischer, J., and Phinney, C.S., 1994, Ground-water contamination by petroleum hydrocarbons: Natural biodegradation in a dynamic hydrologic and geochemical system, American Chemical Society, Washington, D.C. [Proceedings] August 21-26, 1994.

Cozzarelli, I.M., Baedecker, M.J., Eganhouse, R.P., and Goerlitz, D.F., 1994, The geochemical evolution of low-molecular-weight organic acids derived from the degradation of petroleum contaminants in groundwater: Geochemical et Cosmochimica Acta, v. 58, p. 863-877.

Eganhouse, R.P., Dorsey, T.F., Phinney, C.S., and Westcott, A.M. 1996, Processes affecting the fate of monoaromatic hydrocarbons in an aquifer contaminated by crude oil: Environmental Science & Technology, v. 30, no. 11, p. 3304-3312..

Essaid, Hedeff I., Barbara A. Bekins, William N. Herkelrath, and Geoffrey N. Delin. "Crude Oil at the Bemidji Site: 25 Years of Monitoring, Modeling, and Understanding." *Ground Water* 49.5 (2009): 706-26. Web. 26 July 2012.

Fahrenfeld, Nicole, Jeffrey Zoeckler, Mark A. Widdowson, and Amy Pruden. "Effect of biostimulants on 2,4,6-trinitrotoluene (TNT) degradation and bacterial community composition in contaminated aquifer sediment enrichments." 10 Jan. (2012). Web. 26 July 2012.

Kuntze, Keven, Carsten Vogt, Hans-Herman Richnow, and Matthias Boll. "Combined Application of PCR-Based Functional Assays for the Detection of Aromatic-Compound-Degrading Anaerobes." *Applied Environmental and Microbiology*77.14 (2011). Print.

Li, Y., Porter, A., Mumford, A., Zhao, X., & Young, L. (2012). Bacterial community structure of and *bam*A gene diversity in anaerobic degradation of toluene and benzoate under denitrifying conditions. *Journal of Applied Microbiology*, *112*(2), 269–279.

Ma, Yanjun, Christopher A. Wilson, John T. Novak, Rumana Riffat, and Sebnem Aynur. "Effect of Various Sludge Digestion Conditions on Sulfonamide,Macrolide, and Tetracycline Resistance Genes and Class I Integrons." *Environmental Science & Technology* 454 Aug. (2011): 7855-61. Web. 26 July 2012.

Pereyra, L P., S R. Hiibel, M V. Prieto Riquelme, K F. Reardon, and A Pruden. "Detection and Quantification of Functional Genes of Cellulose-Degrading, Fermentative, Sulfate-Reducing Bacteria, and Methanogenic Archaea." *Applied Environmental Microbiology* Feb. (2010). Web. 6 Aug. 2012. <http://aem.asm.org/content/early/2010/02/05/AEM.01285-09.full.pdf>.

Rooney-Varga, Juliette N., Robert T. Anderson, Jocelyn L. Fraga, David Ringelberg, and Derek R. Lovely. "Microbial Communities Associated with Anaerobic Benzene Degradation in a Petroleum-Contaminated Aquifer." *Applied and Environmental Microbiology* 65.7 (1999). Web. 26 July 2012.

Singh, Gargi, Amy Pruden, and Mark A. Widdowson. "Influence of Petroleum Deposit Geometry on Local Gradient of Electron Acceptors and Microbial Catabolic Potential." *Environmental Science & Technology* 4610 May (2012): 5782-88. Web. 26 July 2012.

USGS. *Bemidji Crude-Oil Spill*. N.p., 2001. Web. 26 July 2012. <http://water.usgs.gov/nrp/organic/bemidji.htm>.

Weisburg W, Barns S, Pelletier D, Lane D (1991) 16S ribosomal DNA amplification for phylogenetic study. J Bacteriol 173 (2):697-703

Hot Water Recirculating System Design: Effects on Water Quality Parameters Affecting Premise Plumbing Pathogen Growth

Josh Caldwell*, William J. Rhoads**, Dr. Marc Edwards**

** NSF-REU fellow, Virginia Polytechnic Institute and State University*
(Home Institution: Agriculture and Environmental Sciences, University of Georgia)
***Department of Civil and Environmental Engineering, Virginia Polytechnic Institute and State University*

ABSTRACT

The most common source of waterborne disease in developed countries arise from opportunistic premise plumbing pathogens (OPPPs), which pose special challenges because they grow (amplify) in building plumbing systems beyond the jurisdictional reach water treatment authorities. Hot water heater system design can significantly affect water quality parameters associated with OPPP growth. For instance, pipe orientation and hot water heater temperature settings can affect temperature stratification, disinfectant residual concentrations, and mixing rates within a model hot water heater system. Upward oriented pipes developed temperature gradients that promoted internal mixing even during stagnation events, and had temperatures 7° - 22°C hotter at thermal steady-state than did downward oriented pipes which did not mix (water heater set point 40°C - 66°C). The internal mixing maintained higher disinfectant residuals (up to 0.4 pmm) in upward oriented pipes when compared to downward oriented pipes after 24 hours of stagnation at 48°C. Tracer studies confirmed relatively rapid exchange of water from distal upward facing pipes (64% exchange in 24 hours) versus no exchange of water after 4 days in downward facing pipes.

Keywords: Hot water heater, recirculating system, premise plumbing, pathogens

Introduction

The advent of modern water treatment technology has significantly decreased public health risks from traditional waterborne pathogens in potable water (WSTB, 2006). The largest source of waterborne disease from potable water are now bacteria known as opportunistic premise plumbing pathogens (OPPPs); specifically, *Legionella pneumophila* has been identified as the most common OPPP known to cause illness. There are 8,000 – 18,000 cases of Legionnaires' Disease annually (CDC, 2008). Additionally, other notable OPPPs like *Naeglaria fowleri*, *Mycobacterium avium* complex, and *Acanthamoeba* cause thousands of infections annually (Pruden et al., Water Research Foundation, 2012 - in progress). Studies indicate that in the United States (U.S.), *Legionella* can colonize residential water supplies, commercial and private buildings, hospitals, cooling towers, hotels, and spas (Lee et al. 1993; Flannery et al., 2006; Brennen et al. 1987; Hedges and Roser 1991; Borella et al., 2005; as cited in Williams et al., 2006). *Legionella* infection accounts for half of all reported drinking water disease outbreaks, and a fraction of *Legionella* outbreaks occurred as a result of plumbing system colonization (Yoder et al., 2008). There are several factors that can affect the growth of *Legionella* and other OPPPs including stagnation, pipe material, temperature, and disinfectant residual.

Variations in stagnation times within a building's plumbing are thought to have a profound effect on OPPP growth. Traditional knowledge dictates that stagnation in plumbing systems promotes OPPP populations in industrial settings (Ciesielski et al. 1984). Other research suggests that turbulent conditions can be beneficial to OPPP presence in biofilms of plumbing systems (Liu et al. 2004). Stagnation times in premise plumbing applications, residential or industrial, are typically much higher than in water distribution systems (Edwards et al., 2003). For example, in a typical residential setting, there are high water demands in the mornings and evening; however, during the day, there is a long stagnation time

while consumers are at work. Recommendations for installation of new HWH systems exclude deadlegs and other fixtures which promote stagnation (ASHRAE, 2011). According to this standard installation of recirculation HWH systems is also preferred when compared to non-recirculating systems in terms of preventing excessive stagnation.

Pipe materials can also affect OPPP populations in premise plumbing systems (Rogers et al., 1994; van der Kooij et al., 2005). Plumbing materials can react with disinfectants, causing accelerated decay as well as provide or inhibit delivery of important nutrients to microbes. Typical building plumbing materials include copper, cross-linked polyethylene (PEX), polyvinyl chloride (PVC), and chlorinated polyvinyl chloride (cPVC). Results of studies conducted to quantify the influence of pipe material on the occurrence of *Legionella* spp. have suggested that PEX and other elastomeric materials sustain the most *Legionella* spp. when compared with other plumbing materials (Rogers et al., 1994; van der Kooij et al., 2005) whereas copper pipes are thought to have an inhibitory effect on *Legionella* colonization (Zacheus and Martikainen, 1994; Leoni et al., 2005; Marrie et al., 1994; States et al., 1985, as cited from Williams et al., 2006). Conversely, iron pipes are generally recognized to promote *Legionella* colonization (Rogers et al., 1994); however, some other research suggests that iron presence is negatively correlated with *Legionella* growth (Borella et al. 2004).

Disinfectant type and concentration levels alter microbial populations in plumbing applications (Moore et al. 2006). Two secondary disinfectants are used for potable water applications, chlorine and monochloramine (EPA, 2009). Secondary disinfectants are applied to potable water to maintain disinfection as water travels through distribution systems. Monochloramine is a compound resulting from the combination of chlorine and ammonia. It became widely used after US EPA issued regulations on disinfectant by-products (Stage 1 Disinfectants/Disinfectant Byproducts Rule, EPA, 2003), as it produces less regulated by-products than chlorine; however, chlorine is still the most commonly used secondary disinfectant. Although maintaining a disinfectant residual is important to limit microbial re-growth potential, contrasting levels of 0.1 - 1.5 ppm (Thomas et al., 1999) and 2 – 6 ppm (Lin et al., 1998) free chlorine residual were found to be effective to reduce and control planktonic *L. pneumophila* as long as the residual levels are maintained in the system. *Legionella spp.* present in biofilm requires a much higher level of free chlorine for disinfection of >3ppm free chlorine for 24 hours (Muraca et al., 1987; Skaliy et al., 1980).

Disinfectant residuals can also be difficult to maintain in some systems. Both disinfectants decompose naturally, whereby the compounds slowly decay over time according to natural decay kinetics. Disinfectants can also react with pipes materials, which can drastically accelerate decay rates. For example, decay rate constants for reactions with ductile iron pipe walls for chlorine were an order of magnitude higher than bulk water decay rate constants (Rossman, 2006). Monochloramines are also affected by microbial decay, in the form of nitrification. Nitrifying bacteria oxidize the nitrogen in ammonia as an electron acceptor. Nitrifiers are present in much higher numbers in chloraminated water systems than chlorinated systems due to the excess ammonia bound in the chloramine disinfectant (Lipponen et al. 2002). Monochloramine is thought to better control occurrences of Legionnaires' Disease from premise plumbing pathogens (EPA, 2009). A study to quantify differences in OPPP presence after switching from chlorine to monochloramine found that presence of *Legionella* spp. was reduced 13.8%, while presence of *Mycobacteria* spp. was increased 21.3% (Pryor et al., 2004).

Water temperature within pipes can play a critical role in numerous aspects of premise plumbing performance, including microbial populations, corrosion and disinfectant decay rates. Thermal disinfection is a common means of eliminating OPPPs from HWH systems, and is recommended under ASHRAE guidelines to control *Legionella* (ASHRAE, 2011). Thermal disinfection is ideally achieved at temperatures >70ºC for short periods of time; at lower temperatures, more time is required to inactivate the bacteria. Temperatures within a typical HWH system fluctuate, depending on HWH system type, HWH temperature setting, pipe orientation, among other things. ASHRAE recommends that water temperature within a HWH system should not fall below 51ºC at any point for microbial control. On the other hand the US EPA recommends that HWH temperature settings remain at 48°C to reduce scalding potential, which will produce much lower temperatures throughout the system. Research has shown that

Legionella can grow from 20-50ºC, with an ideal growth range of 32-42ºC (Konishi et al., 2006; Yee and Wadowsky, 1982). This makes parts of HWH systems ideal for *Legionella* proliferation in terms of temperature under the EPA recommended scenario, but under the ASHRAE standard no part of the system would be in the ideal growth range.

Differences in HWH system design can be expected to influence the temperature profile, and by extension the microbial environment within the system. Pipe orientation with respect to HWH installation can drastically alter water temperatures inside pipes (Rushing and Edwards 2004). Pipes which are upward oriented above the HWH are subject to convective mixing within the pipe, due to the instability of having more dense (cooler) water on top of less dense (warmer) water. This causes convective mixing and warmer, more uniform temperatures in the upward oriented pipes. In the opposite scenario, in which the pipes are downward oriented with respect to the HWH recirculation line, the coldest, most dense water is at the bottom of the pipe and the warmer water is at the top, creating very stable stratification in which mixing is resisted.

Experimental Objective

The goal of this experiment was to examine the effects of hot water recirculating system design on key water quality parameters that influence OPPP growth. Specifically, the effects of pipe orientation on temperature, disinfectant residual and stagnant mixing rates were examined.

Materials and Methods

A model plumbing system was built to simulate conditions found in typical premise plumbing systems. A 20 gallon hot water heater (HWH) with a continuously recirculating system consisting of ¾ inch cPVC pipe was used in these experiments. The key design parameter evaluated was pipe orientation. There were eighteen 1.5 m long sample pipes, arranged into triplicates. Each pipe in each triplicate was separated by 7.6 cm with 61 cm between each set of triplicates. Three sets of three sample pipes were slanted upward and three sets of three pipes were slanted downward. Each sample pipe was equipped with a sample port at the end of the pipe for taking aliquot water samples and flow was regulated by ball valves. Influent water into the system was Blacksburg, VA tap water, containing approximately 2 ppm monochloramine disinfectant residual.

There were a series of HWH recirculating system orientations evaluated. In the first, the recirculating line branched off the top of the hot water heater, formed a loop, and fed back into the bottom of the hot water heater (referred to as "setup A"). Branched off of this main loop were two secondary pipes; one containing the three sets of triplicate upward slanted pipes and one with the three sets of triplicate downward slanted pipes (Figure 3.1). The second setup was identical to the first; however, there was a 1.2 meter section added to the secondary lines to minimize turbulent mixing near the main recirculating loop (referred to as "setup B"; Figure 3.2). The last configuration used the secondary lines in the first two setups as the recirculating line (Figure 3.3) to minimize the differences in each triplicate set as a function of distance away from the recirculating line ("setup C").

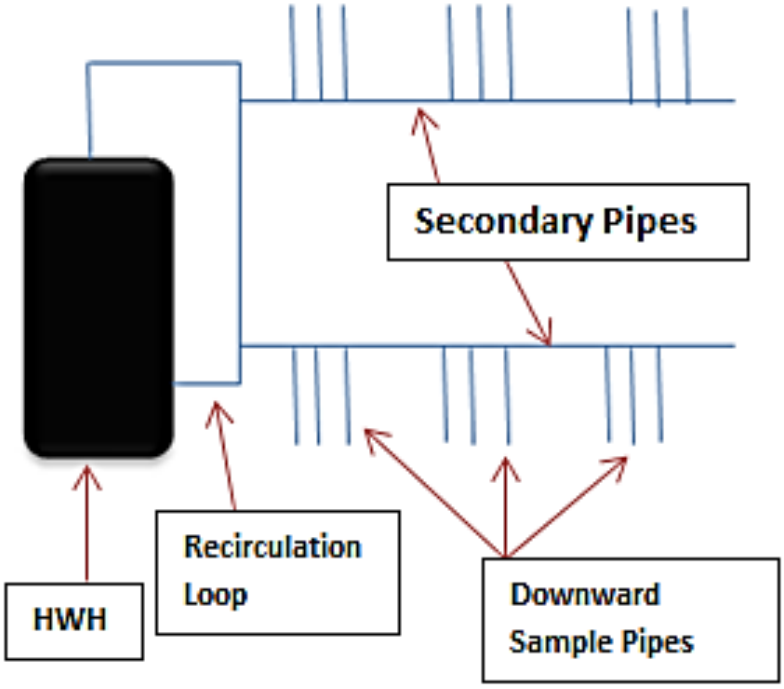

Figure 3.1 Setup A: recirculating loop setup with secondary pipes, no extension

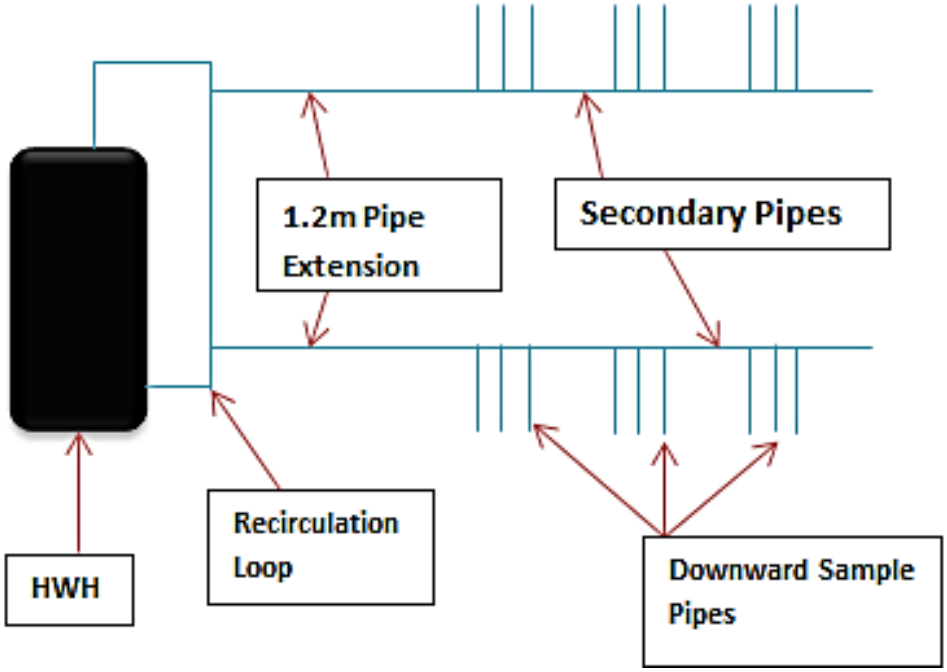

Figure 3.2 Setup B: recirculating loop setup, with secondary pipes, 1.2 meter extension before secondary pipes

Testing for thermosyphon (Setup A and B)

Using both setup A and B, water was flushed through both secondary pipes for 5 minutes, and then left stagnant for two hours to allow steady state temperatures to be reached. Pipe surface temperature was then measured at the mid-point of the sample pipe using an infra-red thermal emissivity gun (Kintrex,

Vienna, VA). Pipe surface temperature was recorded as a function of distance away from the main recirculation loop.

Full recirculation loop, test for thermosyphon (Setup C)

Setup C was used to eliminate all dependency of mixing on the distance from the recirculating line. For this experiment, the hot water in the HWH was initially set at 40°C and allowed come to steady state. Pipe surface temperature was measured at the recirculation loop, middle of sample pipe, and at the end of the sample pipe for upward and downward oriented pipes two hours after setting the HWH temperature. A similar protocol was followed with hot water heater settings of 43°C, 48°C, 54°C, 60°C, and 66°C.

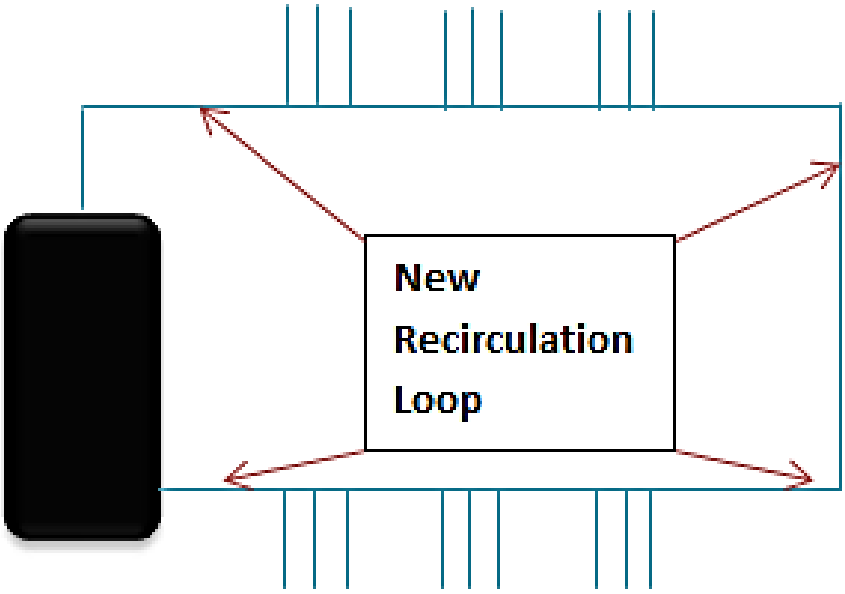

Figure 3.3 – Setup C: recirculating loop setup, secondary pipes connected to form larger recirculating loop

Disinfectant Residual (Setup C)

Again with the third setup orientation, the hot water heater was set to 35°C. All the hot water in the tank was replaced with fresh, cold tap water and water was run through each sample pipe for two minutes to establish a common starting concentration for disinfectant residual. The tank was turned on and allowed to heat up the recirculating line. An aliquot of water was taken from each sample pipe. Total chlorine was measured using a HACH brand Permachem DPD total chlorine reagent packets and a HACH brand pocket colorimeter initially, at one and two hours, and after overnight stagnation. Over the course of the experiment, pipe temperature at the recirculating line and middle of the sample pipes were monitored at 0.5, 1, and 2 hours or until the pipe temperature remained unchanged to ensure that steady state mixing was occurring. This process was repeated for two more hot water heater settings (48°C and 61°C).

Tracer Study (Setup C)

A final experiment quantified the convective mixing rate in the model HWH system using a potassium chloride salt tracer. A 2.4 mg K^+/L increase (Blacksburg tap water contained approximately 1.6 mg K^+/L) was targeted in the 81 L hot water system (tank + pipe volume). To make a stock solution of tracer used, 4.63 g KCl was dissolved in 0.5 L of distilled water, making a 9.28 mg KCl/L solution. Forty milliliters of the 9.28 g KCl/L solution was injected into the 81 L system at the end of one upward and downward oriented pipe. Potassium was measured using Inductively Coupled Plasma Mass

Spectrometer (ICP-MS) at a sample port on the HWH. Samples were acidified with 2% nitric acid. This was performed for HWH settings of 40ºC, 54°C and 66°C.

Results and Discussion

Testing for thermosyphon (Setup A)

The temperatures observed in the HWH system in setup A and B were dependent on the distance away from the main recirculating line for all HWH temperature settings tested. At HWH temperature setting of 44°C in setup A, the triplicate of sample pipes closest to the recirculation loop had measured temperatures of ~27ºC-35°C, whereas sample pipes in the next two triplicate sets showed a constant temperature of ~26°C (Figure 4.1). The same conditions were repeated for setup B; however, temperatures were constant throughout all three sets of triplicates. This indicates that the temperatures observed in a typical HWH system are a function of distance away from the main recirculation loop. In setup A, the first triplicate of pipes was seen to demonstrate a thermosyphon, elevating the pipe surface temperature; but when a 1.2m secondary pipe extension was added, no thermosyphon was seen throughout the system. This demonstrates the inability of the recirculation loop in setup A and B to maintain water temperature above the ASHRAE standard throughout the HWH system.

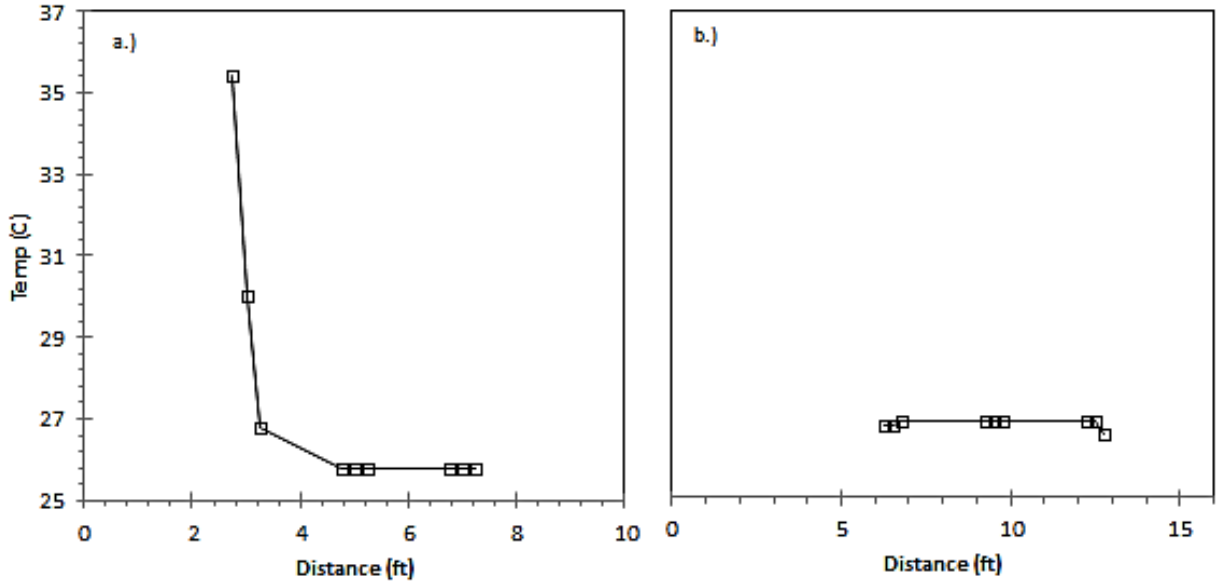

Figure 4.1 – Upward oriented pipes: Pipe surface temperature measured as a function of distance away from recirculating line; a). represents measurements taken with setup A, b). represents measurements taken with setup B. Each point represents surface temperature of the mid-point of a sample pipe, and points from left to right represent increasing distance from recirculation loop. Results for a temperature set point of 44°C.

Full recirculation loop, test for thermosyphon (Setup C)

Once the rig was adjusted such that the sample pipes were directly attached to the recirculation line (Figure 3.3), a thermosyphon was fully developed in all upward slanted pipes but none of the downward slanted pipes. At the highest HWH temperature setting (66°C), pipe surface temperatures for all upward oriented pipes were 15-21ºC hotter during steady state stagnation than pipe surface temperatures for downward oriented pipes (Figure 4.2). This illustrates the thermosyphon effect in upward oriented pipes in the HWH system and the stratification which occurs in downward oriented pipes of the same system. Once again, under no circumstance is the temperature at which the HWH is set maintained throughout the system. For instance, at the hottest HWH temperature setting (66ºC), a difference in temperature of at least 11°C was observed between the recirculating line and the end point of the upward oriented sample pipe, and much of the pipe was in the temperature range considered ideal

for OPPP growth although it was still much higher than the ideal temperature range for *Legionella* growth. The downward oriented pipes also dropped into the range for ideal growth (Figure 4.2). This has major implications for thermal disinfection of *Legionella*, as it shows that thermal disinfection temperatures are not maintained even at HWH temperatures above recommended settings. Both upward and downward oriented pipes were suitable for *Legionella* growth in terms of temperature, but the upward pipes maintained temperatures which were within the ideal growth range for *Legionella* across the range of HWH temperature settings.

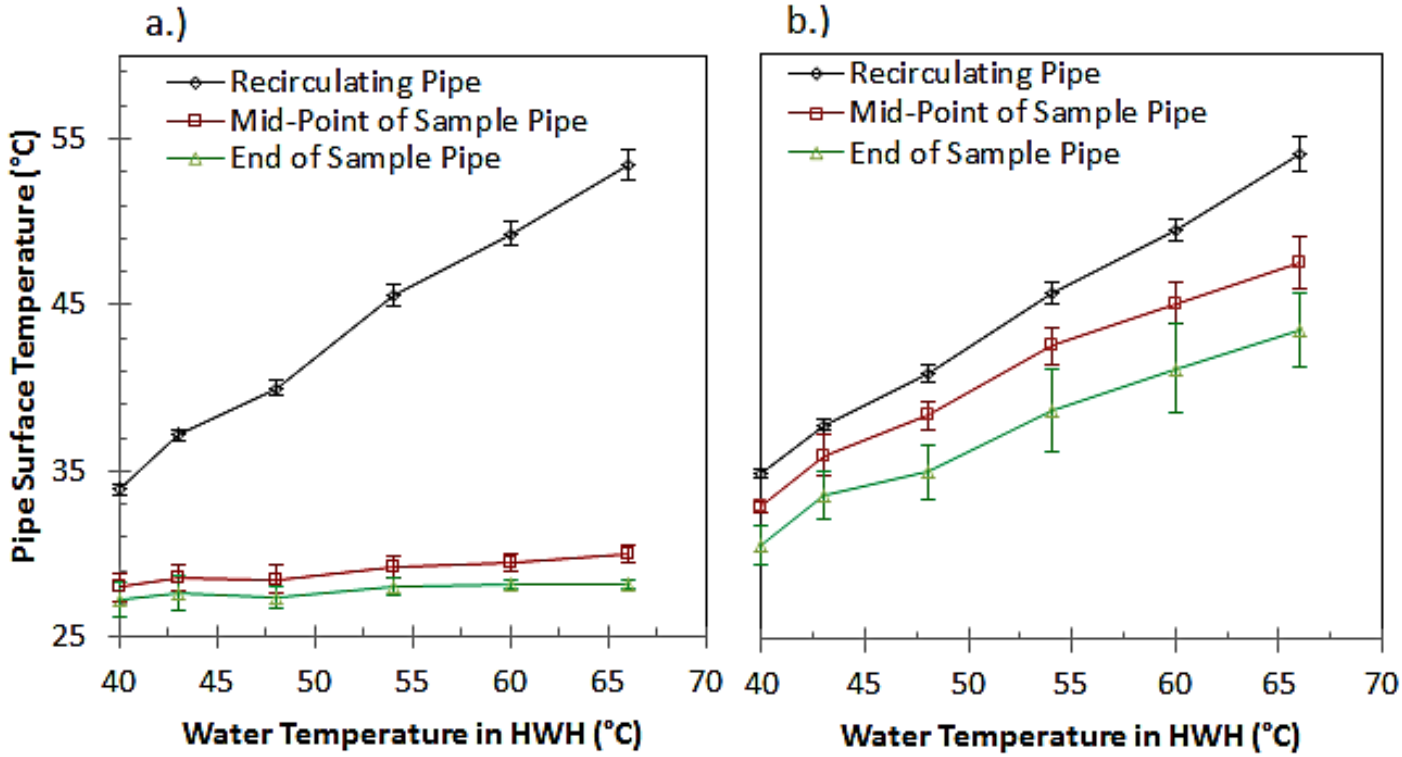

Figure 4.2 – Pipe surface temperature at recirculation pipe, mid-point of sample pipe, and end of sample pipe, across several HWH temperature settings during steady-state stagnation. Figure a) represents downward oriented pipes and no thermosyphon, and figure b) represents upward oriented pipes and a thermosyphon. Error bars represent 95% confidence interval.

Full recirculation loop, chlorine (Setup C)

Disinfectant decay was measured as a function of time in a stagnant system over a range of HWH temperature settings. As stagnation time increased in the system, disinfectant decayed in the recirculating line (Figure 4.3), upward, and downward oriented pipes (Figure 4.4). Disinfectant was decayed in the HWH tank and recirculating line from an initial concentration of 2.28 ppm total chlorine as Cl_2 to 1.92 ppm after two hours of stagnation (Figure 4.3). A greater extent of disinfectant decay was seen in upward and downward sample pipes, but downward oriented pipes had lower levels of disinfectant at nearly every measured point after the onset of stagnation. This is contrary to the conventional wisdom that monochloramine decays faster at higher temperatures (Vikesland and Valentine, 2000) and suggests the higher disinfectant residual levels in upward oriented pipes may be attributed to the higher amount of influent water received from convective mixing (thermosyphon) taking place. The convective mixing could have introduced more influent water with a higher disinfectant residual into the pipes. Average initial concentrations of 2.1 ppm total chlorine as Cl_2 at a HWH setting of 61°C were reduced to an average concentration of 0.23 ppm after 24 hours of stagnation (Figure 4.4).

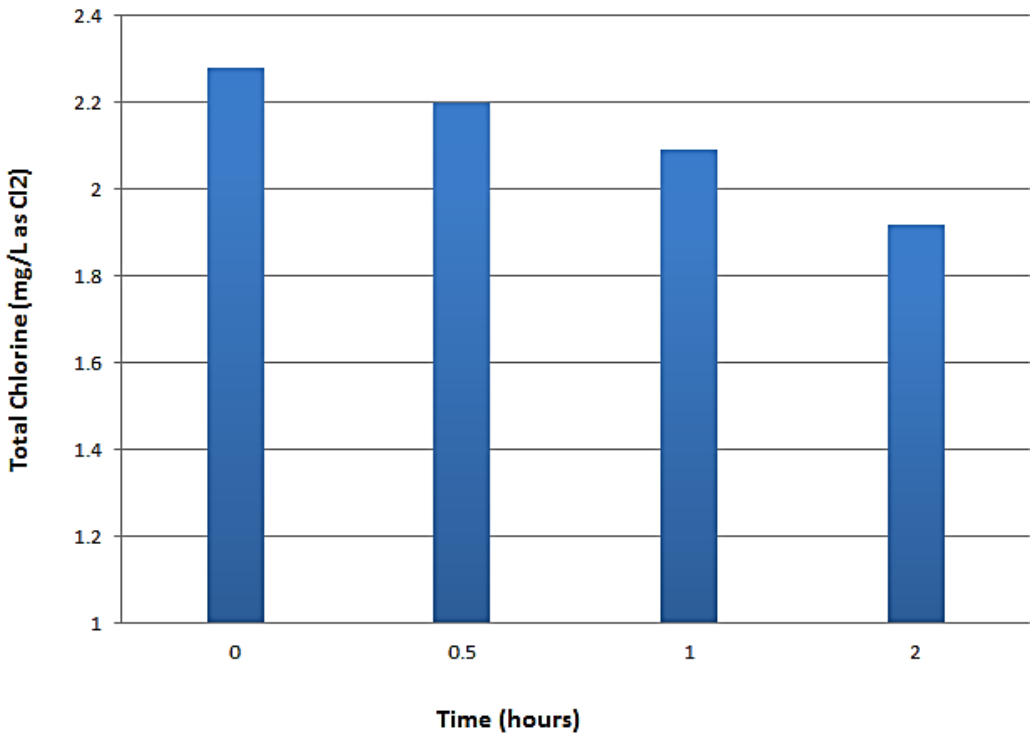

Figure 4.3 – Chlorine decay over time in recirculating line at HWH temperature setting of 61°C; each bar represents one total chlorine measurement at specified time after onset of stagnation.

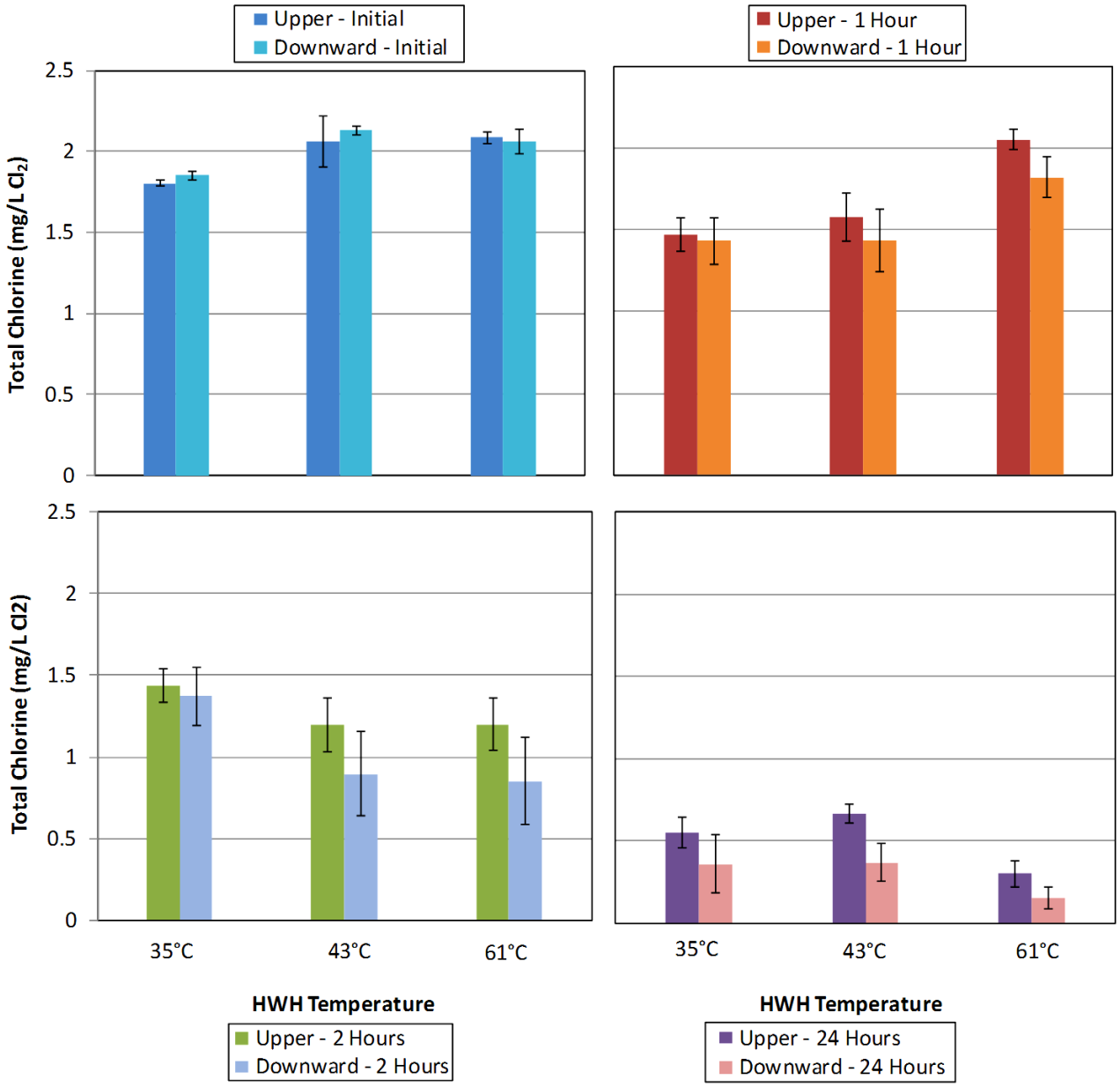

Figure 4.4 – Measured values of total chlorine as a function of stagnation time at initial, 1, 2, and 24 hours. Error bars represent 95% confidence interval.

Tracer study

In the tracer study, convective mixing was quantified by observing increases in K^+ ion concentration in both upward and downward oriented pipes after addition of a KCl tracer. The increase in potassium ion concentration was monitored during stagnation for both upward and downward slanted pipe over HWH settings of 35°C and 54°C. At 35°C, only 64% of K^+ injected was recovered in upward facing pipes after 24 hours of stagnation. The data were fit to an exponential function with a rate of 0.055 hr^{-1} (R^2 of 0.94). Based on this model, monitoring for 52 hours would be necessary to recover 95% of the potassium. Convective mixing was observed at HWH temperature setting of 54°C, where 95% of injected KCl stock solution was recovered after 24 hours of stagnation with an exponential rate of 0.18 hr^{-1}. This suggests that convective mixing in the HWH system is accelerated by an elevation in HWH temperature

setting (Figure 4.5). Convective mixing caused an increase in K^+ ions in the system, whereby heated water within the system traveled to the end of the sample pipe (injection point of KCl stock), and mixed with the main reservoir water recirculated between the heater tank and recirculation lines.

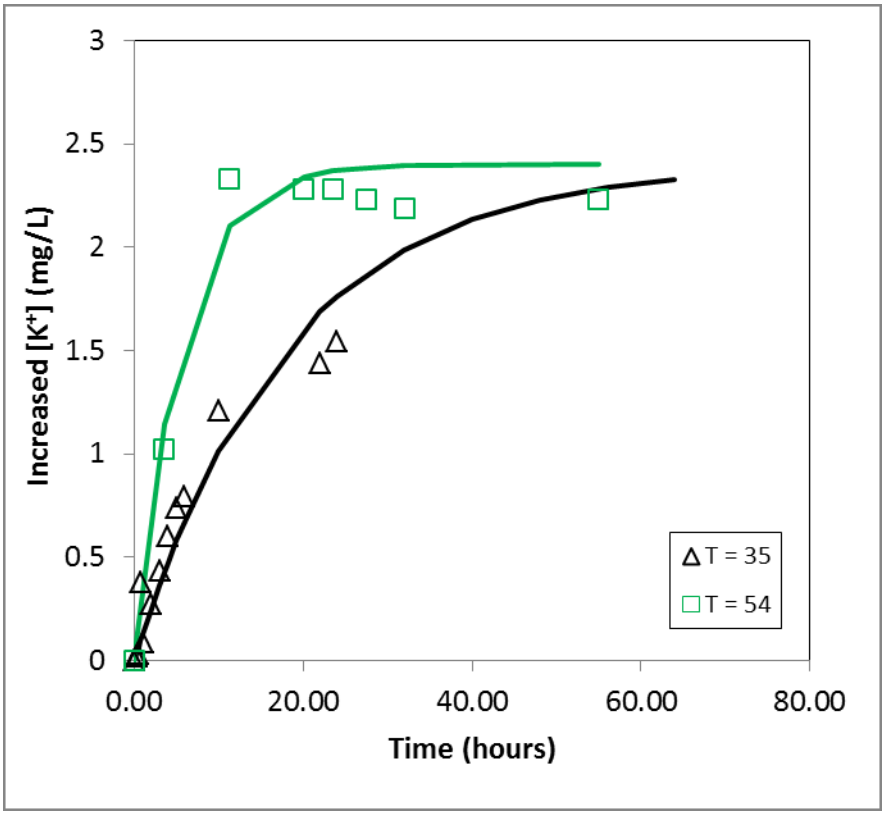

Figure 4.5 – Measured increase in values of K^+ ions after addition of KCl stock solution in upward oriented pipes. HWH was set to 35ºC, and 54°C. Data points are measured values, line is exponential decay curve, with R^2 values of 0.94 (35ºC) and 0.98 (54°C) respectively.

The opposite trend was observed in downward oriented pipes. Virtually no increase in K^+ ions was observed in the system after 4 days of stagnation at 35°C and 54ºC (Figure 4.6). This is likely due to the fact that there was no convective mixing within the system. Since water stratifies in downward oriented pipes, the KCl stock solution would have only come into contact with the coldest, most dense water which stratified to the bottom of the sample pipe.

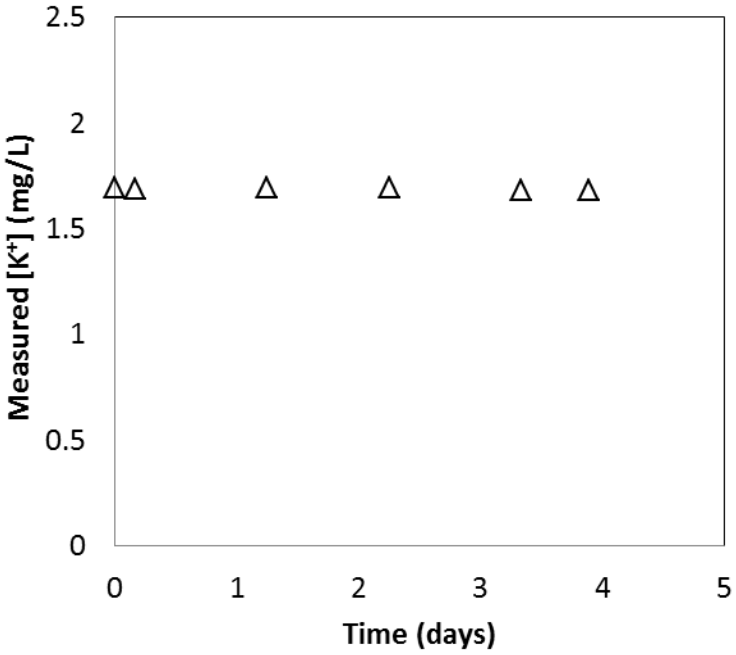

Figure 4.6 - Measured increase in values of K^+ ions after addition of KCl stock solution in downward oriented pipes. Data points are measured values. HWH was set to 35°C and 54ºC, graph is representative of both HWH temperature settings, as no significant difference in data points was observed between temperature settings.

Conclusions

This study demonstrated significant differences in temperature and mixing rates between upward oriented and downward oriented pipes of the same HWH system during stagnation. Although not as pronounced as differences in temperature and mixing rates, differences in disinfectant residual can be observed between upward and downward oriented pipes. Future work should include a study to quantify differences in microbial activity between upward and downward oriented pipes in similar experiments incorporating flow rate and flow frequency.

Acknowledgements

We acknowledge the support of the National Science Foundation through NSF/REU Site Grant EEC-1062860. Any opinions, findings, and conclusions or recommendations expressed in this paper are those of the authors and do not necessarily reflect the views of the National Science Foundation.

I would like to personally thank the National Science Foundation for providing me the opportunity to participate in this experience and my graduate mentor, William Rhoads, who was an ever-present source of help and encouragement throughout this process. I thank my mentor, Dr. Marc Edwards, for his expert advice and insight into my research, and for always making time to assist in any way possible.

References

ASHRAE (2011, June 10). Prevention of Legionellosis Associated with Building Water Systems. *BSR/ASHRAE Standard 188P*. Retrieved from http://www.ashrae.org/technology/page/331

Borella, P., Montagna, M. T., Romano-Spica, V., Stampi, S., Stancanelli, G., Triassi, M., Neglia, R., et al. (2004). Legionella Infection Risk from Domestic Hot Water. *Emerging Infectious Diseases*, *10*(3), 457–464. doi:10.3201/eid1003.020707

Borella, P., M. T. Montagna, et al., (2005). "*Legionella* contamination in hot water of Italian hotels." Applied & Environmental Microbiology **71**(10): 5805-5813.

Brennen, C., R. M. Vickers, et al., (1987). "Discovery of occult *Legionella* pneumonia in a long stay hospital: results of prospective serological survey." Br.Med.J.(Clin.Res.Ed). **295**: 306-307.

Ciesielski, C. A., Blaser, M. J., & Wang, W. L. (1984). Role of Stagnation and Obstruction of Water Flow in Isolation of Legionella pneumophila from Hospital Plumbing. *Applied and Environmental Microbiology*, *48*(5), 984-987.

Drinking Water Distribution Systems: Assessing and Reducing Risks. (n.d.). Retrieved August 4, 2012, from http://www.nap.edu/openbook.php?record_id =11728&page=15

Edwards, M.; Bosch, D; Loganathan, G. V. Dietrich, A. M. (May, 2003). The Future Challenge of Controlling Distribution System Water Quality and Protecting Plumbing Infrastructure: Focussing on Consumers. IWA Leading Edge Conference. Noordwijk, Netherlands.

Flannery, B., L. B. Gelling, et al., (2006). "Reducing *Legionella* colonization in water systems with monochloramine." Emerging Infectious Diseases **12**(4): 588-596.

Hedges, L. J. and D. J. Roser (1991). "Incidence of *Legionella* in the Urban Environment in Australia." Water Research **25**(4): 393-399.

Heim, T. H., & Dietrich, A. M. (2007). Sensory aspects and water quality impacts of chlorinated and chloraminated drinking water in contact with HDPE and cPVC pipe. *Water Research*, *41*(4), 757–764. doi:10.1016/j.watres.2006.11.028

Kim, B. R., Anderson, J. E., Mueller, S. A., Gaines, W. A., & Kendall, A. M. (2002). Literature review—efficacy of various disinfectants against Legionella in water systems. *Water Research*, *36*, 4433-4444.

Konishi, T., Yamashiro, T., Koide, M., & Nishizono, A. (2006). Influence of Temperature on Growth of Legionella pneumophila Biofilm Determined by Precise Temperature Gradient Incubator. [10.1263/jbb.101.478]. *Journal of Bioscience and Bioengineering, 101*(6), 478-484.

Lee, G. F. and A. Jones-Lee (1993b). Public Health Significance of Waterborne Pathogens, G. Fred Lee & Associates.

Lipponen, (2002). Occurrence of nitrifying bacteria and nitrification in Finnish drinking water distribution systems. Water research (Oxford), 36(17), 4319.

Liu, Z., Lin, Y. E., Stout, J. E., Hwang, C. C., Vidic, R. D., & Yu, V. L. (2006). Effect of flow regimes on the presence of Legionella within the biofilm of a model plumbing system. *Journal of Applied Microbiology*, *101*, 437-442.

Moore, M. R., Pryor, M., Fields, B., Lucas, C., Phelan, M., & Besser, R. E. (2006). Introduction of Monochloramine into a Municipal Water System: Impact on Colonization of Buildings by Legionella spp. *Applied and Environmental Microbiology*, *72*(1), 378–383. doi:10.1128/AEM.72.1.378-383.2006

Muraca, P., J. E. Stout, et al., (1987). "Comparative assessment of chlorine, heat, ozone, and UV light for killing *Legionella pneumophila* within a model plumbing system." Applied and Environmental Microbiology **53**: 447-453.

Nguyen, C., Elfland, C., & Edwards, M. (2012). Impact of advanced water conservation features and new copper pipe on rapid chloramine decay and microbial regrowth. *Water Research*, *46*, 611-621.

NRC. (2006). Alternatives to premise plumbing, in: Drinking Water Distribution Systems: Assessing and Reducing Risk (pp. 316-340): National Research Council.

Pryor, M., Springthorpe, S., Riffard, S., Brooks, T., Huo, Y., Davis, G., & Sattar, S. A. (2004). Investigation of opportunistic pathogens in municipal drinking water under different supply and treatment regimes. *Water Science and Technology*, *50*(1), 83-90.

Rogers, J., Dowsett, A. B., Dennis, P. J., Lee, J. V., & Keevil, C. W. (1994). Influence of Plumbing Materials on Biofilm Formation and Growth of Legionella pneumophila in Potable Water Systems. *Applied and Environmental Microbiology*, *60*(6).

Rossman, L. A. (2006). The effect of advanced treatment on chlorine decay in metallic pipes. *Water Research*, *40*(13), 2493–2502. doi:10.1016/j.watres.2006.04.046

Rushing, J. C., & Edwards, M. (2004). The role of temperature gradients in residential copper pipe corrosion. *Corrosion Science*, *46*, 1883-1894.

Skaliy, (1980). Laboratory studies of disinfectants against Legionella pneumophila.. Applied and environmental microbiology, 40(4), 697.

Strickhouser, A., Edwards, M., Jochym, A., Falkinham, J., Reindorf, D., & Tomlinson, A. RE-GROWTH OF LEGIONELLA PNEUMOPHILA IN POTABLE WATER DURING STORAGE IN DOMESTIC WATER HEATERS.

Thomas, W. M., Eccles, J., & Fricker, C. (1999). Laboratory observations of biocide efficiency against Legionella in model cooling tower systems. *ASHRAE TRANS, 105*, 607-623.

Van der Kooij, D., Veenendaal, H. A., & Scheffer, W. J. (2005). Biofilm formation and multiplication of Legionella in a model warm water system with pipes of copper, stainless steel and cross-linked polyethylene. *Water Research*, *39*, 2789-2798.

Vikesland, P. J., Ozekin, K., & Valentine, R. L. (2001). MONOCHLORAMINE DECAY IN MODEL AND DISTRIBUTION SYSTEM WATERS. *Water Research*, *35*(7), 1766-1776.

Williams, K., Strickhouser, A., Pruden, A., & Edwards, M. Legionella in Potable Water Distribution Systems.

Yee, R. B., & Wadowsky, R. M. (1982). Multiplication of Legionella pneumophila in unsterilized tap water. *Applied and Environmental Microbiology, 43*(6), 1330-1334

Taste and Visual Thresholds of Manganese in Drinking Water

Ashley E. Griffin*, Amanda Sain**, Dr. Andrea Dietrich**

** NSF-REU fellow, Virginia Polytechnic Institute and State University*
(Home Institution: Civil Engineering, Auburn University)
***Department of Civil and Environmental Engineering, Virginia Polytechnic Institute and State University*

ABSTRACT

Manganese is a micronutrient commonly found in drinking water at 0.001 – 0.1 mg/L Mn concentrations. The US-EPA issued a secondary maximum contaminant level (SMCL) of 0.05mg/L for manganese; above this concentration, oxidized manganese causes a black-brown discoloration and stains plumbing fixtures. This regulation also ascribes a "bitter metallic taste" to manganese in drinking water, but no known studies confirm this description. The goal of this study is to determine the human taste threshold for aqueous reduced Mn (II) to know if consumers can protect themselves by detecting an off-taste. Visual threshold tests of insoluble oxidized Mn (IV) at and below the SMCL were also conducted. Thirty-one volunteers (15 female) participated in 1-in-5 choice tests where one sample contained soluble Mn^{2+} in deionized water at concentrations from 8.8 mg/L to 506 mg/L and four samples contained deionized water. Each volunteer repeated the 1-in-5 choice test at varying concentrations to accurately determine their threshold. Individual thresholds were calculated using geometric means. Results indicate that 108 mg/L is the population taste threshold, which is much higher than typical Mn concentrations in water. A concentration this high indicates that consumers are unlikely to observe any taste in their drinking water due to soluble manganese.

Keywords: Manganese, drinking water, taste threshold, visual threshold, bitter metallic taste

Introduction

Manganese (Mn) is a necessary micronutrient that assists in multiple facets of human health, including bone health, production of reproductive hormones, and calcium absorption. Manganese is necessary for the body to produce superoxide dismutase (SOD), an antioxidant enzyme (UMMC, 2011). Experimental observation of manganese deficiency in humans resulted in decreased amounts of healthy cholesterol and clotting proteins in the blood (Expert, 2003). In animals, insufficient intake of manganese has been known to lead to poor bone alignment and malformations, infertility, and seizures (UMMC, 2011; Expert Group on Vitamins and Minerals, 2003).

Humans obtain manganese through a variety of sources including whole grain foods, green vegetables, and nuts (UMMC, 2012; Expert Group, 2003). The World Health Organization (WHO) has not specified a Recommended Dietary Allowance (RDA) for manganese due to the lack of clear biomarkers in nutritional and toxicological studies (Greger, 1998). Basing their decision on typical manganese daily consumption, the US National Research Council has set a Estimated Safe and Adequate Daily Dietary Intake (ESADDI) for manganese for infants, children, and adults at 0.3-1, 1-3, and 2-5 mg/day respectively (Greger, 1998, Expert Group, 2003). Manganese from food sources may have less effective solubility as compared to manganese in drinking water.

Overexposure to manganese under specific conditions, most notably airborne manganese particles, may lead to buildup of excess manganese in the brain (Oberdorster, 2004). Manganese miners who are exposed to and inhale airborne microparticles of manganese or those who receive manganese intravenously may experience neurotoxic effects similar to Parkinson's disease and schizophrenia. Excess manganese exposure during development may impact neurodevelopment (UMMC, 2011).

A recent study by Bouchard and colleagues (2011) correlates manganese levels in drinking water with neurotoxic effects in children. In this study, researchers obtained readings of manganese concentration in drinking water in Quebec homes where elementary school children had resided for over

six months consecutively. The tested drinking water contained manganese between 0.1 µg/L and 2,700 µg/L. The study evaluated the children using Performance and Verbal IQ tests and observed trends of lower IQ scores among children whose home drinking water possessed a higher manganese concentration (Bouchard, 2011). The trend referred specifically to drinking water manganese content; total manganese intake had a weaker correlation to low IQ scores. Studies like the one referenced here raise concern among consumers as to the potential neurotoxic effects of soluble manganese in drinking water.

US drinking water providers are not required to monitor or restrict manganese levels in drinking water. The US-EPA has set a non-enforceable Secondary Maximum Contaminant Level (SMCL) for manganese at 0.05mg/L (see Table 1). Secondary Maximum Contaminant Levels were established as a result of the amended Safe Drinking Water Act, section 1412. Secondary contaminants, also called nuisance chemicals, may result in unsavory aesthetic, cosmetic, or technical effects at concentrations higher than their respective SMCLs (US-EPA, 2011). This prompts water treatment managers to minimize these substances in their water. Examples of aesthetic issues caused by secondary contaminants include off tastes or odors, staining, and discoloration. However, secondary contaminants are not considered harmful at concentrations commonly found in drinking water; thus drinking water providers are encouraged but not required to comply with secondary standards.

Table 1: US-EPA Secondary Maximum Contaminant Levels (SMCL)
(Code of Federal Regulations)

Contaminant	Level
Aluminum	0.05 to 0.2 mg/L
Chloride	250 mg/L
Color	15 color units
Copper	1.0 mg/L
Corrosivity	Non-corrosive
Fluoride	2.0 mg/L
Foaming agents	0.5 mg/L
Iron	0.3 mg/L
Manganese	0.05 mg/L
Odor	3 threshold odor number
pH	6.5-8.5
Silver	0.1 mg/L
Sulfate	250 mg/L
Total dissolved solids (TDS)	500 mg/L
Zinc	5 mg/L

Manganese is specifically listed as a secondary contaminant because at concentrations above the SMCL, 0.05mg/L Mn, oxidized insoluble manganese [Mn (IV)] causes a black-brown tint in water and also stains plumbing fixtures (Figure 1). Because of these aesthetic problems, water treatment authorities in the United States regularly maintain manganese levels ranging from 0.001 to 0.1 mg/L Mn, most commonly around 0.01 mg/L Mn (Expert Group, 2003). The EPA's SMCL guidelines also attribute a bitter metallic taste to manganese above the 0.05 mg/L concentration (US-EPA, 2012). However, no available studies confirm this reference. This study is the first to attempt to establish a taste threshold for detectable concentrations of soluble manganese in drinking water. Taste thresholds vary widely among people and can be dependant on age, genetics, taste preferences, and the type of water that a person usually drinks.

Figure 1: Manganese discoloration on a glass pipe

Previous studies on iron and copper, two other metals categorized in the SMCL list, were found to have population taste thresholds below their respective SMCL concentrations. In a study by Omur-Ozbek and Dietrich, ferrous (Fe^{2+}) was found to have population taste thresholds of 0.031 and 0.05 mg/L, determined by logistic regression and geometric mean respectively, as compared to a SMCL of 0.3 mg/L for iron (Omur-Ozbek and Dietrich, 2011). In the same study, population taste threshold for cupric ion (Cu^{2+}) was determined to be 0.61 mg/L, while the SMCL value for copper is 1.0 mg/L.

In addition, many US residents rely on well water, which may have higher manganese content than water that issues from a large-scale treatment facility. As shown in Figure 2, manganese concentrations in US groundwater varies from less than 1µg/L (0.001mg/L) to above 300µg/L (0.3mg/L), well exceeding the SMCL (Ayotte 2011). Thus, well-water drinkers may be exposed to higher amounts of manganese through their drinking water and may be concerned about aesthetic problems and potential health consequences resulting from the manganese content of their water.

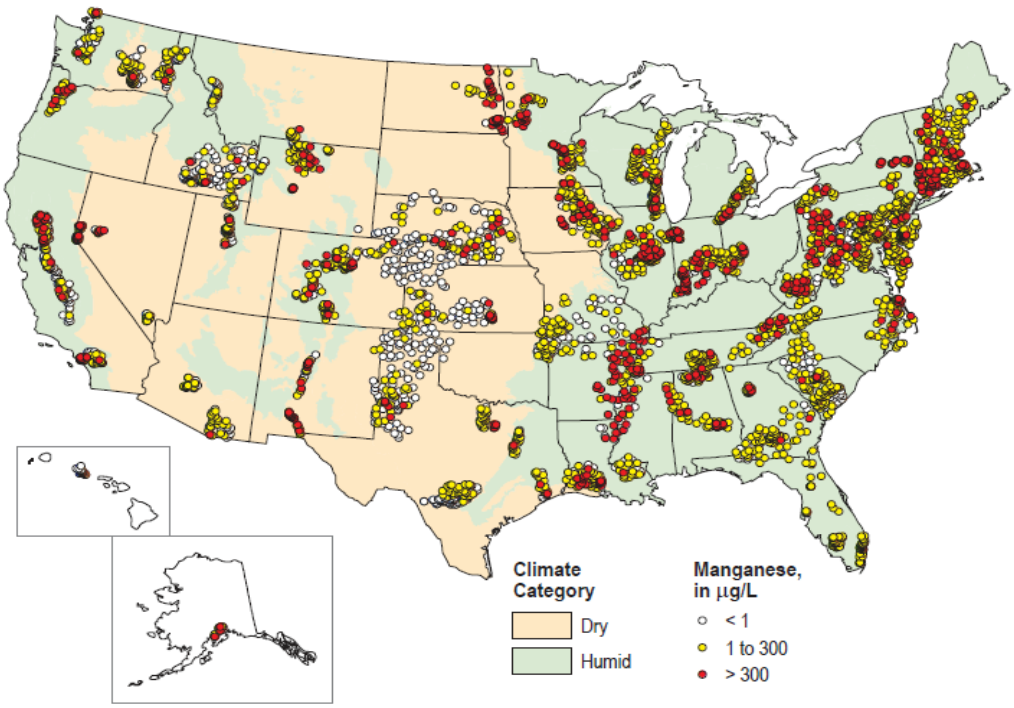

Figure 2: Manganese in US groundwater, US Geological Survey (Ayotte 2011). The white dots represent regions with manganese concentrations below 0.001mg/L, the yellow dots represent areas with groundwater manganese between 0.001mg/L and 0.3mg/L, and the red dots indicate a manganese concentration of above 0.3mg/L.

The only previous study to attempt to quantify a taste threshold for soluble manganese is a 1960 study by Cohen and associates. This study used a panel taste-testing method called the duo-trio method and tested manganous sulfate solutions in spring water and distilled water adjusted to a pH value of 6.4 (Cohen, 1960). Based on feedback from 15-19 pre-trained taste-and-odor-testing judges, researchers estimated a taste threshold for 50 percent of the population as 180 mg/L. However, this study incorporated extensive extrapolation from the panelists' answers, and the duo-trio test (a force-choice test wherein the subject must choose between two solutions) offers a 50 percent chance of choosing the correct answer solely by guessing. Table 3 shows the extrapolated threshold frequencies found in this study (Cohen, 1960).

Table 2: Taste Threshold Frequencies at Various Concentrations of Manganese Ion (Cohen, 1960)

Manganese Concentration ppm	Distilled Water	Spring Water
	Cumulative Threshold Distribution—%	
1	0.7	0
4	6	0
8	14	0
16	26	0.05
32	47	1
64	67	7
128	82	43

This current study aims to establish the human taste threshold for soluble reduced manganese [depicted as Mn^{2+} or Mn (II)] in drinking water. Specifically, researchers hoped to confirm or deny the accepted notion that manganese causes a bitter, metallic taste at the EPA secondary maximum contaminant level of 0.05mg/L. The study also examined human visual detection of soluble reduced manganese, [Mn (II)] and insoluble oxidized manganese, Mn (IV), at lower mg/L concentrations than 0.05 mg/L under various conditions to determine if humans can visually detect excess manganese in their drinking water.

Research Methods

Human Subjects

Since taste is a subjective quality and humans have a wide variety of taste sensitivities and preferences, it was essential for this study to obtain a broad spectrum of volunteers. Researchers obtained approval from the Institutional Review Board (IRB) at Virginia Tech (IRB #09-506). Subjects were recruited by email and consisted of 31 multinational persons (15 out of the 31 were female, 84% were North American/European) made up of faculty, staff, and students of Virginia Tech, as well as undergraduate summer research students from various United States universities. Subjects were competent adults ages 18-61 (mean age 26), some of whom had participated in previous taste threshold research with other metals. All subjects were free to withdraw at any point during the study. Each subject was assigned a random two-digit numerical code associated with his/her data results. Names and email contact information for the volunteers was kept separate from their data results. At each person's first taste session, he or she read an approved consent form, which included the test procedure, and gave verbal informed consent to participate, in keeping with an IRB exemption that this study received. Subjects were instructed to refrain from consuming food or non-water beverages for one hour prior to each testing session. Each participant performed multiple taste test sessions lasting approximately 7 minutes each, with a maximum of 3 tests performed in one day; sufficient time was given between tests to ensure no

overlap of taste residual. Subjects were compensated with snacks upon completing each session.

Pilot taste tests were conducted where staff members of the Virginia Tech Civil and Environmental Engineering Taste and Odor Lab voluntarily performed preliminary taste tests to determine an appropriate Mn concentration with a taste that was noticeably different from de-ionized Nanopure water. Preliminary tests consisted of soluble Mn^{2+} concentrations of 2.0, 5.0, 10.0, 50.0, and 85.0 mg/L. Researchers concluded that further volunteer tastes should commence at 100 mg/L and increase or decrease by a factor of 1.5 depending on correct or incorrect responses by the volunteers.

Taste Test Procedure

This study used food grade manganese sulfate (Spectrum, CA, CAS 10034-96-5). Fresh solutions were prepared daily and verified for accuracy using atomic absorption (AA) spectroscopy (Perkin Elmer 5100). The concentrations of soluble manganese used in this study were 0.8, 8.9, 13.3, 20, 30, 45, 66, 100, 150, 225, 337.5, and 506 mg/L Mn^{2+}. A stock solution ranging from 100 to 506.25mg/L was prepared initially and other concentrations were dilutions of the stock solution and Nanopure water. Solutions were stored in sealed volumetric flasks at room temperature and were poured into 5oz. cups anywhere from 1-60 minutes prior to each test.

The taste threshold identification protocol used in this study replicated the procedure used by Omur-Ozbek and Dietrich (2011) and Mirlohi et al. (2011) to assess the taste thresholds of cupric (Cu^{2+}) and ferrous (Fe^{2+}) ions in drinking water. An exception is that this study did not incorporate nose-clips to isolate taste sensation from flavor sensation (Omur-Ozbek and Dietrich, 2011). Each test session consisted of a single-blind 1-in-5 force choice test where four 3oz. cups contained approximately 20mL of Nanopure water each and one 5oz. cup contained a predetermined concentration of approximate 20mL of soluble manganese in Nanopure water. All five cups are labeled with random three-digit numbers. Participants had a 20% chance of guessing the correct cup even if they could not correctly identify the correct choice by taste.

Testing sessions occurred in open ventilated rooms without distracting noises or odors. At the beginning of each test session, subjects rinsed their palates with approximately 60mL of Nanopure water to serve as the control. Subjects were instructed to wait for one minute in between tasting each sample. At the conclusion of each testing session, subjects used a pH indicator strip to measure their oral pH (EMD Chemicals 9588). Out of the 226 testing sessions, only 6 sessions did not measure oral pH.

The primary statistical method used to analyze the subjects' taste threshold answers consisted of a geometric mean between the lowest Mn (II) concentration that each subject correctly identified and the highest Mn (II) that same subject incorrectly identified. These individual taste thresholds were analyzed by a second geometric mean to compute the best estimate threshold (BET). Further comparisons were made to identify potential correlations between individual taste threshold and oral pH, age, and gender.

Visual Test Procedure

A 1-in-5 test similar to the test used for taste threshold was prepared using solutions of Nanopure water in 16oz Styrofoam cups. Visual testing used manganese (II) chloride tetrahydrate, $MnCl*4H_2O$ (Fisher Scientific, NJ, CAS 13446-34-9). Concentrations tested for visual threshold were 0.075mg/L, 0.05mg/L, 0.02mg/L, 0.01mg/L, and 0.005mg/L oxidized manganese, Mn (IV), in addition to 10.0mg/L reduced manganese, Mn (II).

Figure 3: Visual 1-in-5 test set up. Cups are labeled with random three digit numbers. Subject observes the five cups and chooses the sample that appears different. In this particular test, the cup containing oxidized manganese [0.03 mg/L Mn (IV)] is second-from-the-right.

For each test session, five cups were labeled with random three-digit numbers and contained 200mL of fluid each. Four of the five cups were filled with 200mL of Nanopure water, and the remaining cup was filled with 200mL of the manganese solution. 200µL of Clorox bleach was added to all five cup solutions to oxidize the manganese to MnO_2. Oxidation reaction time was 30 minutes, and solutions were occasionally stirred using glass stirring rods. All visual tests for a particular day occurred approximately 1-5 hours following the addition of the bleach. Volunteer participants (n=15) observed the samples and selected the sample that appeared different (see Figure 3). One series of visual tests with 4 human subjects used 10oz clear flexible plastic cups and tested a concentration of 0.05 mg/L Mn (VI). An additional series with 8 human subjects used soluble reduced manganese (Mn^{2+}) at 10.0 mg/L in 16 oz Styrofoam cups to evaluate participants' ability to identify soluble manganese.

Results

Taste Study

For twenty-seven (27) of the 31 subjects, individual populations thresholds were calculated by geometric mean and ranged from 10.9 mg/L to 267 mg/L Mn^{2+}. Some subjects were sporadic in their responses and did not appear to have a distinct threshold at which they could consistently taste the manganese solution. Figure 4 shows the individual thresholds plotted against age for the 27 subjects whose thresholds were calculable. The remaining subjects either had extremely inconsistent responses, were unable to complete the study, or had taste thresholds outside the range of this study (could not correctly identify the manganese solution at any concentration). Both of the highest and lowest individual taste thresholds occurred among subjects in the 21-24 age range, suggesting that there is no significant correlation between age and threshold. The best estimate population threshold (BET) was determined using geometric mean on these individual taste thresholds and was determined to be 108 mg/L Mn^{2+}, indicating that 50 percent of the population would be likely to taste soluble manganese at this concentration in drinking water. Figure 5 shows a histogram of the subjects' taste thresholds, indicating that 122.5 mg/L was the most common individual taste threshold. This was the result when a subject could not correctly determine the 100 mg/L Mn^{2+} sample solution, but correctly determined the 150 mg/L Mn^{2+} solution during consecutive 1-in-5 tests

.

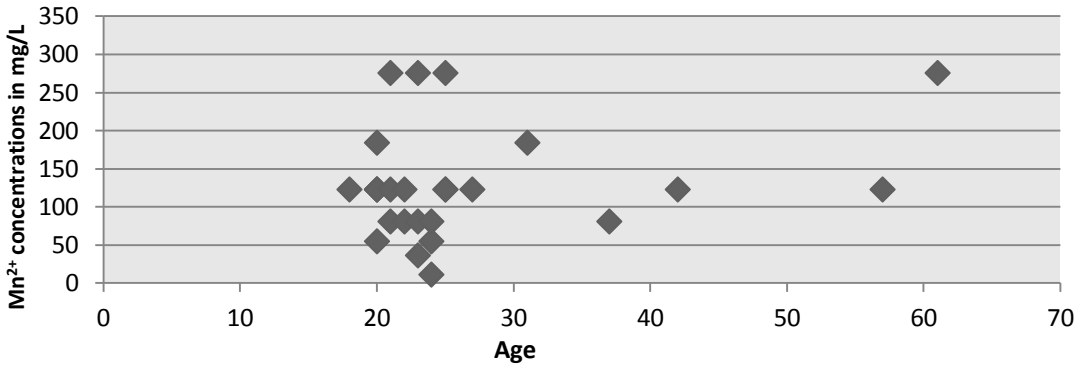

Figure 4: Individual Thresholds by Age for Mn^{2+}

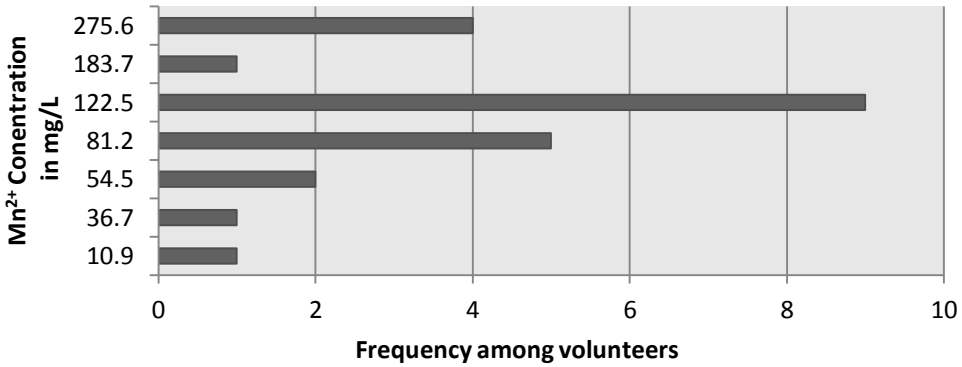

Figure 5: Histogram of Taste Thresholds for Mn^{2+}

Estimated population threshold was also calculated by a preliminary logistic regression (see Figure 6) using seven concentrations (0.8, 20, 100, 150, 225, 337.5, 506 mg/L Mn^{2+}) over 10 subjects who had complete data sets. Based on this model, 50% of the population will be able to detect soluble reduced manganese in drinking water at a concentration of 54.6 mg/L Mn^{2+}, significantly lower than the best estimate threshold of 108 mg/L Mn^{2+}. Using Abbott's correction to account for the 20% possibility of guessing the correct solution in the 1-in-5 taste test, the 60% population threshold results in 96.5 mg/L Mn^{2+}.

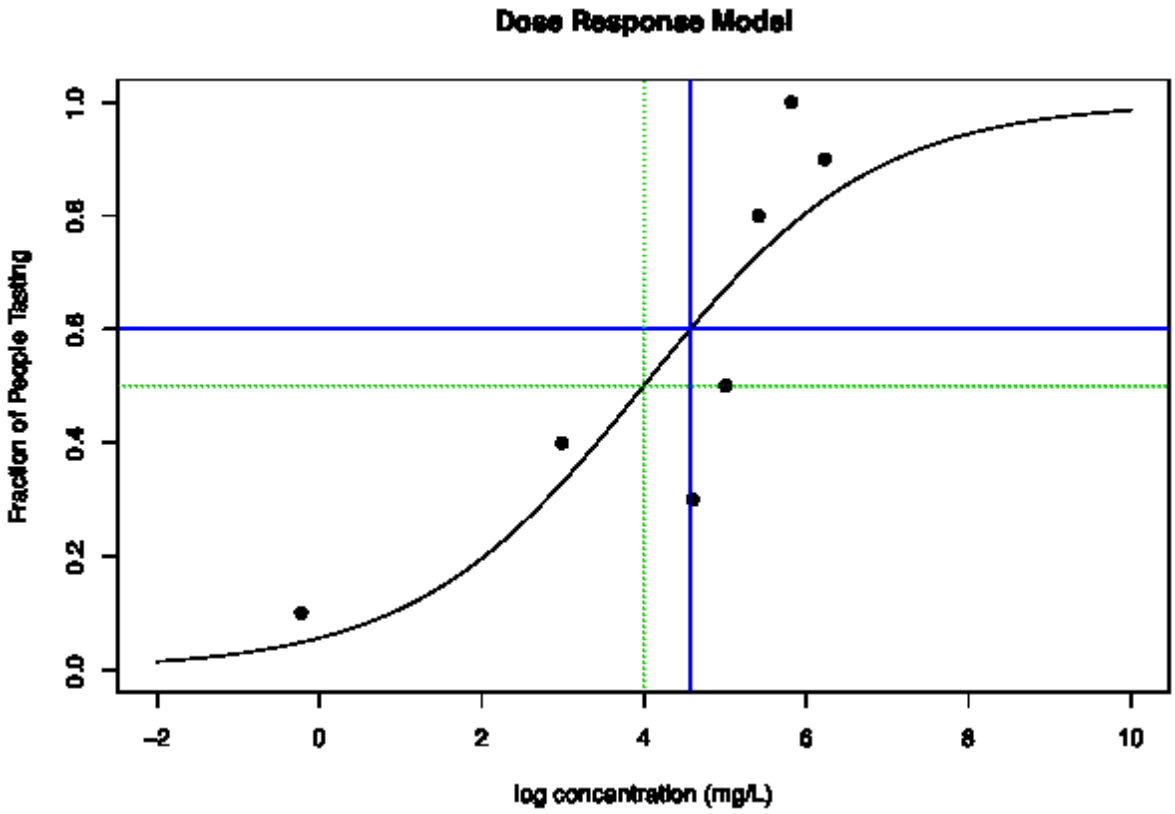

Figure 6: Logistic regression on complete participant data. Green intersecting lines represents 50% population threshold at 54.6 mg/L Mn^{2+}. Blue intersect represents 60% population threshold at 96.5 mg/L Mn^{2+}, accounting for the 20% chance of guessing in the 1-in-5 test.

Subjects described the taste of manganese in a variety of ways (see Figure 7). Out of 130 test sessions where the subject correctly identified the manganese solution, 62 tests (representing 21 of the 31 participants) included some kind of remark or feedback on their chosen correct solution. The most common taste description was "bitter", which was mentioned by 6 subjects over 15 total tests of concentrations ranging from 20 mg/L to 506.25 mg/L Mn^{2+}. This description was followed in frequency by "metallic", which 5 subjects commented on over the course of 12 tests, with concentrations of 0.8 mg/L to 337.5 mg/L Mn^{2+}. The third most common description was sour (2 tests, 2 subjects, 150 mg/L to 22 mg/L). 3 subjects noted that the solution containing manganese had a different "texture" or mouth-feel than the solutions containing only Nanopure, describing the flavor as astringent or fluoride. 4 persons noted an aftertaste and described it as bitter or sweet. In some cases, subjects also noted that the solution containing manganese tasted more like regular drinking water than the Nanopure, which they described as having a metalic taste.

Figure 7: Word cloud depicting frequency of subjects' descriptive responses. Increasing size of words indicates more frequent occurrence of description.

Visual Study

All subjects (n = 15) successfully identified the solution of oxidized manganese, Mn (IV) at the SMCL standard of 0.05 mg/L Mn (IV) in both the white Styrofoam cups and the semi-transparent plastic cups. Subjects described the samples of water containing oxidized manganese as "yellow", "slightly opaque", "darker" and "green". None of the subjects (n = 8) identified the solution containing 10 mg/L of soluble reduced manganese, Mn^{2+}. Of these same 8 subjects, all except one correctly detected an oxidized manganese solution of 0.005 mg/L Mn (IV). Some subjects did note that this lowest concentration was "more of a guess" and that it was "hard to tell" even though they chose the correct solution. This again indicates that it would be difficult for a homeowner to visually detect manganese in drinking water at these concentrations.

Discussion and Recommendations

The concentrations at which participants tasted and correctly identified manganese in drinking water are considerably higher than the levels of manganese typically found in US municipal water systems. Therefore, consumers need not worry about tasting manganese in their city tap water. Even for residents who rely on well water, which has higher concentrations of many minerals than treated water, manganese levels will still be undetectable under normal circumstances.

Further research will replicate the visual 1-in-5 test under other circumstances to replicate realistic situations where humans may encounter water which contains manganese. A different arrangement for the visual difference test would be to use cups similar to restaurant glasses and perform the test over a plain white surface (mimicking a tablecloth) instead of the dark lab countertop.

Another option for additional research is to perform taste tests using oxidized manganese (Mn^{4+}). However, if oxidized manganese was tested at concentrations similar to those used in the reduced manganese taste test study, volunteer subjects would need to be blindfolded as to avoid a bias towards the visually different solution. Previous studies performed by Omer-Ozbek and Dietrich indicate that oxidized metal ions are likely to have weaker tastes than their respective reduced ions (2011). To confirm this trend for manganese, researchers would perform 1-in-5 tests using oxidized manganese at the population taste threshold for soluble reduced manganese, to see if a statistically significant percentage of

the volunteers identify the manganese solution.

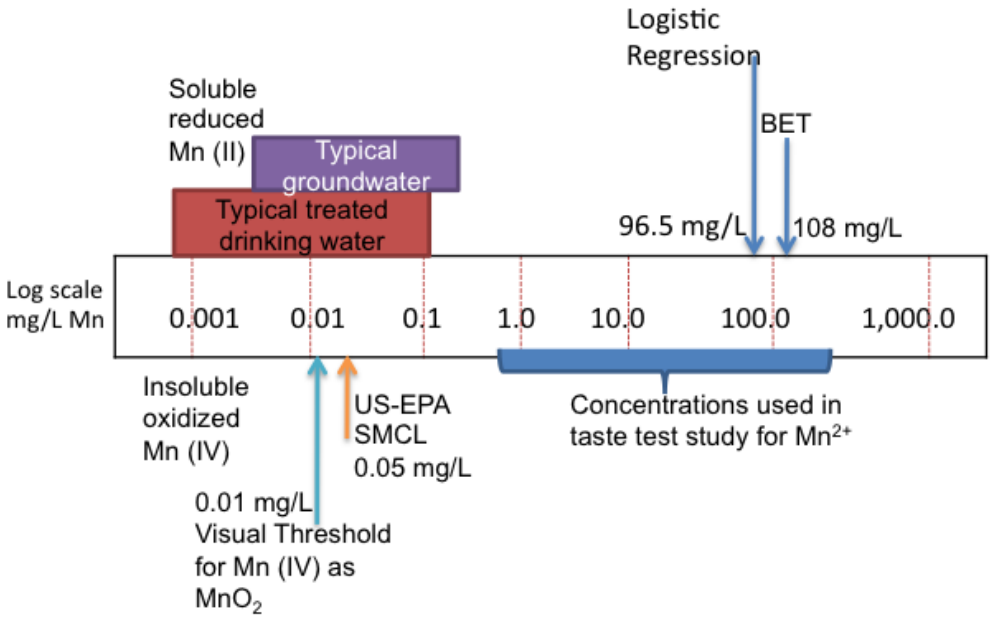

Figure 8: Log scale of Mn in mg/L, depicting notable concentrations determined or referenced in this study

Conclusions

This study dismisses the notion that humans can regularly taste soluble reduced manganese (Mn^{2+}) at concentrations found in drinking water (see Figure 8 above). The human taste threshold is considerably higher than the SMCL value of 0.05mg/L Mn, while the detectable color threshold may be as low as 0.01mg/L Mn for insoluble oxidized manganese [Mn (IV)]. With these results in mind, manganese concentrations in typical processed drinking water systems are undetectable to humans, and off tastes in drinking water should be attributed to other chemical sources. Persons with extremely acute sensitivity may detect some manganese-induced taste in well water systems with abnormally high manganese concentrations. If consumers are concerned about potential manganese concentrations in their drinking water, they should check their local water distributer for information about their water's manganese levels, rather than relying on taste differences to make them aware of higher manganese levels. This is especially a concern for well-water consumers. Since manganese naturally oxidizes very slowly as compared to iron and other metals, manganese concentrations in well water could be higher than 0.05 mg/L Mn without a noticeable color difference.

Acknowledgements

The student author wishes to thank the volunteers for their participation in this study, particularly the fellow REU summer students and staff members of the Taste and Odor Laboratory. Hopefully they enjoyed the fruit gummies. Particular thanks to Amanda Sain and Dr. Andrea Dietrich for designing the research project and mentoring this study. Thanks to the Virginia Tech Department of Civil and Environmental Engineering and Department of Engineering Education for hosting the REU program. Additional thanks to all the seminar presenters who did an excellent job conveying the responsibilities and options for graduate school, and also thanks to the field trip guides at the Blacksburg-Christiansburg-VPI Water Authority, the Blacksburg-VPI Sanitation Authority, the National Weather Service Blacksburg site, and the LEED Gold buildings in Roanoke.

We acknowledge the support of the National Science Foundation through NSF/REU Site Grant EEC-1062860. Any opinions, findings, and conclusions or recommendations expressed in this paper are those of the author(s) and do not necessarily reflect the views of the National Science Foundation.

References

Ayotte, J. D. Gronberg, J. M., and Apodaca, L.E. 2011 Trace elements and radon in groundwater across the United States. *U.S. Geological Survey Scientific Investigations Report* 2011-5059, 115

Bouchard, M. F., S. Sauvé, B. Barbeau, M. Legrand, M. E. Brodeur, T. Bouffard, E. Limoges, D. C. Bellinger, D. Mergler. 2011 Intellectual impairment in school-age children exposed to manganese from drinking water. *Environmental Health Perspectives* **119**, 138–143

Code of Federal Regulations Title 1.D.143 2002. – National secondary drinking water regulations. 613-615

Cohen, J. M., Kamphake, L. J., Harris, E. K., and Woodward, R. L. 1960 Taste threshold concentrations of metals in drinking water. Jourenal of American Water Works Association **52**, 660-670

Expert Group on Vitamins and Minerals, Food Standards Agency. 2003 *Safe Upper Levels for Vitamins and Minerals.* "Risk assessment: manganese". 213-218

Greger, J. L. 1998 Dietary standards for manganese: overlap between nutritional and toxicological studies. Journal of Nutrition **128**, 368S-371S

Marshall, K., Lang, D. G., Jinks, A. L., Hutchinson, I. 2006 The capacity of humans to identify components in complex odor-taste mixtures. *Chemical Senses* **31**, 539-545

Mirlohi, S., Dietrich, A. M., Duncan, S. E. 2011 Age-associated variation in sensory perception of iron in drinking water and the potential for overexposure in the human population. *Environmental Science and Technology* **45**, 6575-6583

Oberdorster, G., Sharp, Z., Atudorei, V., Elder, A., Gelein, R., Kreyling, W., Cox, C. 2004 Translocation of inhaled ultrafine particles to the brain. *Inhalation Toxicology* **16**, 437-445

Omur-Ozbek, P., A. M. Dietrich. 2011 Retronasal perception and flavour thresholds of iron and copper in drinking water. *Journal of Water and Health* **9**, 1-8

United States Environmental Protection Agency (US-EPA) 2012. "Secondary drinking water regulations: guidance for nuisance chemicals". Accessed July 25, 2012. http://water.epa.gov/drink/contaminants/secondarystandards.cfm

University of Maryland Medical Center (UMMC) 2011. "Manganese". Accessed July 26, 2012. http://www.umm.edu/altmed/articles/manganese-000314.htm

Antibiotic Resistance Genes in Recycled Water

Maureen O'Brien*, Mark Mazzochette**, Dr. Amy Pruden**

** NSF-REU fellow, Virginia Polytechnic Institute and State University*
(Home Institution: Colorado School of Mines)
***Department of Civil & Environmental Engineering, Virginia Polytechnic Institute and State University*

ABSTRACT

Water shortages around the United States are causing regions to rely on recycled wastewater as an inexpensive and sustainable option for irrigation. Recycled water is distributed to the point of use via purple pipes, which distinguish them from potable and waste water pipes. While this water is being treated to a high standard, there has been evidence that suggests certain pathogens survive the treatment process and remain in the distributed reclaimed water. Antibiotic resistant bacteria (ARB) are an example of potentially persistent pathogens. In order to quantify antibiotic resistant genes (ARGs), which are markers of ARB presence, samples from irrigation systems in Flagstaff, AZ and Santa Barbara, CA utilizing recycled "purple pipe" wastewater were analyzed using DNA extraction and quantitative polymerase chain reaction (qPCR). qPCR analysis allows direct detection and quantification of ARGs, which are of interest because culture-based methods overlook the vast majority of bacteria and because ARGs can be shared, even between dead and living bacteria. Analysis has detected ARGs in all but two of the twenty-three samples. Notably, frequency of detection and levels of ARGs were higher in the purple pipe water at point of use than coming out of the treatment plant. Some sampling locations indicated more kinds and quantities of ARGs in the purple pipe biofilm, and others in the bulk water. This study suggests that purple pipe distribution systems should be further researched for persistence of ARB and ARGs and that risk assessments for ARGs in recycled water are urgently needed.

Keywords: Antibiotic Resistance Genes (ARGs), Purple pipe, Quantitative polymerase chain reaction (qPCR), and Recycled/reclaimed wastewater

Introduction

Water shortages around the United States are encouraging regions to rely on recycled wastewater as an inexpensive and efficient option for non-potable water uses. Reclaimed water is now being used in urban, industrial, agricultural, environmental, and recreational areas across the country (EPA, 2004). The use of reclaimed water is more cost-effective and sustainable, in that money and energy is saved by using recycled wastewater in place of drinking water (EPA, 2004). This wastewater is treated to a lower standard than drinking water, depending on its intended reuse, and then distributed through pipelines. While this method does reduce stress on water reserves, recent concerns believe treatment is insufficient at eliminating micropollutants found in wastewater (D. Fatta-Kassinos, et al., 2010). Humans and animals are potentially at risk from this water through physical contact or the ingestion of crops that are irrigated with reclaimed wastewater, but risk has not been modeled or quantified with respect to the potential to spread antibiotic resistant disease.

Purple Pipe Water

The demand for recycled or reclaimed wastewater comes from communities that are at or reaching the limits of their water supplies. Recycled water also provides an alternative for wastewater treatment plants (WWTP) for beneficial reuse of wastewater instead of discharging into a water source. Water reclamation can only be used for nonpotable reuse, which means it is not suitable to drink. In order to distinguish reclaimed water from potable water, it is distributed through pipes painted purple, hence giving the water its name.

Typical treatment for recycled water is similar to wastewater treatment with a few more steps to ensure it is at a high enough standard. The process goes through primary and secondary treatment the

same as wastewater, but then is followed by a filtration and disinfection step to treat for reuse (CDPH, 2009). Various methods are used for the disinfection stage, including chlorination or UV ~~sterilization~~disinfection. In some cases where a large amount of reclaimed water is used by a single customer, the EPA requires further treatment to be performed onsite by the customer themselves, similar to potable water requirements (EPA, 2004). [M1]

Reclaimed wastewater is generally regulated by the EPA and those regulations vary depending on the intended use. The highest regulations will be placed upon the water used for irrigating crops intended for human consumption humans while irrigation for forage crops or pastures will be lower (EPA, 2004). California and Florida have kept inventories of their reuse projects and the reclaimed water applications in order to create guidelines for the different types. Other states such as Arizona, California, Colorado, Florida, Hawaii, Nevada, New Jersey, Oregon, Texas, Utah, and Washington have statewide regulations that cover a wide range of end uses for the water (EPA, 2004). The following table shows the ten categories that are used to generate regulations:

Table 1: Recycled Water Reuse*

Category	Examples
Unrestricted urban reuse	Unlimited public access: parks, playgrounds, schoolyards, and residences (toilet flushing, fire protection, etc.)
Restricted urban reuse	Limited public access: golf courses, cemeteries, highway medians
Agricultural reuse on food crops	Crops intended for direct human consumption
Agricultural reuse on non-food crops	Fodder, fiber, and seed crops, pasture lands, commercial nurseries and sod farms
Unrestricted recreational reuse	Body-contact water recreational activities
Restricted recreational reuse	Non body-contact water recreation: fishing, boating
Environmental reuse	Manmade wetlands, enhance natural wetlands, sustaining or augmenting stream flows
Industrial reuse	Cooling systems, boiler-feed water, process water, general washdown
Groundwater recharge	Using infiltration basins, percolation ponds, or injection wells
Indirect potable reuse	Highly treated water discharged into surface waters or groundwater that will be used for source of potable water

*EPA, 2004

California has specific regulations for recycled water presented in Title ~~s 17 and~~ 22 of the California Code of Regulations. The water focused on in this project was used for irrigation which is found under Section 60301.320 in Article 5 of Title 17 (CDPH, 2009). This section includes standards for turbidity, number of total coliform bacteria, ~~chlorine residual,~~ and polio virus removal and/or inactivation shown in Table 2 (CDPH, 2009)~~. For irrigation using recycled water in California, the turbidity of the filter effluent must be below 2 NPU (nephelometric turbidity units), the total coliform bacteria MPN (most probable number) of the disinfected effluent must not exceed 2.2 per 100 mL, and the filtration process must remove 99.999% of the polio virus in the wastewater~~. This is comparable to Arizona's standards; the other area looked at in this project, found in Title 18, Article 11 of the Arizona Administrative Code. ~~For Class A water~~Shown in Table 2 are regulations for Class A water, which is used for many applications of reclaimed water including irrigation for school grounds and residential landscapes (AAC, 2008).~~, which is used for residential and schoolground irrigation, the 24-hour average turbidity of the filtered effluent must also be less than 2 NTU, the maximum concentration of fecal~~

~~coliform organisms is less than 23 per 100mL, and there can be no detectable enteric viruses found in four of the last seven reclaimed water samples taken (AAC, 2008).~~ [M2]

Table 2: Recycled Water Regulations for Irrigation Reuse

State	Turbidity[1]	Bacteria[2]	Virus Removal
California*	< 2 NTU	Total Coliform Bacteria: MPN < 2.2 per 100mL	99.999% removal of polio virus
Arizona**	< 2 NTU	Fecal Coliform Organisms < 23 per 100mL	No detectable enteric viruses found in 4 of last 7 water samples

*California Code of Regulations, 2009
**Arizona Administrative Code, 2008
[1]NTU - Nephelometric Turbidity Units
[2]Total coliform bacteria include bacteria found in soil, water, and human waste. Fecal coliform represent bacteria found in the intestines and feces of people and animals (Washington, 2012)

It[a3] is important to have different regulations for these categories of reuse because of the degree of human contact associated with the recycled water. Even with the regulations in place, contaminants can find their way through the treatment process and can potentially harm humans (Cooper et al., 2008).

Antibiotic Resistance Genes

Last year, the World Health Organization (WHO) recognized antimicrobial (which includes antibiotics) resistance as the topic of top priority for World Health Day and going into the future (WHO, 2011). The year 1998 brought 2.2 million deaths as a result of multi drug-resistance, and in the United States, 14,000 individuals die each year from illnesses caused by drug-resistant microbes in hospitals (WHO, 2000). These microbes are resistant to antibiotics due to their ARGs. The cause of the increased presence of these genes has been the focus of many new studies.

Over-prescription of antibiotics has been linked to the rise of antibiotic resistance as a result of mutation or horizontal gene transfer by microorganisms (Martinez, 2008). Overuse of antibiotics for livestock as growth stimulants and infection prevention could also be attributed to increased resistance (Novick, 1981)[a4]. Each ARG is targeted to resist a certain antibiotic; for example the *vanA* gene is resistant to vancomycin, a common antibiotic used to treat penicillin resistant *Staphylococcus aureus*. Vancomycin has been used as a "last resort" drug when other antibiotics have failed but may become obsolete due to resistant microorganisms and newer antibiotics (Levine, 2006). These new antibiotics are starting to see antibiotic resistance as well, thus perpetuating the antibiotic resistance cycle continues (Tsiodras, 2001). Studies are currently being done to identify the presence of ARGs in areas that consistently use recycled water, a possible transport of antibiotic resistant bacteria (McLain, 2010).

Research Methods

Site Description

The first set of recycled wastewater samples used in this experiment came from areas watered by the Rio de Flag Wastewater Reclamation Facility in Flagstaff, Arizona. This facility came about in the early 1990's when the city started to reach the limits of their drinking water supplies and the Wildcat Hill plant was reaching its design capacity (Rio, 2011). The reclamation plant diverts between four and six million gallons per day of raw sewage from the WWTP and treats it using primary sedimentation, aeration (nitrification and denitrification), primary and secondary clarifiers, filters, and UV sterilization. This last step avoids the addition of chemical additives for disinfection. The final product has about 99.5% of the pollutants removed and is considered "full body contact" quality so it can be used for recreational swimming areas and acceptable for industrial and commercial uses as well (Rio, 2011). Rio de Flag provides recycled water for twelve elementary schools, seventeen public parks/landscaping uses, and various golf courses and cemeteries. The eleven water samples came from a range of areas that the reclamation plant serves, including baseball fields, parks, and soccer fields (see Table 3~~2~~ for complete list of sample names and locations).

Table 3: Recycled Water Samples

Sample Origin	Sample ID	Sample Type	Sample Location
Flagstaff, AZ Rio de Flag (RdF)	RdF1	Water	Thorpe Park, Baseball Field North
	RdF2	Water	Bushmaster Park
	RdF3	Water	Thorpe Park
	RdF4	Water	Rio de Flag Construction Outlet
	RdF5	Water	Wildcat WWTP Outlet
	RdF6	Water	Rio de Flag WWTP Outside Faucet
	RdF7	Water	Thorpe Park, Baseball Field South
	RdF8	Water	Coconino HS, Baseball Field
	RdF9	Water	Foxglen Soccer Field
	RdF10	Water	Thorpe Soccer Field North
	RdF11	Water	Wheeler Park
California	1s	Swab	DPHS, upper baseball diamond sprinkler
	1w	Water	DPHS, upper baseball diamond sprinkler
	2s	Swab	DPHS, pitcher's mound
	2w	Water	DPHS, pitcher's mound
	3	Soil	DPHS, football field
	4	Swab	UCSB, student services building sprinkler
	5	Water	UCSB, baseball field sampling spigot
	6s	Swab	UCSB, student housing complex sprinkler
	6w	Water	UCSB, student housing complex sprinkler
	7	Water	UCSB manifold
	SBCCs	Swab	SBCC, campus sprinkler
	SBCCw	Water	SBCC, campus sprinkler

The second set of samples came from Dos Pueblos High School (DPHS) in Goleta, CA, University of California at Santa Barbara (UCSB), and Santa Barbara City College (SBCC). SBCC is currently using water from the El Estero Wastewater Treatment Plant while Dos Pueblos High School and UCSB are using water from the Goleta Sanitary District (City of Santa Barbara, 2012; Goleta Water District, 2012). Five of these samples are swabs of biofilms, or collections of bacteria growing on a surface. These were collected using a sterile cotton swab that was rubbed against the biofilm to pick up bacteria and then placed in a sterile centrifuge tube for testing. The biofilm samples from sprinklers were taken from inside a dismantled sprinkler head in order to prevent contamination. The soil sample was taken from the center of the high school football field while the grass was still wet from recently being watered and placed in a sterile centrifuge tube. The water samples were taken from either sprinkler heads or sampling spigots and also placed in sterile centrifuge tubes.

~~**Table 2: Recycled Water Samples**~~

~~Sample Origin~~	~~Sample ID~~	~~Sample Type~~	~~Sample Location~~
~~Flagstaff, AZ Rio de Flag (RdF)~~	~~RdF1~~	~~Water~~	~~Thorpe Park, Baseball Field North~~
	~~RdF2~~	~~Water~~	~~Bushmaster Park~~
	~~RdF3~~	~~Water~~	~~Thorpe Park~~
	~~RdF4~~	~~Water~~	~~Rio de Flag Construction Outlet~~
	~~RdF5~~	~~Water~~	~~Wildcat WWTP Outlet~~
	~~RdF6~~	~~Water~~	~~Rio de Flag WWTP Outside Faucet~~

	RdF7	Water	Thorpe Park, Baseball Field South
	RdF8	Water	Coconino HS, Baseball Field
	RdF9	Water	Foxglen Soccer Field
	RdF10	Water	Thorpe Soccer Field North
	RdF11	Water	Wheeler Park
California	1s	Swab	DPHS, upper baseball diamond sprinkler
	1w	Water	DPHS, upper baseball diamond sprinkler
	2s	Swab	DPHS, pitcher's mound
	2w	Water	DPHS, pitcher's mound
	3	Soil	DPHS, football field
	4	Swab	UCSB, student services building sprinkler
	5	Water	UCSB, baseball field sampling spigot
	6s	Swab	UCSB, student housing complex sprinkler
	6w	Water	UCSB, student housing complex sprinkler
	7	Water	UCSB manifold
	SBCCs	Swab	SBCC, campus sprinkler
	SBCCw	Water	SBCC, campus sprinkler
California	1s	Swab	DPHS, upper baseball diamond sprinkler
	2s	Swab	DPHS, pitcher's mound
	3	Soil	DPHS, football field
	4	Swab	UCSB, student services building sprinkler
	6s	Swab	UCSB, student housing complex sprinkler
	SBCCs	Swab	SBCC, campus sprinkler
	1w	Water	DPHS, upper baseball diamond sprinkler
	2w	Water	DPHS, pitcher's mound
	5	Water	UCSB, baseball field sampling spigot
	6w	Water	UCSB, student housing complex sprinkler
	7	Water	UCSB manifold
	SBCCw	Water	SBCC, campus sprinkler

Experimental Setup

In order to quantify and identify the bacteria using qPCR, DNA had to first be extracted. For the water samples, samples were preserved via a freeze drying process. In order to freeze dry the water samples, they were first put into 50mL aliquots and then stored in a -80°C freezer. A Labconco FreeZone Freeze Dry 4.5L Plus machine was used to remove the water from the frozen samples through a sublimation process. This process is done by lowering the temperate and pressure of the samples so the water can go from a solid state to a gaseous state while maintaining the integrity of the sample (Labconco, 2004). The samples containing the concentrated bacteria were placed back into the -80°C freezer until the DNA extraction could be performed.

An MPbio FastDNA Spin Kit (MP Biomedicals, Solon, OH) was used to extract the DNA from the sixteen water samples. Before the initial lysing step, the freeze dried samples had to be resuspended using the provided lysing buffer and nano-pure water. The kit could then utilize its lysing matrix and FastPrep machine to homogenize the samples. The released DNA was cleaned with a binding matrix and filtered into a catch tube for PCR analysis. The MPbio FastDNA Spin Kit for Soil was used for the soil and swab samples. This kit also utilizes a lysing matrix tube, but ensures proper lysing with ceramic beads and silica particles within the tubes. Buffers and the FastPrep machine were then used again to homogenize the sample and remove only the DNA, followed by a binding matrix and filter similar to the regular kit (MP Biomedicals, 2012).

Table 4: Genes of Interest

Gene Name	Antibiotic Resistance	Common Carrier	Pathogen Effects
16s rRNA	N/A	All heterotrophs	N/A
***mec*A**	Methicillin	*Staphylococcus aureus* (MRSA)	Known as staph infection, is a common cause of hospital infections that can spread to the heart, bones, lungs, and bloodstream with fatal results (ISDA, 2004)
***erm*F**	Erythromycin	*Staphylococcus aureus*	
***van*A**	Vancomycin	*Enterococcus spp.*	Can cause infections in blood, urinary tract and heart, and can be life-threatening (ISDA, 2004)
***tet*A**	Tetracycline	*Escherichia coli* (*E. coli*)	Virulent E. coli can cause gastroenteritis, UTI's, neonatal meningitis, HUS, peritonitis, mastitis, sepsis, and pnuemonia (Todar, 2007)
***tet*W**	Tetracycline		
***tet*O**	Tetracycline		
***sul*1**	Sulfonamide		
***sul*2**	Sulfonamide		

After the DNA was extracted, a qPCR analysis was completed. In order to use this machine, proper primers, an *Evagreen* master mix, and standards were needed. The Ssofast *Evagreen* master mix was mixed with water to a specific recipe and added to a designated tray for the machine. The standards and samples were added to this mix on the tray in triplicates before it is added to the machine. Primers are specific to the targeted gene and diluted to a concentration of 5µM to be used for the qPCR solution. *Evagreen* was the master mix being used for these tests and a component of this mix known as a fluorescence oligonucleotide, binds to the DNA within the samples and emits a fluorescence that is measured by the qPCR machine (Bio-Rad, 2012). Each gene (shown in Table 3) had a specific protocol used for the qPCR machine, varying the annealing temperatures and time based on past tests completed.

~~**Table 3: Genes of Interest**~~

A dilution of 1:50 was used for the samples for the following genes: *mec*A[a5], *van*A, *tet*A, *tet*W, *sul*1, and *sul*2. No samples were showing any *mec*A presence and only one was showing a consistent vanA presence with this dilution so optimization tests were performed for the qPCR. The optimization involved running a test with a temperature gradient in order to find the best annealing temperature for these genes using undiluted samples[a6]. Neither of the genes showed any presence during either optimization test. It was decided after this to use undiluted samples for the last two genes, *tet*O and *erm*F.

Data Collection & Analysis

The initial results obtained from the qPCR analysis included quantities of target genes in the samples for the triplicate measurements. In order to find the number of copies in the original samples, the triplicates' starting quantities [a7]were first averaged to give an average starting quantity for each sample. These numbers were then corrected to account for the DNA dilution and the overall treatment of the original samples. [a8]The water samples from Flagstaff originally had 50mL of water before freeze drying while the California water samples had 13-15mL. The final unit for the water samples is number of copies

per mL. The swab samples are given in units of copies per swab. For the soil sample, an original amount of 500mg was weighed out for the DNA extraction so this final unit is in number of copies per gram of soil.

It should be noted that the presence of the genes, *mec*A and *tet*W, was measured as well. The first test, using the 1:50 dilution of the DNA sample showed no presence of the genes. For *mec*A, the qPCR test was optimized to determine a better annealing temperature, but the gene still showed no presence using a temperature gradient. Both *mec*A and *tet*W are therefore being left out of the quantification data. Other data being excluded includes starting quantities that were below the detectable limit. With these samples, that included anything below ten copies because that was the lowest standard used for comparison.

Results & Discussion

Flagstaff, AZ

The set of 11 water samples from the Flagstaff area showed a presence for five out of the seven ARGs tested; *tet*W and *van*A were not detectable. The 16S rRNA gene was included as an indicator of the total bacterial density in each sample. Figure 1 shows the quantification of the genes for the Rio de Flag samples including the 16S rRNA gene as a comparison to see how much of the total bacteria contained the ARGs. Figure 2 shows the same samples normalized to the 16S rRNA gene.

The group of samples can be categorized by these results into samples that came from WWTP outlets and then distribution sites. Samples 4, 5, and 6 were from outlets of the WWTPs, and showed either one or zero ARGs present. This is substantially different from the distribution site samples (1-3, 7-11) which show three to five of the ARGs present. This difference suggests that the ARGs could be multiplying in the distribution system or transferring into the water from potential biofilms before dispersion.

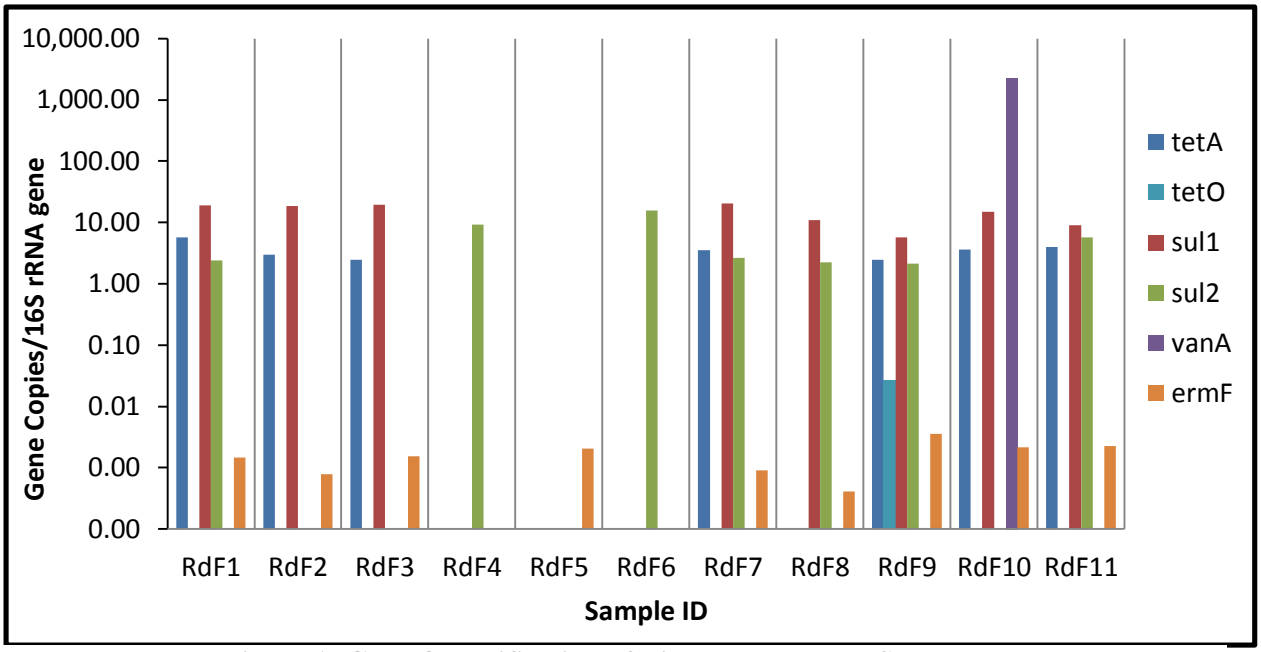

Figure 1: Gene Quantification of Rio de Flag Water Samples

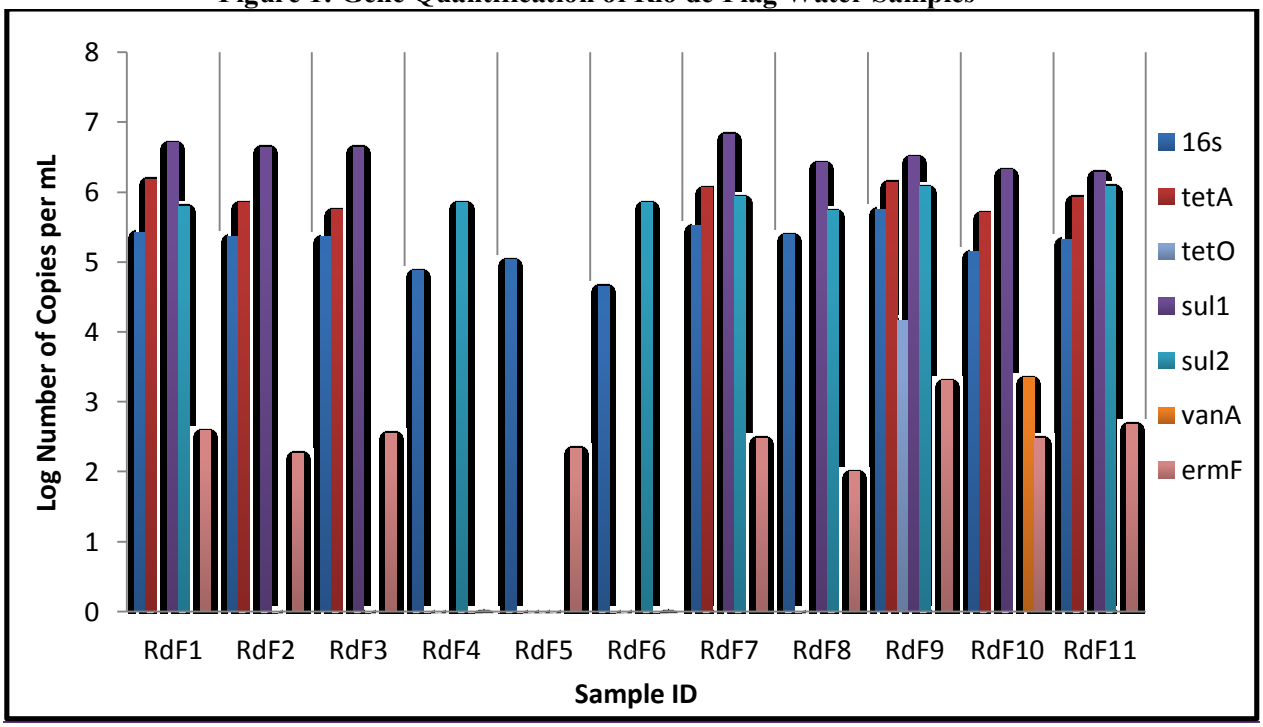

Figure 2: Gene Quantification of Rio de Flag Water Samples Normalized to 16S rRNA Gene

~~**Figure 1: Gene Quantification of Rio de Flag Water Samples**~~

G

~~The group of samples can be categorized by these results into samples that came from WWTP outlets and then distribution sites. Samples 4, 5, and 6 were from outlets of the WWTPs, and showed either one or zero ARGs present. This is substantially different from the distribution site samples (1-3, 7-11) which show three to five of the ARGs present. This difference suggests that the ARGs could be multiplying in the distribution system or transferring into the water from potential biofilms before dispersion.~~

~~[M9]Figure[a10] 2: Gene Quantification of Rio de Flag Water Samples Normalized to 16s[M11]~~

~~G~~oleta and Santa Barbara, CA

The samples from California include swabs and a soil sample, along with water from the recycled water distribution sites. Figure 3 shows the quantification of the ARGs including the 16s gene within the

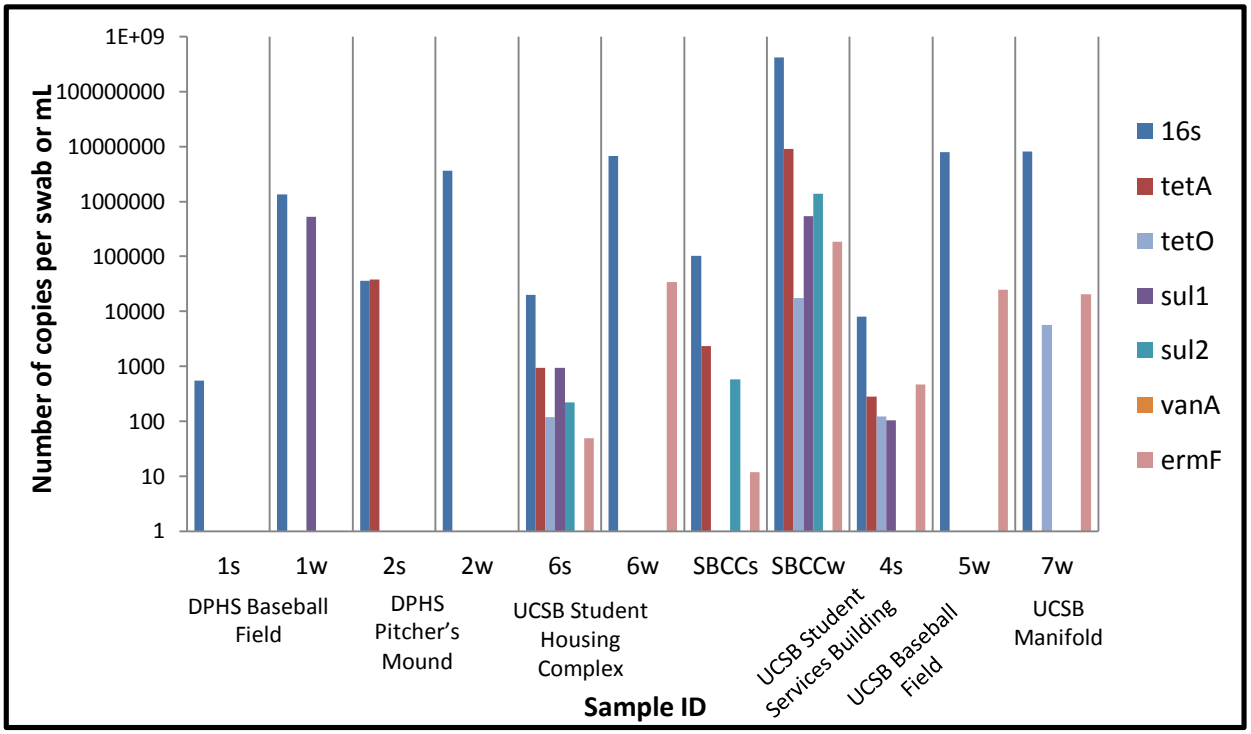

~~Figure 3: Gene Quantification of California Swab Samples~~

water and swab samples. As with the samples from Flagstaff, five of the seven ARGs appeared in the samples from California.

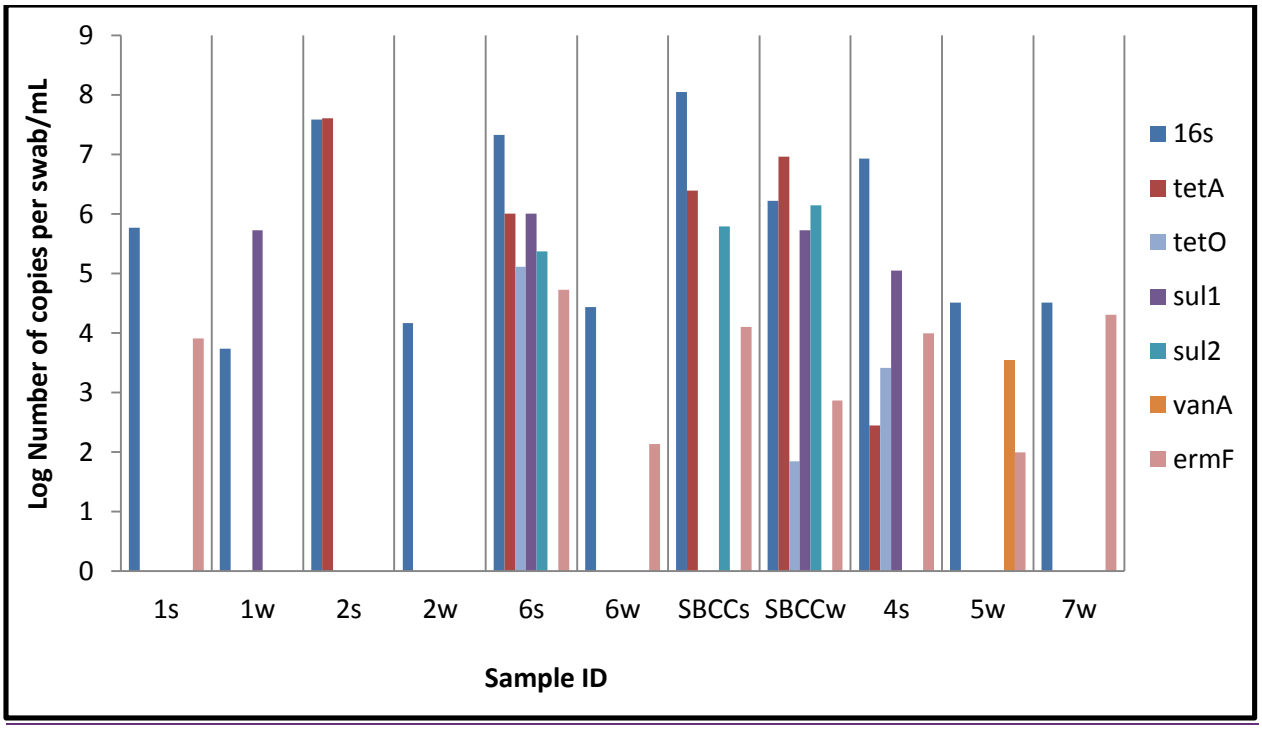

Figure 3: Gene Quantification of California Swab Samples

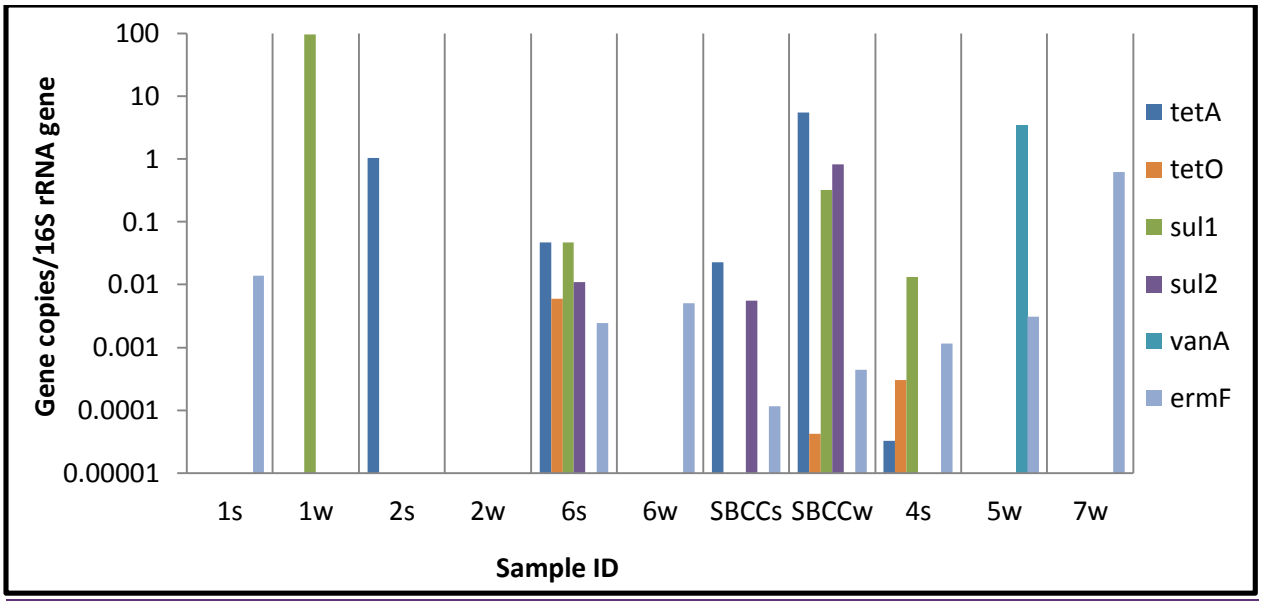

Figure 4: Gene Quantification of California Swab Samples Normalized to 16S rRNA Gene

From this data, there are no clear conclusions that can be made as to the ARGs being a result of the treatment plant or the swabbed biofilms. Figure 4 shows that in the samples from the UCSB student housing complex (6s, 6w) there were four more ARGs found in the swab sample, and in larger quantities. The opposite is shown for the samples from SBCC, in which the water sample contained the most ARGs. The units for comparing the swabs and water make it difficult to compare the two quantitatively, but the qualitative results show that biofilms should be researched more in how they potentially increase ARGs in

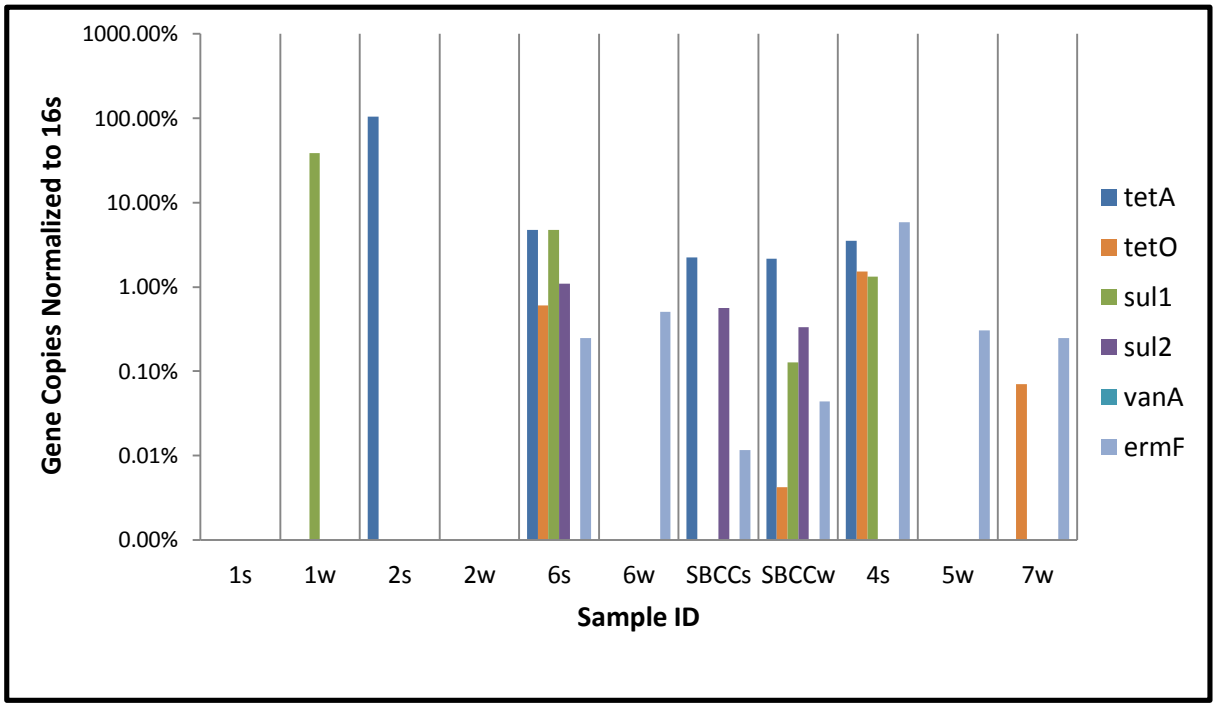

recycled water prior to distribution.

~~**Figure 4: Gene Quantification of California Swab Samples Normalized to 16s**~~[a12]

Figure 5: Gene Quantification of Soil Sample

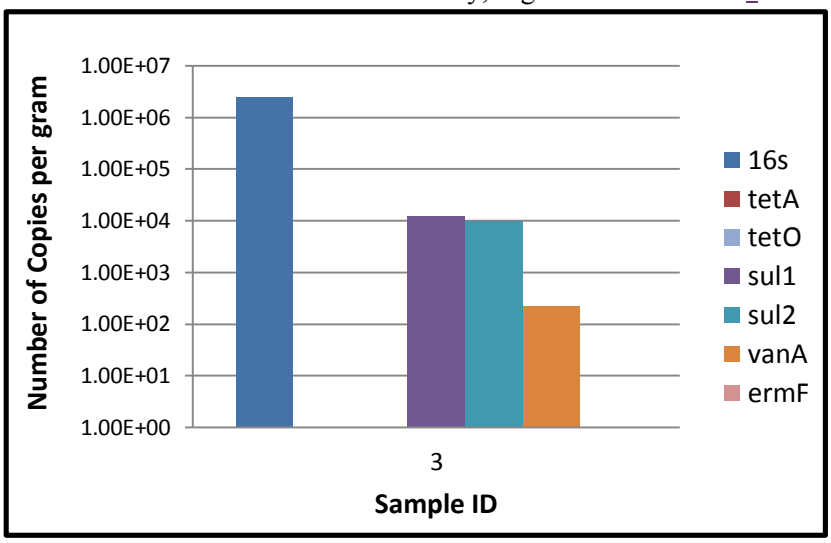

Lastly, Figures ~~5 and 6~~ shows the quantification for the soil sample from the football field at Dos Pueblos high school. This sample is being highlighted because of the *van*A that was detected~~, making it the only sample showing any vanA~~. Identifying any vancomycin resistant bacteria is important because vancomycin is used as a last resort antibiotic. Therefore, that resistance should be kept minimal if possible (Pruden et al., 2006). This sample is also showing higher amounts of the sul1 and sul2, indicating resistance to sulfonamides. While other samples may have more ARGs in higher amounts present, soil is a concerning medium to find presence of ARGs because of the high human contact associated with soil on athletic fields.

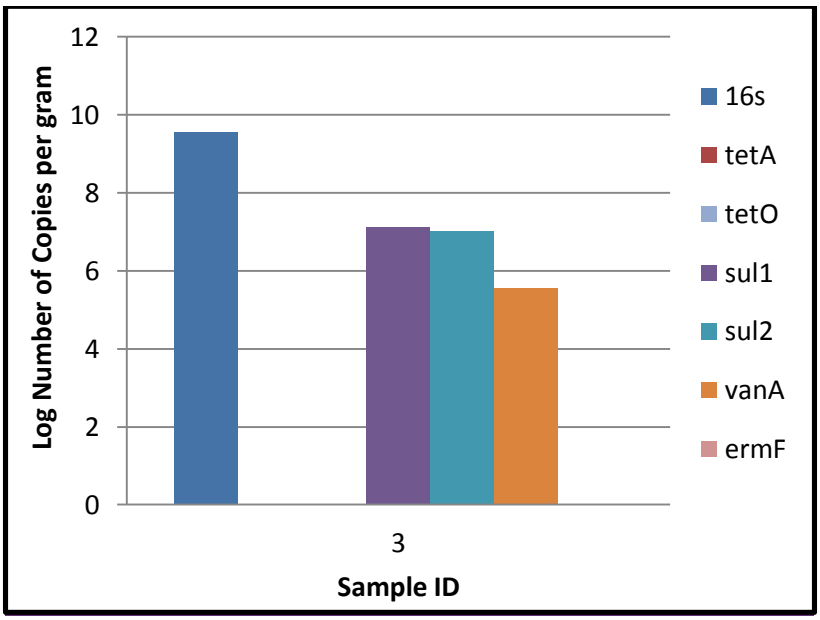

Figure 5: Gene Quantification of Soil Sample

Conclusions

There is no doubt based on the results above that ARGs are present within recycled wastewater. While some samples showed more genes than others, it was important to show the presence of the ARGs and check for the major players~~,~~ ; *mec*A and *van*A. Overall, the results from Flagstaff, AZ show that biofilms may play an important role in the propagation of ARGs within reclaimed wastewater. The concerned citizen who provided the samples, Dr. Silver, can use these results in his work to have schools use less reclaimed wastewater in areas that have higher amounts of direct student contact, and for more research to be done on the distribution of the recycled water itself. This is also true for Dr. McGowan,

who provided the samples from California, in his attempts to stop new housing developments in California from using reclaimed water for the unrestricted public reuses described in Table 1.

The WHO provided a slogan for their World Health Day last year which focused on antimicrobial resistance: "No action today, no cure tomorrow," (WHO, 2011). WHO's six step plan that was proposed last year includes developing a financed national plan, rationing the use of antibiotics for humans and animal husbandry, enhancing infection prevention, as well as continuing research and development of the issue. This plan will hopefully lead to the quantification of risk involving ARGs so regulations can be put into place in the future. While researchers, government officials, and WWTP operators have important roles to play in the suspension of ARGs being released into the environment, the public can help fix the problem as well. If more people are aware of the issue, more will check with their doctors about alternative treatments to antibiotics before accepting them and more will be conscious about the disposal of antibiotics within the household. Preventing ARG spread is a complex issue, but the more action taken now, the better of a chance future generations have in stopping it.

Acknowledgments

Funding for this project was provided by the National Science Foundation. We acknowledge the support of the National Science Foundation through NSF/REU Site Grant EEC-1062860. Any opinions, findings, and conclusions or recommendations expressed in this paper are those of the author(s) and do not necessarily reflect the views of the National Science Foundation. I would like to thank Dr. Vinod Lohani and Virginia Tech for the opportunity to perform research here through the Interdisciplinary Water Sciences and Engineering REU. A big thank you~~-~~ goes to Dr. Amy Pruden for ~~her~~ advising me throughout the research process this summer and for the opportunity to work on this project in the Pruden lab ~~at ICTAS II~~.[a13] I would like to especially thank Mark Mazzochette for his mentorship this summer. It was an honor to be taught by him and help with his thesis project. The lab work performed for the project, this paper, and my final presentation would not have been possible without him. My gratitude goes out to all of the members of the ICTAS II lab and those working under Dr. Pruden this summer, especially to Hong Wang and Virginia Riqeulme for their aid in using the freeze drying machine, and to Chad McKinney for his excellent "grand-mentoring" skills involving the qPCR process. Thank you to Dr. Robin Silver and Dr. Edo McGowan for providing the samples and motivation for my project. Lastly, I would like to thank my REU colleagues for all of their help and support this summer.

References ~~(still needs to be alphabetized)~~

Arizona Administrative Code, "Article 3. Reclaimed Water Quality Standards," Chapter 11. Department of Environmental Quality Water Quality Standards, *Title 18. Environmental Quality,* pp. 61-63, 2008.

Bio-Rad Laboratories, Inc., "Ssofast EvaGreen Supermix," Amplification: PCR Reagents, Bulletin 5816, Rev. B, 2012, http://www.bio-rad.com/webroot/web/pdf/lsr/literature/Bulletin_5816.pdf.

California Department of Health, "Article 3. Uses of Recycled Water," *Title 22 Code of Regulations*, pp. 12-17, 2009.

City of Santa Barbara, "Map of Recycled Water User Sites," El Estero Wastewater Treatment Plant, Jun. 2012, http://www.santabarbaraca.gov/Resident/Water/ Wastewater/WWRecycledWater.htm.

Cooper, Emily R, Thomas C Siewicki, and Karl Phillips. "Preliminary Risk Assessment Database and Risk Ranking of Pharmaceuticals in the Environment." *The Science of the total environment* 398.1-3 (2008): 26–33. Web. 2 Aug. 2012.

"Development of Antibiotic Resistance in Bacteria of Soils Irrigated with Reclaimed Wastewater."

Fatta-Kassinos, D. et al. "The Risks Associated with Wastewater Reuse and Xenobiotics in the Agroecological Environment." *Science of The Total Environment* 409.19 (2011): 3555–3563. Web. 28 June 2012.

Goleta Water District, "Recycled Water," 2012, http://www.goletawater.com/water-supply/recycled-water/.

Labconco, "A Guide to Freeze Drying for the Laboratory," pp. 4-6, 2004, http://chiron.no/pdf/Labconco_guide_to_freeze_drying.pdf.

Levine, D. P. "Vancomycin: A History." *Clinical Infectious Diseases* 42.Supplement 1 (2006): S5–S12. Web. 28 July 2012.

Martínez, José L. "Antibiotics and Antibiotic Resistance Genes in Natural Environments." *Science* 321.5887 (2008): 365–367. Web. 28 July 2012.

MP Biomedicals, "FastDNA SPIN Kit for Soil," 2012, http://www.mpbio.com/product_info.php?family_key=116560200.

Novick, Richard P. "THE DEVELOPMENT AND SPREAD OF ANTIBIOTIC-RESISTANT BACTERIA AS A CONSEQUENCE OF FEEDING ANTIBIOTICS TO LIVESTOCK*." *Annals of the New York Academy of Sciences* 368.1 (1981): 23–60. Web. 9 Aug. 2012.

Pruden, Amy et al. "Antibiotic Resistance Genes as Emerging Contaminants: Studies in Northern Colorado" *Environmental Science & Technology* 40.23 (2006): 7445–7450. Web. 28 June 2012.

Rio de Flag Wastewater Reclamation Facility, "Rio de Flag Reclaimed Water Plant," Flyer, 2011.

Tsiodras, Sotirios et al. "Linezolid Resistance in a Clinical Isolate of Staphylococcus Aureus." *The Lancet* 358.9277 (2001): 207–208. Web. 28 July 2012.

U.S. Environmental Protection Agency, "Guidelines for Water Reuse," Office of Wastewater Management: Municipal Support Division, Sep. 2004, pp. 1-4 http://www.epa.gov/nrmrl/wswrd/dw/smallsystems/pubs/625r04108.pdf

Washington State Dept. of Public Health, "Coliform Bacteria in Drinking Water," Web, 2012.

"WHO | World Health Day 2011: Policy Briefs." *WHO*. Web. 2 Aug. 2012.

~~A. Pruden, R. Pei, H. Storteboom, and K. H. Carlson, "Antibiotic Resistance Genes as Emerging Contaminants: Studies in Northern Colorado," Environmental Science & Technology, vol. 40, no. 23, pp. 7445–7450, Dec. 2006.~~

~~J. L. Martínez, "Antibiotics and Antibiotic Resistance Genes in Natural Environments," *Science*, vol. 321, no. 5887, pp. 365–367, Jul. 2008.~~

~~U.S. Environmental Protection Agency, "Guidelines for Water Reuse," Office of Wastewater Management: Municipal Support Division, Sep. 2004, pp. 1-4 http://www.epa.gov/nrmrl/wswrd/dw/smallsystems/pubs/625r04108.pdf~~

D. Fatta-Kassinos, I. K. Kalavrouziotis, P. H. Koukoulakis, and M. I. Vasquez, "The risks associated with wastewater reuse and xenobiotics in the agroecological environment," Science of The Total Environment, vol. 409, no. 19, pp. 3555–3563, Sep. 2011.

E. R. Cooper, T. C. Siewicki, and K. Phillips, "Preliminary risk assessment database and risk ranking of pharmaceuticals in the environment," Sci. Total Environ., vol. 398, no. 1–3, pp. 26–33, Jul. 2008.

"WHO | World Health Day 2011: policy briefs," WHO. [Online]. Available: http://www.who.int/world-health-day/2011/policybriefs/en/index.html.

J. L. Martínez, "Antibiotics and Antibiotic Resistance Genes in Natural Environments," Science, vol. 321, no. 5887, pp. 365–367, Jul. 2008.

A. Pruden, R. Pei, H. Storteboom, and K. H. Carlson, "Antibiotic Resistance Genes as Emerging Contaminants: Studies in Northern Colorado," Environmental Science & Technology, vol. 40, no. 23, pp. 7445–7450, Dec. 2006.

D. P. Levine, "Vancomycin: A History," Clinical Infectious Diseases, vol. 42, no. Supplement 1, pp. S5–S12, Jan. 2006.

S. Tsiodras, H. S. Gold, G. Sakoulas, G. M. Eliopoulos, C. Wennersten, L. Venkataraman, R. C. Moellering Jr, and M. J. Ferraro, "Linezolid resistance in a clinical isolate of Staphylococcus aureus," The Lancet, vol. 358, no. 9277, pp. 207–208, Jul. 2001.

J. McLain, C.F. Williams, "Development of Antibiotic Resistance in Bacteria of Soils Irrigated with Reclaimed Wastewater," 5th National Decennial Irrigation Conference, Vol. 1, Dec 2010.

Rio de Flag Wastewater Reclamation Facility, "Rio de Flag Reclaimed Water Plant," Flyer, 2011.

City of Santa Barbara, "Map of Recycled Water User Sites," El Estero Wastewater Treatment Plant, Jun. 2012, http://www.santabarbaraca.gov/Resident/Water/Wastewater/WWRecycledWater.htm.

Goleta Water District, "Recycled Water," 2012, http://www.goletawater.com/water-supply/recycled-water/.

Labconco, "A Guide to Freeze Drying for the Laboratory," pp. 4-6, 2004, http://chiron.no/pdf/Labconco_guide_to_freeze_drying.pdf.

MP Biomedicals, "FastDNA SPIN Kit for Soil," 2012, http://www.mpbio.com/product_info.php?family_key=116560200.

Bio-Rad Laboratories, Inc., "Ssofast EvaGreen Supermix," Amplification: PCR Reagents, Bulletin 5816, Rev. B, 2012, http://www.bio-rad.com/webroot/web/pdf/lsr/literature/Bulletin_5816.pdf.

R. P. Novick, "THE DEVELOPMENT AND SPREAD OF ANTIBIOTIC-RESISTANT BACTERIA AS A CONSEQUENCE OF FEEDING ANTIBIOTICS TO LIVESTOCK*," *Annals of the New York Academy of Sciences*, vol. 368, no. 1, pp. 23–60, 1981.

Arizona Administrative Code, "Article 3. Reclaimed Water Quality Standards," Chapter 11. Department of Environmental Quality Water Quality Standards, *Title 18. Environmental Quality*, pp. 61-63, 2008.

California Department of Health, "Article 3. Uses of Recycled Water," *Title 22 Code of Regulations*, pp. 12-17, 2009.

Study and Application of a Real-Time Environmental Monitoring System

Manuel Martinez*, Aaron Bradner**, Daniel Brogan***, Mark Rogers**, Parhum Delgoshaei*** and Vinod K. Lohani***

** NSF-REU fellow, Virginia Polytechnic Institute and State University*
(Home Institution: Virginia Polytechnic Institute and State University)
*** Department of Civil and Environmental Engineering, Virginia Polytechnic Institute and State University*
**** Department of Engineering Education, Virginia Polytechnic Institute and State University*

ABSTRACT

A LabVIEW Enabled Watershed Assessment System (LEWAS) Lab has been under development on VT campus since 2008. The outdoor site of LEWAS is located on the Webb Branch, just upstream of Duck Pond. The goal is to collect, store, and wirelessly communicate real-time water (quality and quantity) and weather data for water sustainability research and education. This interdisciplinary lab supports research work of students in various disciplines including engineering education, civil and environmental engineering, electrical and computer engineering and chemical engineering. The LEWAS uniquely integrates LabVIEW's data acquisition capability with the water and weather hardware. Specifically, it includes a Hydrolab which collects water quality data; a Flow Meter, which measures flow and stage of the stream; and a weather station which collects weather data. In this research, calibration procedures for water and weather hardware were established. Real-time water and weather data were collected for a number of storm events in summer 2012 and rainfall-runoff analysis is in progress. Using LabVIEW File I/O, a Virtual Instrument (i.e., program) for storing weather data was written. A case study to analyze environmental impacts of a water main break in the town of Blacksburg is developed to show the importance of a real-time environmental monitoring system.

Keywords: Real-Time Monitoring, Environmental Monitoring System, LabVIEW, Stroubles Creek, Water Main Break

Introduction

Since 2008, a LabVIEW Enabled Watershed Assessment System (LEWAS) Lab is being developed at Virginia Tech. This work was initiated as part of a NSF project funded under the Department-Level Reform (DLR) program (Lohani, et al., 2011). The goal is to collect, store, and wirelessly communicate real-time water (quality and quantity) and weather data for water sustainability research and education To achieve this goal, the LEWAS Lab uses a Hydrolab Sonde MS5, which measures water temperature, pH, conductivity, turbidity, and dissolved oxygen; a Sontek Flow Meter, which measures flow and stage of the stream; and a Vaisala Weather Station, which measures barometric pressure, air temperature, relative humudity, speed and direction of the wind, and amount of precipitation. LabVIEW, a programming software, developed by the National Instruments (www.NI.com), created to deploy measurement and control system through hardware integration , is used to remotely collect data through its data acquisition capability. LabVIEW communicates with all hardware components to aquire data and then processes the data and makes it available over the Internet using its web publishing capability. A schematic representation of LEWAS is shown in figure 1. As can be seen, digital data from various hardware components are processed by LabVIEW and resulting data graphs are made availbale to potential users over the Internet.

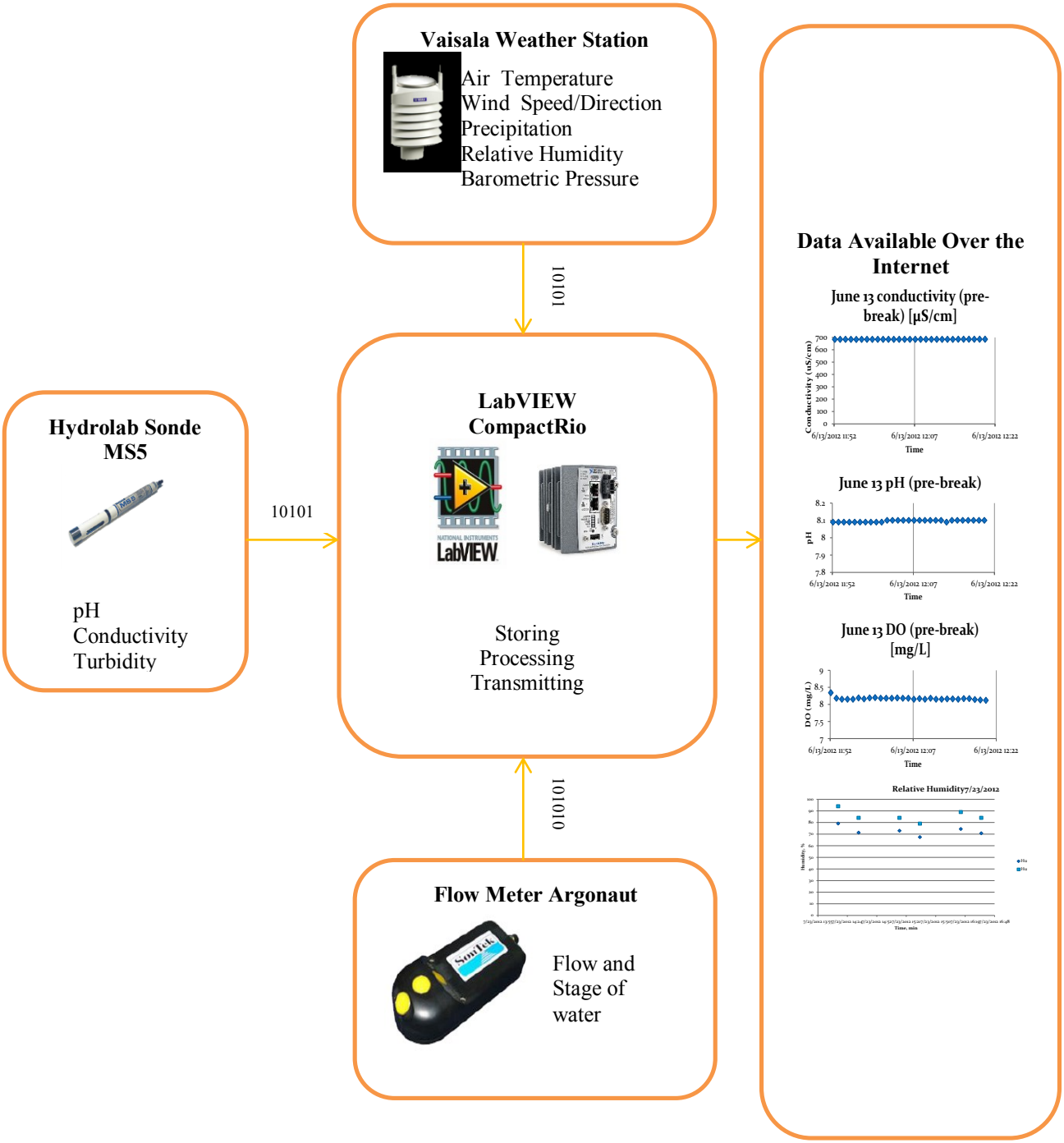

Figure 1: Operational Diagram of LEWAS

LEWAS Site

The outdoor site of LEWAS is located on Webb Branch, just upstream of the Duck Pond, of the Stroubles Creek. This stream originates in the town of Blacksburg and flows through Virginia Tech campus, an area that is mainly urban and residential (see figure 2). . It meets with Stroubles Creek at the outlet of the Duck Pond and flows into the New River. Webb Branch is part of the Stroubles Creek Watershed, a 1,975 acres watershed (Parece, et al. 2010). The current set up of the lab is shown in figure 3. The box shown is this figure houses an embedded computer for processing data.

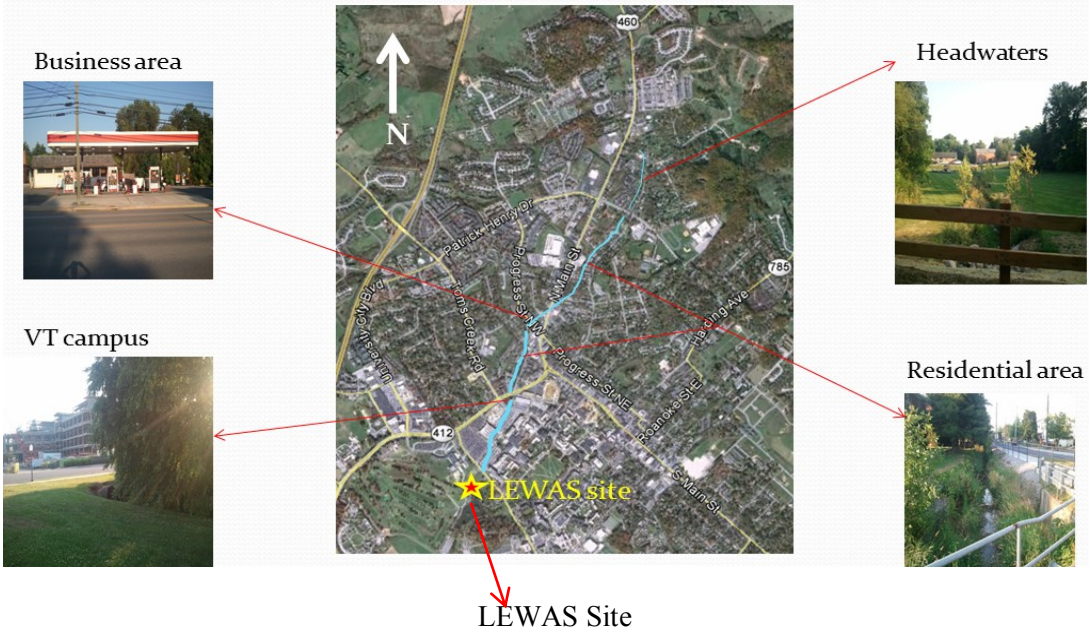

Figure 2: Satalite Picture of Webb Branch from its Headwaters until LEWAS Site

Figure 3: A closer look to LEWAS Site

A system similar to LEWAS is deployed by the Southern Nevada Water Authority (SNWA). It has on-site hydrolabs to monitor the quality of the water of the Wash, an urban river that runs through Southern Nevada. This system measures temperature, pH, turbidity, conductivity, and dissolved oxygen.

It is reported that observations at this system are taken every 20 minutes and the data can be accessed hourly (Las Vegas Wash Coordination committee, 2012). LEWAS sensors can collect data as often as every second and the data can be observed in a real-time.

Calibration of Hardware Components of LEWAS

In order to collect high quality data, each instrument deployed at LEWAS site must be periodically calibrated. Based on experience and consultation with researchers, it is decided to calibrate the sensors of the Hydrolab Sonde MS5 every two weeks. The calibration of the flow meter is being conducted by a graduate student as part of his M.S. thesis (Rogers, 2012).

The Vaisela Weather Station is calibrated by its manufacturer. However, it was decided to validate the data collected by this station by making comparisons with data collected at neighboring meteorologic stations such as the National Weather Service Office in Blacksburg.

Research Methods

Calibration of the Hydrolab MS5 Sonde

Figure 4: Calibration of Hydrolab Sonde

The calibration process of sonde typically requires two people (see figure 4). A software by Hack Hydromet called Hydras3 LT is used to assist in the calibration process. Hack Hydromet has provided calibration videos which were followed to calibrate the Hydrolab: (http://www.hydrolab.com/web/ott_hach.nsf/id/pa_videos_and_transcripts.html). Briefly, the first step was to clean all the sensors using a soft brush and mild soap. Then the Hydrolab was connected to a laptop through an USB port and Hydras3 LT software was executed which enables the connection between the hardware and software. Once connected, the calibration tab was opened to perform the calibration process. More details on Hydrolab calibration are given in Welch, et al., 2011. In the following, a brief discussion of the calibration process for various water parameters is given.

pH

pH is a measurement of the amount of Hydrogen ions in the water. It determines whether a solution is acidic, basic, or neutral. To support a diverse aquatic population, a stream must have a pH between 6 and 9 (NC State University, 2012). Blacksburg is located in a limestone area so the stream water is expected to have high pH values. The pH sensor of sonde includes two electrodes, one for a measurement and the other as a reference. The measuring electrode, which is the glass bulb, is chemically "doped" with lithium ions so that it reacts with the hydrogen ions in the water outside the bulb. This causes an electrochemical reaction generating voltage across the glass bulb, which then corresponds to a certain pH level (Welch, et al., 2011). The pH calibration is a two-point calibration. We started by checking whether the reference junction looks worn or the circle is brown, if so, it had to be replaced. For this research, there was no need to replace it. For the first calibration, the electrolyte solution inside the pH sensor was replaced. For the first point calibration, a pH 7 buffer solution was used. For the second point calibration, he could have used either a pH 4 buffer solution or a pH 10 buffer solution, depending on the expected pH range. Since Blacksburg is located in a limestone area, and the pH is normally relatively high, a pH 10 buffer solution was used.

Turbidity

Turbidity is a measurement of the cloudiness of the water. This cloudiness is produced mainly by the presence of sediments in the water. To support a diverse aquatic population, the turbidity of a stream must be lower than 30 NTUs (NC State University, 2012). As per the reference manual, the Self Cleaning Turbidity sensor measures the intensity of light scattered by particles in the water sample at 90 degrees from an infrared light source and reports that value in NTUs (Hach Hydromet, 2012). For the calibration process, deionized water was used to establish the zero point calibration and a standard solution that was 100 NTU was used for the high end point calibration.

Conductivity

Conductivity is a measurement of the ability of water to pass electric current. It is due mainly to the presence of dissolved inorganic solids in the water (EPA, 2012). To support a diverse aquatic population, a stream should have a conductivity that ranges between 150 and 500 µS/cm (NC State University, 2012). Hach Hydromet recommends calibrating the conductivity sensor before calibrating the DO (Clark Cell) sensor. The conductivity sensor contains a cathode and an anode and it measures the current between the ions (Welch, et al, 2011). For the calibration process, deionized water was used for the zero-point calibration and a standard solution of 1412 µS/cm was used for the high-end-point calibration.

Dissolved Oxygen

Dissolved oxygen (DO) is a measurement of the amount of free oxygen in the water. DO is affected by water temperature, the higher the temperature, the lower the amount of dissolved oxygen in the water; by nutrients which produce excessive plant grow, those plant consume the dissolved oxygen, and by sediments, the higher the amount of sediments in the water, the lower the amount of dissolved oxygen (EPA, 2012). To support a diverse population, a stream must have more than 5 ppm of dissolved oxygen (NC State University, 2012). The DO sensor consists of two electrodes surrounded by an electrolyte solution and covered with an oxygen permeable membrane. As oxygen crosses the membrane, it is consumed in a chemical reaction which generates a small electrical current between the electrodes. The current measured is directly proportional to the amount of oxygen in the water sample (Hach Hydromet, 2011). For the calibration process, the absolute barometric pressure was used. This number was obtained from the National Weather Service website and was uncorrected using the equation BP'=BP-2.5(A/100), where BP' is the absolute barometric pressure, and A is the altitude in ft.

Deployment of the Hydrolab Sonde MS5 for data collection at LEWAS Site

Figure 5: Deployment of Hydrolab at the LEWAS site

For this research, Hydras3 LT was used to collect the data using the Hydrolab. First, the Hydrolab was connected to a computer, using a USB port that had the Hydras3 LT software loaded. The software was opened and a communication between the software and the hardware was established. Once connected, the System tab was selected and the Hydrolab time was synchronized with the computer clock. Next step was to select the Log File tab, and create a name for the file. LEWAS researchers name the files using the following format: month_day_year_brief_explanation.
For example, July_10th_2012_24_hours_test. Then the starting time and end time were set, and the logging interval was chosen. For this research, a 3- minute logging interval was used. Then the parameters to be measured were selected. In this study, water temperature (ºC), pH (units), conductivity (µS/cm), dissolved oxygen (mg/l), turbidity (NTU), and % voltage left on internal batteries were chosen. These setting were then saved and system was enabled. It is very important to remember to click the Enable button. Once the setting were, chosen the Hydrolab was unplugged from

the computer and set in the water (see figure 5). Once data was collected, the Hydrolab is removed from the water and connected back to the computer. The Hydras3 LT software was opened and a connection between the software and hardware was established. The Log File tab was opened and the data was downloaded and saved in an Excel sheet. It is recommended to delete the data from the Hydrolab after it has been saved in a computer because the Hydrolab can only hold four log files. Examples of the data collected are given in results and discussion section.

Data Logging System in LabVIEW for the Vaisala Weather Station and Data Validation

The existing weather data LabVIEW VI implemented into LEWAS can display data in real-time, but it cannot store this data. The VI was edited and a File I/O was written that enabled the VI to store data into an SD card. Also, the user interface of the VI was edited to make it look cleaner and user-friendly. In addition, units were added to the graphs, the color was changed to blue, and the LEWAS Logo was added to the VI. The data from the Vaisala Weather Station was validated by comparing LEWAS station data with the data available from the National Weather Service in Blacksburg. Also, a contact was made with a faculty member in the Biological System Engineering Department to obtain data from their weather station.

Results and Discussion

Water Main Break Case Study

On June 26th, 2012, around 4:30 pm, a water main broke in the town of Blacksburg, VA. By 9:00 pm, the water spill was contained. Approximately 760 m^{3}of drinking water was spilled into Webb branch watershed during this 5.5 hours-long water main break. LEWAS lab started collecting data for this event at 7:45 pm. Figure 6 displays flow conditions at LEWAS site during normal flow and after the water main broke. This event impacted the quality of water in Webb Branch for a few hours and as a result a large number of fish died. Most of the water quality parameters returned to their normal levels within 24 hrs. or so.

Figure 6: LEWAS Site during normal flow **LEWAS Site after the water main broke**

As can be seen in figure 7, after about 3 hours of the water main break, turbidity increased to 300 NTU from a pre-break level of 1-2 NTU. Also, it can be seen that within 24 hrs or so the tubidity value returned to its normal base flow range (between 0 and 3 NTU).

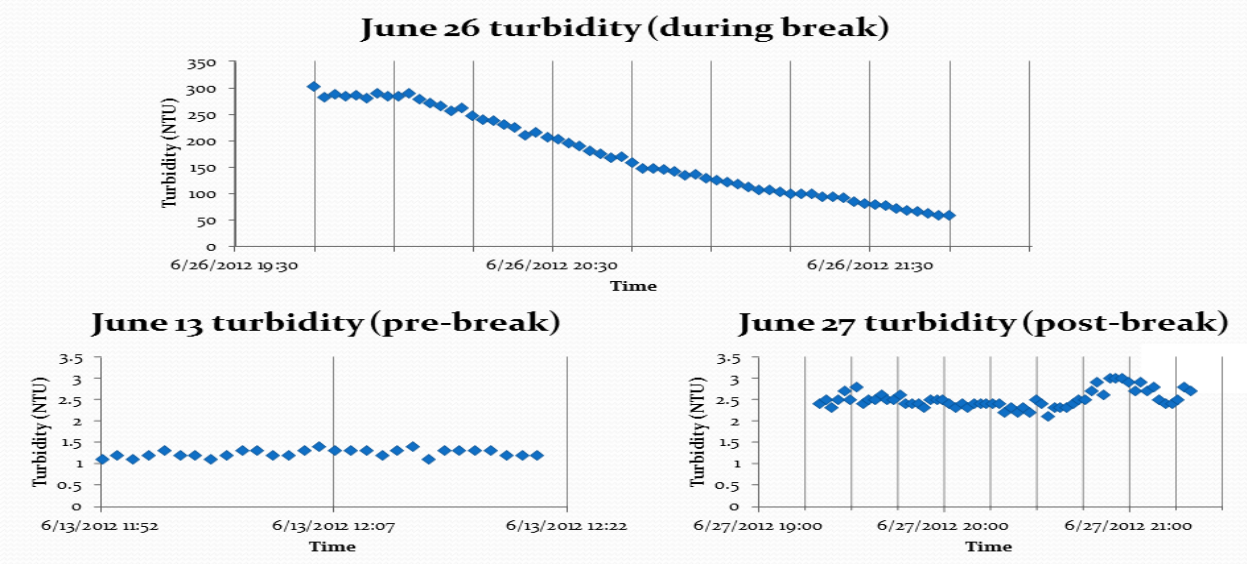

Figure 7: Effect of the broken main on turbidity

Figures 8 shows that conductivity went down from its normal range between 600 and 700 µS/cm to about 300 µS/cm, which is expected because the water spilled was drinking water. The conductivity of Blacksburg tap water was later tested and it was 150 µS/cm.

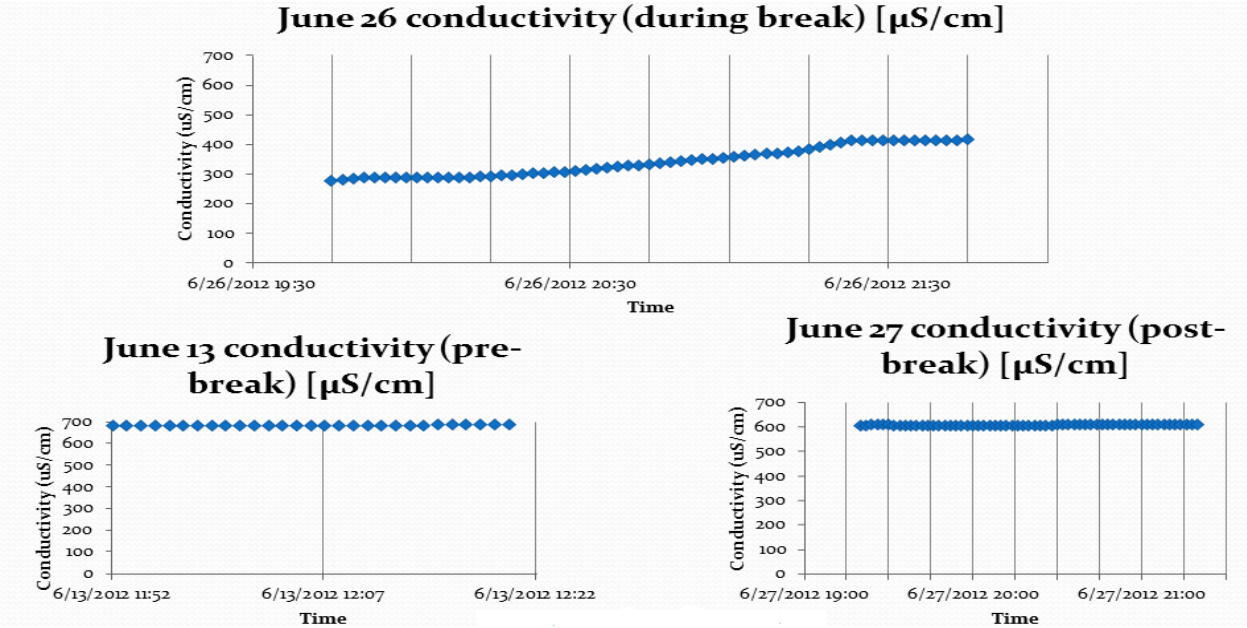

Figure 8: Effect of the broken main on conductivity

Figure 9 shows impact on DO levels as a result of water main break. It went down from its normal range of about 8.5 mg/L to 7.1 mg/L and it was not completely recovered the next day. This was probably due to the large amount of sediments getting into the water.

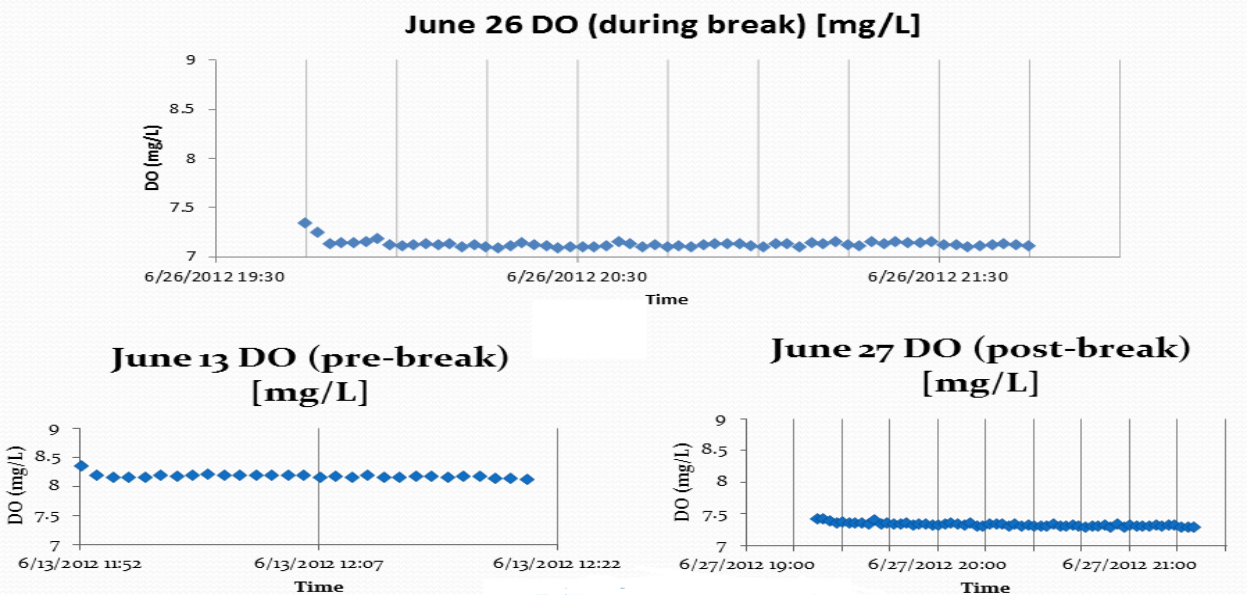

Figure 9: Effect of broken main on DO

Figure 10 shows impact on pH of creek water and the change seen is within the margin of error of the sensor (0.2 units)

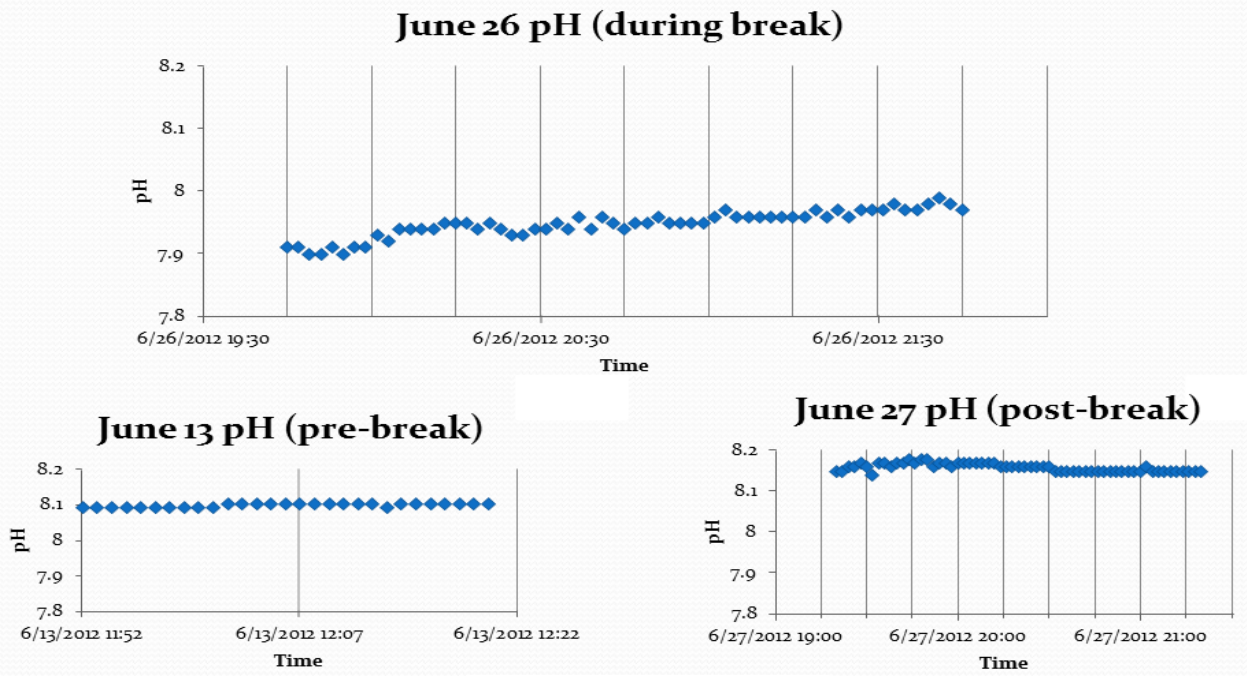

Figure 10: Impact of broken main on pH

Ecological Impacts

Authors observed dead fish all over the Webb Branch downstream of the water main break point (see figure 11). After consulting with two experts (Dr. Orth from the Fishery Department and Dr. Benfield from the Biological Sciences Department) the dead fish was identified as Blacknose Dace and two possible explanations were given for the fish kill. 1. Dr. Orth felt that fish died due to the chlorine contained in the drinking water. 2. Dr. Benfield believes that the high turbidity suffocated the fish. It may be noted that impact of this event lasted a few hours only and continuous data from LEWAS site provided some reasonable explanation for fish kill.

Figure 11: Fish kill at LEWAS Site

LabVIEW Weather Station Virtual Instrument (VI)

The Block Diagram of the weather VI was edited to store data. A subVI which receives data from the weather station and writes it to a file in the SD card contained in an embedded computer at LEWAS site computer was created.

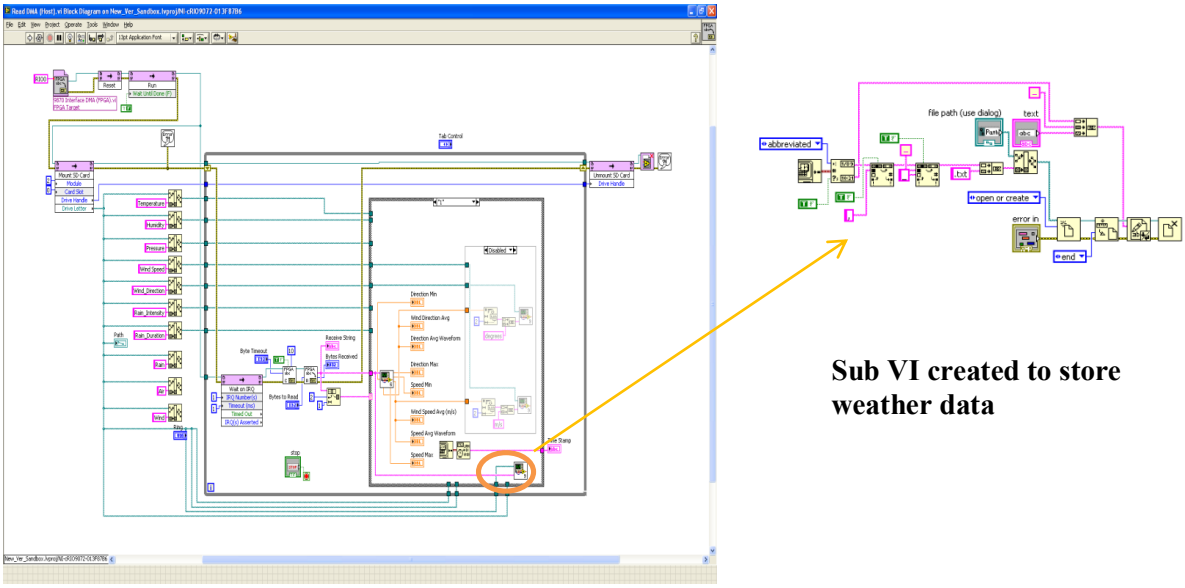

Figure 12: Weather VI Block Diagram

The Front Panel of the weather VI was edited to make it more user-friendly. Proper names and correct units were added to each parameter. Graphs were spaced evenly. Background color was changed to blue and LEWAS logo was added (see figure 13).

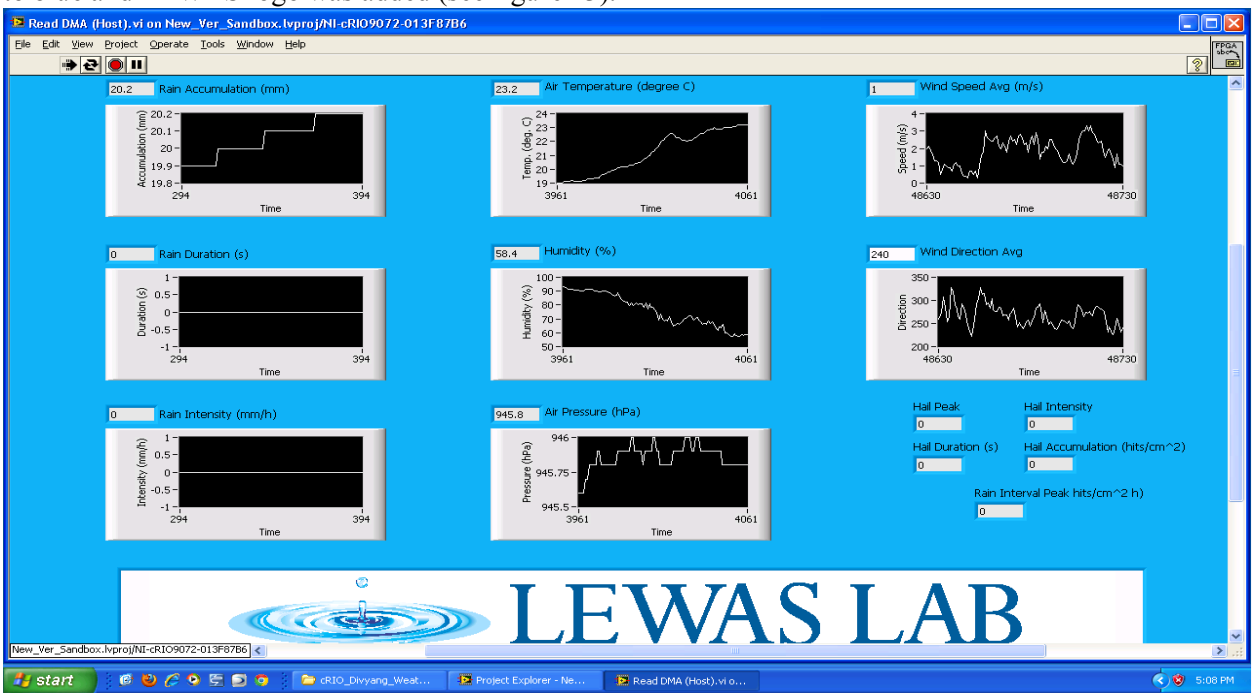

Figure 13: Front Panel of the Weather VI

Vaisala Weather Station Data Validation

Figure 14 shows the location of the LEWAS site and its nearby weather stations, National Weather Service, and BSE weather station.

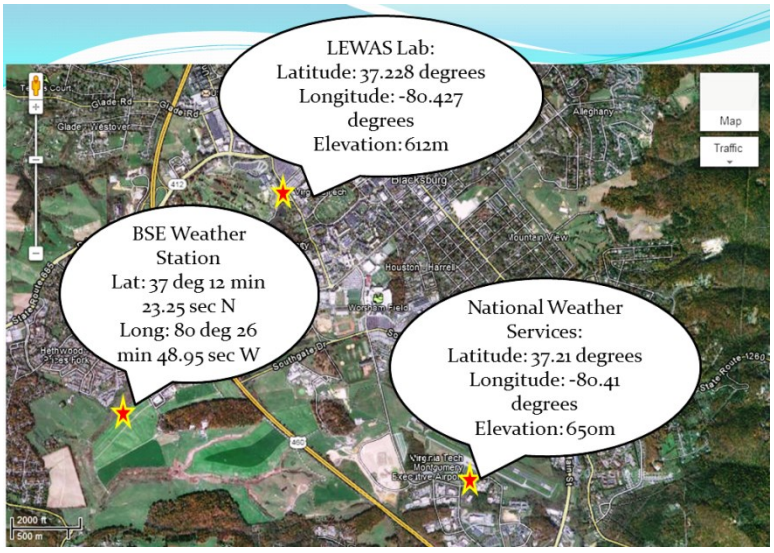

Figure 14: Location of the LEWAS outdoor site, National Weather Service, and BSE weather station

Weather parameters were recorded at LEWAS Site on July 23rd, 2012 and these are compared with data from other station. The barometric pressure reported by the LEWAS Lab is about 0.1 in Hg lower than that of the National Weather Service (figure 15). Though these numbers are very close, it does not make sense because LEWAS Lab is located at a lower altitude than the National Weather Service and one would expect the air pressure to be higher at a lower altitude. This suggests some kind of calibration problem.

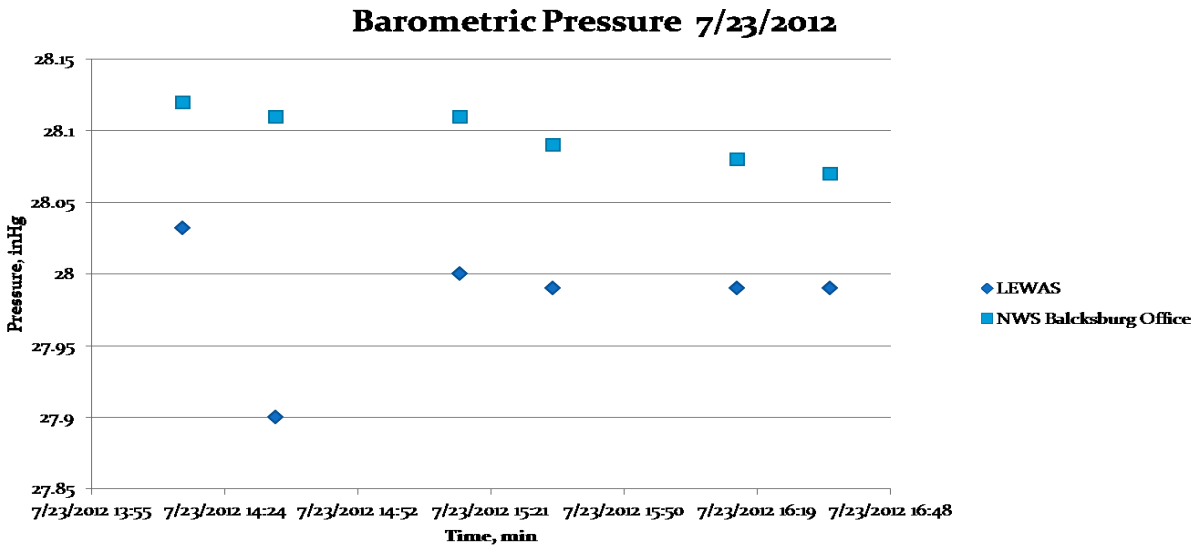

Figure 15: Barometric Pressure at LEWAS site and National Weather Service station on July 23rd, 2012

The humidity reported at LEWAS station is between 11% - 14% lower than the humidity reported by the National Weather Service (see figure 16). The two sites are very close to have such a large difference in humidity. This also suggests some kind of calibration problem.

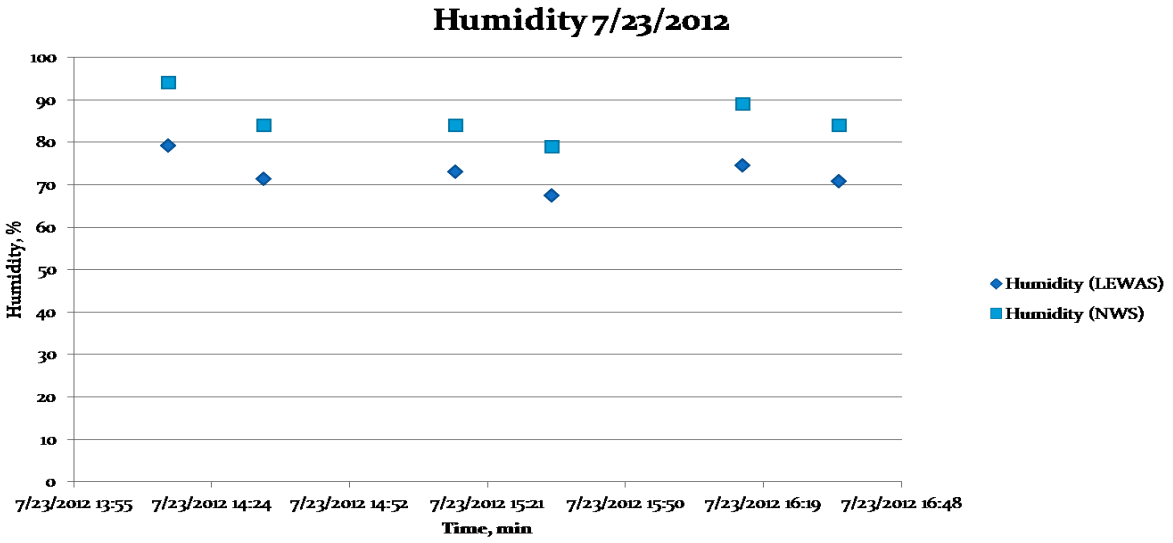

Figure 16: Humidity at LEWAS site and National Weather Service station on July 23rd, 2012

As seen above, the humidity and air pressure data collected by the Vaisala Weather Station are off when compared with the data from the National Weather Service Office located in Blacksburg After consulting the manufacturer, it was learned that the PTH (pressure, temperature, and humidity) module of the sensor needs replacement and actions to replace the module are in progress.

Summary

During the 10-week summer project, the lead author had the opportunity to work in an interdisciplinary team to study a real-time environmental monitoring system. This taught him how to work with students from different majors to solve environmental related problems. It gave him skills to solve problems that are not directly related to his chemical engineering background. Examples of some scientific concepts that he learned during the study are:

- Relationship between land use and water quality
- Relationship between water quality and ecology
- Basics of LabVIEW programming and data acquisition
- Integration of software and hardware components of a real-time environmental monitoring system

The broken water main case study is a good example of the importance of having a real-time environmental monitoring system. This event was responsible for killing a large number of fish. For many days, there was a strong odor of dead fish all over the Webb Branch. Real-time monitoring provides a way to identify impacts of short-term events such as the water main break. Using traditional methods for collecting water quality data, impacts of such short-term events cannot be identified unless the events cause permanent change to the water quality regime of the stream.

Last academic year, I took ENGE 1024, which is the first course that all engineering students have to take at Virginia Tech. In this course I learned the basic of LabVIEW programming. The last day of class we were given a LEWAS demo to demonstrate the application of LabVIEW in solving real-world problems. I thought that the project was very interesting and that is why I decided to join the LEWAS team. I attended an NSF project workshop on August 2nd in which it was discussed to incorporate LEWAS into a Virginia Tech senior hydrology course at VT and to Virginia Western Community College in Roanoke. It feels good to know that data I am helping to collect will be used for educational purposes.

Recommendations for Future Work

The broken main demonstrated that there is a need for a chlorine ion sensor in the system. Also, it would be good to start monitoring biological parameters of the stream such as amount of chlorophyll and algae. It is necessary to solve the programing issues with the cRio computer so that the three instruments can be used at the same time. Finally, it is necessary to edit the VIs to make it possible for users to switch between tabs and instruments, add help files so that users know what each parameter represents, and finally to give the opportunity for users to download data.

Acknowledgements

I would like to thank my research mentor Dr. Vinod K Lohani and his graduate students Aaron Bradner, Daniel Brogan, Mark Rogers and Parhum Delgoshaei for their continuous help and support during this 10- week summer project. It has been a great opportunity and a great experience to work these interdisciplinary researchers. We acknowledge the support of the National Science Foundation through NSF/REU Site Grant EEC-1062860. Any opinions, finding, and conclusion or recommendations expressed in this paper are those of the author (s) and do not necessarily reflect the views of the National Science Foundation.

References

Biological Systems Engineering (BSE), Virginia Tech, 2012. Stroubles Creek Watershed Stormwater BMPs. Accessed July 2012<http://www.tmdl.bse.vt.edu/stormwater/C131/>

Environmental Protection Agency (EPA), 2012. Monitoring and Assessment.Accessed June 2012. <http://water.epa.gov/lawsregs/lawsguidance/cwa/tmdl/index.cfm>

Hach Hydromet, 2010. Calibration Videos and Transcripts. Accessed June 2012. <http://www.hydrolab.com/web/ott_hach.nsf/id/pa_videos_and_transcripts.html>

Las Vegas Wash Coordination Committee, 2012. "Real Time Water Quality Monitoring" Accessed July 2012. < http://www.lvwash.org/html/being_done_research_realtime.html>

Lohani, V. K.; Wolf, M.; Wildman, T.; Mallikarjuna, K.; and Connor, J., 2011. Reformulating General Engineering and Biological Systems Engineering Programs at Virginia Tech, Advances in Engineering Education Journal, ASEE, vol 2, no. 4, pp. 1-3.

North Carolina State University, Biological and Agricultural Engineering Department, 2012. Water Quality. Accessed June, 2012 <http://www.bae.ncsu.edu/programs/extension/wqg/volunteer/man_ch3.htm>

Parece, Tammy; DiBetitto, Stephanie; Sprague, Tiffany; Younos, Tammi. 2010. "The Stroubles Creek Watershed: History of Development and Chronicles of Research" Virginia Polytechnic Institute and State University, Blacksburg, VA.

Rogers, M. 2012, Calibration of flow at LEWAS site, M.S. thesis. Submitted to VT, Fall 2012.

Welch, Stephanie; Rogers, Mark; Lohani, V. K. 2011. "Calibration of Real-Time Water Quality Monitoring Devices." Virginia Polytechnic Institute and State University, Blacksburg, VA.

Investigating the Occurrence and Fate of 4-Nonylphenol in a Watershed Impacted by Urban Development

Jennifer Moutinho*, Theresa Sosienski**, Dr. Kang Xia**

** NSF-REU fellow, Virginia Polytechnic Institute and State University*
(Home Institution: Chemical Engineering, Worcester Polytechnic Institute)
***Department of Crop & Soil Environmental Science, Virginia Polytechnic Institute and State University*

ABSTRACT

Urban development has prompted increasing concerns about organic chemical concentrations in fresh water sources due to urban and agricultural runoff. Endocrine disrupting compounds are of particular concern due to their effect on ecosystems and wide use in many consumer products and crop fertilizers. Investigating the level of a common anthropogenic endocrine disrupting compound, 4-nonylphenol, will improve understanding the extent of impact urban development has on the water quality of urban watersheds. The purpose of this study is to determine the occurrence of 4-nonylphenol within the Stroubles Creek Watershed in Blacksburg, Virginia to help gain a better understanding of the environmental impacts of urban development. Throughout this study, water and sediment samples were collected at six different locations along the creek. Extraction and cleanup of 4-nonylphenol in the water samples was performed using solid phase extraction. 4-nonylphenol in the sediment samples was extracted using ultrasonication and cleaned up using silica gel. The analysis of 4-nonylphenol in the final extract was conducted on a gas chromatography-tandem mass spectrometer. The levels of 4-nonylphenol in the water samples were detected at 100's ng/L, while in the sediment samples they were detected at 1000's μg/kg. This investigation helped determine the relationship between the concentration of 4-nonylphenol and different types of urban development.

Keywords: endocrine disrupting compound, 4-nonylphenol, water, sediment, gas chromatography-tandem mass spectroscopy, and urban development

Introduction

Endocrine Disrupting Compounds

The endocrine system exists in all animals. The role of the endocrine system is to produce hormones to regulate basic functions including development and reproduction. Certain chemicals, when absorbed by an organism, can act as endocrine disruptors due to their similar structure to natural hormones. When anthropogenic (man-made) chemicals act as endocrine disruptors, organisms can experience brain and sexual developmental problems as well as birth defects (Diamanti-Kandarakis E et al., 2009). A wide range of endocrine disruptors exist in the environment, as shown in Figure 6 below. Each endocrine disruptor mimics a different hormone allowing it to bind to the specific hormone's receptor decreasing the number of produced hormones that are able to create the correct response within the organism.

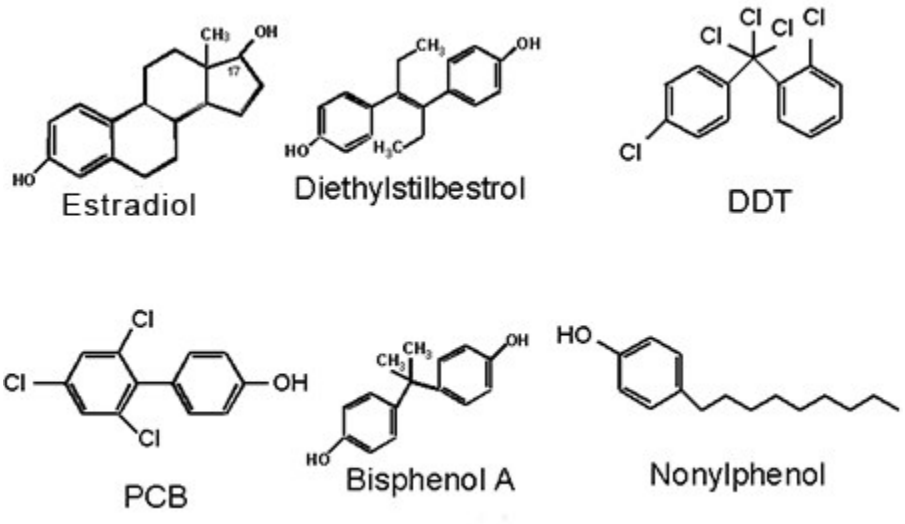

Figure 6: Examples of different Endocrine Disrupting Compounds (Southern California Coastal Water Research Project, 2011)

4-Nonylphenol

The basic structure of 4-nonylphenol is a compound with a hydroxyl group (OH group) in para position to a nine carbon chain on a benzene ring. The configuration of the nine carbon-chain however is unspecified giving 4-nonylphenol many different isomers. Shown in Figure 7 are a number of 4-nonylphenol isomers. Shown in Figure 8 are two 4-nonylphenol isomers that compare closely with the structure of estradiol, a natural hormone used to help regulate reproduction and sexual function. Due to this similar structure, 4-nonylphenol has been studied for the effects it has on reproduction and sexual development within various ecosystems (Cox, 1996). A statewide endocrine disrupting monitoring study in Minnesota sampled a wide range of lakes and rivers as well as fish to determine the presence of endocrine disrupting compounds in the different locations around the state. The fish were specifically studied to determine if levels of the protein vitellogenin increased signifying feminization in male fish since vitellogenin is associated with reproduction in female fish. The study found detectible levels of vitellogenin in male fish in all locations signifying that fish are affected by endocrine disrupting compounds in the environment (Mark Ferrey, et al., 2010). Another study testing the effects of 4-nonylphenol on Japanese Medaka fish reported both disruptions in reproduction as well as development. The Medaka fish were exposed to different concentrations of nonylphenol for the first three months of their development. The study found that 50% of the male fish had both testicular tissue and true oocytes (ovarian tissue) in the gonad when they were exposed to 50 ppb aqueous solutions of 4-nonylphenol for 3 months. At 100 ppb for 3 months, 86% of male fish developed testis-ova, an intersex condition where both testicular and ovarian tissue in the gonad (Gray & Metcalfe, 1997).

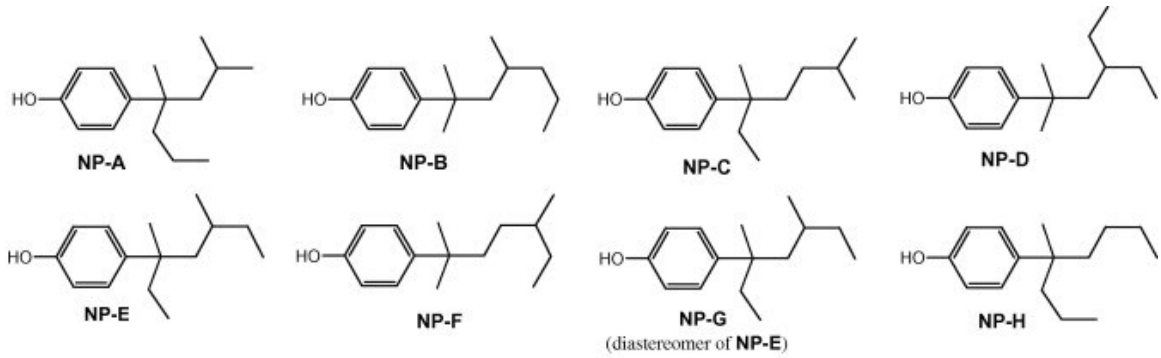

Figure 7: Examples of 4-nonylphenol isomers (Uchiyama, Makino, Saito, Katase, & Fujimoto, 2008)

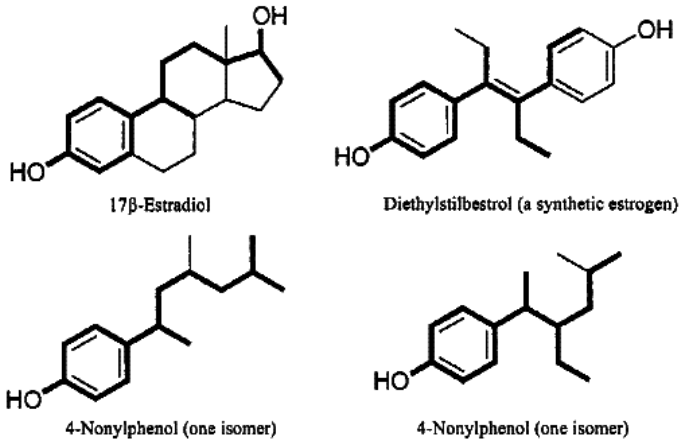

Figure 8: Structure comparison of estradiol and 4-nonylphenol isomers (Reinhard & Montgomery-Brown, 2003)

While nonylphenol can be used directly, the majority of all nonylphenol produced is used in intermediate steps when producing other chemicals. A common chemical is nonylphenol polyethoxylates used as nonionic surface active agents since the 1940s in many industrial processes including textile and plastic manufacturing, paper production and recycling, agricultural fertilizers and pesticides, industrial oil soluble detergents, lubricants, and household cleaning supplies (Office of Water, 2005) (Starratt & Topp, 2000). Nonylphenol polyethoxylates were common in household laundry detergents; however by 2010 the EPA had worked with manufacturers to eliminate their use. Industrial laundry detergents still contain a large amount of nonylphenol polyethoxylates, however it is projected that by 2013 nonylphenol polyethoxylates will be no longer in liquid detergents and by 2014 nonylphenol polyethoxylates will no longer be in power detergents commonly used at industrial laundry facilities such as textile rental shops (U.S. Environmental Protection Agency, 2012). The major route of entry for nonylphenol polyethoxylates into the environment is wastewaters discharged by industries and municipal sewage treatment plants (Soares, Guieysse, Jefferson, Cartmell, & Lester, 2008) (Ahel, Giger, & Koch, 1994). Although the nonylphenol polyethoxylates are relatively hydrophilic and nontoxic, microbial degradation of these compounds both in wastewater treatment plants and the environment leads to the formation of hydrophobic and more toxic nonylphenol compounds (Writer, Ryan, Keefe, & Barber, 2012). Due to its high use in commercial products, 4-nonylphenol contaminate levels can be used as indicator of urban influence on an ecosystem (Strauch, et al., 2008) (Kolpin, et al., 2006).

Nonylphenol is a pale yellow color with an octanol/water partition coefficient or K_{OW} of 4.48 explained by the hydrophobic hydrocarbon chain giving the compound a low solubility in water (Ahel & Giger, 1993) (Brix, Hvidt, & Carlsen, 2001)(White, House, & John, 2000). Concentrations of nonylphenol existing in the environment has been studied around the globe (Bennie D. T., 1999). A study around the Great Lakes region reported concentration levels in water samples ranging from <0.010 to 0.92µg/L and concentration levels in dry weight sediment samples ranging from 0.17 to 72 µg/g (Bennie, Sullivan, Lee, Peart, & Maguire, 1996). Sewage treatment plants in Canada were studied finding levels of 4-nonylphenol in effluent ranging from 0.32 to 3.21µg/L(Lee, Peart, & Svoboda, 2005) and a study performed on samples from wastewater treatment plant effluent in North Carolina found concentrations of 4-nonylphenol between 1 and 2.5µg/L (Naylor & Kubeck, 1990). An investigation of three wastewater treatment plants reported biosolid concentrations of 1.3mg/kg, 1.24mg/kg, and 300mg/kg (Xia, Keller, Bhandari, & Wagner, 2001) and a study performed on 20 different active sewage treatment plants found 4-nonylphenol in 11 at concentrations up to 12.400µg/kg(Hale, et al., 2000). In a report released by the EPA in 2010, fresh water quality criteria for nonylphenol are 28µg/L for acute and 6.6µg/L for chronic exposure (U.S. Environmental Protection Agency, 2012).

Relationship between Sediment and Water

Due to its hydrophobic characteristics and high K_{OW} value, 4-nonylphenol has an affinity to organic matter in sediment as well as dissolved organic matter in water (Zwolsman & Goossens, 1996). Both natural events such as rain and anthropogenic activities have the potential to resuspend the organic contaminant within the sediment into the water increasing the possible degradation process (Thomas & Eggleton, 2004). Most studies focus on laboratory and model based results helping to explain the effects of natural and anthropogenic disturbances, there is a need then for field-based research to better understand the effects of disturbances on resuspension (Roberts, 2012).

Stroubles Creek Watershed

Historically the town of Blacksburg, Virginia was founded due to the existence of Stroubles Creek as a drinking water source and benefit to business (Randolph, 1993). With the development of many large apartment complexes, residential neighborhoods, and the Virginia Tech campus located within the Stroubles Creek Watershed, the majority all residential and agricultural runoff now collects in the creek. Figure 9 shows a Stroubles Creek Watershed and its relationship with the Town of Blacksburg.

Figure 9: Stroubles Creek Watershed (Department of Biological Systems Engineering)

Due to the extent of runoff collecting in the creek, Stroubles Creek has been added to the Clean Water Act list of impaired waters. With this notification, the Stream Restoration, Education, and Management (StREAM) Lab was starting in the Virginia Tech community in an effort to remove Stroubles Creek from the impaired waters list. Efforts include a long-term stream quality monitoring program focusing on nutrient loading and biological indicators as well as on microbial contamination from cattle and bank restoration to reduce erosion. The StREAM Lab currently doesn't monitor the organic contaminant concentrations that are possibly present in the creek water or bed sediment. An important side note, while Stroubles Creek is no longer the drinking water source for Blacksburg, Stroubles Creek drains into the New River, which is currently the drinking water source for the town of Blacksburg and many other neighboring communities.

Overall Goal

Determine the occurrence of 4-nonylphenol within the Stroubles Creek Watershed in Blacksburg, Virginia to help gain a better understanding of the environmental impacts of urban development.

Research Methods

Field Work

About 800mL of water and 400mL of sediment samples were collected each Monday along with an 800ml field blank. Preparation for sampling began about 30 minutes before departure time where 20 – 500ml amber sampling bottles are collected and labeled. Two bottles were filled with ultrapure water before leaving for field blank samples. A cooler was also filled with ice to ensure that the samples stayed chilled during the sampling. A small crate containing a shovel for sediment collection, paper towels, a solution of 50:50 methanol/water for sterilizing the shovel between sites, a small dropper-topped bottle containing concentrated hydrochloric acid, and nitrile gloves was refilled and carried during sampling. Sampling occurred in conjunction with a PhD student under Dr. Kromeitis from BSE who drove a truck to each sampling site. At each sampling site, two bottles were used to collect water samples from the center of the creek and one bottle was used to collect sediment from the top centimeter of the creek bed. All samples were preserved using five drops of hydrochloric acid and stored in the ice cooler. The field blanks were exposed to the air at the last site and preserved using the same process. After returning to the lab with the samples, six 10mL glass vials are filled with each sediment sample and all the samples are frozen with the caps removed to prevent the glass bottles from breaking.

Water and sediment samples were collected for six different sites along the Stroubles Creek Watershed. The sites are located at the inlet of the Duck Pond where the creek first emerges from under the Drillfield, the outlet of the Duck Pond after the dam, the bridge on Plantation Road, Bridge 1, Bridge 2, and Bridge 3. Bridge 1 is located directly after a large apartment complex while Bridge 2 and 3 are located within agricultural fields. Sampling is collected from downstream to upstream to reduce effect of sediment sampling on other samples. Figure 10 and Table 2 shows and explains a map of the sampling sites as well as the lab location.

Table 2: Sampling Site Map Key

Sampling Site	Colored Marker
Smyth Hall	Purple
Duck Pond in (DPin)	Green
Duck Pond out (DPout)	Light Blue
Plantation Road Bridge (PR)	Pink
Bridge 1 (B1)	Orange
Bridge 2 (B2)	Blue
Bridge 3 (B3)	Yellow

Figure 10: Sampling Site Map

Extraction and Cleanup Procedure for Water Samples

200mL of each samples was measured out and transferred into a clean amber bottle after melting no more than 48 hours before the samples were to be run. Along with the seven samples and the field blank, 200ml of ultrapure water and 200ml of ultrapure water spiked with 4-nonylphenol to 1 µg/L were used to help determine the method recovery for 4-nonylphenol. All nine samples were extracted using with Solid Phase Extraction (SPE) with a vacuum pump to regulate the flowrate of the treatment. To pre-condition the SPE, Oasis HLB cartridges (3ml/60mg, Waters) were conditioned by passing 3ml of methanol followed by 3 ml of ultrapure water to equilibrate the cartridge at the flow rate of 5 ml/minute. The 200ml of water was then passed through the HLB cartridge at a flowrate of 2ml/minute. To remove the unwanted components from the cartridge and partially remove the interfering organic material, the cartridge was washed with 5ml of 5% methanol aqueous solution and 5 ml of ultrapure water respectively at a flow rate of 4ml/min. The cartridge was then dried under vacuum for 45 minutes to remove all moisture. The final step was to elute the 4-nonylphenol from the cartridge into a 12ml glass vial placed under the cartridge using two 3 ml washes of dichloromethane/acetone (7:3, v/v) at a flow rate of 2ml/min. The 6ml of eluted sample was concentrated under a stream of nitrogen gas at 7 psi until completely dry, re-dissolved with 0.5ml of acetone, transferred to a 2ml GC vial, and analyzed using a gas chromatography-tandem mass spectrometer (GC/MS/MS).

Extraction and Cleanup Procedure for Sediment Samples

Two grams of freeze dried sediment (particle size < 2mm) was mixed with 10mL of acetone/hexane (1:1, v/v) solution in a 12ml glass vial. Along with the 6 samples, 10ml of pure acetone/hexace (1:1, v/v) solution and 10ml of 4-nonylphenol spiked solution at 1 μg/L were used to help determine the method recovery for 4-nonylphenol. All eight samples were mixed thoroughly and sonicated for 20 minutes in a room temperature ultrasonication bath. The samples were then centrifuged at 3500rpm for 10 minutes at 22°C. Simultaneously, silica gel cartridges are prepared using cleaned 3ml cartridges by layering one gram of silica gel followed by one gram of sodium sulfate. The silica gel cartridge was pre-conditioned with 3ml of methanol and 3ml of hexane. A 15ml vial was used to collect the sample passing through the conditioned cartridge. Keeping the cartridge wet was important throughout the whole conditioning and eluting process. The 6mL of eluted samples was concentrated under a stream of nitrogen gas at 7 psi until completely dry, re-dissolved with 0.5mL of acetone, and analyzed using a gas chromatography-tandem mas spectrometer (GC/MS/MS).

GC/MS/MS Analytical Procedure

GC-MS/MS analysis was performed using a gas chromatograph (7890A, Agilent, USA) coupled with an Agilent 7000 series triple quadrupole GC/MS detector and a 7693 autosampler. The GC/MS/MS conditions were as follows: The initial column was held at 60°C for 0.5 min, increased to 100°C at 15°C min^{-1} ramp rate, further increased to 200 °C at 5°C min^{-1} ramp rate, and finally increased to 280°C at 25°C min^{-1} ramp rate. The backflush time is 3.0188min making the whole time for a cycle 26.867min. The inlet temperature, transfer line temperature, and the ion source temperature were set at 200°C, 250°C, and 200°C, respectively. The analytical column is HP-5MS (30 m × 0.250 mm i.d., 0.25um film thickness, Agilent, USA) and with a backflush column of Agilent res. (0.78m×150 um ×0 um). Splitless mode was used at a Helium gas flow rate of 2.25 mL min^{-1}. The injection volume was 1 uL and the collision gas used was nitrogen. The x compound was qualified by electron impact at 70 eV using multiple reaction monitoring (MRM) mode. The MS/MS quantification and confirmation ions are m/z (107+121+135+149). According to the elute pattern of the isomers, four time segments were set in the MRM method. Transitions used are listed in Table 3.

Table 3: Time segment, confirmation and quantization ions and transitions for MS/MS analysis

Time Segment (min)	Quantification and confirmation ions (m/z)	Quantification and confirmation Transitions (m/z)			
5-19.50	121+135	--	121→103 121→77	135→107 135→77	--
19.50-19.97	107+121+135+149	107→77 107→51	121→103 121→77	135→107 135→77	149→121 149→107
19.97-20.17	107+121+135+149	107→77 107→51	121→103 121→77	135→107 135→77	149→121 149→107
20.17-20.57	107+121+135+149	107→77 107→51	121→103 121→77	135→107 135→77	149→121 149→107
20.57-21.50	107+121+135+149	107→77 107→51	121→103 121→77	135→107 135→77	149→121 149→107

The results from the GC-MS are displayed as chromatograms. Figure 11 below shows the chromatogram of a 400μg/L standard. Technical grade 4-nonylphenol purchased from Sigma Chemical (St. Louis, MO) was used as external standard for the qualification and the quantification of total 4-nonylphenol (summation of areas of all the 4-NP peaks). The graph is created as counts vs acquisition time in minutes. In order to quantify the concentration of the 4-nonylphenol each sample, the peak area is determined using the program from 19 to 19.2 minutes and from 19.8 to 21.5 minutes. In Figure 11, this is

shown by the shaded area under the peaks within this range. Since 4-nonylphenol has many isomers, the different peaks represent the different isomers all of which are important to include when determining the concentration of 4-nonylphenol in the samples.

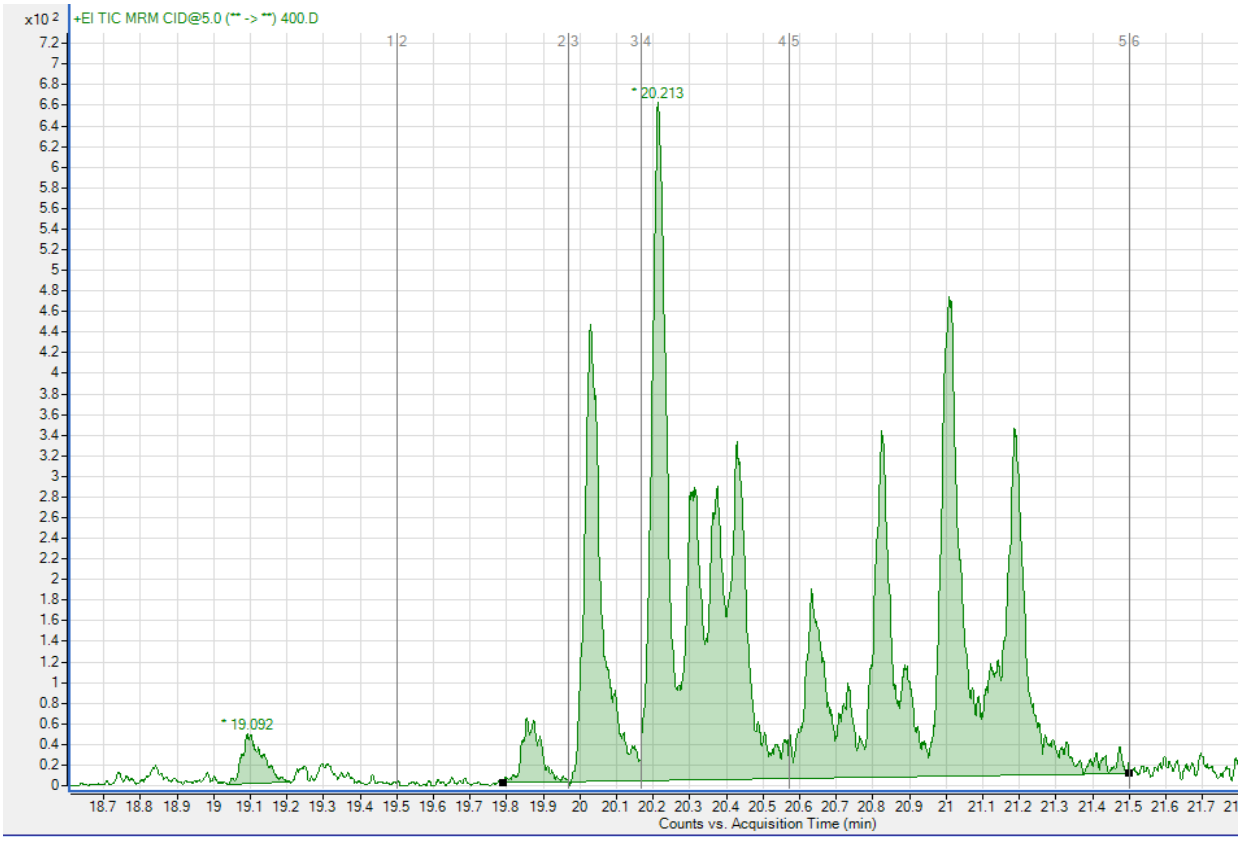

Figure 11: Chromatogram of the 400µg/L standard run on July 3, 2012

The area of the peaks is used in conjunction with the calibration curve to determine the 4-nonylphneol concentration in the final extract. The concentration of the final extractant in the 2mL GC vial multiplies the extraction concentration factor of the corresponding result in 4-nonylphenol concentration in the water or sediment sample.

Results and Discussion

Figure 12 shows a chromatogram for a 400ppb 4-nonylphenol standard. Figure 13 shows a chromatogram of a water sample and Figure 14 shows a chromatogram of a sediment sample. The similarity of the isomer pattern between the standard and that of the samples implies that the 4-nonylphenol existing in the environment has a low degradation rate leading to the buildup of the compound.

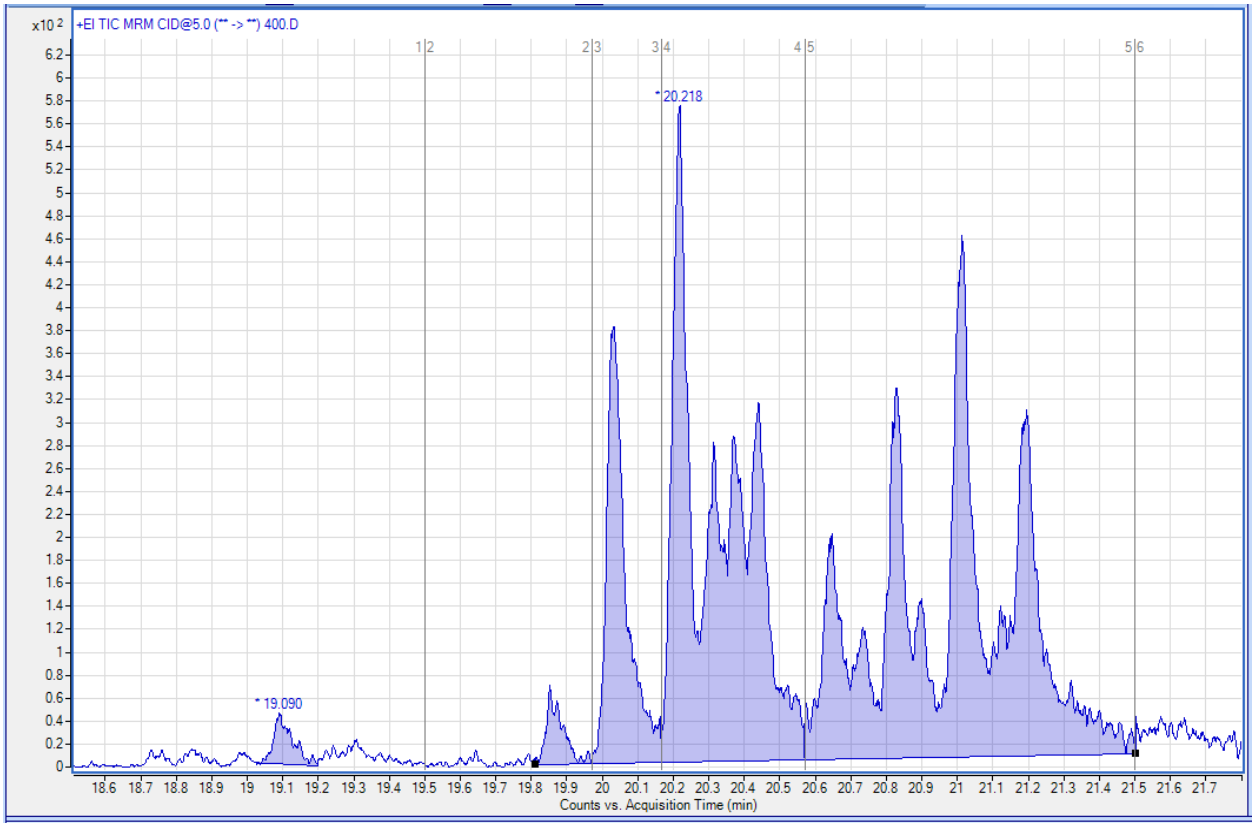

Figure 12: 400 ppb Standard

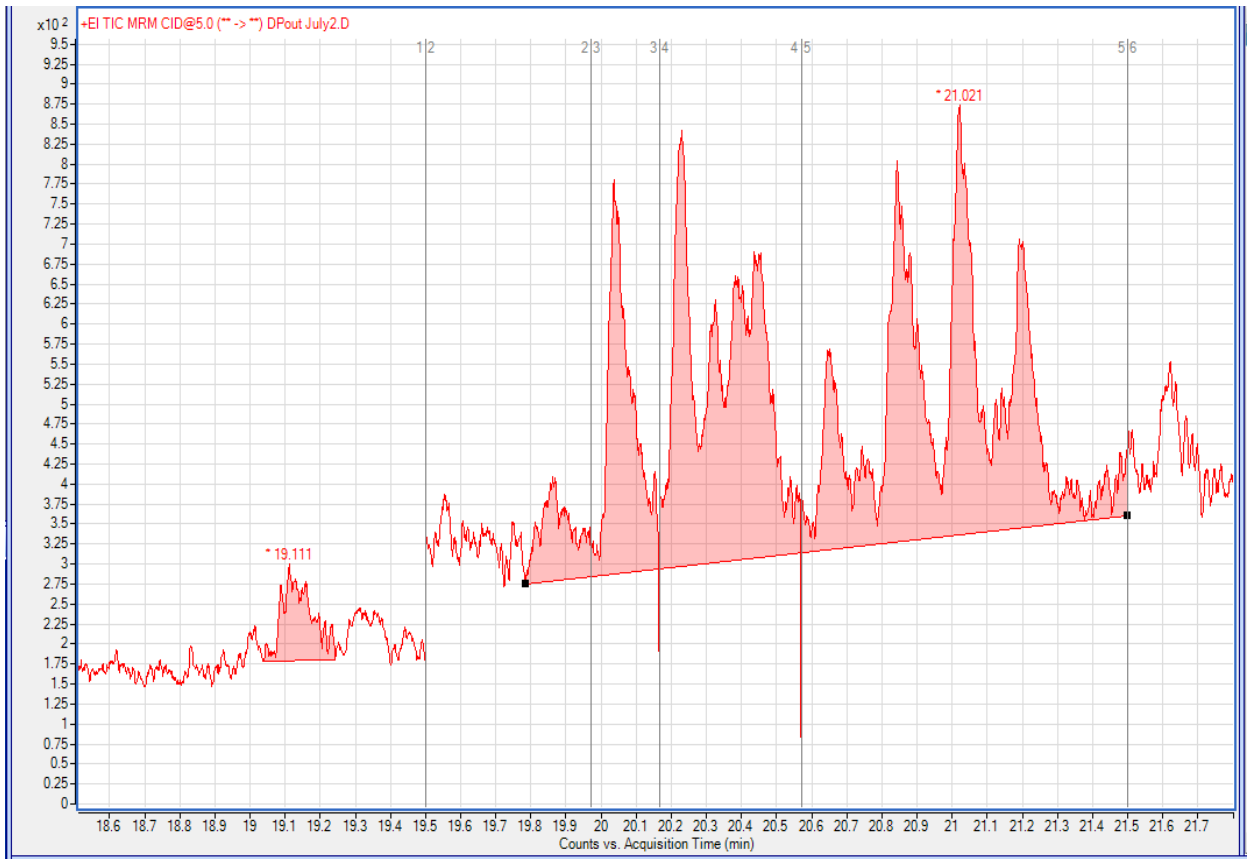

Figure 13: Water Sample from Duck Pond out Site collected on July 2

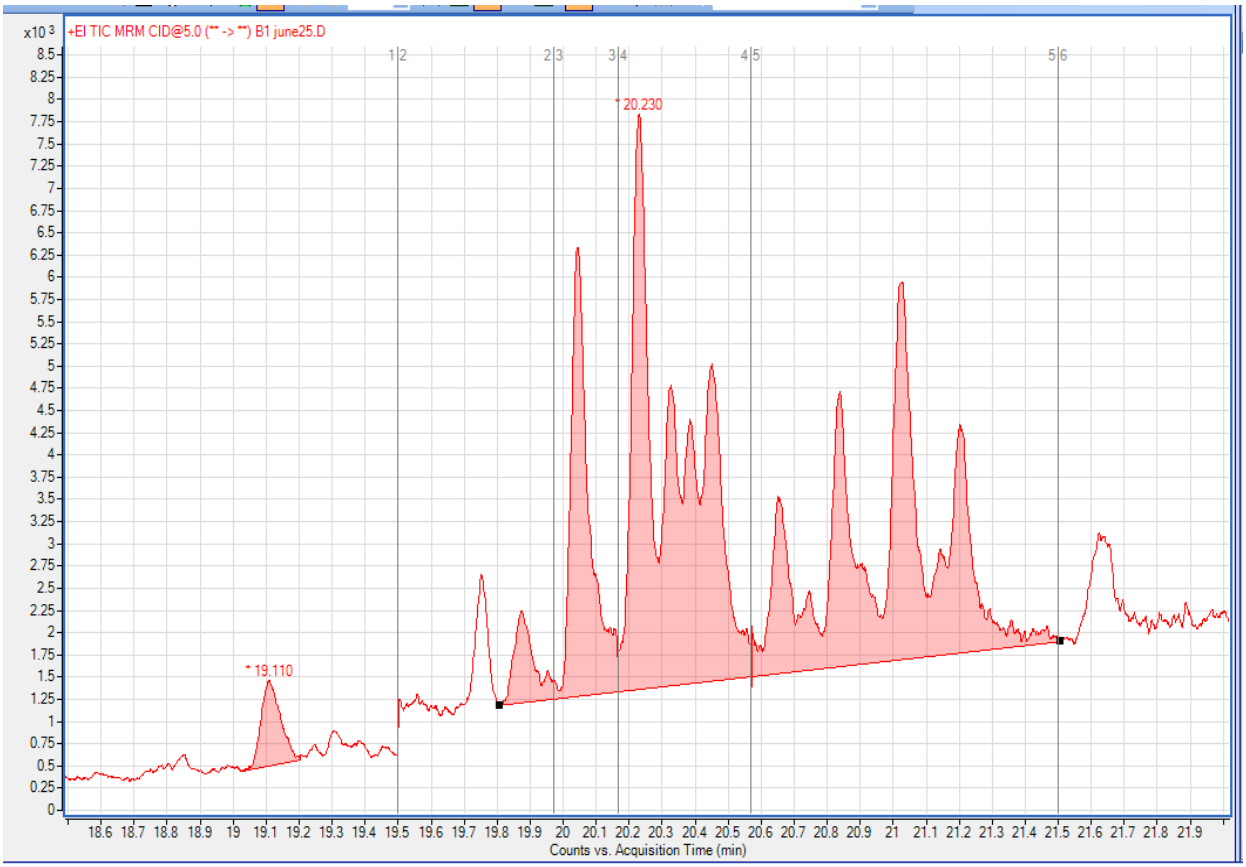

Figure 14: Sediment Sample from Bridge 1 Site collected on June 25

Shown in Figure 15 is the concentration relative to each samples site where each bar represents a different day. The sampling sites are labeled relative to Table 2 and Figure 10. The range for the concentration of water samples was between 0.01 and 1.6µg/L. Figure 16 shows the relationship between the concentration and the rainfall in terms of the sampling data. The concentration of the water samples increased considerably during the significant rainfall seen on July 2nd.

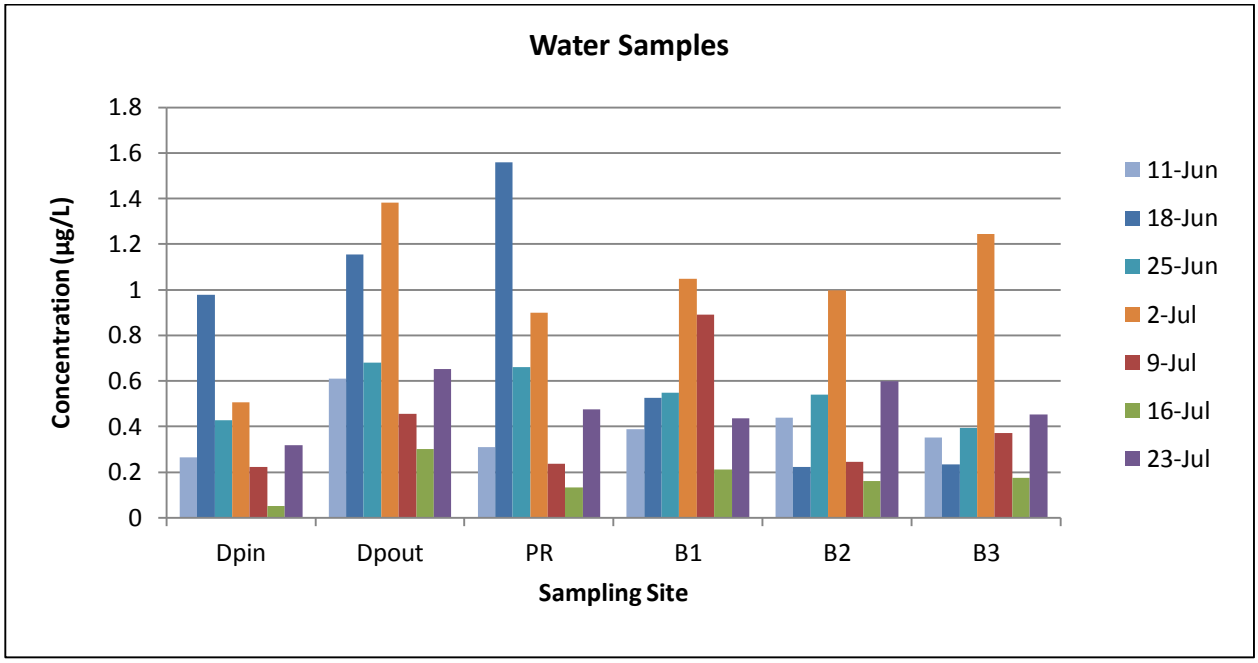

Figure 15: Change in Water Concentration relative to Sample Site

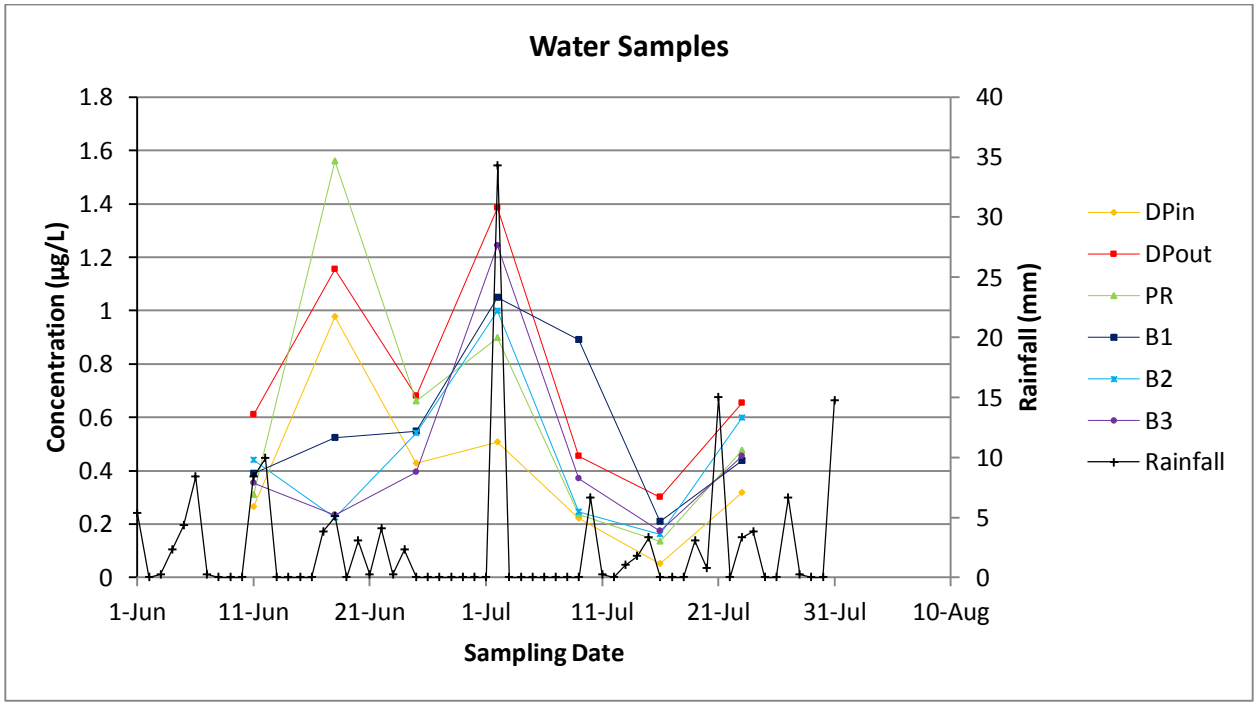

Figure 16: Relationship between Concentration and Rainfall relative to Time

Shown in Figure 17 is the sediment concentration relative to each samples site where each bar represents a different day. The concentration of sediment samples was around 1000µg/kg with the maximum being 10,000µg/kg. Figure 18 shows the relationship between the 4-nonylphenol sediment concentration and the rainfall in terms of the sampling data.

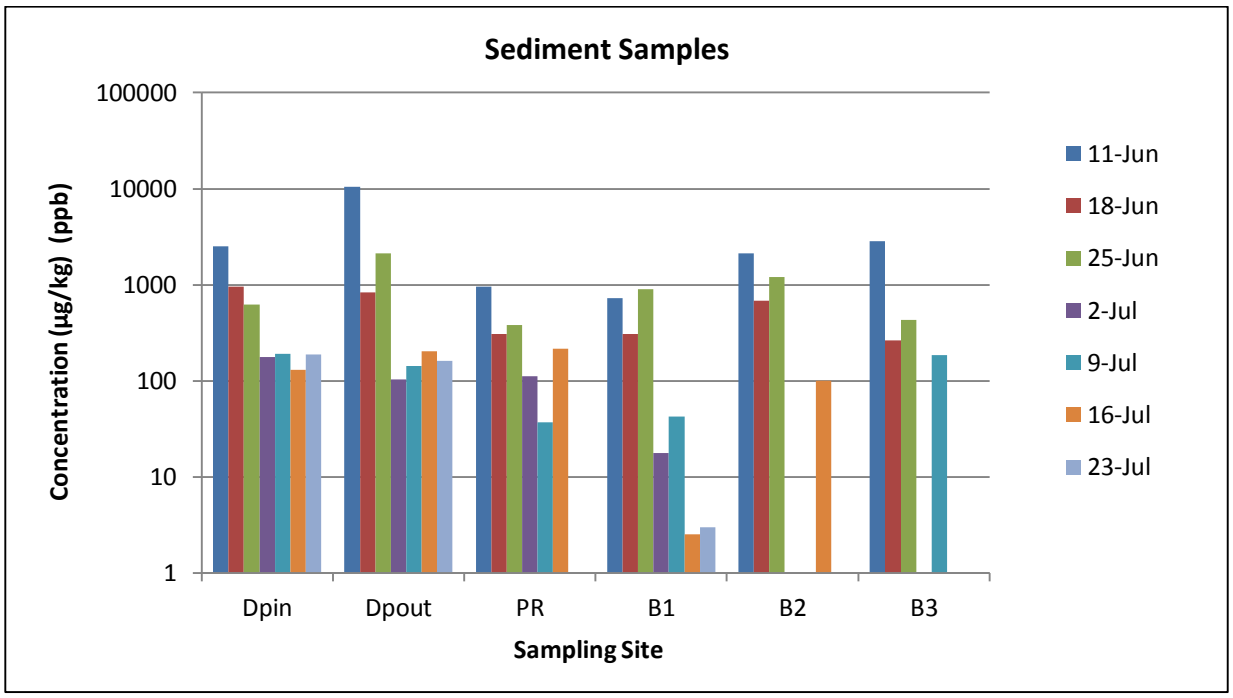

Figure 17: Change in Sediment Concentration relative to Sample Site

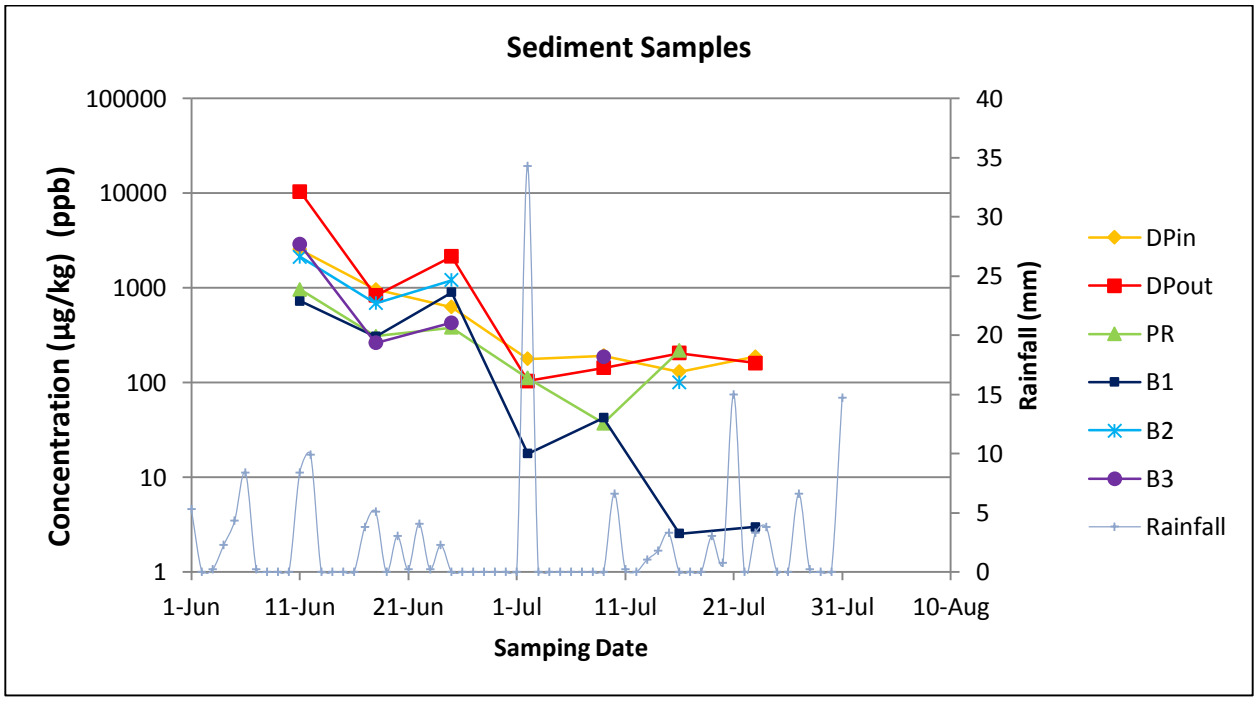

Figure 18: Relationship between Sediment Concentration and Rainfall relative to Time

Conclusions

Throughout this study 4-nonylphenol has been investigated in both the water and sediment of Stroubles Creek to determine the extent of impact urban development has on a watershed. The concentration of 4-nonylphenol in the water samples ranged from less than 0.05 to 1.6 ppb while the concentrations of the 4-nonylphenol in the sediment samples was 1,000ppb reaching a maximum of 10,000ppb. Other work has determined stream water sample 4-nonylphenol concentrations less than 1 ppb with wastewater treatment effluent 4-nontlphenol concentrations higher than 3 ppb (Bennie, Sullivan, Lee, Peart, & Maguire, 1996) (Lee, Peart, & Svoboda, 2005). Sediment samples in other work were also comparable to the levels found in this study with dry weight sediment samples ranging from much lower at 170ppb to much higher at 72,000ppb (Bennie, Sullivan, Lee, Peart, & Maguire, 1996). Wastewater treatment plant biosolid concentrations have also been reported from 1,300ppb to 300,000ppb (Xia, Keller, Bhandari, & Wagner, 2001). Within this study the concentration in the water samples tended to increase after rain events. Concentrations of both water and sediments samples were higher coming out of the Duck Pond compared to entering the Duck Pond which lead to considerations as to whether the Duck Pond was truly acting as a retention pond, as originally designed.

Future Work

As research continues further trends will be assessed including possible trends between 4-nonylphenol concentrations and other environmental parameters such as water flow, temperature, pH, turbidity, sediment redox potential, and other weather related parameters. Conducting sampling trips specifically around rain events in order to better understand the relationship between increased flowrate and concentration levels in both mediums will also be interesting to analyze. In comparison, conducting controlled lab experiments to mimic 4-nonylphenol release from sediment to water during a rain event will enhance our understanding of the fate of 4-nonylphenol in the watershed. In an effort to reduce the amount of 4-nonylphenol entering the creek, it may be of interest to also assess the possible contributions to the runoff in the residential and agricultural areas.

Acknowledgements

I would like to thank Dr. Kang Xia for all her guidance throughout this summer. I would also like to thank Theresa Sosienski for all her help in the lab preparing tests and running them late into the evening. To the rest of the lab members, thank you for all your training on different tools and procedures. Lastly, thank you to Dr. Lohani and all of his graduate students for their organization of the program and all of the seminars.

"We acknowledge the support of the National Science Foundation through NSF/REU Site Grant EEC-1062860. Any opinions, findings, and conclusions or recommendations expressed in this paper are those of the author(s) and do not necessarily reflect the views of the National Science Foundation."

References

Ahel, M., & Giger, W. (1993). Partitioning of Alkylphenols and Alkylphenol Polyethoxylates between Water and Organic Solvents. *Chemosphere*, Vol. 26, No. 8, pp. 1471-1478.

Ahel, M., Giger, W., & Koch, M. (1994). Behaviour of Alkylphenol Poltethoxylate Surfactants in the Aquatic Environment -- I.Occurrence and Transformation in Sewage Treatment. *Wat. Res.*, Vol. 28, No. 5, pp. 1131-1142.

Bennie, D. T. (1999). Review of the environmental occurrence of alkylphenols and alkylphenols ethoxylates. *Water Quality Research Journal of Canada*, Vol. 34 Issue 1, p79-122.

Bennie, D., Sullivan, C., Lee, H.-B., Peart, T., & Maguire, R. (1996). Occurrence of alkylphenols and alkylphenol mono- and diethoxylates in natural waters of the Laurentian Great Lakes basin and the upper St. Lawrence River. *The Science of the Total Environment*, 193, pp.263-275.

Brix, R., Hvidt, S., & Carlsen, L. (2001). Silubility of nonylphenol and nonylphenol ethoxylates. On possible role of micelles. *Chemophere*, 44, pp. 759-763.

Cox, C. (1996). Nonyl Phenol and Related Chemicals. *Journal of Pesticide Reform*, VOL.16, NO. 1.

Department of Biological Systems Engineering. (n.d.). *Historical Marker!* Retrieved from Stream Restoration, Education, and Management (StREAM) Lab: http://streamlab.bse.vt.edu/

Diamanti-Kandarakis E et al. (2009). Endocrine-Disrupting Chemicals: An Endocrine Society Scientific Statement. *Endocrine Reviews*, 30(4):293-342.

Gray, M. A., & Metcalfe, C. D. (1997). Induction of testis–ova in Japanese Medaka (Oryzias Latipes). *Environmental Toxicology and Chemistry*, Vol. 16, No. 5, pp. 1082–1086.

Hale, R. C., Smith, C. L., O. De Fur, P., Harvey, E., Bush, E. O., La Guardia, M. J., & Vadas, G. G. (2000). Nonylphenols in Sediments and Effluents Associated with Diverse Wastewater Outfalls. *Environmental Toxicology and Chemistry*, Vol. 19, No. 4, pp. 946–952.

Kolpin, D. W., Thurman, E. M., Lee, E. A., Meyer, M. T., Furlong, E. T., & Glassmeyer, S. T. (2006). Urban contributions of glyphosate and its degradate AMPA to streams in the United States. *Science of the Total Environment*, 354 pp. 191– 197.

Lee, H.-B., Peart, T. E., & Svoboda, M. L. (2005). Determination of endocrine-disrupting phenols, acidic pharmaceuticals, and personal-care products in sewage by solid-phase extraction and gas chromatography–mass spectrometry. *Journal of Chromatography A*, 1094, pp. 122–129.

Mark Ferrey, et al. (2010). *Statewide Endocrine Disrupting Compound Monitoring Study 2007-2008.* Saint Paul, MN: Minnesota Pollution Control Agency.

Naylor, C. G., & Kubeck, E. (1990). Trace Analysis of Alkylphenol Ethoxylates. *Journal of the American Oil Chemists' Society*, Vol. 67, no. 6.

Office of Water. (2005). *Ambient Aquatic Life Water Quality Criteria - Nonylphenol.* Washington, DC: U.S. Environmental Protection Agency.

Randolph, J. (1993). *The Town of Blacksburg and Virginia Tech's Impact on the Stroubles Creek Watershed.* Environmental Planning Studio.

Reinhard, M., & Montgomery-Brown, J. (2003). Occurrence and Behavior of Alkylphenol Polyethoxylates in. *Environmental Engineering Science*, Volume 20, Number 5, Pages 471-486.

Roberts, D. A. (2012). Causes and ecological effects of resuspended contaminated sediments (RCS) in marine environments. *Environment International*, 40, pp. 230–243.

Soares, A., Guieysse, B., Jefferson, B., Cartmell, E., & Lester, J. (2008). Nonylphenol in the environment: A critical review on occurrence, fate, toxicity and treatment in wastewaters. *Environment International*, 34, pp. 1033–1049.

Southern California Coastal Water Research Project. (2011, November 14). *Background: Endocrine Disruption*. Retrieved from Research Area: Contaminants of Emerging Concern: http://www.sccwrp.org/ResearchAreas/Contaminants/ContaminantsOfEmergingConcern/BackgroundEndocrineDisruption.aspx

Starratt, A., & Topp, E. (2000). Rapid Mineralization of the Endocrine-Disrupting Chemical. *Environmental Toxicology and Chemistry*, Vol. 19, No. 2, pp. 313–318.

Strauch, G., Möder, M., Wennrich, R., Osenbrück, K., Gläser, H.-R., Schladitz, T., . . . Schirmer, M. (2008). Indicators for Assessing Anthropogenic Impact on Urban Surface and Groundwater. *J Soils Sediments* , 8 (1) pp. 23–33.

Thomas, K. V., & Eggleton, J. (2004). A review of factors affecting the release and bioavailability of contaminants during sediment disturbance events. *Environment International*, 30, pp. 973– 980.

U.S. Environmental Protection Agency. (2012). *Nonylphenol (NP) and Nonylphenol Ethoxylates (NPEs) Action Plan [RIN 2070-ZA09]*.

Uchiyama, T., Makino, M., Saito, H., Katase, T., & Fujimoto, Y. (2008). Syntheses and estrogenic activity of 4-nonylphenol isomers. *Chemosphere*, Volume 73, Issue 1, Supplement, August 2008, Pages S60–S65.

White, G. F., House, W. A., & John, D. M. (2000). Environmental Fate of Nonylphenol Ethoxylates: Differential Adsorption of Homologs to Components of River Sediment. *Environmental Toxicology and Chemistry*, Vol. 19, No. 2, pp. 293–300.

Writer, J. H., Ryan, J. N., Keefe, S. H., & Barber, L. B. (2012). Fate of 4-Nonylphenol and 17β-Estradiol in the Redwood River of. *Environmental Science and Technology*, 46, 860−868.

Xia, K., Keller, H., Bhandari, & Wagner, J. (2001). Occurrence, Distribution, and Fate of 4-nonylphenol in Kansas Domestic Wastewater Treatment Plants. *Water Resources*, Issue 120: 41-48.

Zwolsman, J. J., & Goossens, H. (1996). An Evaluation of the Behaviour of Pollutants During Dredging Activities. *Terra et Aqua*, Number 62, pp. 20-28.

Effect of Bioavailable Fe^{3+} on the Sustainability of Monitored Natural Attenuation of Petroleum Hydrocarbons

William J. Raseman*, Dr. Mark Widdowson**

** NSF-REU fellow, Virginia Polytechnic Institute and State University*
(Home Institution: Civil Engineering, University of Notre Dame)
***Department of Civil and Environmental Engineering, Virginia Polytechnic Institute and State University*

ABSTRACT

Petroleum-derived compounds, particularly benzene, remain among the most frequently-cited groundwater contaminants (USGS, 2011). At these sites, Monitored Natural Attenuation (MNA) is often employed to manage residual contamination. MNA is a cost-effective technique which utilizes biodegradation and other natural attenuation mechanisms to remediate petroleum hydrocarbon plumes in the groundwater before reaching points of compliance in a time-frame comparable to alternative methods (USEPA, 1999). In order for microbes to biodegrade contaminants, electron acceptors, such as oxygen and iron, must be available. Due to its abundance in soils, iron often has the most potential for anaerobic biodegradation of organic matter (Lovley et al., 1989). However, only a portion of the iron, known as bioavailable Fe^{3+}, can be utilized by microbes. We are interested in modeling the effect of different bioavailable Fe^{3+} distributions on the sustainability of petroleum hydrocarbon plume biodegradation. To determine representative distributions, we used a bioavailable Fe^{3+} assay in order to characterize borehole samples from Site 45, Marine Corps Recruit Depot, Parris Island, South Carolina. Using iron distributions from these data and other hypothetical scenarios, we numerically modeled the fate and transport of gasoline—including an ethanol-enriched fuel known as gasohol—in hypothetical groundwater systems using SEAM3D (Sequential Electron Acceptor Modeling in 3-Dimensions).

Keywords: bioremediation, monitored natural attenuation, iron, modeling, petroleum

Introduction

Petroleum Hydrocarbon Contamination of Groundwater

Petroleum-derived compounds, particularly benzene, remain among the most frequently-cited groundwater contaminants (USGS, 2011). Benzene, toluene, ethylbenzene, and xylene (BTEX) are petroleum-derived compounds that readily dissolve into the groundwater and can have adverse effects on human health (Ryan, 2010). Benzene is the compound of the highest concern because it is both the most soluble of these compounds and it is a known carcinogen. At petroleum contaminated sites, Monitored Natural Attenuation (MNA) is often employed to manage residual contamination after the source zone has been remediated. MNA is a cost-effective technique which utilizes natural attenuation mechanisms such as sorption, volatilization, and biodegradation. These mechanisms remediate contaminant plumes before reaching points of compliance—such as a well or residential area—in a time-frame comparable to alternative methods (USEPA, 1999). Similar to other methods, MNA uses a system of monitoring wells to determine the extent of the plume over time. The feasibility of this technique is most dependent on the rate of biodegradation at the site.

Local microbial populations can biodegrade contaminants, such as petroleum, if there are available electron acceptors such as oxygen, iron, and sulfate. The contaminant concentration, available electron acceptors, and donors, limit the rate of biodegradation (Lebron et al., 2005). Initially, the contaminants can biodegrade aerobically, but as dissolved oxygen depletes, aerobic biodegradation only occurs along the leading edges of the plume, while various anaerobic conditions dominate within (Figure 1-1).

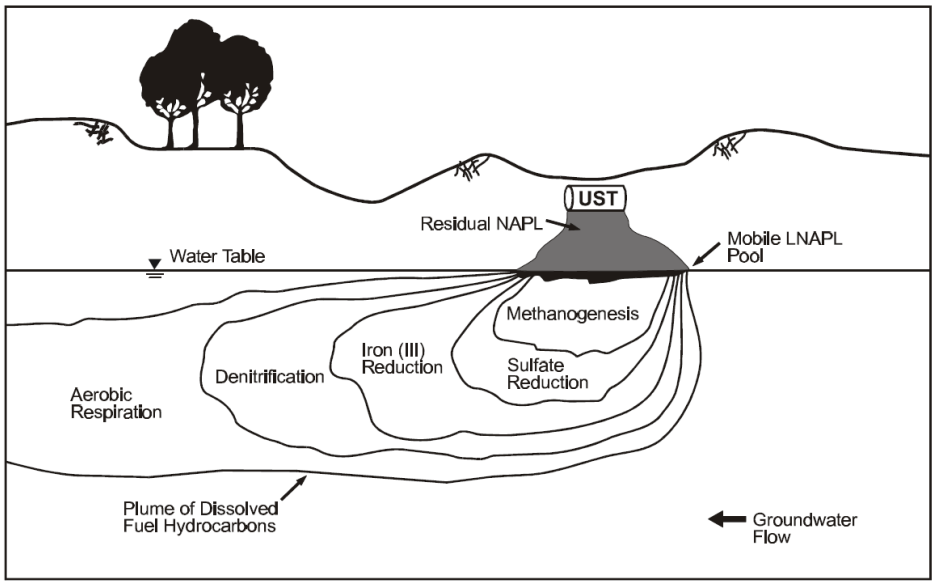

Figure 1-1. Conceptualization of Electron Acceptor Zones in the Subsurface (USEPA, 2012)

The Role of Ferric Iron in Monitored Natural Attenuation

Due to its abundance in soils, ferric iron (Fe^{3+}) often has the most potential for anaerobic biodegradation of organic matter (Lovley et al., 1989). Although, not all types of ferric iron can be utilized by microbes. "Bioavailable Fe^{3+} is ferric iron that is capable of being reduced by microorganisms that oxidize another chemical species and derive energy from the electron transfer" (Lebron et al., 2005). Since bioavailable Fe^{3+} has great biodegradation potential, the amount of bioavailable Fe^{3+} could determine whether MNA is a feasible remediation strategy for a contaminated site.

The role of ferric iron on the natural attenuation of a petroleum hydrocarbon is conceptualized in Figure 1-2. As the hydrocarbon plume migrates in the direction of the groundwater flow toward a point of compliance, the microbes deplete the iron over time. In order to determine how ferric iron impacts the biodegradation of petroleum hydrocarbons, we are modeling the effect of various bioavailable Fe^{3+} distributions on the sustainability of petroleum hydrocarbon plume biodegradation.

Currently, the depositional mechanism and the distribution of bioavailable Fe^{3+} are not well understood, so it is difficult to estimate these distributions for remediation sites (Kennedy et al., 1999). In 2005, New Horizons Inc. created a bioavailable Fe^{3+} assay which can directly measure the bioavailable iron in soil samples (Lebron et al., 2005). This assay was used to characterize borehole samples from a chlorinated solvent-contaminated site in South Carolina in order to research the distribution of bioavailable Fe^{3+} at the site.

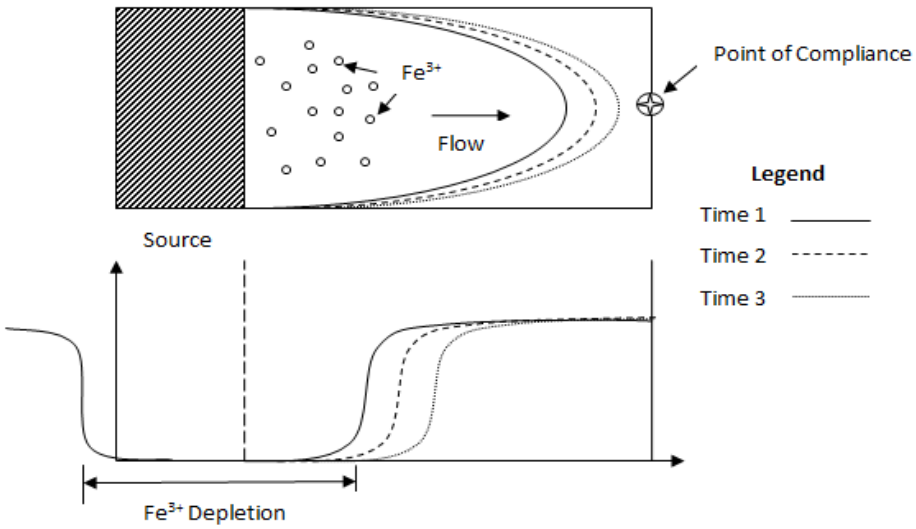

Figure 1-2. Conceptualization of Fe^{3+} Depletion in a Petroleum Hydrocarbon Plume over Time

The Changing Composition of Gasoline and Its Impact on Groundwater Contaminant Fate and Transport

In 1990, Congress amended the Clean Air Act requiring oxygenates to be added to gasoline in order to reduce vehicle emissions (Perciasepe, 2000). Initially, MTBE (methyl tertiary butyl ether) was used to fulfill oxygenate requirements, but due to elevated levels of MTBE found in drinking water, ethanol replaced MTBE (Perciasepe, 2000). This ethanol enriched gasoline, known as gasohol, contains up to 10 percent ethanol by volume. Gasohol, the current standard for gasoline in the United States, and gasoline from the 1990s, which contains no ethanol, are distinct in their fate and transport in groundwater. Ethanol is infinitely soluble in water, therefore it dissolves rapidly into the groundwater and moves quickly in the direction of groundwater flow (Weaver et al., 2009). Additionally, ethanol is preferentially biodegraded over the BTEX compounds in gasoline; consequently, as the ethanol migrates down gradient it depletes available electron acceptors, reducing the biodegradation potential of the contaminated site. This could cause increased BTEX plume lengths, which increases the likelihood of BTEX-contaminated drinking water (Weaver et al., 2009).

Numerical Modeling

Using the numerical model SEAM3D (Sequential Electron Acceptor Modeling in 3-Dimensions), the fate and transport of a 1990s gasoline and gasohol were modeled in hypothetical groundwater systems. The composition used for gasohol was based off of data reported by Haskew et al. in 2007.

Modeling Assumptions

In SEAM3D, two 3D-Grids were generated. Grid 1 had dimensions of 40, 20, and 3 meters (Figure 2-1) and 80, 40, and 30 cells in the x, y, and z direction, respectively. Grid 2 had dimensions of 160, 40, and 3 meters and 160, 40, and 30 cells in the x, y, and z direction, respectively. Grid 1 was used for all models except those represented in Figures 4-7 and 4-8. Along the centerline of the domain, a four by four meter gasoline source was placed in layers 14, 15, 16, and 17. This source was placed two meters in the positive x-direction. There were no flow boundary conditions along the perimeter of the grid except for the faces along the zy-plane. On these faces, constant head boundary conditions were applied to create a hydraulic gradient of 0.0025m/s. The head value closest to the origin was 5m, and the head on the opposite end of the grid was dependent on the length of the grid to keep a constant hydraulic gradient in each simulation. The cells were modeled as fully saturated, and each layer was confined. The horizontal

hydraulic conductivity was set to 1 m/d, the vertical anisotropy was set to 2, and the porosity was set to 0.3.

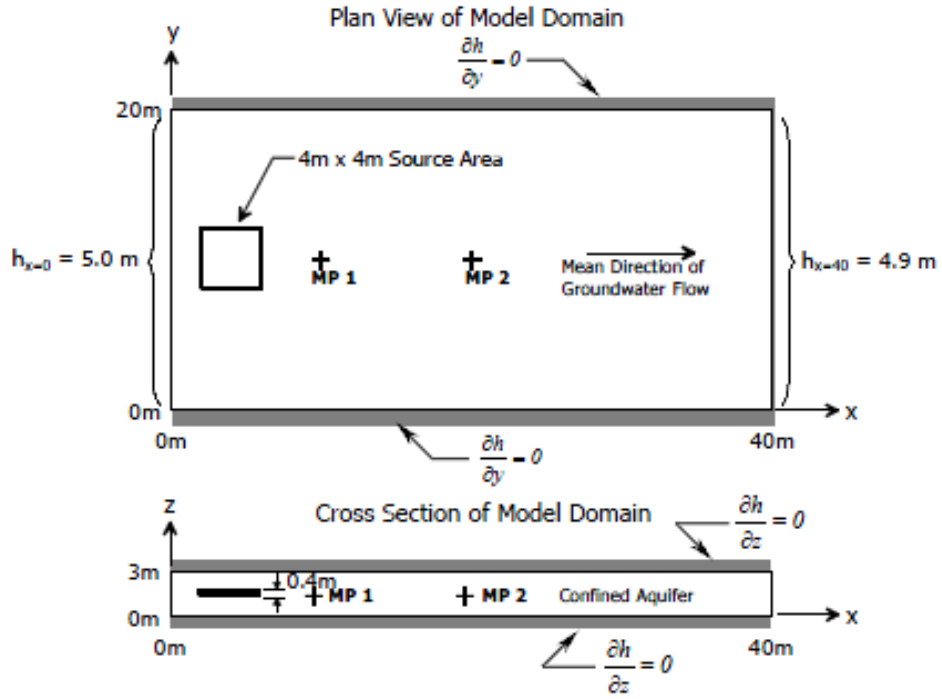

Figure 2-1. Boundary Conditions and Dimensions for the Hypothetical Numerical Model Domain (Brauner, 2000)

The Advection, Dispersion, Source/Sink Mixing, Chemical Reaction, Biodegradation, and NAPL Dissolution Package were enabled for SEAM3D. The parameters for these packages are detailed in the appendix except for the Advection Package, which was left at its default setting, and the Chemical Reaction Package, in which the soil bulk density was set to 1.6×10^6 g/m^3 for each layer. In order to isolate the importance of ferric iron, only aerobic and iron-reducing biodegradation were simulated.

Methods of Analysis

Numerical Modeling

In order to monitor contaminants of concern (COC) in SEAM3D, a hypothetical monitoring well was placed at 25 meters from the source that could generate a concentration time curve of contaminants, biodegradation mass data grouped by electron acceptor was analyzed, and the mass of COC in the plume was calculated at different time steps.

Three biodegradation conditions were modeled: aerobic, iron-reducing, and no biodegradation. A tracer represents transport of benzene if there is no biodegradation. A mid-range aerobic biodegradation was modeled with a starting concentration of 3 mg/L of oxygen. Mid-range iron-reducing conditions were modeled using a uniform distribution of ferric iron of 400 mg/kg. These values were chosen by our research group based on values Dr. Widdowson had observed in the field and as a result of model sensitivity testing.

Site Description and Sample Collection

A total of twelve borehole samples were collected from the chlorinated solvent-contaminated Site 45, Marine Corps Recruit Depot, Parris Island, South Carolina (Figure 2-1). After collection, the borehole samples were separated into one foot sections, homogenized, transported in chilled jars, and stored at 4°C

until testing began. Eight samples from boreholes 1 and 3 were examined (Figure 2-1). Borehole 3 was chosen in order to examine iron depletion that occurs near the source. Since borehole 1 is located outside of the contaminated area, it was chosen to observe the unaltered distribution of iron.

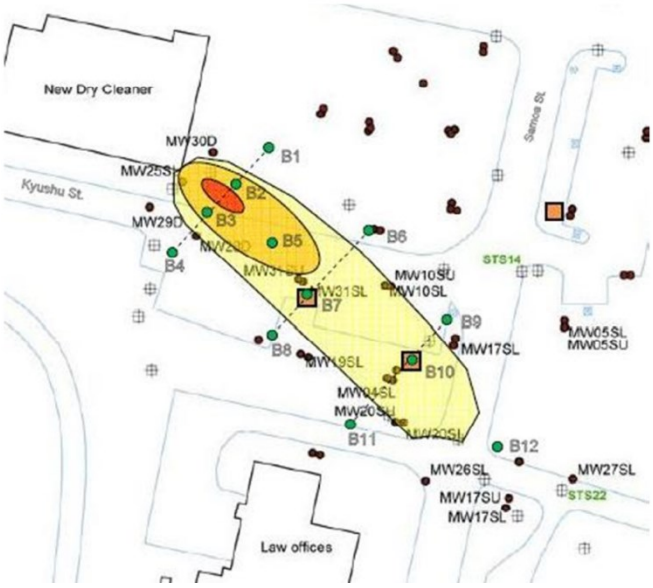

Figure 3-1. Borehole Sample Locations Relative to Chloroethene Plume at Site 45, Marine Corps Recruit Depot, Parris Island, South Carolina (Boncal, 2011)

Laboratory Tests

The borehole samples were tested in triplicate following the Bioavailable Ferric Iron Assay from New Horizons Inc. (Lebron et al., 2005). First, two samples of 5 ± 0.5g were placed into 20mL test tubes labeled T_0 and T_{30}. After adding the soil, the T_0 test tubes were filled halfway with distilled water and tapped until all air bubbles were released from underneath the soil. 1 mL of HCl was added in order to acidify the solution within the pH range necessary for a colorimetric test. Next, distilled water was added until the solution reached the top of each test tube. The solutions were then capped, mixed by inversion, and placed on a shaker table in a dark room for 48 hours. After 48 hours, the solutions extracted using a 3 mL syringe, and filtered into containers. Finally, the concentration of Fe^{2+} in the solution was measured using the ferrous iron Hach test 255 in a DR5000 model.

After the addition of the soil, the T_{30} test tubes were filled up to the neck with distilled water solution and tapped in order to minimize air bubbles trapped beneath the soil. Freeze-dried bacteria (Reagent B) were added to each solution, followed by the addition of distilled water until the solutions reached the top of each test tube. The solutions were capped, inverted several times, and incubated in a dark room for 30 days. Following the same procedure as the T_0 test, the T_{30} solutions were acidified with HCl, set on the shaker table for 48-hours, and colorimetrically analyzed for ferrous iron.

The T_{30} test measures the ambient Fe^{2+} plus the Fe^{2+} byproduct of bioavailable ferric iron degradation. The bioavailable ferric iron in the soil is calculated by taking the difference between the ferrous iron concentrations of the T_{30} and T_0 tests, divided by a concentration conversion factor for liquid to soil Fe^{2+} (Equation 1).

Equation 1. Bioavailable Fe^{3+} calculation

$$Bioavailable\ Fe^{3+} = (T_{30}Fe^{2+}\text{-}T_0Fe^{2+})/(217)$$

Results and Discussion

Model Sensitivity to Varying Iron(III) Distributions

A monitoring well was placed in layer 15—the middle of the 30 layer domain—25 meters from the source and concentration curves of this data were generated (Figure 4-1 and Figure 4-2). Various biodegradation conditions were modeled in order to determine their effect on both benzene and the BTEX compounds as a whole.

At this monitoring well, aerobic biodegradation reduced the peak concentration of benzene by less than 0.5 mg/L (Figure 4-1). The addition of ferric iron decreased the concentration by another 1 mg/L. Aerobic biodegradation had less of an effect on the concentration of BTEX compounds, but reduced the peak concentration by almost 10 mg/L (Figure 4-2).

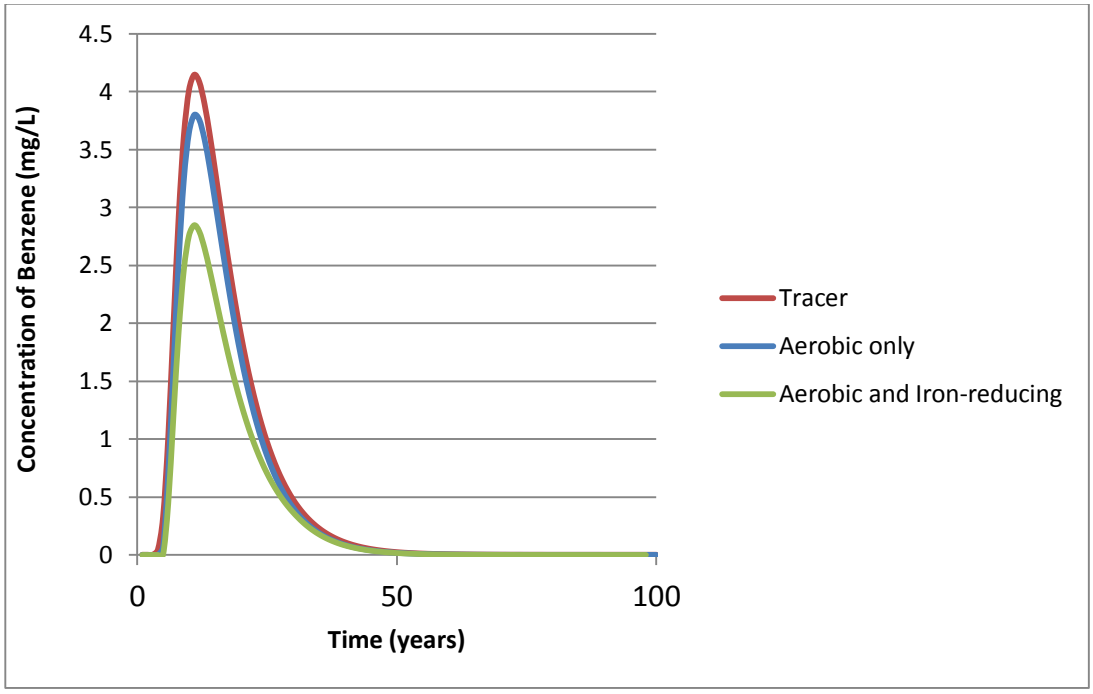

Figure 4-1. Concentration of Benzene Over Time at a Monitoring Well 25m from the Source

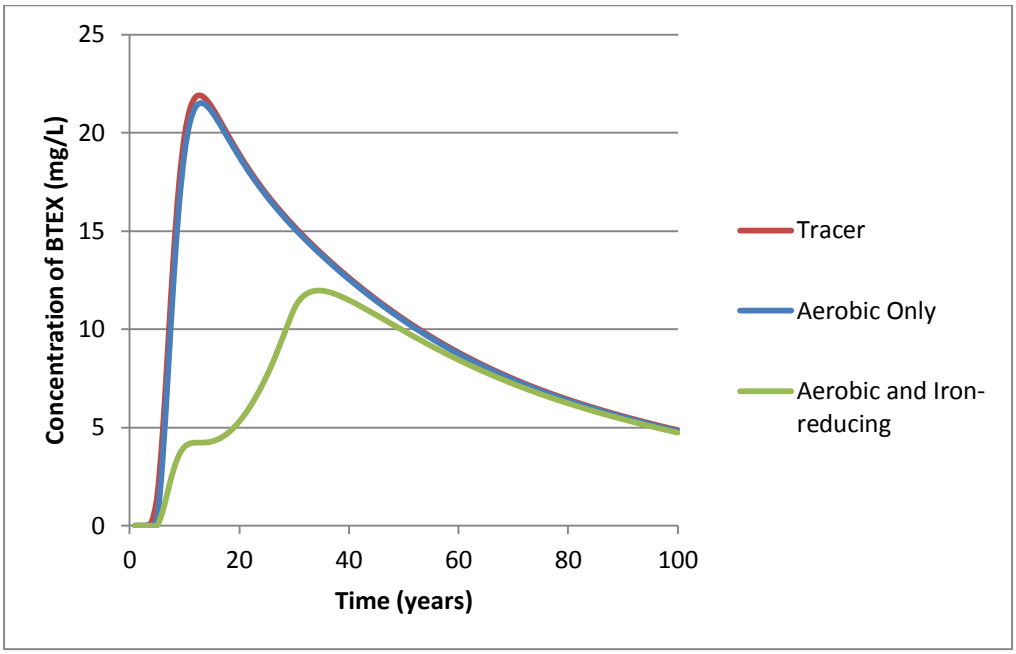

Figure 4-2. Concentration of BTEX Over Time at a Monitoring Well 25m from the Source

Figures 4-1 and 4-2 highlight the contribution the introduction of iron can have on the attenuation of COC. However, they do not express the effect of varying the amount of ferric iron in the domain. This is significant to explore because the distribution of electron acceptors varies greatly from site to site. To determine how iron affects the biodegradation of benzene, values of ferric iron ranging from 50 to 1200 mg/kg were modeled. At the monitoring well specified previously, there is a negligible effect on peak benzene concentration when increasing ferric iron beyond 100mg/kg (Figure 4-3). However, when comparing the 100 and 1200 mg/kg scenarios between 20 and 40 years, the concentration of benzene decreases faster in the presence of higher amounts of iron.

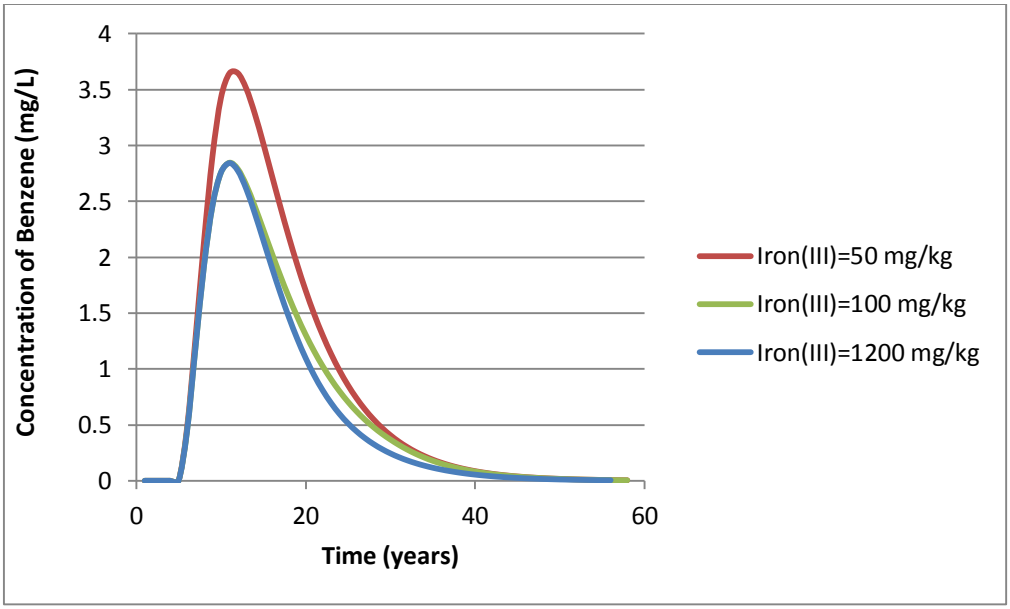

Figure 4-3. Sensitivity of Benzene Concentration Over Time to Changes in the Amount of Iron(III) in the Domain at a Monitoring Well 25m from the Source

The capability of SEAM3D to simulate monitoring wells is an important feature because it represents data that researchers may observe in the field. Researchers cannot visualize the concentration and extent of the contaminant plume beneath the subsurface. Instead, they can only track the plume based on data from a series monitoring wells. SEAM3D has additional capabilities that let the user analyze data that a field researcher cannot.

SEAM3D has the ability to output quantities of each biodegraded compound and the electron acceptor responsible for the amount of mass degraded. This information was used to analyze how distribution variations of ferric iron affect the mass of BTEX compounds that was biodegraded from the entire plume (Figures 4-4 and 4-5). In these figures, the amount of contaminant broken down due to ferric iron and oxygen were compared with changing amounts of ferric iron in the domain. The amount of mass biodegraded due to oxygen was compared with the amount due to iron as a point of reference in order to demonstrate the relative contributions of oxygen and iron to biodegradation.

The slope of the mass biodegraded over the amount of iron curve decreases as iron levels increase (Figures 4-4 and 4-5). This relationship can be explained by two limiting factors: the amount of iron available and the rate of biodegradation due to iron. With low iron concentrations, the iron depletion is the limiting factor to biodegradation, but when there is sufficient iron available, the rate of biodegradation limits the mass of benzene biodegraded and the curve reaches an asymptote. Additionally, it is apparent that iron-reducing biodegradation has much more of an impact on BTEX compounds than benzene when compared to aerobic biodegradation (Figures 4-4 and 4-5).

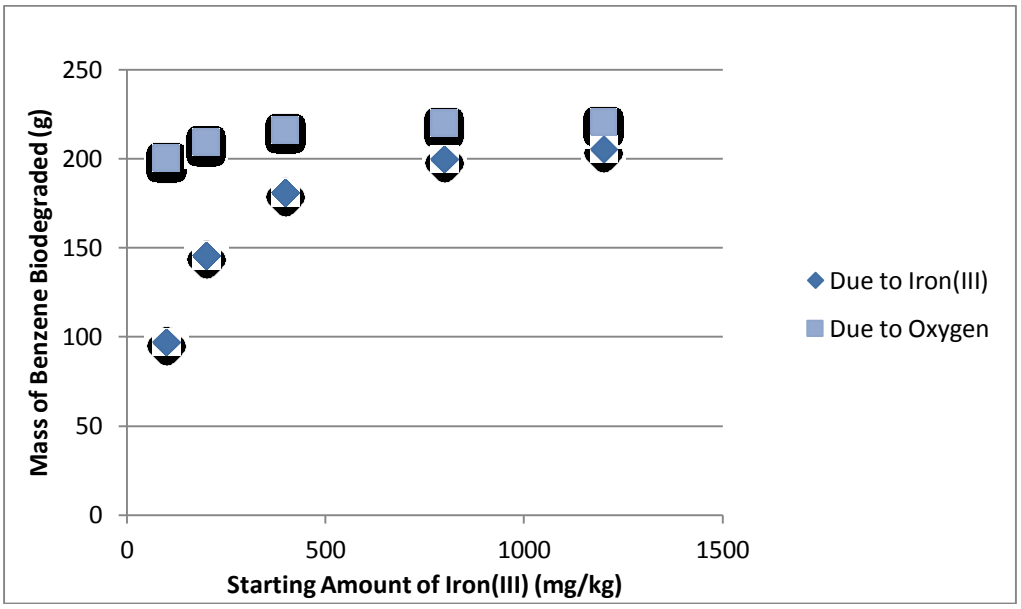

Figure 4-4. Model Sensitivity of the Total Mass of Benzene Biodegraded Due to Iron(III) and Oxygen with Variable Starting Amounts of Iron(III)

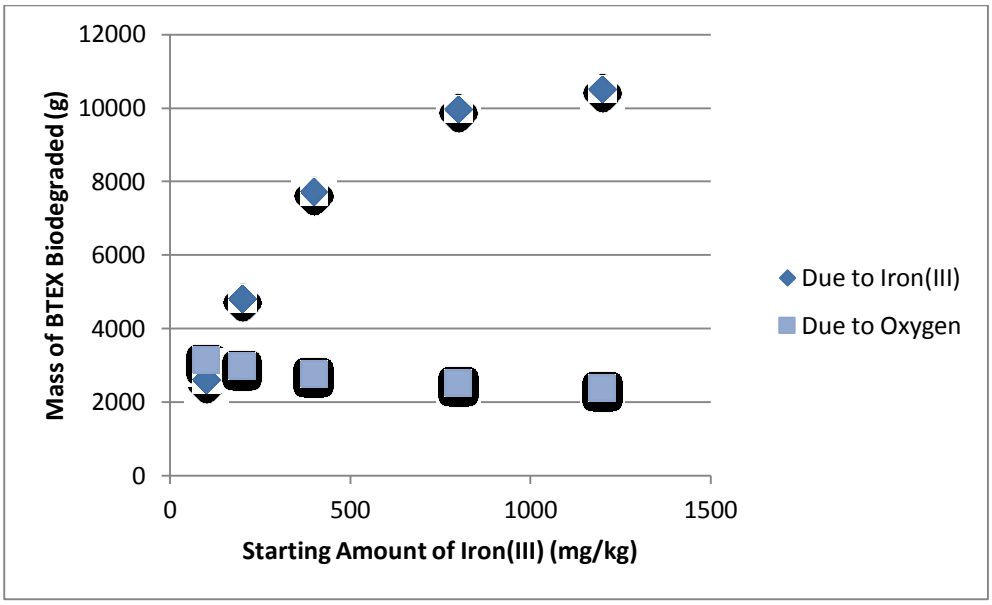

Figure 4-5. Model Sensitivity of the Total Mass of BTEX Biodegraded Due to Iron(III) and Oxygen with Various Starting Amounts of Iron(III)

The Fate and Transport of Gasohol

The models that were discussed thus far each used a 1990s composition of gasoline as the contaminant input. It is still relevant to model older compositions of gasoline because remediation of contaminated sites normally last for decades; therefore, gasoline from the 1990s is likely prevalent in sites across the country. Modeling current gasoline compositions is also important in the event of future groundwater contamination.

Since ethanol has been added to gasoline after the 1990s, the fate and transport is different for each type of gasoline. Ethanol affects the fate and transport because ethanol is infinitely soluble and preferentially biodegraded over BTEX compounds. This inhibits the biodegradation for the BTEX compounds, most likely causing increased BTEX plume lengths. For instance, the percentage of benzene biodegraded due to both iron and oxygen is less in gasohol than the 1990s fuel (Figure 4-6). This decrease in biodegradation increases the mass flowing out of the domain defined in SEAM3D, which causes increased plume lengths.

Additionally, the sensitivity of gasohol and the 1990s gasoline to varied amounts of ferric iron was analyzed at 50 years—just before the plumes left the SEAM3D domain (Figure 4-7). As expected, the mass of benzene in the domain was greater for gasohol than the 1990s gasoline at every level of iron.

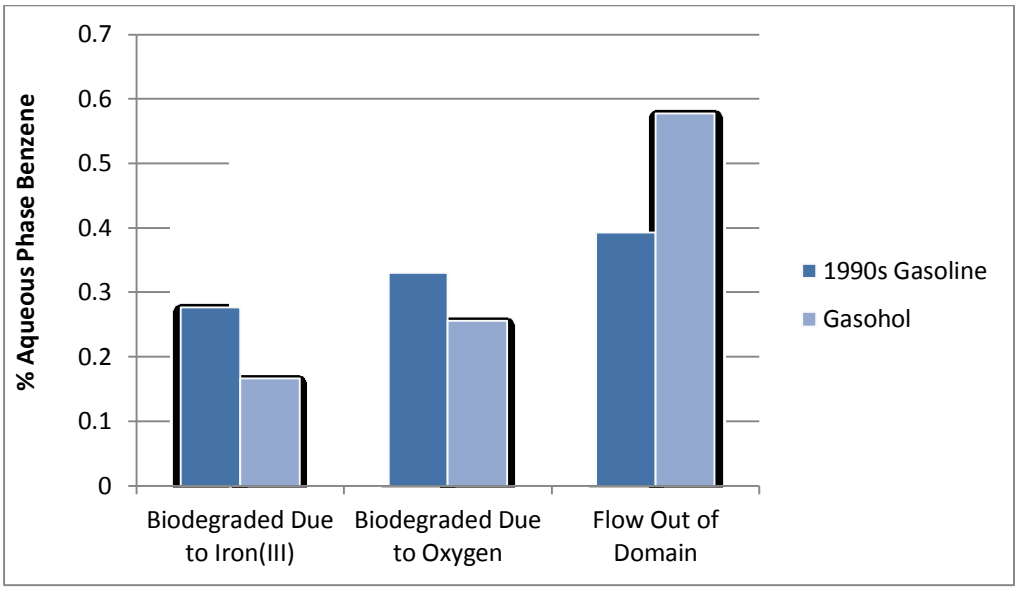

Figure 4-6. The Aqueous Phase Percentage of Benzene that Flows of the Domain, that is Biodegraded Due to Iron(III), and Due to Oxygen

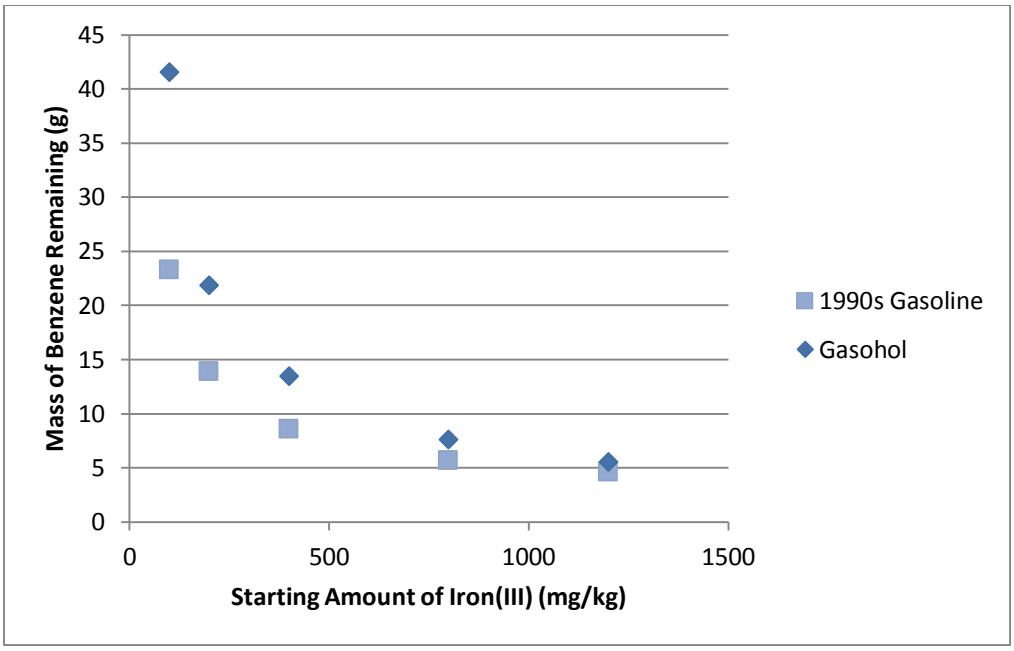

Figure 4-7. Mass of Benzene Above Remaining in Domain After 50 years with Varied Starting Amounts of Iron(III)

Bioavailable Fe^{3+} Assay and Model Application

The bioavailable Fe^{3+} results from borehole 1 serve two purposes (Table 4-1); to determine a realistic ferric iron distribution for our model, and to research the depositional patterns of bioavailable Fe^{3+} in the subsurface. Since the borehole 3 was located within the contaminant plume, iron recorded in these samples can tell us more about the spatial depletion of bioavailable Fe^{3+}. The data from sections of two boreholes are not substantial evidence for bioavailable Fe^{3+} trends; however, in the future, more evidence will be gathered from the remaining boreholes at the site.

Table 4-1. Mean Value of Bioavailable Fe^{3+} in Borehole Triplicates

Borehole Sample	Depth (ft)	Bioavailable Fe^{3+}(mg/kg)
1-B	3 to 4	360.6
1-C	6 to 7	621.9
1-D	7 to 8	141.6
1-F	10 to 11	58.1
1-G	13 to 14	56.5
1-I	16 to 17	129.4
3-G	13 to 14	459.5
3-H	14 to 15	103.5

From Table 4-1, it is apparent that the distribution of bioavailable ferric iron is heterogeneous with depth at this borehole. For instance, comparing sample 1-C to 1-F, whose starting elevations are only 4ft apart, there is over an order of magnitude decrease: from 621.9 mg/kg to 58.1 mg/kg. These results show that ferric iron distributions can be highly heterogeneous, and until there is a better understanding of the deposition of this substance, more samples will need to be analyzed to be able to predict a bioavailable ferric iron distribution.

In order to compare heterogeneous and uniform distributions, the ferric iron data from borehole 1 was applied to a SEAM3D model. Since there were gaps in depths between boreholes that were sampled (Table 4-1), the boreholes were assumed to be equally spaced. Thus, the amount of ferric iron for layers 1-5 was 129.4 mg/kg, layers 6-10 was 56.5 mg/kg, layers 11-15 was 58.1, and so forth. For the uniform model, the average amount of iron in each of the borehole 1 samples was distributed homogeneously through the grid. The mass of benzene in the domain was similar for the heterogeneous and uniform distribution, although, it is apparent that the distribution of the iron has an effect on the biodegradation of COC (Figure 4-7).

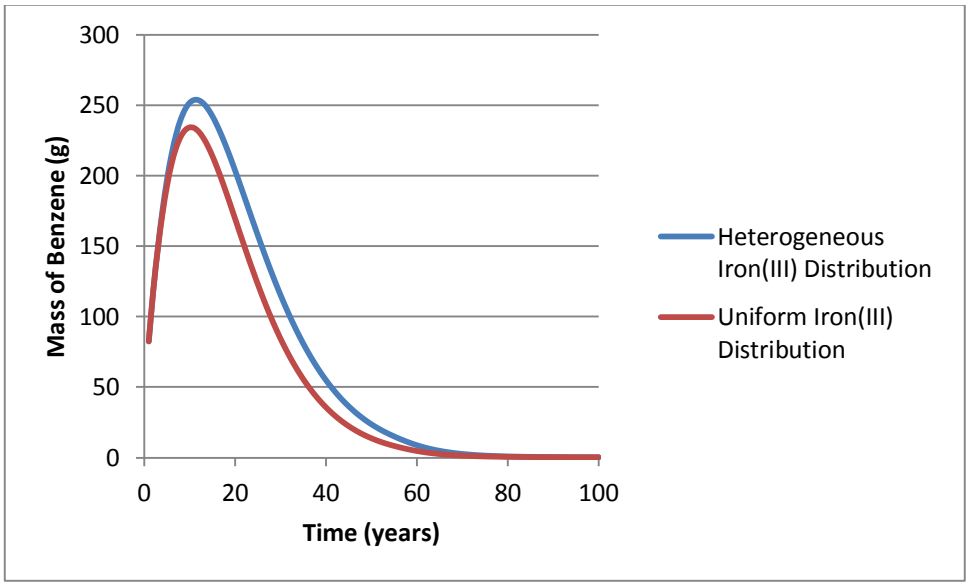

Figure 4-8. The Mass of Benzene in the Domain with a Heterogeneous Iron(III) Distribution from Borehole 1 Data and a Uniform Iron(III) Distribution Using the Average Value of Iron(III) from Borehole 1 Data

It was expected that samples from borehole 3 would have low amounts of iron because they were located near the source of the contamination. However, the amount of iron exceeded 400 mg/kg in borehole 3-G, and the iron in 3-H was over 100 mg/kg as well (Table 4-1). The samples that were tested

were relatively deep—from 13 to 15 feet—so it is possible that the plume may not have reached that elevation. Thus, the original amount of bioavailable ferric iron could have been maintained at these depths.

Summary and Conclusions

SEAM3D programs were created in order to model aerobic and iron-reducing biodegradation of gasoline. The goal was to test various distributions of bioavailable ferric iron in order to quantify their effect on the sustainability of biodegradation. Sustainable biodegradation is significant because it determines whether MNA is an applicable remediation strategy for a remediation site.

After running various SEAM3D models, it became apparent that mid-range levels of oxygen and iron decreased peak levels of the concentration of COC at a monitoring well 25 meters from the source. Peak benzene concentration was decreased by over 1 mg/L, while the peak BTEX concentration was decreased by over 10 mg/L. Further study was done to determine how different amounts of iron affected these concentrations. The monitoring well study showed negligible change in benzene concentration with iron levels above 100 mg/kg. Contrastingly, by analyzing the effect that different amounts of iron have on the total mass of benzene biodegraded due to iron, it was found that the relationship was asymptotic. This suggests that for low iron levels, there is too much contaminant to sustain iron reduction. With increasing levels of iron, there are sufficient available electron acceptors, although, the biodegradation rate of iron becomes limiting. It was also determined that biodegradation due to iron-reduction had less of an impact on benzene than it did the remaining BTEX compounds when compared to aerobic biodegradation. Additionally, the fate and transport of gasohol and 1990s gasoline was evaluated. Due to the infinite solubility and high rate of biodegradation of ethanol, the biodegradation of BTEX compounds are lessened. Modeling showed almost a 50 percent decrease in the amount of benzene biodegraded due to ferric iron in gasohol compared to the 1990s gasoline.

In addition to numerical modeling, an assay was performed on two boreholes from a chlorinated solvent-contaminated site in South Carolina in order to quantify bioavailable ferric iron. The measured ferric iron was highly heterogeneous with depth; two samples only four feet apart contained iron levels over an order of magnitude apart. Unexpectedly, borehole samples taken nearby the contamination source had relatively high amounts of iron. These samples were thought to be contaminated by a chlorinated solvent source; therefore, any bioavailable iron would likely be depleted via biodegradation. It is possible that the contaminant never reached the depths of borehole samples, in which case, the soils would not have become depleted of iron. More boreholes must be analyzed in order to better predict bioavailable ferric iron distributions in the subsurface.

Lastly, using data from borehole 1, models of realistic and uniform iron distributions were created. The total iron in the domain was constant, although the distribution was variable. The mass of benzene in the domain was similar in each model, but it is apparent that the both the amount and distribution of iron are significant for iron-reducing biodegradation.

Acknowledgements

"We acknowledge the support of the National Science Foundation through NSF/REU Site Grant EEC-1062860. Any opinions, findings, and conclusions or recommendations expressed in this paper are those of the author(s) and do not necessarily reflect the views of the National Science Foundation."

I would like to thank Dr. Vinod Lohani for setting up the Interdisciplinary Water Sciences and Engineering REU program this summer, and my advisor Dr. Mark Widdowson, who shared his vast expertise of computer modeling and contaminant transport while guiding me through this project. I want to thank Julie Petruska for keeping me safe in the laboratory and Dr. Nicole Fahrenfeld for her help with the bioavailable ferric iron assay. Dr. Lashun King-Thomas, thank you for collecting the borehole samples that we had the opportunity to analyze. Lastly, I want to thank all of my REU fellows, Josh Caldwell, Maureen O'Brien, Jennifer Moutinho, Meghan Rissky, Zach Bailey, Manuel Martinez, Ashley Griffin, and Kate Aulenbach, for being great friends and teachers this summer.

References

Baukal, C. E. (2001). "Production, Refining, and Chemistry." *The John Zink Combustion Handbook.* CRC Press, Boca Raton, Florida, 177.

Brauner, J. S. (2000). "Impacts of Sequential Microbial Electron Accepting Processes on Natural Attenuation of Selected Petroleum Hydrocarbons in the Subsurface Environment." (Unpublished doctoral dissertation). Virginia Polytechnic and State University, Blacksburg.

Boncal, J.E. (2011). "Spatial Relationships Between Potential Bioavailable Organic Carbon and Sediment Grain Size at a Chlorinated Solvent-Contaminated Site." (Unpublished doctoral dissertation). Virginia Polytechnic and State University, Blacksburg.

Charbeneau, R.J. (2000). "Groundwater Contamination." *Groundwater Hydraulics and Pollutant Transport.* Prentice Hall, Inc. Upper Saddle River, NJ, 266-267.

Deeb, R.A., Sharp, J.O., Stocking, A., McDonald, S., West, K.A., Laugier, M., Alvarez, P.J., Kavanaugh, M.C., Alvarez-Cohen, L. (2002). "Impact of Ethanol on Benzene Plume Lengths: Microbial and Modeling Studies." *Journal of Environmental Engineering*, 868-875.

Harayama, S., Kishira, H., Kasai, Y., Shutsubo, K. (1999). "Petroleum Biodegradation in Marine Environments." *J. Molec Microbiol. Biotechnol.*, 1(1): 63-70.

Haskew, H.M., Liberty, T.F., McClement, D. (2007). "Fuel Permeation from Automotive Systems: E0, E6, E10, and E85." *Coordinating Research Council*. Alpharetta, Ga.

Lebron, C., Sugiyama, B., Evans, P., Trute, M., Olsen, R., Chappell, R. (2005). "Final Report-ER-0009 Field Demonstration and Validation of a Bioavailable Ferric Iron Assay." *Naval Facilities Engineering Command.*

Lovley, D.R., Baedecker, M.J., Lonergan, D.J, Cozzarelli, E.J., Phillips, P., Siegel, D.I. (1989) "Oxidation of Aromatic Compounds Coupled to Microbial Iron Reduction." *Nature (London)*, 339, 297-299.

Molson, J. W., J. F. Barker, E. O. Frind, and M. Schirmer (2002). "Modeling the impact of ethanol on the persistence of benzene in gasoline-contaminated groundwater." *Water Resour. Res.*, 38(1), 1003, doi:10.1029/2001WR000589.

Perciasepe, R. (2000). "Robert Perciasepe Assistant Administrator Office of Air & Radiation U.S. Environmental Protection Agency before the Subcommittee on Health and Environment of the Committee on Commerce U.S. House of Representatives." *U.S. Environmental Protection Association.* Retrieved from: http://www.epa.gov/otaq/consumer/fuels/mtbe/3200test.pdf

Powers, S.E. Hunt, C.S., Heermann, S.E., Corseuil, H.X., Rice, D., Alvarez, P.J.J. (2001). "The Transport and Fate of Ethanol and BTEX in Groundwater Contaminated by Gasohol." *Critical Reviews in Environmental Science and Technology*, 31(1), 79-123.

Ryan, J. (2010). "Leaking Underground Storage Tanks." *Boulder Area Sustainability Information Network.* Retrieved from: http://bcn.boulder.co.us/basin/waterworks/lust.html/

Weaver, J.W., Skaggs, S.A, Spidle, D.L., Stone, G.C. (2009). "Composition and Behavior of Fuel Ethanol." *U.S. Environmental Protection Agency.* Retrieved from:

http://www.epa.gov/athens/publications/reports/Weaver_EPA600R09037_Composition_Fuel_Ethanol.pdf

Wypych, George (2008). "Solubility and Miscibility." *Knovel Solvents- A Properties Database.* ChemTech Publishing. Toronto, Ontario, Canada.

"Basic Information about Benzene in Drinking Water." *U.S. Environmental Protection Agency.* (2012). Retrieved from: http://water.epa.gov/drink/contaminants/basicinformation/benzene.cfm

"Cleaning Up UST System Releases." *U.S. Environmental Protection Agency.* (2012). Retrieved from: http://www.epa.gov/oust/cat/releases.htm

"Monitored Natural Attenuation." *U.S. Environmental Protection Agency.* (2012). Retrieved from: http://www.epa.gov/oust/pubs/tum_ch9.pdf

Appendix

Figure A-1. Dispersion Package

TRPT	0.1
TRVT	0.01
Longitudinal Dispersivity	1.0 m

Figure A-2. NAPL Dissolution Package input for 1990s gasoline

	Initial Mass Fraction	**Solubility**	**Molecular Weight**
Tracer	0.01	1780	78.1
Benzene	0.01	1780	78.1
Toluene	0.08	515	92.1
Ethylbenzene	0.05	140	106.2
Xylene	0.12	180	106.2
Aromatics	0.1	166	120.0
Aliphatics	0.55	12	97.0
Inert Fraction			150.0

Figure A-3. NAPL Dissolution Package input for gasohol

	Initial Mass Fraction	**Solubility**	**Molecular Weight**
Tracer	0.00675	1790	78.1
Benzene	0.00675	1790	78.1
Toluene	0.07607	526	92.1
Ethylbenzene	0.0167	169	106.2
Xylene	0.08535	191.09	106.2
Aromatics	0.1184	54.93	121.45
Heavy Aliphatics	0.239887	22.04	86.3
Light Aliphatics	0.074109	68.55	71.33
Ethanol	0.11347	11600	46.07
Inert Fraction			90.1

Figure A-4. Source parameters

Residual Saturation	0.05
NAPL concentration (g/g)	0.0064
Dissolution Rate (1/day)	0.1

Figure A-5. Biodegradation Package: maximum specific rates for the 1990s gasoline

Microcolony	EA	Benzene	Toluene	Ethylbenzene	Total Xylene	Other Aromatics	Aliphatics
Unit		1/day	1/day	1/day	1/day	1/day	1/day
Aerobes	O2	0.64	0.64	0.64	0.64	0.64	0.64
Iron reducers	Fe(III)	0.0009	0.009	0.009	0.009	0.009	0
Methanogens		0	0	0	0	0	0

Figure A-6. Biodegradation package: maximum specific rates for gasohol

Microcolony	EA	Benzene	Toluene	Ethylbenzene	Total Xylene	Other Aromatics	Heavy Aliphatics	Light Aliphatics	Ethanol
Unit		1/day	1/day	1/day	1/day	1/day	1/day	1/day	1/day
Aerobes	O2	0.64	0.64	0.64	0.64	0.64	0.64	0.64	3.2
Iron reducers	Fe(III)	0.0009	0.009	0.009	0.009	0.009	0	0	0.045
Methanogens		0	0	0	0	0	0	0	0

Figure A-7. Biodegradation package: biodegradation constants

		Half Saturation Constant							
Microcolony	EA	Hydrocarbon	Electron Acceptor	Yield Coeff.	Use Coeff.	Inhib. Coeff.	Production Coeff.	Initial Biomass	Decay Constant
Unit		g/m^3	g/g	g/g	g/g	g/m^3	g/g	g/g	1/day
Aerobes	O_2	5	0.5	0.5	3.2	0.1		0.3	0
Iron reducers	Fe(III)	5		0.2	42	10	0.2	0.3	0
Methanogens		5		0			0.8	0.3	0

Figure A-8. Biodegradation Package: concentration parameters

	Dissolved Oxygen	Fe(III)	Hydrocarbons
Initial concentration:	N/A	400	N/A
Minimum Concentration	0.01	10	0.0001

Influence Of The Phosphorus Circulation On The Eutrophication And Algal Blooms At Falling Creek Reservoir Leading

Meghan Frances Rissky*, Rick Browne**, Dr. John Little**

** NSF-REU fellow, Virginia Polytechnic Institute and State University*
(Home Institution: Civil Engineering, Texas Tech University)
***Department of Civil and Environmental Engineering, Virginia Polytechnic Institute and State University*

ABSTRACT

Cyanobacteria can control their depth within water allowing them to bloom in ideal conditions and cause taste and odor changes, as well as release possible toxins, which cause problems in the drinking water at Falling Creek Reservoir. In order to understand the conditions in which cyanobacteria bloom, the amount of phosphorus going into the lake, as well as that in the lake at different depths, temperature, dissolved oxygen, and turbidity have been recorded. The phosphorus in the lake also increases the rate of eutrophication allowing cyanobacteria to thrive as the different layers created during thermal stratification are closer together allowing the cyanobacteria to reach sunlight easier and use photosynthesis to bloom. In an attempt to control this, Western Virginia Water Authority will be installing a side steam oxygenation system to introduce oxygen into the Hypolimnion layer in order to control anoxic conditions. Monitoring phosphorus levels before and after the oxygenation system is installed will be assed in order to determine its effectiveness in suppressing phosphorus release as phosphorus is a major problem in eutrophication, leading to the growth of cyanobacteria.

Keywords: phosphorus, eutrophication, cyanobacteria

Introduction

Nearly one-third of the world is influenced by a lack of drinkable water and water scarcity making it a priority to increase water quality (Schindler, 2008). Algae blooms cause taste and odor changes in water supplies as well as various toxins that can lead to harm within all life forms. Many consumers are wary to drinking water that tastes or smells unusual as it causes people to be skeptical as to how clean the water is. Water treatment plants have to take the different tastes and odors, as well as the toxins and cloudiness from the algae, out using various processes that are costly (Henderson-Sellers, Markland, 1987). Therefore, water treatment plants are trying to take out the need for these treatments by suppressing the amount of algae growing in water by means of lowering the nutrients that algae feed on—mainly phosphorus and nitrogen—thus cutting costs.

Cyanobacteria growth has been shown to be limited with both chemicals, used as algaecides, and destratification systems. Western Virginia Water Authority has tried various methods to try to control the algae blooms at Falling Creek Reservoir including a surface circulator in 2007. A surface circulator is similar to a water fountain underwater in that it takes the water from the hypolimnion and redistributes it in the epilimnion, thus disrupting the thermal stratification taking place and oxygenating the hypolimnion. The effectiveness on suppressing algae growth at Falling Creek Reservoir was studied in 2008 and was proved to be ineffective. In 2005, Western Virginia Water Authority also tried to suppress the amount of phosphorus available to cyanobacteria by using the most common algaecide, copper sulfate. Although algaecides do well at controlling algae, they can also change the taste and odor of the reservoir; thus not eliminating the extra costs in treatment. Later this summer (2012), they plan on installing a side stream oxygenation system (SSO) in order to try to fix this problem. This acts like the destratification system in the fact that they both provide oxygen to the hypolimnion. The main difference is that the destratification system disrupts the thermal stratification, where the SSO injects oxygen directly into the hypolimnion.

Research Objective

The primary objective of this project was to determine the effect of an oxygenation system on the amount of phosphorus in the reservoir. In order to do this, one must determine the main source of phosphorus into the reservoir—internal versus external—and the amount of phosphorus in the lake before and after the circulator has been installed. To accomplish this, samples are taken from five different inlets, to determine the concentration of the phosphorus, as well as the flow rate of the water. These with the cross-sectional area of each inlet helps determine the rate at which phosphorus is flowing into the reservoir. Also, samples are taken off a catwalk at seven different elevations to determine the amount of phosphorous already in the reservoir. Dissolved oxygen levels, turbidity, and the temperature of the reservoir are collected, at five different locations using a CTD, to help determine the effect of phosphorus on the reservoir.

Background

Bodies of water contain nitrogen, phosphorus, and carbon dioxide, among other elements, and depending on the quantities of these main three, it can lead to eutrophication and eventually the increase of algae blooms. To try to minimize the effect of these elements on eutrophication, the effects of each element have been studied intensely in many controlled instances to determine which is the most influential. It was determined that the limitation of phosphorus has been said to be an effective way of controlling eutrophication as it is more of a catalyst than both nitrogen and carbon dioxide (Schindler, Vallentyne, 2008). Carbon, which often comes as a result of algae photosynthesizing due to the nutrient loading of phosphorus and nitrogen, has been shown, that when limited, to have a negative effect on eutrophication as it can cause an increase in phosphorus and nitrogen and thus an increase in algae blooms (Schindler, Vallentyne, 2008). Phosphorus gets into the water through both internal and external nutrient loading; internal including coming from the sediments in the lake and external coming from various human influences. Internal nutrient loading in the case of Falling Creek Reservoir comes from the decomposition of various plant life and animals in the water as algae blooms block sunlight to the vegetation in the hypolimnetic layer that provide shelter and food to various species in the water; although internal nutrient loading can also come from photosynthesis of various plants and chemosynthesis (Henderson-Sellers, Markland, 1987). External nutrient loading of phosphorus mainly comes from erosion of the land, animal excrements, and lawn fertilizers—as well as herbicides and pesticides—that run off during storms (Schindler, Vallentyne, 2008). This build of nutrients along the bottom of the water leads to anoxic conditions—there is history of this happening at Falling Creek Reservoir—as the

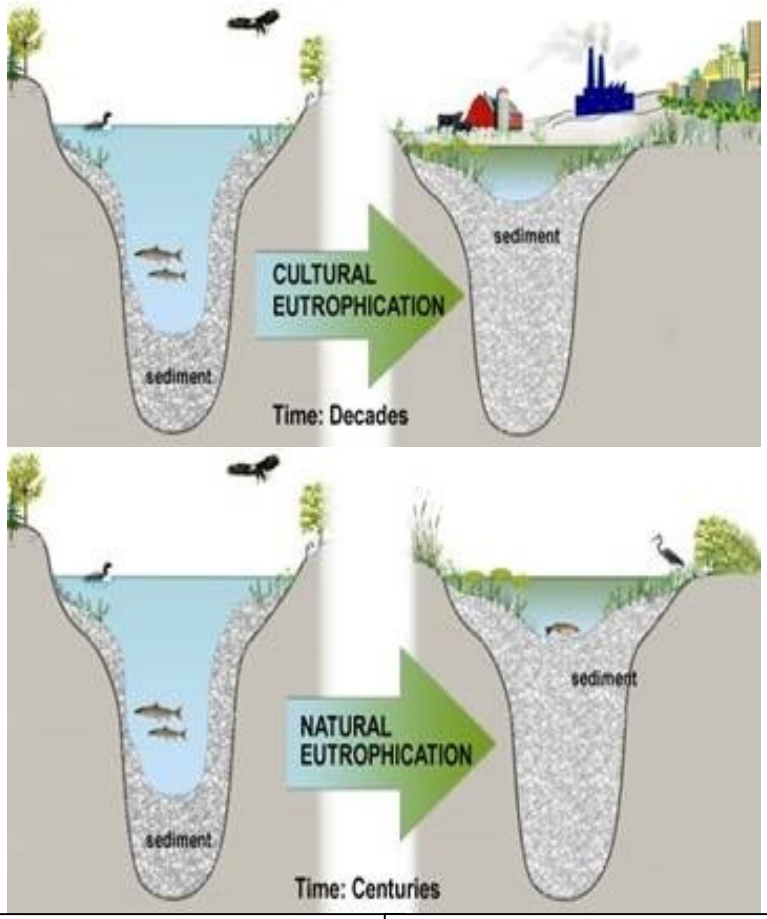

Source: "Eutrophication." 2012	Figure 1. Eutrophication Effects

nutrient layers in the water are thinner and longer thus not allowing the water mix as well. Therefore the nutrients are scattered throughout the layers and the dissolved oxygen is only replenished in the epilimnion (Henderson-Sellers, Markland, 1987). More reasons that eutrophication is a problem is that it increases the biomass of the body of water as well as increasing turbidity, the amount of sediments, and the algae blooms ("Effect of Eutrophication and Algal Bloom," 2009). This can be shown in Figure 1 as well as the effect that human interaction has on eutrophication.

As a result of phosphorus nutrient loading, an increase in algae blooms occurs. At Falling Creek Reservoir, cyanobacteria are the main vegetation that have taken over. Algae increases turbidity—thus blocking sunlight to lower vegetation causing it and the organisms that survive on it to die out and decompose; therefore increasing the eutrophication of the body of water—as well as decreasing the amount of dissolved oxygen in the water. When dissolved oxygen levels get too low in the hypolimnion anoxic conditions occur ("Effect of Eutrophication and Algal Boom," 2009). The effects of algae can be shown in Figure 2. Although this is not a picture of Falling Creek Reservoir, it gives a good idea of how algae affect the clarity of water.

Figure 2. Algae Effects	Source: "Harmful Algae Blooms," 2012

Cyanobacteria can grow in both dark and light situations due to the adenosine triphosphate (ATP) synthase gene—a generating system that allows the cyanobacteria to photosynthesize. This is because the ATP can adjust to the different light levels in the water; where in the darker levels, the ATP has a decreased interaction of concentration (Rogers, Gallon, 1988). Phosphorus comes into this as cyanobacteria stores phosphorus and nitrogen in order to complete a process called oxidative phosphorylation where the cyanobacteria uses energy from when the nutrients are oxidized to produce more ATP (Rogers, Gallon, 1988). This makes growth in the dark equivalent to when in sunlight when oxygen-dependent respiration uses internal polyglucose storing (Rogers, Gallon, 1988). As algae is continuing these process, it releases toxins that are responsible for the costly taste and odor changes; some of which are removed naturally in the lake, while others have to be removed at the treatment plant. Not all algae blooms are producing toxins at all times, and it is impossible to tell when they are producing toxins and which ones are producing toxins as testing takes a couple days and the toxin production varies. Some of the various toxins that cyanobacteria produce include: microsystins, the most common and a hepatotoxin; nodularin, also a hepatotoxin; clindrospermopsis, a hepatotoxin and cytotoxins; anatoxins, a neurotoxin; and lyngbya, a dermatotoxin and gastrointestinal toxin (Schindler, Vallentyne, 2008). An example of a toxin outbreak in drinking water occurred in 1993 in Milwaukee, WI when the drinking water was infected with cryptosporidium, a protozoan that is chlorine resistant. It went undetected for a short time leading to forty thousand people infected, four thousand hospitalized, and between fifty and seventy dead (Schindler, Vallentyne, 2008).

One of the main factors that lead to phosphorus nutrient loading in the reservoir is that thermal stratification that takes place in warmer months. This is where the water is not mixing itself due to the temperature differences in the summer; as hot water rises about colder water and the water at the top is getting the heat radiation from the sun not allowing it to sink. This allows the dissolved oxygen to not get replenished in the hypolimnion when the algae and other organisms in the water use it up; thus leading to anoxic conditions. Anoxic conditions when a lake is stratified leads to an increase in phosphorus in the water as well and therefore causing an influx of algae. This happens when organics decompose and the sulphate turns into hydrogen sulphide ($2CH_2O + SO_4^{2-} + 2\ H^+ \rightarrow H_2S + 2CO_2 + 2\ H_2O$). As this happens, the hydrogen sulphide reacts with phosphates of iron to produce free phosphate ions ($2FePO_4 +$

$3H_2S \rightarrow 2FeS + 2PO_4^{3-} + S + 6H^+$) (M, B, 2007). In the winter this isn't a problem as the water in the epilimnion has less heat radiation from the sun, thus being cold and sinking to the bottom making the water almost all the same temperature—with the lowest level being warmest—and the water well mixed. This decreases the phosphorus nutrient loading as the phosphorus is suppressed and therefore decreasing the amount of algae growth, thus solving the problem of taste and odor changes. When high winds occur, as Falling Creek Reservoir as it is shallow, it does disrupt thermal stratification for a short period of time but not enough to solve the taste and odor problems caused by the algae. To decrease thermal stratification in the water throughout the summer when natural mixing does not occur, a destratification (like the one previously used) system can be used. At Falling Creek Reservoir there are currently plans to install a side-steam saturation system towards the end of the summer. This injects oxygen into the hypolimnion layer and suppresses the nutrients to avoid nutrient loading and thus disrupting the algae growth. (Elam, 2008). Although this does not destratify the reservoir, it allows the hypolimnion to become oxygenated as the bubbles injected carry the water from the hypolimnion up to the epilimnion where it gets oxygenated by the atmosphere.

Site Study

Falling Creek Reservoir, located in Bedford County, is maintained by the Western Virginia Water Authority and supplies part of the drinking water to Roanoke, VA. To give an estimate of the size, about 322ML of water can be held in Falling Creek Reservoir when completely full. Figure 3 shows a mp of Falling Creek Reservoir showing the inlets and drainage into FCR due to the topography of the area. Taste and odor problems, connected with the algae and cyanobacteria growth, have been an issue here for quite some time; Falling Creek Reservoir also suffers from anoxic conditions due to this. To try to solve this problem, first in 2005, they used an algaecide known as a copper sulfate mixer. Although algaecides tend to be effective, they are not preferred as they can also lead to taste and odor alterations. Then, in 2007 (in 2006, nothing was used to control algae), a surface circulation system was installed. This is similar to a water fountain underwater in that it takes the water from the hypolimnion layer and dispenses the water into the epilimnion layer, thus mixing the water (Henderson-Sellers, Markland, 1987). This was proved to be ineffective at Falling Creek Reservoir to control algae growth. Therefore later this year, around August 2012, a side stream oxygenation system is intended to be installed.

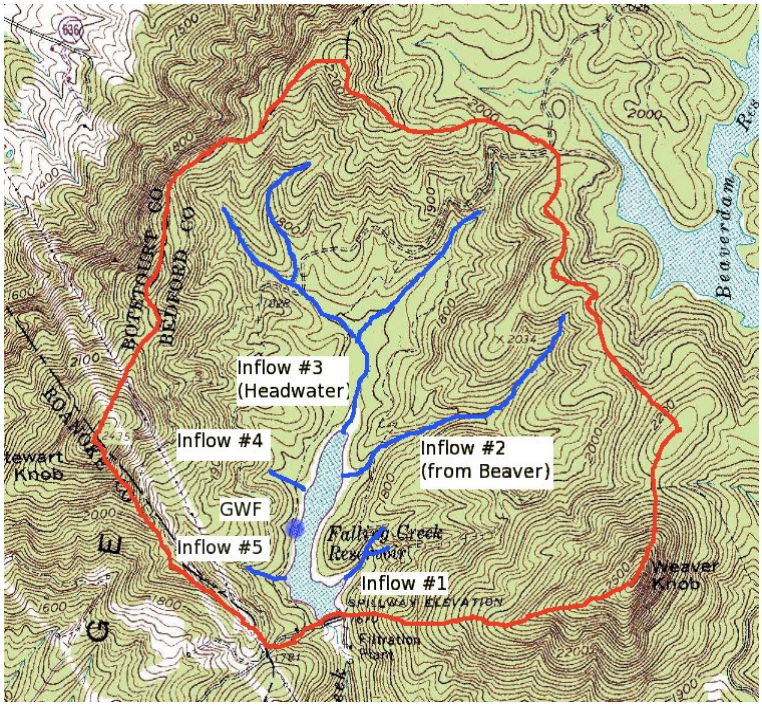

Figure 3. Map of Falling Creek Reservoir

Data Collection

To create a phosphorus balance for Falling Creek Reservoir samples are taken from seven different elevations of the lake, from all five inflows, and a CTD is used at five different sites. Measurements were taken of total phosphorus, orthophosphate, dissolved oxygen, temperature, chlorophyll, algae count, and water velocity through the course of the summer. It is planned that Rick

Browne will continue to take measurements after the side stream oxygenation system has been installed later this year to determine the effectiveness.

CTD

The CTD—standing for conductivity, temperature, and depth—measures the chlorophyll, temperature, and dissolved oxygen throughout the water at five different locations. Figure 4 shows the locations on Falling Creek Reservoir. The temperature and dissolved oxygen were measured to determine the thermal stratification of the lake as well as the extent of the anoxic conditions throughout the water. As the reservoir is stratified, it is expected to have higher dissolved oxygen near the top of the water as well as a temperature that gradually drops as the CTD lowers in the water. Chlorophyll is also measured by the CTD and this helps determine how deep light is penetrating in the water. This is important for the growth of other organisms in the water, as well as the growth of algae. The farther light penetrates the father organisms travel near the bottom and fewer algae tends to be blocking light.

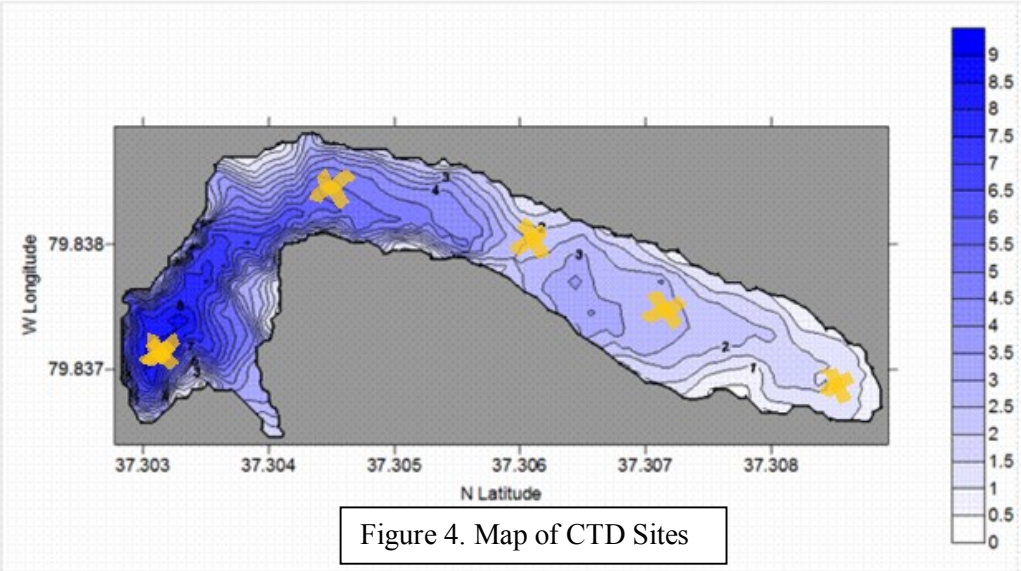

Figure 4. Map of CTD Sites

Water Velocity

Water Velocity is taken at all the intakes to determine how much water is flowing in from each; we can combine this information with the phosphorus levels to determine how much phosphorus is flowing into the reservoir from each inlet. Over the course of the summer inlet one and three were stagnant and inlet four had dried up so no flow rates were taken at these sites. Two reading were taken from each viable source and were averaged. Figure 5 shows the flow being read at inlet 2; a current is obvious to the naked eye. This was then combined with the cross sectional area to determine the flow rate each week using Q=A*V; where A is the cross-sectional area of the inlet, V is the average water velocity, and Q is the flow rate. Measurements for the cross-sectional area were taken at the point of fastest flow and half way between the point of fastest flow and the edge on each side; as well as the width measurement—each week measurements were taken at the same location on the inlet.

Figure 5. Water Flow Rate Being Recorded

Phosphorus

Figure 6. Samples Being Taken At FCR

Water samples were taken from each inlet, when viable, to determine the amount of orthophosphate and total phosphate in the water each week. Figure 6 shows samples being taken from inlet two. Samples were also taken off a catwalk at seven different elevations—1663 ft, 1660.5 ft,1658 ft, 1654.5 ft,1651 ft,1647 ft, and 1643 ft—within the water to compare how much phosphorus was flowing in to how much phosphorus was in the reservoir. These can be compared to determine whether the main source of phosphorus in the reservoir is from external—from the inlets—or internal nutrient loading—from the sediments; thus determining if Falling Creek Reservoir is storing or releasing phosphorus in the sediments.

Orthophosphate

Orthophosphate is phosphorus in the water that is inorganic and soluble that is often used by plants; it is only a fraction of the phosphorus in the water (Murphy, 2007). Samples measured for orthophosphate had to be tested the same day they are taken as the samples do not preserve unless frozen. To measure for orthophosphate, first a calibration curve is taken using phosphorus concentrations of 0.00, 0.010, 0.025, 0.050, 0.25, and 0.50 (using DI water and adding a stock sample of phosphorus to create this concentration). Sulfuric acid, ammonium molybdate- antimony potassium tartrate, and ascorbic acid are added to the sample. This makes the sample turn a shade of blue which is then measured in a spectrophotometer—measures the absorbance of the blue wavelength at 880nm. This is then used with the samples from the reservoir to determine the concentration based on the reading from the spectrophotometer. The samples from the reservoir are tested almost the same in that they are filtered beforehand through .7um pore filters (also the 0.00 for the calibration curve is filtered).

Total Phosphorus

Total phosphorus is all phosphorus including dissolved and inorganic in a sample (Murphy, 2007). These samples are preserved and put in the refrigerator until being tested the next week. A calibration scale is created here using the same concentrations as when testing for orthophosphate. To test for total phosphorus in a sample ammonium peroxidisulfate is added for digesting, as well as sulfuric acid. The samples are then put into an autoclave for 30 minutes in which the water is boiled under high temperature and high pressure; often this is called the digestion stage. Then it mimics the test for orthophosphate in that ammonium molybdate- antimony potassium tartrate and ascorbic acid are added to change the water a shade of blue before being put into the spectrophotometer.

Quality Assurance and Quality Control

While testing for both orthophosphate and total phosphorus, blanks—about every ten samples, duplicate samples, spiked samples, and QC samples using an outside standard source, are used to make sure that contamination has not occurred.

Results and Discussion

All results shown are from the current year and before the side stream oxygenation system installation.

Temperature, Dissolved Oxygen, and Algae Count

When anoxic conditions are present, dissolved oxygen levels should be low in the hypolimnion layer. According to this year's data shown in Figure 7, Falling Creek Reservoir is not currently in anoxic conditions; although there is a difference in the amount of oxygen between the hypolimnion and epilimnion. But, thermal stratification is still taking place. This can be seen in Figure 8 as the temperature is not constant in the summer month. In the colder months shown on Figure 8, the temperature is pretty consistent at around seven degrees Celsius throughout the different elevations. However, in the warmer months, the higher elevation of 1663 ft is warmer than the lower elevation of 1643 feet. This shows that mixing is not going to occur as the warmer water on the top will not fall. Shown in Figure 9, the amount of algae has been on the rise though through the warmer months. The correlation between these three can be seen all throughout the warmer months. As the temperature is increasing, thermal stratification begins to start and dissolved oxygen begins to drop in the hypolimnion and algae growth is increasing. The 31st of May, 2012 shows a great example of this as all graphs show number spikes. This can be shown in Figure 10. The turbidity has increased on the 31st as well showing the effect that the increased algae have on the clarity of the water.

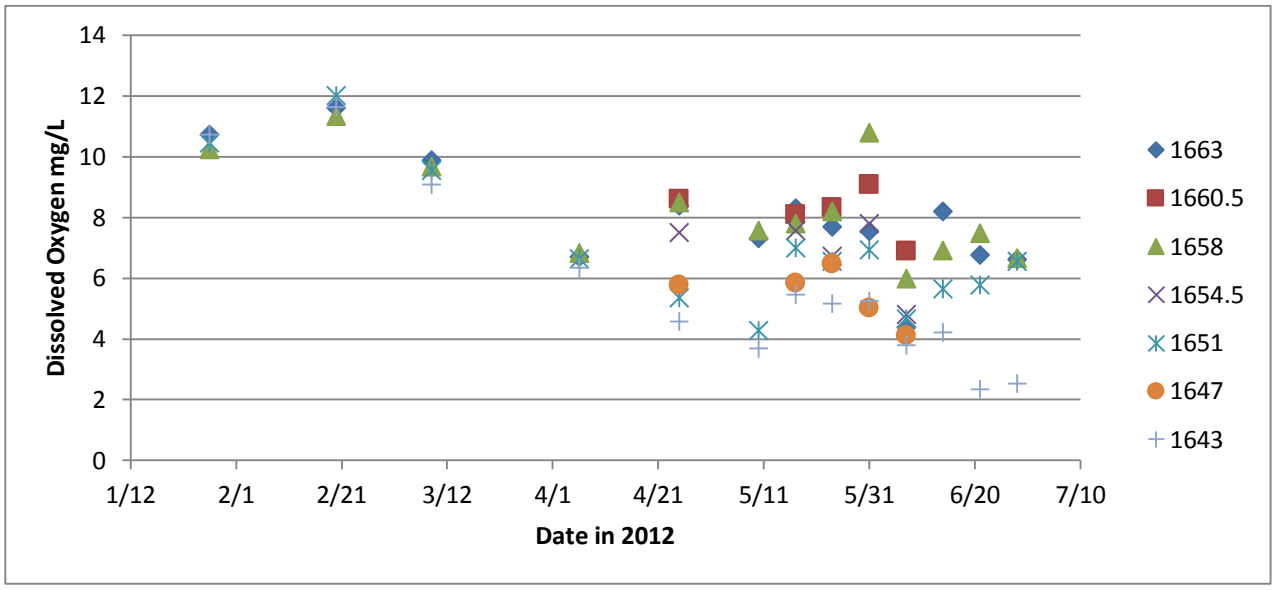

Figure 7. Dissolved Oxygen Over Time

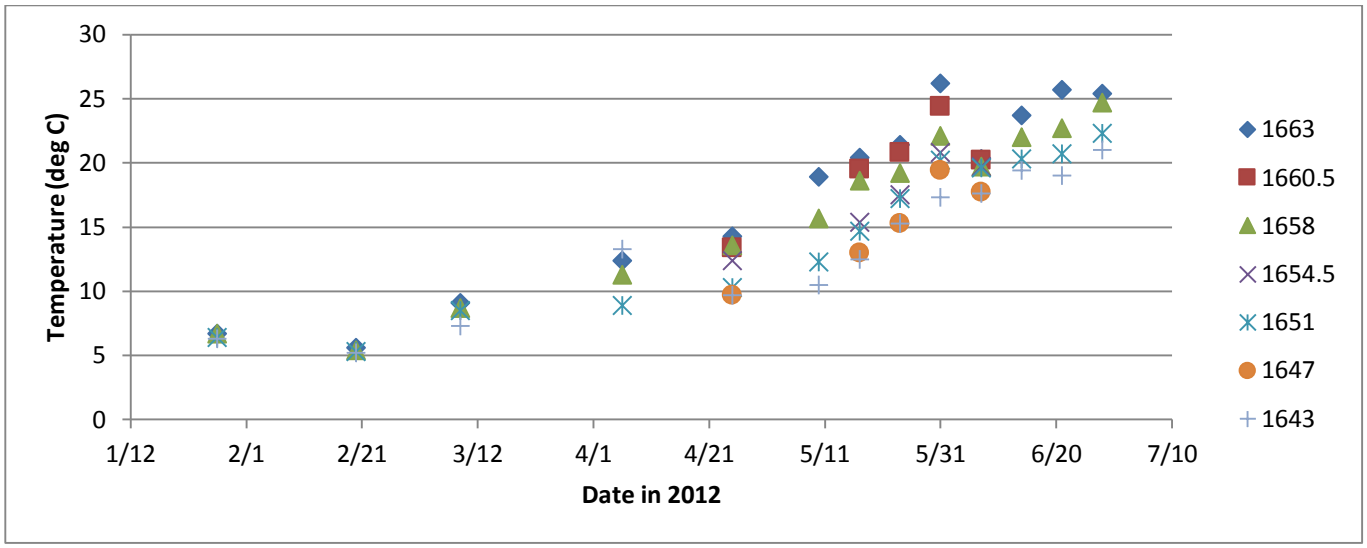

Figure 8. Temperature Over Time

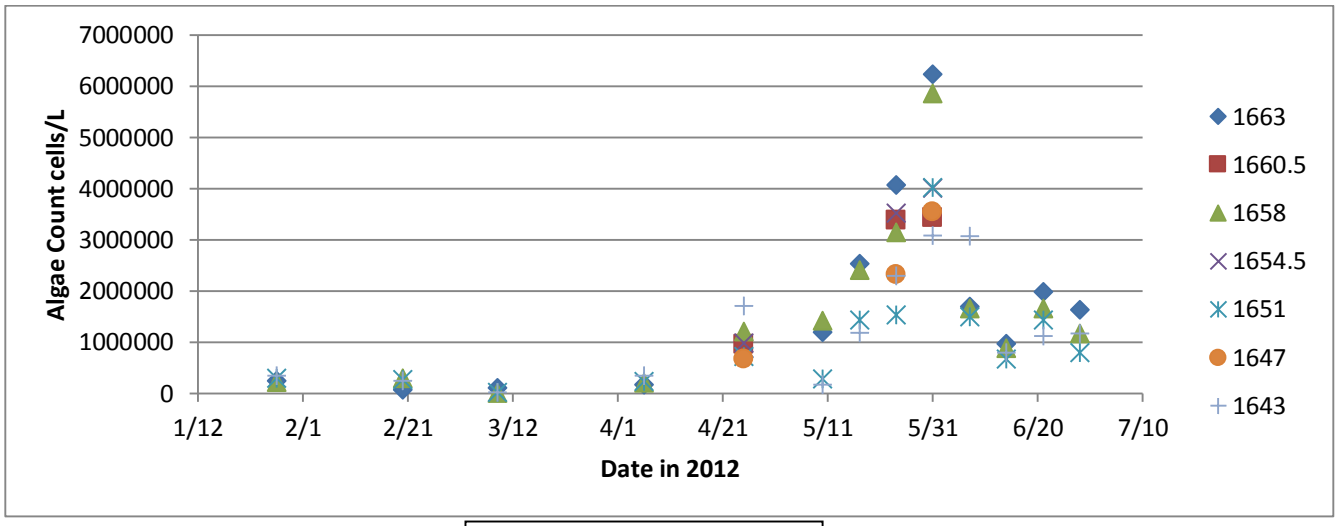

Figure 9. Algae Over

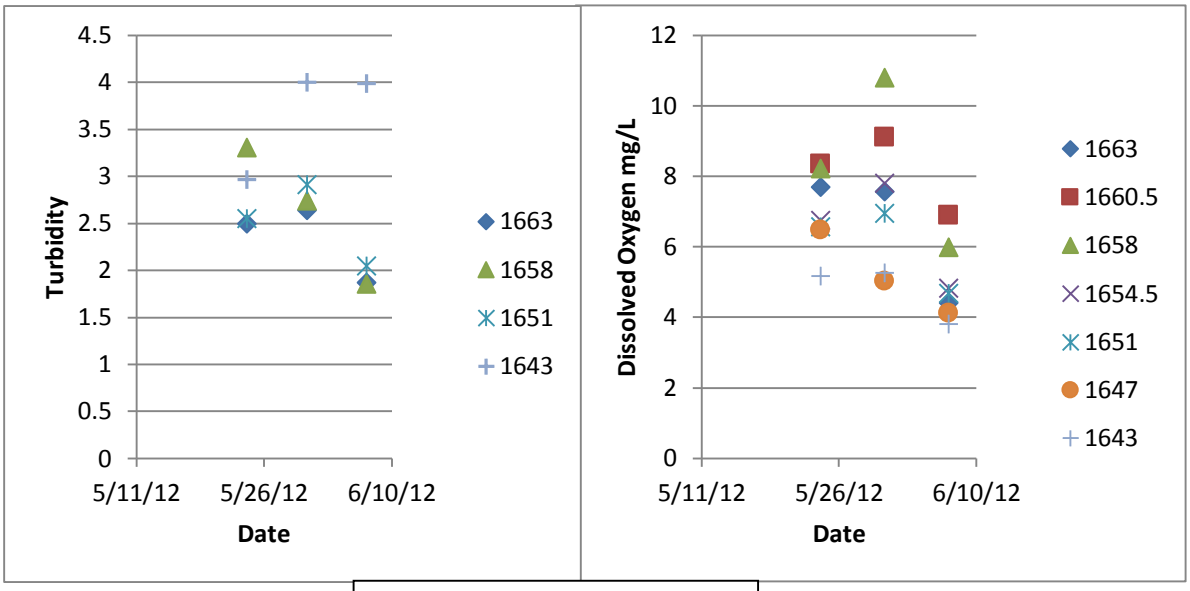

Figure 10. May 31st, 2012

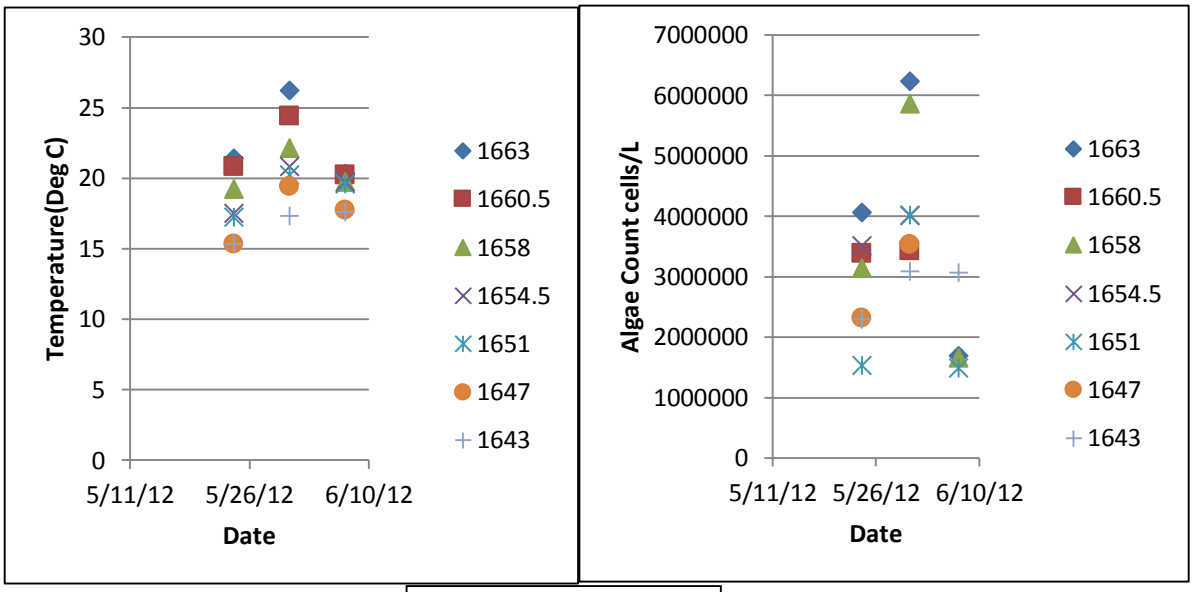

Figure 11. Flow Rates

Phosphorus and Water Flow

Total Phosphorus, as it includes orthophosphate, was the main result studied in terms of water flow. It can be observed in Figure 11 and 12 that most of the water flowing into the reservoir is coming from Inlet 2. Figure 13 shows that the highest concentration of phosphorus flowing into the reservoir is from inlet 5; although this doesn't account for the flow rate. Based on the flow rate and the phosphorus concentration, the amount of phosphorus flowing into the lake, and out, can be seen in Figure 15. Inlet 1 and 3 were stagnant and inlet 4 has dried up throughout this testing so flow into the reservoir is irrelevant. The main source of water flowing in, shown in Figure 13 come from inlet 2. It should be noted that inlet 2's flow increases because Beaver Dam which feeds into inflow 2 was opened during the beginning of the summer. When comparing the graph in Figure 15, it can be determined that as the net flow is negative, there is more phosphorus flowing into the lake then out of it. Therefore it can be determined that Falling

Creek Reservoir is being filled with phosphorus more than releasing phosphorus. It can also be determined from Figure 14 that the main source of phosphorus flowing into the water is from inlet 2. Therefore, with the main source of phosphorus determined, a side stream oxygenation system can be implemented.

Date (Inflow 2)	Calculated Area (ft^2)	Mean Flowmeter velocity (ft/s)	Calculated water flow (cfs)
2/20/2012	0.37942708	0.4	0.151770833
3/19/2012	0.88541667	0.567	0.50203125
4/25/2012	0.88541667	0.7	0.619791667
5/17/2012	1.77083333	1.2	2.125
5/24/2012	1.77083333	0.85	1.505208333
6/7/2012	1.77083333	1.55	2.744791667
6/14/2012	1.77083333	1.233	2.1834375
6/21/2012	1.77083333	0.93	1.646875
6/28/2012	1.27083333	1.4	1.779166667
7/5/2012	1.27083333		0
7/12/2012	1.82291667	1.1	2.005208333
7/19/2012	1.67708333	1.5	2.515625
7/26/2012	1.39583333	1.5	2.09375
Date (Inflow 5)	**Calculated Area (ft^2)**	**Mean Flowmeter velocity (ft/s)**	**Calculated water flow (cfs)**
3/19/2012	0.55164931	0.2	0.110329861
5/17/2012	0.34027778	0.25	0.085069444
6/14/2012	0.34027778	0.35	0.119097222

*Inlets 1 and 3 were stagnant so flow rate was irrelevant
** Inlet 4 was dried up so there was no flow rate
*** Inlet 5 dried up before summer 2012 was over so readings stopped

Figure 12. Flow of Water At FCR

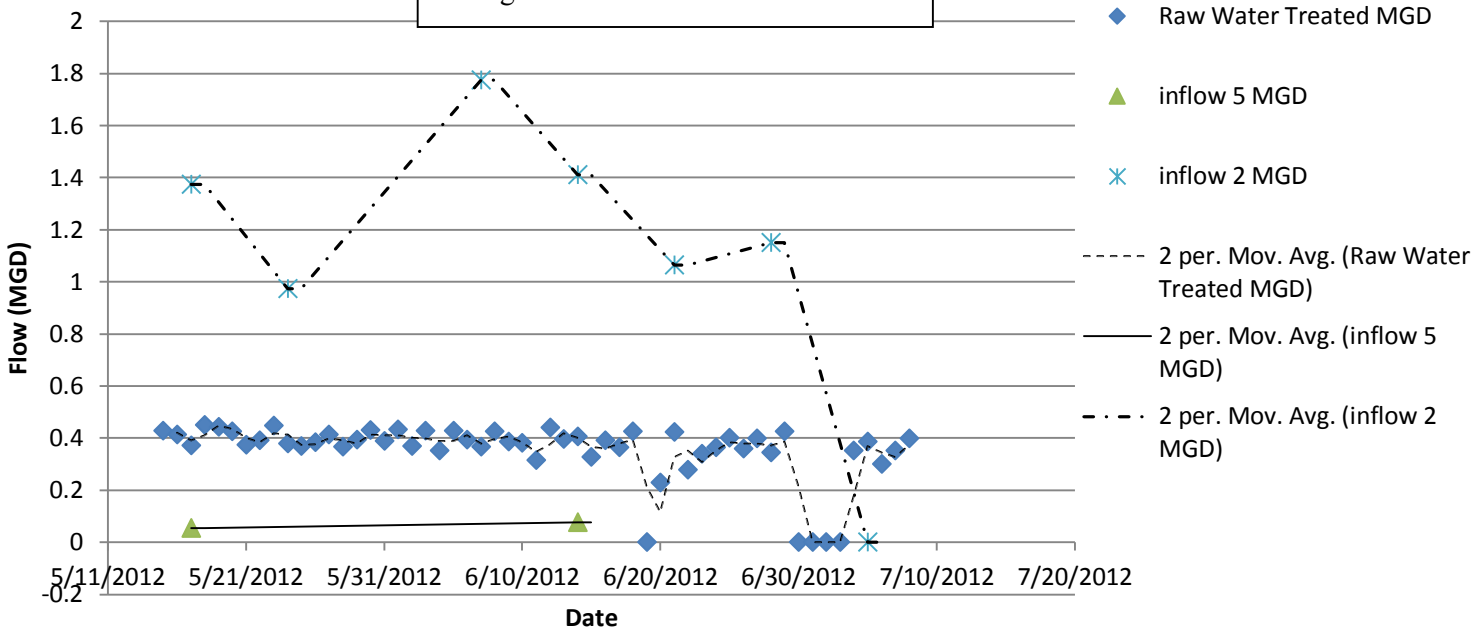

TP Over Time At 7 Different Elevations Within FCR

Figure 13

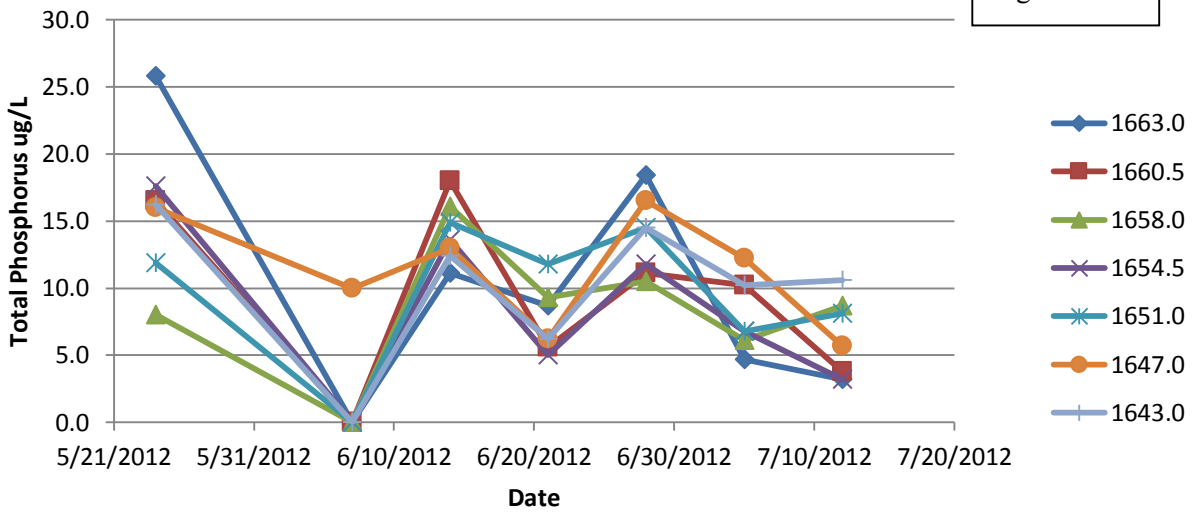

TP From Each Inflow

Figure 14

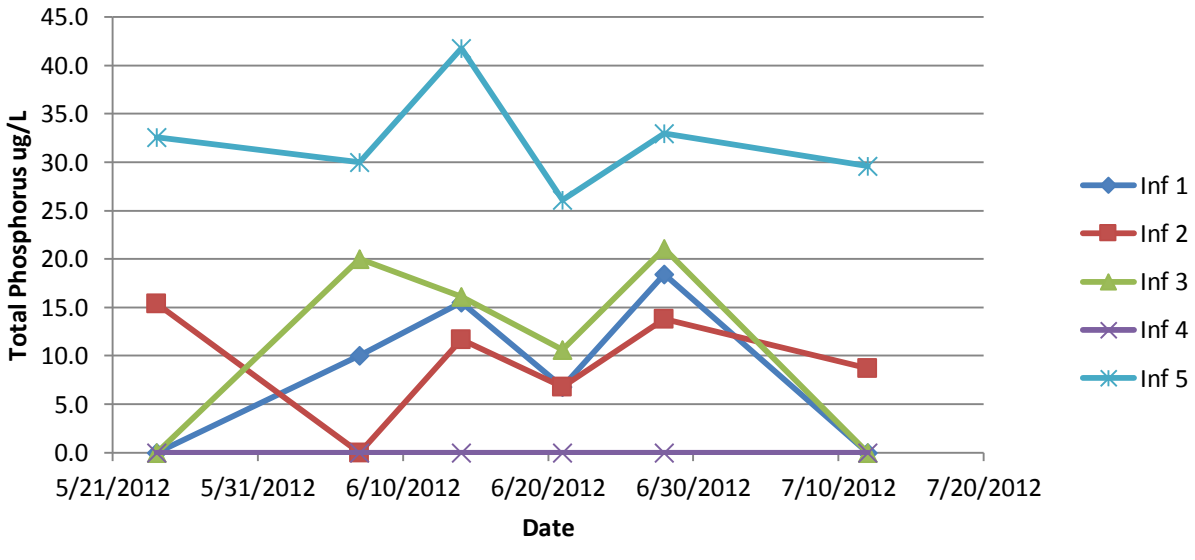

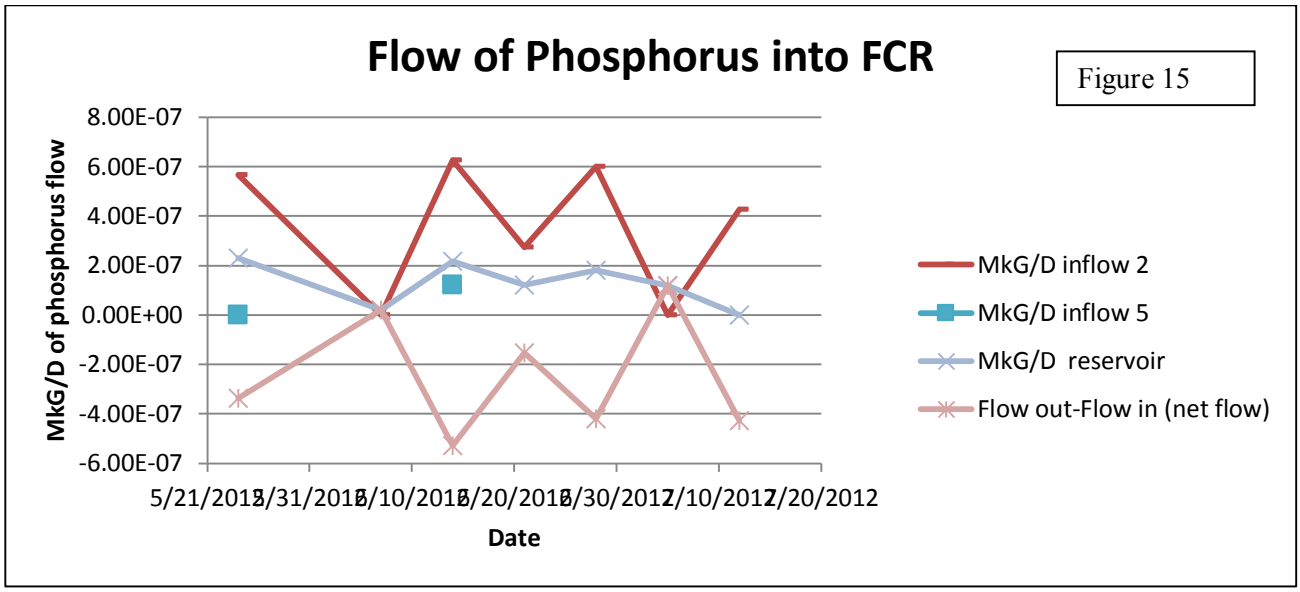

Conclusion

The purpose of the side stream oxygenation system to be installed is to provide oxygen to the hypolimnion layer which should suppress the amount of phosphorus in the reservoir and thus decrease the amount of algae. Although it has not been installed yet, one can see from the data already collected that algae blooms do increase over the warmer months. It is expected that when the side steam oxygenation system is installed, the amount of algae blooms will be decreased and thus solve the taste and odor difference caused by them; this will then reduce the cost of treatment of water. A side stream oxygenation system has been chosen as the main source of phosphorus has been concluded to come from the inlets. By suppressing the phosphorus at the source, it reduces chances that the phosphorus will be released from the sediment and cause an influx of algae blooms in the years to come.

Acknowledgements

We acknowledge the support of the National Science Foundation through NSF/REU Site Grant EEC-1062860. Any opinions, findings, and conclusions or recommendations expressed in this paper are those of the author(s) and do not necessarily reflect the views of the National Science Foundation.

I would like to thank my mentor, Rick Browne, and the support of Dr. John Little. I would also like to thank Western Virginia Water Authority for their support and the use of their equipment. This program would not be possible without Dr. Lohani, and so I thank him for all his support and organization with keeping everyone on track throughout the summer. I would also like to thank all the guest speakers that spoke this summer to the NSF REU Interdisciplinary Water Science and Engineering group who brought knowledge of various subjects to the group.

References

"About Eutrophication." *World Resources Institute*. N.p., n.d. Web. 24 July 2012. <http://www.wri.org/project/eutrophication/about>.

"Blue-Green Algae (Cyanobacteria) Blooms." *Blue-Green Algae (Cyanobacteria) Blooms*. California Department of Public Health, 20 Sept. 2011. Web. 10 July 2012. <http://www.cdph.ca.gov/healthinfo/environhealth/water/pages/bluegreenalgae.aspx>.

Cooke, Rosa-lee. "Lesson 9: Taste and Odor." *Lesson 9: Taste and Odor*. Mountain Empire Community College, 21 Aug. 2011. Web. 10 July 2012. <http://water.me.vccs.edu/courses/env110/lesson9.htm>.

"Effect of Eutrophication and Algal Boom." *Effect of Eutrophication and Algal Boom*. N.p., 25 September 2009. Web. 24 July 2012. <http://www.ychlpyss.edu.hk/~bio/share/0405/ecologyessay/sam/7.htm>.

Elam, Kevin P. "Effects of a Surface Circulator on Temperature, Dissolved Oxygen, Water Velocity, and Photosynthetic Yield in Falling Creek Reservoir." Thesis. Virginia Polytechnic Institute and State University, 2008. Print.

"Eutrophication." *Lake Scientist*. Lake Scientist, n.d. Web. 10 July 2012. <http://www.lakescientist.com/learn-about-lakes/water-quality/eutrophication.html>.

Gantzer, Paul. Mark Mobley. (2012, January 27). Falling Creek Reservoir Hybrid Management Strategy. Western Virginia Water Authority.

Henderson-Sellers, Brian, and H. R. Markland. *Decaying Lakes: The Origins and Control of Cultural Eutrophication*. Chichester [West Sussex: Wiley, 1987. Print.

"Harmful Algal Blooms." *Lake Scientist*. Lake Scientist, n.d. Web. 10 July 2012. <http://www.lakescientist.com/learn-about-lakes/water-quality/harmful-algal-blooms.html>.

M, Drabkova, and Marsalek B. "A Review of In-lake Methods of Cyanobacterial Blooms Control." *CyanoData*. CyanoData, Apr. 2007. Web. 1 Aug. 2012. <http://www.cyanodata.net/review.php>.

Murphy, Sheila. "BASIN: General Information on Phosphorus." *BASIN*. City of Boulder/USGS Water Quality Monitoring, 23 Apr. 2007. Web. 31 July 2012. <http://bcn.boulder.co.us/basin/data/NEW/info/TP.html>.

"Oxygenation (environmental)." *Wikipedia*. Wikimedia Foundation, 07 Mar. 2012. Web. 10 July 2012. <http://en.wikipedia.org/wiki/Oxygenation_(environmental)>.

Rogers, L. J., and J. R. Gallon. *Biochemistry of the Algae and Cyanobacteria*. Vol. 28. Oxford [England: Clarendon, 1988. Print.

Seckbach, J. *Algae and Cyanobacteria in Extreme Environments*. Dordrecht: Springer, 2007. Print.

Schindler, David W., and John R. Vallentyne. *The Algal Bowl: Overfertilization of the World's Freshwaters and Estuaries*. Edmonton: University of Alberta, 2008. Print.

"Taste- and Odor-Causing Compounds In Drinking Water."*Engamerica*. TrojanUV Water Confidence, 2005. Web. 10 July 2012. <http://www.engamerica.com/uploaded/Doc/Trojan_ECT_Facts.pdf>.

"Water Oxygenation." *Wikipedia*. Wikimedia Foundation, 26 June 2012. Web. 10 July 2012. <http://en.wikipedia.org/wiki/Water_oxygenation>.